2017

Evaluation of building demand and PV system output in order to devise an improved tariff and operational strategy for sharing PV power

Bosui Li
University of Wollongong

UNIVERSITY
OF WOLLONGONG
AUSTRALIA

Evaluation of building demand and PV system output in order to devise an improved tariff and operational strategy for sharing PV power

Bosui Li

This thesis is presented as part of the requirements
for the conferral of the degree:

Master of Philosophy

August 2017

Supervisors:
Duane Robinson, Ashish Agalgoankar

The University of Wollongong
School of Electrical, Computer & Telecommunications Engineering

DECLARATION

I, *Bosui Li*, declare that this thesis submitted in partial fulfilment of the requirements for the conferral of the degree *Master of Philosophy*, from the University of Wollongong, is wholly my own work unless otherwise referenced or acknowledged. This document has not been submitted for qualifications at any other academic institution.

_____

Bosui Li

August 31, 2017

ABSTRACT

Governments in a number of countries have developed policies to support the utilisation of solar energy. These policies drive the adoption of new electricity tariffs such as: Feed-in tariff (FiT), net metering (NM), and virtual net metering (VNM). In recent years, VNM has attracted greater attention due to its improved performance for extending the utilisation of PV power. In the U.S., VNM has been widely applied to operate community solar projects and a number of studies have been done to evaluate the policy issues of VNM. However, studies focusing on policy and regulation are not enough to develop a comprehensive understanding of a solar tariffs because other contributing factors, such as load behaviour, PV system output and network service charges, have potential impact on the performance of solar schemes. The motivations of this thesis are to increase the understanding of VNM tariff by considering the above factors, and subsequently propose potential improvements. Furthermore, this thesis proposes an alternative to solar tariffs in order to share PV power where such solar tariffs are unavailable.

In this thesis an evaluation of VNM, FiT and NM was first developed using micro-economic models for the general comparison of the three widely applied solar tariffs in an Australian context. The results indicate that FiT generally provides the worst performance and VNM illustrates potential to be the best option, depending on the ability to minimize surplus credits.

To evaluate the impact of variations in building demand and PV system output on solar tariffs, this thesis developed several characteristic profiles of solar generation and load consumption using MATLAB simulations and analysis of real data. For the preliminary work, two types of Australian utility retail tariffs, time of use (TOU) and fixed-rate, were introduced to link the profiles to financial performance. The developed profiles of load demand and PV system output are also utilised for the financial evaluation of other solar tariffs such as VNM.

The research presented here on a credit based VNM tariff demonstrates that customer profiles with high peak load tend to provide a shorter payback period, and the percentage of VNM tariff participants also has significant impact on payback period.

It is also shown that the value of VNM declines with increasing surplus (un-allocated) credits. Thus minimizing surplus credits and adjusting participant composition could be two approaches to improve the financial performance of VNM tariff. In addition, the shared PV system of a VNM program is generally only sized by referring to the capacity of overall loads. This study develops several sizes of PV solar system to illustrate the impact of sizing the PV system has on a VNM project.

Service charges of transmission and distribution utilities associated with solar sharing, also called wheeling costs, are studied using an approach of tracing power flow and MW-mile method. The results indicate that the percentage of power shared is more significant to the value of wheeling charges than the distance the shared power passes through and the amount of shared power. It is also demonstrated how the value of wheeling costs are influenced by the installation location of the shared PV system, the methodology for allocating wheeling costs to end users and the profile of load demand.

The last component of this study proposes a conceptual network as an alternative to solar tariff for sharing solar in a small-scale installation. The simulated results indicate that the network can implement solar sharing without the support of utility tariffs and energy storage, but the irregularity and variation of daily PV system output significantly challenge the network operation. Consequently, a probability-based methodology is proposed to minimise the impact from PV system output variation.

The profiles of load demand and PV system output are identified as the most critical components to successful PV sharing schemes, however, further research into the behaviour of load demand and PV system output is required. In addition, the evaluation of wheeling costs associated with solar sharing is at the initial stage, so the verification of relevant achievements still needs further research.

ACKNOWLEDGEMENTS

To my parents who gave me the full supports to commence this research project and the thesis, to my supervisors who guided me to initiate the academic research and provided the direction and encouragement to complete my thesis.

TABLE OF CONTENTS

DECLARATION ii
ABSTRACT iii
ACKNOWLEDGEMENTS v
TABLE OF CONTENTS vi
LIST OF FIGURES x
LIST OF TABLES xiii
Chapter 1 Introduction 1
1.1 Background to sharing PV power 1
1.2 Research gaps 3
1.3 Purpose and scope 4
1.4 Objectives and contributions 5
1.5 Thesis layout 6
Chapter 2 Literature Review 8
2.1 Introduction 8
2.2 PV system performance and utilisation of PV power 8
2.2.1 PV system performance 8
2.2.2 Strategy of locally utilising PV power 10
2.2.3 Load behaviour 12
2.3 Precinct networks for sharing PV power 15
2.3.1 Stand-alone network 15
2.3.2 Utilising utility grid 18
2.4 Incentives for encouraging sharing of PV power 21
2.4.1 Feed-in tariff (FiT) and net metering (NM) tariff schemes 21
2.4.2 Community solar and virtual net metering (VNM) 25
2.5 Summary 31
Chapter 3 Comparison of Existing and New Tariff Schemes Using Microeconomic Model…….. 32
3.1 Tariffs for utilising PV power 32
3.1.1 Feed-in tariff (FiT) 32
3.1.2 Net metering (NM) 33
3.1.3 Virtual net metering (VNM) 34

3.1.4 Review of FiT, NM and VNM 35
3.2 Comparison of FiT, NM and VNM by microeconomic model 36
3.2.1 Microeconomics 36
3.2.2 Microeconomic models of FiT, NM and VNM 36
3.3 Results and analyses in different scenarios 39
3.3.1 Scenario 1 - no excess solar power 40
3.3.2 Scenario 2 - excess solar power exported and total generation less than load consumption 42
3.3.3 Scenario 3 - excess solar power exported and total generation more than load consumption 45
3.4 Summary 49
Chapter 4 Daily Profiles of Building Electrical Demand and PV System Generation Based on Australian Fixed and TOU Tariffs 51
4.1 Daily trends of building demand and PV generation 51
4.2 Evaluation of electrical demand and simulation of PV system output 52
4.2.1 Building daily demand 52
4.2.2 PV system daily output 56
4.3 Categorising daily profiles of building electrical demand and PV system outputs 59
4.3.1 The profiles of electrical demand 59
4.3.2 The profiles of simulated grid-connected PV system output 62
4.4 Profiles of building consumption and PV generation based on utility tariff…. ……64
4.4.1 Utility tariffs in Australia 64
4.4.2 Proportion of building consumption and PV generation under utility tariffs…… 66
4.4.2.1 Proportion of building consumption 66
4.4.2.2 The proportion of PV generation 74
4.5 Summary 78
Chapter 5 Economic Performance of VNM Based on Daily Trends of Building Demand and PV Generation 79
5.1 Financial evaluation of VNM 79
5.2 Establishing mathematic models 80
5.2.1 Cost of building consumption 81

5.2.2 Cost saving from VNM 83
5.3 VNM credits allocated to customer's bill 83
5.4 Financial evaluation 85
5.4.1 Payback period 85
5.4.2 Assumptions for case study 90
5.4.3 Evaluation under assumed 'pure' TOU schedule 94
5.4.3.1 Investigation for individual building 95
5.4.3.2 Investigation for a group of buildings 99
5.4.4 Evaluation under assumed 'hybrid' schedule 106
5.4.5 Reflective value 108
5.5 Summary 111
Chapter 6 Wheeling Cost Associated with Using Utility Grid to Share PV Power 113
6.1 Wheeling cost associated with sharing PV power 113
6.2 The methodology for evaluating wheeling cost 114
6.2.1 MW-Mile for wheeling cost evaluation 114
6.2.2 Generation matrix for tracing power flow 116
6.3 Demonstration on model LV network and evaluation 119
6.3.1 Model LV network and scenarios 119
6.3.2 Modelling result and discussion 123
6.3.2.1 Evaluation under Scenario 1 124
6.3.2.2 Evaluation under Scenario 2 131
6.3.2.3 Evaluation related to the profile of load demand 137
6.4 Summary 138
Chapter 7 Improvements Arising from The Application of Sharing PV Power ... 140
7.1 Solar tariff limitations 140
7.1.1 Pricing of FiT and NM for distributed generation projects 140
7.1.2 Addressing PV generation by VNM 141
7.2 A conceptual network for limitation breaking 141
7.2.1 Application range 141
7.2.2 Network structure and operation principle 142
7.2.2.1 Network structure 142
7.2.2.2 Utilisation of PCC voltage and reverse power for switchable loads control…. 143

7.3 Case study implementation 147
7.4 Challenges of the network operation and solutions 152
7.4.1 Challenges 152
7.4.2 Solutions 155
7.5 Financial analysis 160
7.6 Summary 162
Chapter 8 Conclusions and Future Work 164
8.1 Conclusions 164
8.2 Constraints and recommendations 166
REFERENCES 167
APPENDIX A Simulation Models of Grid-Connected PV System 177

LIST OF FIGURES

Fig. 2.1 Load profiles of domestic appliances: fridge, freezer, cooling, TV, microwave and others [22]. 13
Fig. 2.2 Comparison of the hourly PV output, building load [23]. 14
Fig. 2.3 Distribution flexible network [24]. 17
Fig. 2.4 Sharing PV power in radial LV distribution [30]. 20
Fig. 2.5 Community solar business models [38]. 26
Fig. 3.1 Scenario 1. 40
Fig. 3.2 Comparison under condition 1 - $p_{FiT, NM} = r$. 41
Fig. 3.3 Comparison under condition 2 - $p_{FiT, NM} < r$. 41
Fig. 3.4 Comparison under condition 3 - $p_{FiT, NM} > r$. 42
Fig. 3.5 Scenario 2. 43
Fig. 3.6 Comparison under condition 1 - $p_{FiT, NM} = r$. 43
Fig. 3.7 Comparison under condition 2 - $p_{FiT, NM} < r$. 44
Fig. 3.8 Comparisons under condition 3 - $p_{FiT, NM} > r$. 44
Fig. 3.9 Scenario 3. 45
Fig. 3.10 Comparison under condition 1 - $p_{FIT, NM} = r$. 46
Fig. 3.11 Comparison under condition 2 - $p_{FIT, NM} < r$. 47
Fig. 3.12 Comparison under condition 3 - $p_{FIT, NM} > r$. 49
Fig. 4.1 Annual maximum, minimum, average daily changing trend. 55
Fig. 4.2 Daily profile of electrical load demand changing of large hotel in per unit. 56
Fig. 4.3 Schematic diagram of grid-connected PV system [71]. 56
Fig. 4.4 Schematic diagram of stand-alone PV system [71]. 57
Fig. 4.5 Annual average curve of PV systems generation. 64
Fig. 4.6 Electricity charges for residential customer [75]. 65
Fig. 4.7 Electricity charges for business customer [75]. 65
Fig. 4.8 Transformed profile of load demand under fixed-rate tariff. 67
Fig. 4.9 Transformed profile of load demand under TOU. 67
Fig. 4.10 Annual percentage of energy consumed during the shoulder period over total daily energy consumption under TOU. 68
Fig. 4.11 Annual percentage of energy consumed during the off-peak period over total daily energy consumption under TOU. 68

Fig. 4.12 Annual percentage of energy consumed during the peak period over total daily energy consumption under TOU. 69
Fig. 4.13 Transformed profile of PV generation under fixed-rate tariff. 74
Fig. 4.14 Transformed profile of PV generation under TOU. 75
Fig. 4.15 Annual percentage of off-peak PV generation over total daily generation. 76
Fig. 4.16 Annual percentage of shoulder PV generation over total daily generation. 76
Fig. 4.17 Annual percentage of peak PV generation over total daily generation. 77
Fig. 5.1 Schematic of VNM [76]. 79
Fig. 5.2 Transformed profile of building demand under (a) fixed-rate and (b) TOU 80
Fig. 5.3 Transformed profile of PV generation under (a) fixed-rate and (b) TOU. ... 80
Fig. 5.4 Financial presentation of load profile under TOU. 82
Fig. 5.5 Assumed allocation of VNM credits. 84
Fig. 5.6 Assumed allocation of VNM 'left-over' credits. 85
Fig. 5.7 Three groups of buildings with different profiles of demand. 90
Fig. 5.8 Comparison of annual building demand and PV generation. 91
Fig. 5.9 Results of quick service restaurant. 96
Fig. 5.10 Results of stand-alone retail. 96
Fig. 5.11 Results of hospital. 97
Fig. 5.12 Results of assumed stand-alone retail. 99
Fig. 5.13 Results of Group 1. 100
Fig. 5.14 Results of Group 2. 101
Fig. 5.15 Results of Group 3. 101
Fig. 5.16 Results of Group 1 under full sizes of PV system. 103
Fig. 5.17 Results of assumed Group 2 under full sizes of PV system. 104
Fig. 5.18 Results of assumed group 3 under full sizes of PV system. 104
Fig. 5.19 Comparison of critical PV sizes. 105
Fig. 5.20 Comparison of payback periods – 40 kW PV system. 107
Fig. 5.21 Comparison of payback periods – 200 kW PV system. 107
Fig. 5.22 Annual reflective value of VNM credits of Group 1. 109
Fig. 5.23 Annual reflective value of VNM credits of Group 2. 110
Fig. 5.24 Annual reflective value of VNM credits of Group 3. 110
Fig. 6.1 Proportional sharing principle [19]. 117
Fig. 6.2 Segments of MV and LV residential distribution networks in Wollongong City. 119

Fig. 6.3 LV distribution network model. 121
Fig. 6.4 results with 22kW PV output. 124
Fig. 6.5 Results with 30kW PV output 125
Fig. 6.6 Results with 51kW PV output 126
Fig. 6.7 Results with 72kW PV output 126
Fig. 6.8 Results with 89kW PV output 127
Fig. 6.9 Results with 100kW PV output 127
Fig. 6.10 Integrated illustration of the above 6 groups. 131
Fig. 6.11 Results at B1. 132
Fig. 6.12 Results at B2. 133
Fig. 6.13 Results at B3. 133
Fig. 6.14 Results at B4. 133
Fig. 6.15 Results at B4(a). 134
Fig. 6.16 Results at B5. 134
Fig. 6.17 Results at B6. 135
Fig. 6.18 Daily illustration under scenario 2. 136
Fig. 6.19 Impact on typical arguments from load-demand profile. 137
Fig. 7.1 Structure of proposed network. 142
Fig. 7.2 Simplified equivalent circuit of sharing PV power. 144
Fig. 7.3 Daily change of excess solar power. 145
Fig. 7.4 Simulation of PCC reverse power and voltage. 148
Fig. 7.5 PCC voltage drop. 150
Fig. 7.6 Simulation of switchable-loads operation. 151
Fig. 7.7 Irregularity of PV generation. 153
Fig. 7.8 Comparison of P & V under different PV-generation profiles. 154
Fig. 7.9 Annual probability distribution of hourly step changes of PV generation. 156
Fig. 7.10 Annual probability density curve of hourly step changes of PV generation. 157
Fig. 7.11 Payback period under different kW of excess solar power. 161
Fig. A.1 Integrated model of PV systems output 177
Fig. A.2 Model of cell temperature 177
Fig. A.3 Model of PV systems AC output 178

LIST OF TABLES

TABLE 3.1 Notations 37
TABLE 4.1 Year-round daily trend of electrical load demand of large hotel. 53
TABLE 4.2 Daily electrical load consumption in kW and per unit. 55
TABLE 4.3 Daily profile of building electrical load demand of 15 categories of buildings. 59
TABLE 4.4 Year-round daily profiles of grid-connected PV system. 62
TABLE 4.5 Proportions of load consumption of the fifteen categories of buildings. 70
TABLE 4.6 Transformed profile of load demand of the fifteen categories of buildings. 71
TABLE 5.1 Variables. 81
TABLE 5.2 Types of VNM in Australia. 87
TABLE 5.3 Potential sizes of the shared PV system. 92
TABLE 5.4 Daily consumption of individual and group of building(s). 93
TABLE 5.5 Potential sizes of the shared PV system with normalized daily consumption by 34.17 kWh. 93
TABLE 5.6 Summary of assumed sizes of shared PV system with different daily... 94
TABLE 5.7 Summary of assumed sizes of shared PV system with normalized daily consumption. 94
TABLE 6.1 Assumptions related to power flow. 120
TABLE 6.2 Daily change of PV generation. 120
TABLE 6.3 Daily change of residential-building load demand. 121
TABLE 6.4 Daily change of office-building load demand. 121
TABLE 6.5 Financial assumptions and calculated results. 122
TABLE 6.6 Notation of testing parameters. 124
TABLE 6.7 Proportion of load consumption. 138
TABLE 7.1 Assumptions of case study. 147
TABLE 7.2 Assumed economic issues. 160

Chapter 1 Introduction

1.1 Background to sharing PV power

The utilisation of PV systems has rapidly expanded in the global renewable energy market in recent years. This is because solar energy is more accessible than other renewable resources, and the price of PV modules has significantly declined since 2009 [1, 2]. On the other hand, individual focused PV installations shut the door to a large number of potential solar power consumers. For example, in the U.S., only 25% of owner-occupied properties, i.e. 67% of total households (80 million), are well suited to PV installations, and the remaining 33% of households are composed of renter-occupied properties (43 million units) [3]. In Australia, tenants and low-income earners often feel being stuck with high electricity bills because they have ownership-issued and monetary obstacles to use solar power [4]. The cost of installing individual PV systems, space limitations, poor roof orientation, shading from trees and structures, and the ownership are the main barriers for further expanding home solar PV projects. Commercial scale solar faces a similar situation due to the ownership requirements and geographical constraints for installing on-site PV systems.

In order to overcome aforementioned obstacles, solar power sharing has been advocated and implemented in recent years. For example, a group of investors installed a shared PV system with 115 solar panels on the rooftop of Young Henry's Brewery in Newton Sydney, Australia, and it is estimated that the investors will receive a return of 5 to 7 per cent on the investment [4]. To understand and utilize well PV power sharing, a number of research and prototype projects have been developed. A distribution system is required for sharing solar in order to transport locally produced power from one party to another. The distribution system can be achieved by either building up a separate local network or utilising the existing utility grid. The additional costs for establishing a separate network is often more of a financial burden than using the existing grid, i.e. using the grid is normally the more cost-effective option for solar sharing programs.

Government and utility policies must offer financial and administrative support for solar sharing schemes when utilising the grid to distribute PV power. Currently, shared PV-generated electricity can be either sold to the utility or a third party, or rolled over into the electricity bills of participants of a solar sharing program. Therefore, how to price the fed-in solar power or how to treat the rolled-over kWh credits has to be scheduled by relevant policies or utility tariffs. Furthermore, the technical issues such as the size of the shared PV system, the connection conditions and connection of metering systems also need to be regulated and guided. In response to addressing the financial and administrative requirements, some utility renewable (or specific for solar) tariffs were developed such as feed-in tariff (FiT), net metering (NM), net purchase and sale, community solar, and virtual net metering (VNM). However, some of the tariffs like FiT and NM have become inadequate for the increasing requirements of solar sharing programs. By contrast, later-developed solar tariffs or schemes such as community solar and VNM have become more advocated in the solar sharing market due to their improved performance.

In the U.S. 101 community solar projects and 108 MW (cumulative) have been installed. In addition, 26 states and the nation's capital territory had community solar programs active in 2017 [5]. It is forecasted that community solar programs will be implemented across the U.S. as awareness grows. In Australia, there have been around 40 community solar projects installed or launched in some regions or states, and it is presented that the participants can use the electricity generated by the community solar projects for their family loads consumption. For example, in Goulburn community solar farm, a shared PV system with more than 5000 solar panels has the capacity to power 400 homes, and each investor participating this project owns at least one solar panel [4, 6]. However, it is currently hard to find relevant reports and studies about PV power sharing projects and the utilisation of community solar and VNM in China. A comprehensive investigation into VNM and other solar tariffs is still required to improve the financial and technical performance of solar schemes and subsequently expand the benefits of solar sharing to a larger amount of potential PV-energy consumers.

1.2 Research gaps

A solar sharing program generally includes four critical components: a power source (shared PV system); shared-energy consumer (participant's loads); a distribution network (utility grid); and policy support (utility tariff). The variation of each component would influence the performance of a solar sharing program. PV system output changes with the variation of weather conditions, such as irradiation, temperature and cloud shading, during the daytime. PV system output is zero at night time and early morning due to zero or low-level sun insolation. For a building, load demand varies along with time due to the variation of occupant activities. For different categories of buildings such as residential buildings, commercial buildings, education buildings, and hotel buildings, the load demand will generally have various patterns because of the different designs for electrical and mechanical systems based on the corresponding building functions and variable occupant activities. In addition, it is argued that wheeling costs associated with solar sharing should be charged by utilities (distribution network service providers). The addition of wheeling charges would impact the financial performance of solar sharing programs. Utility solar tariffs have direct influence on the revenue of the owner(s) of a shared solar system and the economic benefits of the participants. Furthermore, government or utility policies also function to manage and regulate solar sharing schemes. It is obvious that a comprehensive study on solar sharing must consider all the above aspects.

Although a number of studies have been completed on the technical issues of solar power sharing, little work considers the variation of building consumption and PV generation in the relevant research. Previous research on wheeling costs are applied solely to transmission level systems, and some studies have mentioned that a type of network service fee should be charged for using the grid to transport solar power at distribution level. Few studies contribute investigations and assessments in detail for the wheeling costs associated with sharing PV system power. As to the studies on utility solar tariffs, a majority of them focus on the policies and financial issues. However, the behaviours of PV systems output and load demand could have significant impact on the performance of a solar sharing tariff. This remains unanswered due to few studies considering the variation of PV generation and load

consumption in the evaluation of solar tariffs (a detailed literature review is presented in Chapter 2).

The main research gaps driving this research can be summarised as follows:

- There is a large degree of mismatch between solar-based renewable energy generation and building load profiles, and the mismatch can financially cause appreciable positive impacts on sharing power schemes. Identifying ways to reduce this mismatch and the consequent financial loss to implementing solar sharing schemes is an ongoing area of the research.
- Wheeling costs should be charged for sharing solar power via utility grid, but it is short of relevant investigation and assessment in detail. Establishing a study model of evaluating the wheeling charges associated with solar power sharing will be constructive for the practical application of wheeling charges to PV generation sharing schemes.
- Utility solar tariffs require the behaviour of building load demand and PV generation variation to be considered, there remains opportunities to enhance how such schemes or tariffs reward each of the parties (utility, generation owner, building owner, energy consumers).

1.3 Purpose and scope

As aforementioned, the variation of PV system output and load demand have impact on the financial performance of solar sharing tariffs, and VNM has received significant attention due to its potential for expanding the utilisation of solar power. Therefore, the purpose of this study is to evaluate VNM and the associated wheeling costs from a new perspective – with the assistance of the profiles of PV generation and building consumption to study the solar tariff.

In order to achieve this purpose, this study firstly compares three utility solar tariffs FiT, NM and VNM in terms of financial performance. Subsequently, profiles of PV generation and building consumption are developed for the detailed evaluation of VNM. To establish wheeling costs this study introduces two methodologies used to evaluate transmission and distribution services associated with solar power sharing. In addition, case studies are applied to the investigation and evaluation of VNM and the

associated wheeling costs. A conceptual small-scale network for solar power sharing is proposed and evaluated in response to the unavailability of utility tariff support, and case studies are also used to investigate the technical and financial issues of the proposed network.

1.4 Objectives and contributions

Through this study, four aspects of objectives and contributions are achieved. The first is the identification of a tariff with improved financial performance in terms of revenue brought to end users among FiT, NM and VNM. This evaluation is developed under several assumed scenarios, which are set based on daily PV generation and building consumption, utility retail rate, and purchase price for fed-in solar energy. Microeconomic models are used to evaluate the potential monetary profits customers achieve by subscribing to a solar tariff.

Second, the evaluation of financial performance of VNM considering the profiles of PV generation and building consumption has been developed. The contribution includes the investigation on the correlation of payback period of the investment for a VNM solar system and the variant patterns of building consumption, variation in sizes of the VNM shared PV system, and the assessment of VNM allocated credits.

Third, the evaluation of wheeling costs associated with solar power sharing has been presented. The contribution includes the allocation of a suitable cost structure for wheeling charges raised by solar sharing using the MW-mile approach. Example implementation of wheeling costs associated with solar sharing on a typical precinct LV feeder, which is equally applicable to MV radial networks, is established. The analysis includes determining correlation between the extent of utilising utility grid, and the profiles of building consumption, with wheeling costs.

Fourth, a conceptual small-scale local network has been proposed. This proposal contributes an alternative of utility tariffs to sharing potential excess solar generation, and has advantageous application for maximising utilisation of locally generated solar power without the support of energy storage and utility solar tariffs.

In conclusion, the contributions made by this research can be summarised as follows:

- Identifying which tariff among FiT, NM and VNM can bring the best revenue to end users under several common scenarios related to PV generation, load consumption and utility retail rates, etc. .
- Evaluating financial performance (pay back periods) of VNM with considering the profiles of PV generation and building consumption.
- Evaluating wheeling costs associated with solar power sharing with the application of MW-mile approach.
- Proposing a conceptual small-scale local network as an alternative of existing utility tariffs to sharing potential excess local-generated solar power.

1.5 Thesis layout

This thesis is organised as follows:

Chapter 2 reviews previous research related to the technical, financial and policy issues of solar sharing including the evaluation of PV systems performance and building load behaviour, strategies for local utilisation and precinct sharing of solar power, and utility solar tariffs.

Chapter 3 develops comparisons of financial performances of three existing utility solar tariffs as FiT, NM and VNM by using micro-economic models. The financial evaluation focuses on the profits brought to end-users by subscribing to solar tariffs.

Chapter 4 investigates daily trends of PV system output and building load demand. The profiles of PV generation and load consumption of 15 categories of buildings are established by software simulation and data analysis. The achieved profiles were further evaluated by using Australian utility tariffs.

Chapter 5 evaluates the economic performance of VNM by considering the profiles of PV generation and building consumption. The chapter includes analysis on the correlation of payback period and profile of building consumption, the correlation of payback period and utility electricity tariff, and an assessment of the value of VNM allocated credits.

Chapter 6 investigates and assesses wheeling costs associated with solar power sharing. The evaluation of wheeling costs and related issues is undertaken using a

combined MW-mile and tracing power flow approach, and includes analysis on the correlation of wheeling costs and profiles of building demand.

Chapter 7 proposes a conceptual small-scale network for sharing solar power. The analysis on the voltage and the reverse power at the point of common coupling and the related financial evaluation are included.

Chapter 8 provides conclusions of this study and recommendations for future work.

Chapter 2 Literature Review

2.1 Introduction

As one of the most common technologies utilising renewable resources, solar PV has been globally utilised, and solar schemes and tariffs have been correspondingly designed to support the utilisation of PV power, such as feed-in tariff (FiT), net metering (NM), net purchase and sale, etc. However, recent research has demonstrated that community or group-based solar programs are more economical and practical than individual solar PV tariffs like FiT and NM. There have already been several methodologies developed for sharing PV-generated electricity in precinct or in multi-tenant buildings. Community solar and virtual net metering (VNM) are examples of such schemes, and in the USA, they have been widely applied to overcome the barriers involved with FiT and NM. By contrast, there had been few applications of VNM till 2013 in Australia. Research into VNM for sharing PV power and related technical and financial issues is required to meet increasing energy demand and alleviating environmental crisis.

Through the literature review of previous relevant studies, three main research areas have been identified in terms of the utilisation of PV systems: (i) evaluation of PV system performance and local utilisation of PV power; (ii) technology serving precinct-level PV power sharing; and (iii) utility tariffs and government policies for the utilisation of solar power. The following detailed review is provided on these topics.

2.2 PV system performance and utilisation of PV power

2.2.1 PV system performance

The studies on solar systems performance aim to evaluate or predict PV systems output and help understand influence factors to PV generation. The influence factors of PV system performance include related equipment efficiencies and weather conditions, noting the latter is more critical when developing predictions of PV system

performance [7]. A set of models for evaluating daily solar generation was developed in [7] as Solar Advisor Model (SAM) including a comparison of predicted and actual measured solar generation. The hourly meteorological and irradiance parameters were measured as the inputs to the models for radiation, module performance and the inverter. The comparison showed that inverter and radiation models are very reliable, with only 1-2% disagreement to measured results. The module performance model had a significant disagreement of 5-11%, the reason for which is suggested as being a material-issued matter.

As [7] shows, weather conditions are the fundamental inputs for all developed models. In addition, the evaluation of PV module performance is more complicated than inverter and irradiation, and consequently there is significant research specifically focused on the performance of the PV module. Developed solar module models are commonly based on a function of irradiance and temperature [8-10]. In general, studies either separate the PV system into several components or specifically focus on one component. For the work in this thesis a fragmented evaluation model will make application more complex. In order to investigate utilisation of solar power and related issues, a methodology for evaluating the complete PV systems is required.

An approach to simulate solar generation is outlined in [11] which provides a formula for AC output of the PV inverter with consideration of inverter efficiency and resistance of DC cabling. Meteorological data as radiation and ambient temperature was included from an online database called SoDa. In [11] the simulated and actual annual generation output of a PV system, installed in two locations with different weather conditions, are compared. While undertaken in only two locations due to funding limits, the developed model proved reliable [11]. For the evaluation of PV generation, dirt loss and array loss caused by mismatched modules are two non-negligible coefficients to consider in conjunction with inverter loss and resistance of cabling [12, 13]. The model outlined in [11] could be improved with consideration of these additional loss coefficients.

In conclusion, several simple holistic models based on the most significant considerations of PV system operation are available to evaluate PV systems performance. This is the preferred approach, instead of modelling individual

components. A comprehensive consideration for relevant loss factors is required to achieve reliable evaluation of solar generation.

2.2.2 Strategy of locally utilising PV power

In terms of local utilisation of PV power, the application of energy storage is always one of hot topics. Batteries have been employed for most stand-alone PV systems to store excess PV-generated electricity and subsequently release it when needed [14]. Besides storing excess solar energy, the application of energy storage in PV systems also can have a positive influence on environmental and economic considerations for both stand-alone and grid-tied systems [15]. The study in [15] used two economic indicators, net present cost (NPC) and cost of energy (COE), and two environmental factors, renewable fraction (RF) and greenhouse gas (GHG), to evaluate the implication of employing energy storage. By comparing PV systems integrated with and without storage, it is demonstrated that storage helped significantly with reducing GHG emission, decreasing COE and NPC, and improving RF.

The intermittent nature of PV system output is one of the concerns for stable power supply to loads. In [15] strategies combining alternative generation sources, such as diesel generator, fuel cell, etc. with PV systems, were developed and evaluated for making up the difference between solar generation and load consumption. Hybrid power systems are a solution to addressing the intermittent nature of PV systems output. [16] developed a network integrating PV solar, fuel cell, battery and super capacitor to supply on-site loads. In [16], all power sources and storage device are coupled to a common DC bus, and the load can either be the DC load or the voltage source inverter (feeding power back into grid). The simulation results demonstrate that the hybrid power system was effective in meeting a high degree of power availability and reducing cycling of the battery. It is obvious that a control strategy must be required for the operation of such a hybrid system to incorporate different components, and the size match of power sources and storage is another concern for a technologic and cost-effective operation, which were not included in [16]. In addition, the system was developed based on DC system, so the practicability of the hybrid network for AC load still needs to be further studied.

In [17], a PV micro-grid system was built in Naresuan University of Thailand. Normally, controllable generation source, such as fossil fuel, biomass, biogas, is used in micro-grid system for uncomplicated control. The application of uncontrollable energy resource, such as solar PV, in micro-grid system is a challenge for the control of micro-grid system. The data collection of the studied PV micro-grid system demonstrates that PV generator works well in this micro-grid system, and it meets more than 50% of total monthly load demand in every month except in August, which is caused by the rainy season. On the other hand, this study claims that a comprehensive control strategy must be carefully designed for a decent performance of PV-solar generator in micro-grid systems. It can be seen that the utilisation of micro-grid system could be inapplicable for residential building or other clients with such cost-issued or space-constrained matters by the comparatively high requirements of configuration and control. For a simplified utilisation of PV systems, [18] used a grid-tied PV system and back-up battery with load management to supply a residential client. The loads involved were divided into time manageable, storage capable and the non-manageable, and load management displaced the time manageable and storage capable loads from evening hours to PV generation hours to increase self-consumption by up to 50%. Battery energy storage is still required for grid-tied PV system to achieve complete self-consumption.

From the above studies, energy storage is popularly used for either stand-alone or grid-tied PV systems. However, the high environmental footprint caused in manufacturing process, the sensibility related to weather conditions and financial issues, to some extent, still limit the extensive utilisation of batteries. In addition, it is obvious that the complex configuration of multiple generation sources and storage and complicated control strategy are not practical for residential clients and commercial customers with cost-issued or space-constrained matters.

For the utilisation of a grid-tied PV system without battery, which has the most simplified configuration and control among the existing strategies of utilisation of solar PV systems, the effect of compensating utility energy usage is significant, and the cost saving from utilising the on-site solar power is completely dependent on utility tariff and weather conditions [19]. This study in [19] demonstrates that the solar power reduced daily utility energy consumption by 28%, if solar power directly supplied on-

site loads instead of feeding overall generation back to utility. However, a payback period of 25 years by this method was 11 years longer than selling overall on-site solar generation to the utility directly, in the specific context of that study. In addition, it was shown that the variation of weather conditions, such as the temperature and irradiation, resulted in significantly varying revenues.

As [19] demonstrated, the financial profits from the application of grid-tied PV system without battery, except for the influence of weather conditions on PV generation, is completely depending on the local utility tariff, and consequently an investigation into solar tariffs is required for comprehensive evaluation of PV power.

In terms of the technologic issues of grid-tied PV system, [20] completed a review study. It is pointed out that grid-tied PV systems still need to address the intermittent nature of solar generation, and this will become more significant with an increasing percentage of renewable-generation in power systems. In addition, grid-tied PV systems have advantages that stand-alone systems do not, such as low-cost financial requirement, easy control and simple configuration for both end users and utilities. It should be noted that all the above studies do not include the evaluation of load demand, which could have significant impact on successful application of PV systems, as building load is closely associated with the strategy of local utilisation of solar power, which is implied by [18].

2.2.3 Load behaviour

Energy demand of buildings is non-linear, and it is very difficult to predict with accuracy, which itself has become a popular research area. In terms of building category, non-residential buildings, such as education buildings, commercial buildings and company facilities, make up a large proportion of building stock. Therefore, the investigation into non-residential buildings would significantly contribute to comprehensively understanding building-load behaviour. For non-residential buildings, weather conditions have smaller influence on load demand profile than the occupants' activity inside the building [21]. [21] used 'the work day schedule' to classify load curves as the week-day, the-Saturday and non-work day, which was developed based on the Sunday profile. It is claimed the non-linearity of load profile is directly related to occupant activities on different types of days, which can be

covered by 'the work day schedule'. It can be seen that the methodology applied by [21] includes two key properties, historical data and classification based on the day type. It is also pointed out that the load data is susceptible to evolving over time. [21] only tested five-day forecasting based on the historical data statistics. However, the application of long-term historical data and the long-term forecasting based on historical data are different issues, and that study does not indicate the time range of the applied historical data. In general, the longer the period of data collection, such as year-round, the more reliable and meaningful the evaluation.

[22] proposed an approach to emulate electrical load consumption of buildings, and it is demonstrated that this approach had very good performance with 0.15~0.85% error between the simulated hourly results and the referenced results achieved by an existing tool (Energy Plus). Two fundamental elements used to build up the models are load profile of electric devices, and equipment and building load distribution. The models are finally achieved by aggregating the load model of each electric appliance based on the structure of the building load distribution system. It can be seen that the load profile is the most fundamental input to the proposed model of building energy consumption.

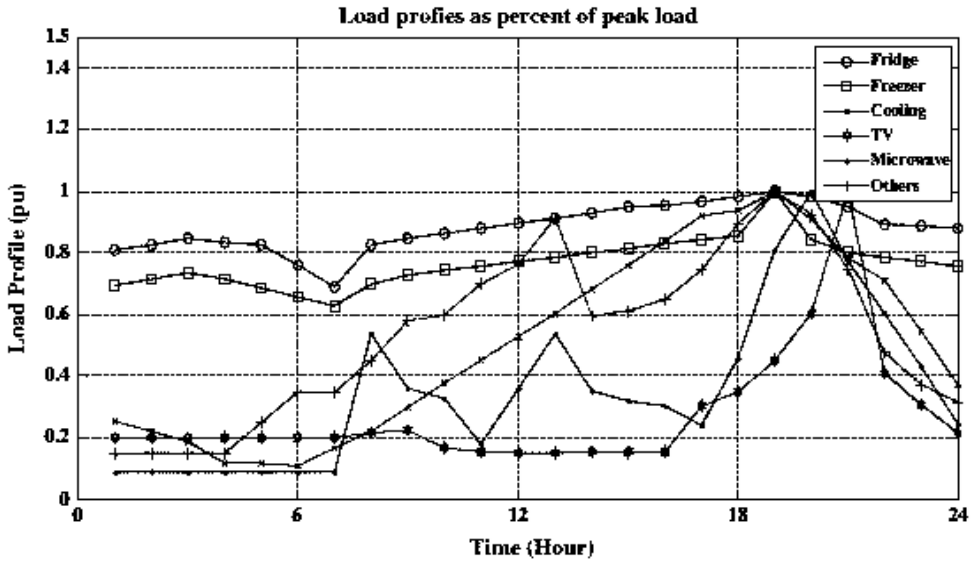

Fig. 2.1 Load profiles of domestic appliances: fridge, freezer, cooling, TV, microwave and others [22].

Fig 2.1 illustrates the load profiles of domestic appliances used in [22]. It can be seen that the load data is presented by the percentage of its peak hourly consumption, and the load consumption is time varying over 24 hours. If known, the load profile in

percentage can be directly inputted to the model, else data such as that available from Electrical Power Research Institute (EPRI), as used in [22], or hourly energy consumption of loads may be introduced from public databases. This approach can be applied to residential buildings and small non-residential buildings. For large buildings, the application of this approach would be impractical due to the vast workload to investigate large numbers of electric appliances and facilities. However, the methodology employed by presenting load consumption as a percentage is a useful tool for the evaluation of building energy consumption.

In order to comprehensively evaluate the utilisation of PV power, the investigation only focusing on one aspect of load behaviour and PV system performance is not enough, and an integral study of PV systems output and building load demand is required. [23] presented an example to evaluate PV generation considering building energy consumption. This study used a computer program, Energy-10, to simulate PV generation based on a realistic building. It is pointed out that if an investigation is only interested in sizing a PV system, and then only a calculation for load demand is enough to achieve that. However, if the correlation between PV generation and load consumption is the objective of a study, then an integral analysis for both PV system and building load is required.

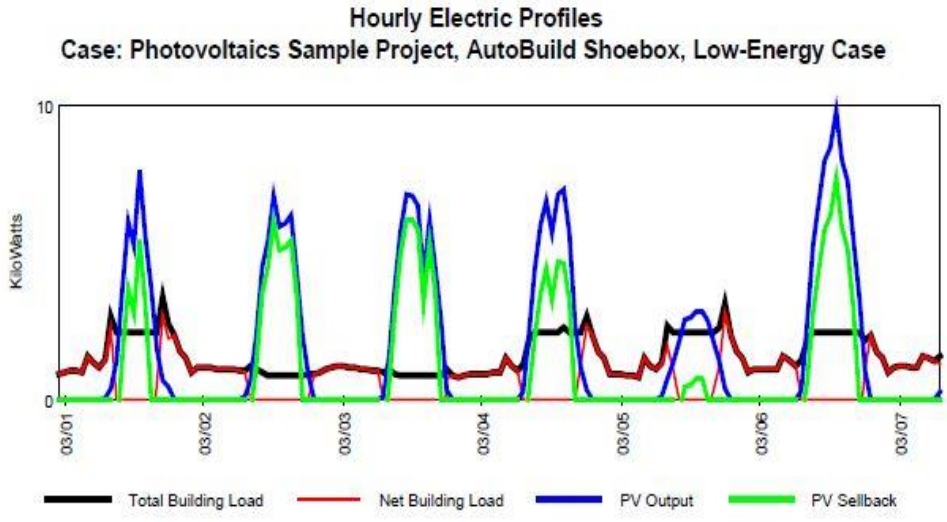

Fig. 2.2 Comparison of the hourly PV output, building load [23].

From Fig 2.2, the hourly load demand, PV system output and PV sellback are presented. Through the illustration, the exact situation about when solar power is generated in relation to when it is needed, when the peak demand occurs, and when

the system feeds excess solar power back into the grid, can be clearly identified. The comparison study of PV system output and load demand is obviously helpful to design a PV system more matching to local demand. In addition, this methodology simultaneously considering PV systems output and load demand has real significance for the comprehensive evaluation of utilising solar power, which could be applicable for studies on solar power sharing and related financial analysis.

In summary, the profiles of PV systems generation and of building load demand are significantly different, which were separately presented by [7]-[11] for PV generation performance and [21]-[23] for load behaviour. It is commonly understood that the mismatch between solar-based energy generation and building load demand financially impacts the implementation of sharing power schemes due to the incomplete utilization of shared solar power the mismatch caused. Therefore, the identifying the potential ways to reduce the mismatch and the consequently financial loss for implementing solar power sharing schemes, which is investigated and evaluated by few previous studies, is one of motivations driving the research.

2.3 Precinct networks for sharing PV power

2.3.1 Stand-alone network

Solar power sharing can more widely spread the environmental and financial benefits of the utilisation of renewable resources compared to local only utilization of PV power. For example, sharing solar power can make more customers, who previously do not have access to install own solar systems due to space or cost-issued matters, consume renewable-generated electricity. In order to share solar power, a network, which can be separately built or take advantage of the existing utility grid, is a fundamental requirement. In terms of using grid, voltage rise and reverse power are two inevitable issues, and the restriction of voltage rise and reverse power caused by the penetration of PV systems in utility distribution network is always a hot topic. Separating from or not connecting to the utility grid, often called stand-alone network, is a solution to solar sharing and simultaneously avoids the propagation of voltage rise and reverse power on the utility grid. A proposal of stand-alone network configuration is provided in Fig. 2.3 (a) to (c) [24].

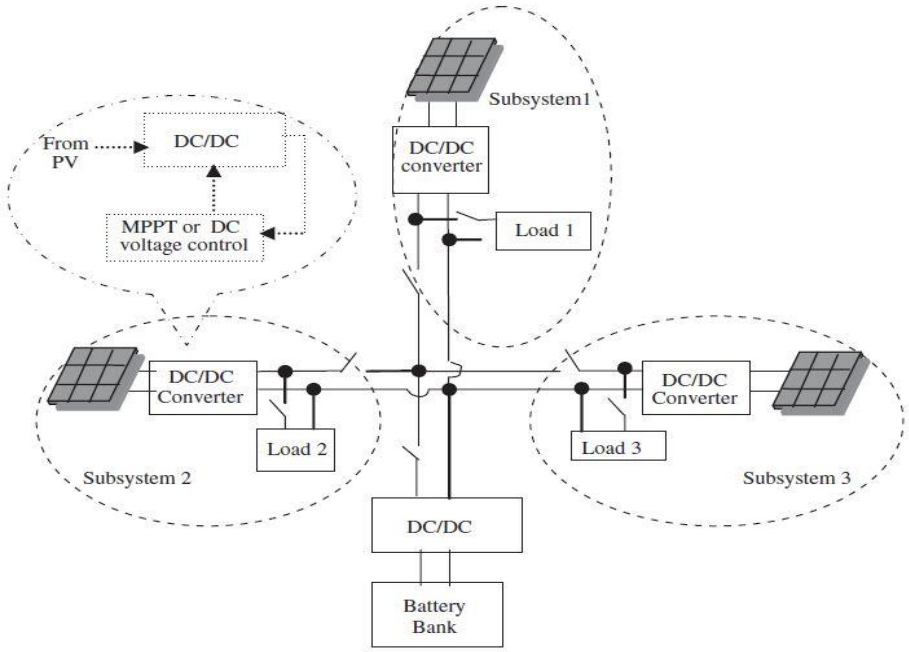

Start network (a)

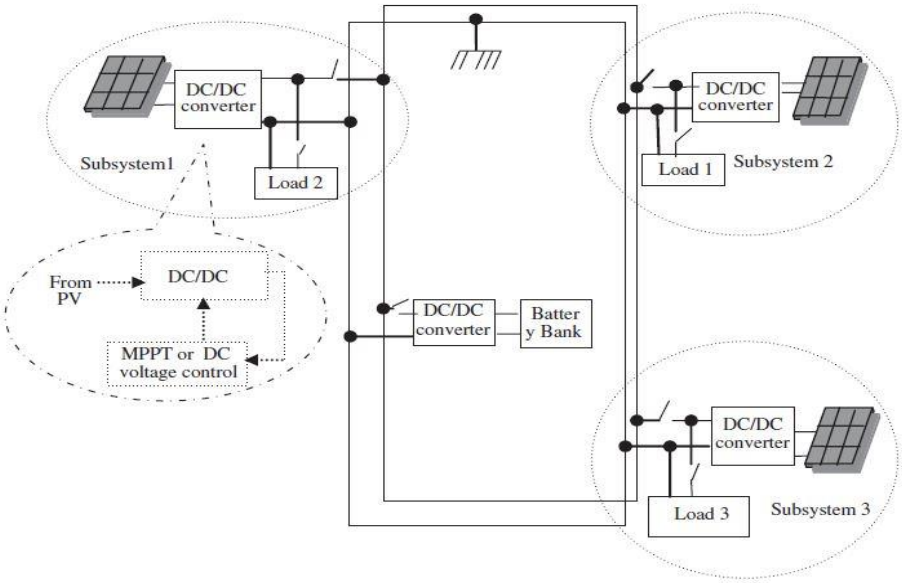

Loop network (b)

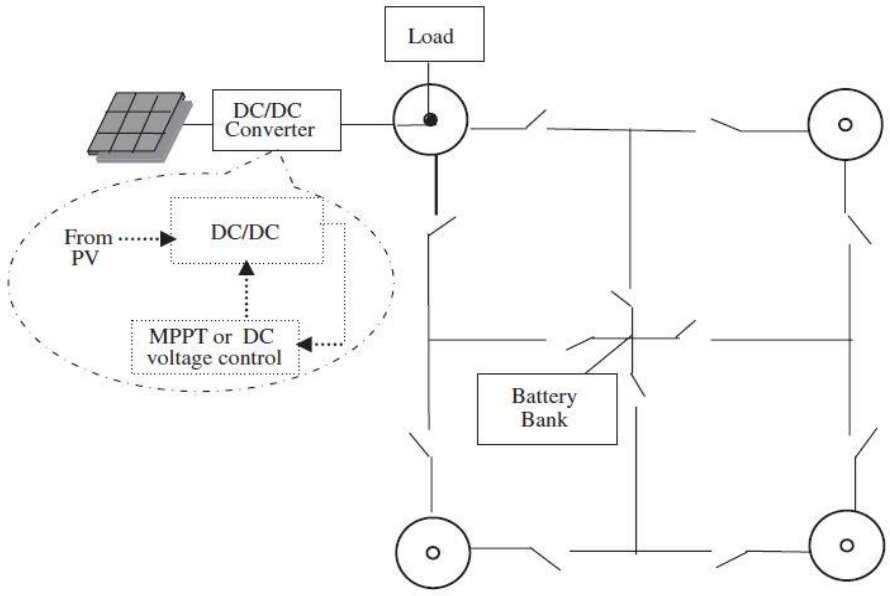

Meshed network (c)

Fig. 2.3 Distribution flexible network [24].

As Fig 2.3 shows, three alternative network configurations are provided, and it is stated that the selection of optimal configuration should depend on the attributes such as location, cost, and loads. However, it can be seen that the three configurations have a common system composition as several sub-PV systems, and a shared battery bank. It is noted that each stand-alone sub-PV system only has PV panels, a DC/DC converter, and the network has a shared energy storage device instead of distributed battery for each sub-system. Sub-PV systems are connected to each other by extra-built network, and the distributed switches operate to isolate the local breakdown from the network. The sub-PV systems can either mutually compensate local load usage or charge the shared battery bank. When demand is higher than the on-site PV generation, either the shared battery bank or other sub-solar systems with excess power can meet the increasing demand. It is clear that the proposed network can reduce the cost of energy storage because of only a battery bank configured instead of several distributed battery devices. In addition, the excess PV power used by local self-consumption is maximised. The network results in an extension of battery lifespan due to decreased charging and discharging.

It should be noted that the concept network from [24] operates at DC voltage, so the applicability for AC loads needs further study. In addition, battery bank is the only power source during PV generation unavailable hours, so the size of the shared energy

storage device and how fully it is charged are the concerns to meet overall load demand for several hours. Furthermore, cable loss constrains the scale of the network (load capacity) and needs to consider limit of voltage drop. In terms of the financial issues, the investment in cables and laying would be a considerable additional cost, which is not assessed by this study. In conclusion, the lack of backup power, constraints on voltage drop, and extra costs for building up an independent network are common limits to the utilisation of a stand-alone network.

2.3.2 Utilising utility grid

The above-analysed limits of stand-alone network do not exist when using utility grid for solar sharing. However, power sharing and restraining reverse solar power are mutually contradictory under the scenario of using the grid, and consequently a balanced solution is required for both implementing power sharing program and satisfying the upper limit of reverse power and voltage rise defined by related codes or regulations.

As to the incidence of reverse solar power, [25] demonstrates that consumer composition in terms of the categories of buildings has impact on the restraint of reverse power of distributed grid-tied PV systems. A 1 km^2 distribution grid in Australia was selected to evaluate the potential reverse power of distributed PV systems by using the profile of measured household demand and simulated commercial-building demand. The results indicate that it could be advantageous to support and give priority to decentralized PV systems development in the area with less households and more commercial consumers, because commercial loads absorb more on-site PV generation than household loads with the same capacity, which results in lower potential reverse flow of distributed solar PV systems. [25] also evaluated the correlation of load profile and reverse power, and demonstrated the consumer composition is one of the critical factors, which is often neglected by related studies, for the successful deployment of distributed grid-tied PV systems. It should be noted that the consumer composition in terms of the categories of buildings is comparatively fixed for a developed precinct area. In this scenario, an alternative method for the reduction of reverse power of PV systems by improving end user's relevant performance must be expected.

Energy management as an approach for end consumers to mitigate reverse power and voltage rise at the point of common coupling point of grid-tied PV systems has been evaluated by a number of studies. [26] proposes an energy consumption scheduling algorithm to shift the operation of deferrable loads from peak consumption hours to high PV-generation hours for a potential maximal self-consumption. Voltage rise and resulted potential extra cost were used as the indicators to show the technical and financial performance of the proposed algorithm. [27] developed a HVAC load direct activation algorithm, which operates depending on a real-time voltage signal. When a voltage rise is detected, the idle HVAC load such as water heater would be activated to consume the potential reverse power. [28] uses a supply and demand interface (SDI) to control the connection and disengagement of loads and other devices, and battery to mitigate the reverse power of on-site solar PV systems. In this study, SDI activates heat pump water heater, which is normally operated at night due to the low price of utility electricity, when PV generation is increasing up to an operation value. If reverse solar power still remains, the battery is subsequently controlled by SDI to be charged by the left-over power.

From [26-28] it can be seen that load management may be implemented by various means, but the operating principle is to increase self-consumption and consequently reduce reverse power. No matter which type of load management methodology, the user must have deferrable loads and a battery is usually applied to completely eliminate reverse power. Another option for load management is deferrable load. Common deferrable (controllable) loads include water heater, water pump, ice making equipment and storage devices. The application of deferrable loads is limited for normal household energy consumers. For non-residential consumer, the deferrable load normally takes a comparatively low proportion of total electric load. Space and cost issues associated with the utilisation of energy storage for reverse power reduction is another barrier for the consumers. Therefore, there is limited application available for deferrable loads.

The restriction of PV system output is an alternative to load management for reducing reverse power flow. [29] compares the approaches of restriction of PV system output and load management. The results from [29] indicate that load management is more effective. It is pointed out that PV system output restriction, which is normally realized

by curtailing grid-tied inverters or completely disconnecting them from the grid, is actually a waste of renewable generation and equipment investment, and it would also cause a loss of potential revenue to the owner of the PV system [30].

In order to implement mitigation of reverse power and voltage rise caused by increasing penetration of PV systems, a balanced solution via solar power sharing and restriction of reverse power and voltage rise is required, however few studies address this.

A methodology for distributed grid-tied PV systems to share solar power via an LV radial distribution feeder, considering the upper limit to voltage rise in the Australian context is proposed in [30].

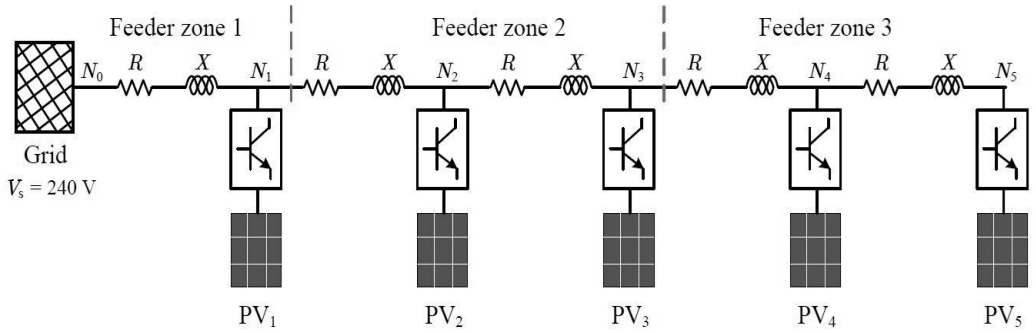

Fig. 2.4 Sharing PV power in radial LV distribution [30].

In a radial LV network, the voltage sensitivity is often highest at the end of feeder, e.g. node N_5 in Fig. 2.4. The maximum voltage that PV systems may stay connected is 230 V+10% (253 V) as defined by AS 4777.2 – 'Grid Connection of Energy Systems via Inverters – part 2: inverter requirements, Australian Std.'. It is understood that the voltage U_{N5} at node N_5 must thus be equal or less than 253 V. When this occurs, the other node voltages were calculated by [30] as 244.4 V, 247.8 V, 250.4 V and 252.1 V for nodes N_1 to N_4, respectively. The allowable injected PV power based on the achieved voltages was also calculated as 2.69 kW for each distributed PV system (PV_1 - PV_5). It can be seen that this proposed methodology pre-sizes each distributed grid-tied PV system by limiting the node voltages, and consequently balances solar sharing and restricts voltage rise. This study does not consider the variation of load consumption and solar generation, which must have impact on the node voltage value due to the net fed-in solar power changing.

In summary, utilising utility grid for solar sharing must consider the mitigation of reverse power and voltage rise, and self-consumption is the most critical approach to achieve that. In addition, the utilisation of grid does negate the need to build up extra network, and the configuration and control system are much simpler than stand-alone networks, as shown by [30]. The advantage of stand-alone network cannot be neglected, such as complete isolation from grid without the issues of reverse power and voltage rise. Therefore, a potential network combining both utilisation of the grid and stand-alone networks, could be worth studying to identify options for implementing solar sharing.

Moreover, wheeling charges should be applied when using utility grid to transport locally-generated solar power in realistic project, but it is always ignored or omitted by the relevant studies for the network of sharing solar power, such as [25]-[30]. Therefore, the evaluation of wheeling costs associated with PV power sharing by modelling a utility LV network, which is similar as [30] presenting, will be needed for the practical application of wheeling charges to PV power sharing schemes.

2.4 Incentives for encouraging sharing of PV power

As Section 2.3 demonstrated, solar sharing can be achieved by using stand-alone or utility grid. Stand-alone networks are invested into by users and are independent of the grid, and consequently the related financial and administrative agreements would be settled by the users themselves. However, using the utility grid requires the support of utility tariffs to value shared power and implement associated management and financial arrangements. The following view is around several existing popularly-applied utility tariffs.

2.4.1 Feed-in tariff (FiT) and net metering (NM) tariff schemes

FiT is designed to incentivise the deployment of the renewables technologies by subsidising investors. The renewable technologies applied to FiT normally include solar PV, wind, geothermal, hydro energy and biomass. The intermittent nature of the renewable resources and uncertain market prices make investment into renewables an inherently risky venture. However FiT can guarantee a set payment for per unit of renewable-generated electricity and thus limit investors' exposure to low market rates for a certain time period [31].

Some new issues have been raised by widespread implementation of FiT. For example, in Japan, since grid-tied renewable generation systems rapidly accelerated under FiT, utilities face substantial increased costs for maintaining network reliability due to the intermittent and variable nature of renewable energy technologies. As a result, utilities refuse the further integration of renewable generation systems into grid, which runs contrary to the purpose of designing FiT. This situation will persist until government has an improved cost-effective manner to bolster the network infrastructure [32]. The investigations of [32] demonstrated another newly-emerged concern in that investments for renewable generation systems are mostly for PV projects, due to the significant reductions of residential and commercial PV prices since 2009. In Japan, PV systems accounted for 98% of total newly approved capacity of renewable-generated electricity, compared to only 1% for wind power by June 2014.

To address the same situation of PV systems deployment developing too fast, Germany introduced an automatic FiT adjustment mechanism which was dependent on ongoing deployment volumes, and attempted to match with the reductions of PV systems price in 2009 compared to previous FiT, which was reduced by specific depression rates and reviewed every 3-4 years [33]. This study also mentioned that the reductions of PV price have been faster than expected since 2009, so the automatic mechanism cannot keep up with the decreasing PV price. Therefore, a responsive FiT was proposed by [33] to have an adjustment with shorter frequency, e.g. quarterly, monthly, or even weekly. The simulation results demonstrated the flexible FiT had better performance than the existing automatic mechanism. However, the practicability of the proposed responsive FiT mechanism based on assumed depression rates is still a question, because too frequent government regulation could bring renewable energy investors uncertainty and insecurity.

Current FiT schemes can be divided into two types: market-independent; and market-dependent [34]. In market-independent, the FiT rate is irrespective of the utility retail price and the rate remains fixed for the duration of a contract. In market-dependent policy, the FiT purchase rate is constantly adjusted based on the fluctuating utility price, and the value could be higher by a premium or bonus, or lower by a percentage of utility retail prices, depending on the diverse incentives of the utility. Fixed rate FiT often comes under criticism as there is no match with electricity price trends and load

demand, so it could lead to higher prices for either electricity customers or the utility due to the variability of utility price. For market-dependent schemes, it was shown that the FiT rate floating along with utility price creates greater uncertainty for investors and renewable generation developers, especially for smaller investors or community-owned projects, due to the unpredicted electricity price. Therefore, some countries, e.g. Germany, Spain, and Greece, have abandoned market-dependent policy and turned to fixed rate FiT. This is because market-independent policy has greater investment security and leads to lower-cost renewable systems deployment [34].

From [34], it is clear that market-independence FiT policy is advantageously applied to reduce investment risks. However, it needs to be noted that fixed FiT rate has been constantly re-valued to match PV market trends, and the target of renewable generation volumes set by government, and the actual profitability for FiT investors must be correspondingly fluctuating. Therefore, detailed financial evaluation must be undertaken to demonstrate if FiT is still a worthwhile scheme for renewable energy investors.

It is suggested in [35] that FiT is becoming unattractive for the solar power market because FiT revenue is considerably low and makes renewable energy investment unprofitable. [35] included five representative European countries and demonstrated that for PV systems rated at 500 kW, the payback period (PBP) under FiT in France, Germany, and U.K. is longer than 25 years. PBP is 19-21 years in Italy, and Greece has the shortest at 14-15 years. For PV systems rated at 3 kW and 20 kW, PBP ranges from 11-22 years in all five countries. The U.K. always had the longest PBP with 15+ years for each size of system. Compared to the normal contract duration of 20 years under FiT, the evaluated PBP makes PV investments for developers less attractive. It was demonstrated that countries where net-metering (NM) and self-consumption is active have the highest profitability indexes, and further PV development has been linked to establishment of self-consumption regulatory mechanisms.

With FiT fading, one proposed scheme to revitalize the PV market is NM, by which self-consumption has a priority to use PV power, and any net generation is fed back to the grid at a set rate. Compared to FiT, which requires a heavy governmental subsidy, NM has more open market conditions for PV energy, and provides continuous growth in a sustainable way [36]. In the U.S., NM as an alternative renewables scheme, was

launched early, e.g. New York state in 1997, Vermont in 1998, and later amendments were done to permit the installation of more net metered capacity, e.g. in 1998 a cap of 15 kW for customers and 100 kW for farm systems, increased to 500 kW per installation in Vermont [37, 38]. In Europe, pilot NM schemes were taking place in Cyprus, Slovenia and Portugal in 2013 [36].

NM defines the priority of self-consumption, any residual local renewable generation is sold to utility, so for NM subscribers, the total revenue includes compensation for utility energy use and a payment by the utility for the fed-back local generation. Therefore, for a NM policy maker, three critical aspects need to be taken into account: utility retail electricity tariff; treatment of excess produced PV energy; and netting period [39]. Utility retail tariff can be generally split into four charge categories: production charges, including both generation and supply charges; network charge; standing fees; and taxes. It is noted that NM schemes deviate slightly in different counties and areas due to the varying regulations and considerations of governments and utilities. Fed-back power may be compensated as a feed-in repayment or renewable energy credit. The former is monetary revenue for the NM subscriber for exporting solar energy back to grid in a billing period, and the repurchase rate can be either a fixed value or varied. The latter is often implemented by transferring the excess energy as credits to the next billing period without monetary transfers. For netting period, the most common option is annual, but shorter netting periods, e.g. monthly, daily or hourly have been reported.

The study in [39] indicated an unfair situation towards utilities and non-NM consumers could occur by a repurchase NM rate at utility retail price, which is much higher than PV LCOE, as was applied in Cyprus, or prolonged rolling credit period (comparison between 1, 6 and 12 months). In addition, the [39] recommended that NM customers should be charged for part of production and/or network charges, based on the imported and exported energy, for compensating utilities investment for network and encouraging NM customers PV power self-consumption, which can lead to a more profitable investment. It was also pointed out that charging NM customers production and network fees would make NM schemes less attractive for investors, so policy makers need to have a balanced solution. Furthermore, it is clear that the profitability

of NM scheme for an investor is heavily influenced by utility electricity tariff, because the revenues raised are directly linked to the utility retail price.

Recommendations for making a successful NM scheme in terms of economic returns by the evaluations of several financial indexes under different assumed amendments of existing NM schemes were outlined in [39]. The study focused on the Mediterranean region and the repurchase rate as one of the critical factors, which heavily impacts on the profitability of NM schemes. To comprehensively understand the current situation of NM schemes, a more extensive review of financial and other relevant issues is required.

From previous studies on NM schemes, monetary payments were more popularly applied than rolling-over credits for fed-back PV power, and the repurchase rate currently is quite low, similar to FiT, e.g. 8.16 ¢/kW in Canada, 5 ¢/kW in Australia and 8.9-16.5 ¢/kW in California, U.S. [40, 41, 42]. NM has an ownership requirement for applicants, which is required by FiT as well, so tenants and other potential customers, who are not the property owner, are unqualified to participate in NM or FiT schemes [43]. A U.S. survey showed that at least 49% of households and 48% of businesses were unable to host a PV system by 2015 when excluding residential renters, homeowners without access to roof space, and other potential renewables consumers living/working in buildings with insufficient roof space [44].

It can be seen that current NM schemes have hampered the development of PV energy. Although the NM scheme is more flexible than FiT, limits of ownership and geographical issues still exist. To address these obstacles, a community solar model was proposed as one of the improved approaches to expand the utilisation of solar power to more potential customers.

2.4.2 Community solar and virtual net metering (VNM)

In the report [44], it was stated that ‘shared solar’ could be the key to expanding the potential solar power consumers to 100% of homes and businesses, and four different shared solar models were presented: community group purchasing; offsite shared solar; onsite shared solar in multi-unit buildings; and community-driven financial models. Refer to Fig. 2.5.

Fig. 2.5 Community solar business models [38].

In [44] it is also pointed out that the grid should support energy generated on individual property sharing, but the current tariff schedules and scheme make 'sharing' difficult in the Australian context. The concept of community ownership was proposed as an approach to overcome barriers involved in FiT and NM schemes, but the report did not provide detailed explanations for what is a suitable community solar model and how it is implemented.

A case study of a utility community solar program launched in Arizona US in 2009 is introduced in [45]. The program sells solar output to customers, who are unable to put a PV system on their roof for various reasons, at a fixed price of around $0.12/kWh for up to 20 years. Customers are permitted to cancel the participation in the program at any time. If customers' energy consumption is less than purchased solar energy during a certain billing cycle, the excess is carried over to future bills for the compensation of utility energy charges. The PV systems in this community solar program are normally large-scale solar farms that can be either utility owned projects or projects operated under a power purchase agreement. It can be seen that participants in this community solar program are only energy buyers, so the purchase price is very critical to encourage customers to participate in it. However, it was introduced with a price of $0.12/kWh, representing a $0.02/kWh premium over standard local utility retail rates, so it negatively impacts the customers' incentive to subscribe this program.

Compared to utility community solar, [46] presented that there are some community solar programs called community owned solar, which allow customers to hold ownership shares by investing directly into the PV system. In London, U.K., a 37 kW roof-mounted PV system was installed on Elmore house, and money for PV installation of this project was raised by selling shares to 103 individuals, 70% of who live within two miles of this housing block [47]. The investors receive up to 3% of the profit back in dividends, and the main source of project income is from the compensation of utility energy usage of the lifts in Elmore house and the export of remaining on-site PV power under local FiT. The remaining profit of about 2% (after investor dividends) goes towards the Community Energy Efficiency Fund, which is used for energy efficiency improvements of Elmore house on which the community PV system was installed. In this case, the utility is the energy buyer, and the investors are local residents. In addition, the PV-produced electricity supplies a third party, Elmore house.

From [46, 47], it is clear that community solar programs do not have a standard design and implementation, but a common point is the substitution of a centralized PV system for distributed private solar systems. In addition, the community solar ownership structure can be summarized as utility-owned, third party-owned or community-owned based on the ownership of the centralized PV system.

In terms of the implementation of community solar, [48] stated that generally there are two options in implementing a community solar program: (i) city designs a program, and then contract the project development and maintenance to a third-party vender who purchases the electricity produced by the community solar project for sale to customers; or (ii) utility develops and manages the entire project. It can be seen that an organization or agency party must be required to operate a community solar program, no matter which option a community solar program takes. In addition, it is also demonstrated that community solar has generally developed to address different local scenarios or overcome implementation challenges.

Although community solar programs have already been implemented to overcome the obstacles existing in FiT and NM policies, they have an obvious technical limitation of solar PV installation site. Many communities do not have suitable sites for installing a centralized PV system, and will thus install their solar systems in other locations,

which could increase required investment. In addition, the number of sites suitable for roof-mounted community solar project often have other technical limitations such as poor conditions of aging buildings, loading requirements of the state's or national building code, and utility distribution network capacity [49]. It is assumed that such limitations are a widespread constraint for expanding solar community program, especially in metropolises. However, metropolis is precisely where community solar should be applied, because of the amount of multi-tenant buildings and potential consumers who currently are shut out by FiT and NM schemes.

There is some urgency to introduce community solar programs in cities, e.g. New York, U.S., due to the increasing impacts of climate change [50]. However, New York residents pay the highest electricity rate within continental U.S., and low-income people spend an average of 20% of their income on electricity bills. In terms of the utilisation of renewable energy, only wealthy homeowners are able to afford their own PV systems. By contrast, community solar model facilitate participation from people of all income levels and is often a more affordable and accessible solar power program. Thus community solar is a promising solution to address big city specific barriers depending on the environmental and social matters. It is perceived that any urgency of bringing community solar to metropolises, and understanding the technical limitation of implementation, will require ongoing research to address the issues.

No matter which type of community solar, the utility distribution system will be needed to receive the solar power generated by the centralized PV systems, as shown in Fig. 2.5, and metering will be required to monitor the fed-in solar power. Currently, three meter tariffs support community solar programs: group billing; meter aggregation; and virtual net metering (VNM) [51, 52]. Group billing requires a central meter to record all electricity usage, including tenant loads within a building, and the utility produces a group bill based on the meter readings, against which the output from a shared PV system is netted. The net metering credits are allocated to participants depending on a pre-agreement. In meter aggregation, multiple accounts (meters) of a customer are aggregated on one bill, and the generation from a solar installation on one of the accounts/meters is allowed to offset the consumption of all the aggregated accounts. VNM is an improved version of meter aggregation, and under such a scheme, all generation from a community solar project is shared among

participants regardless of the energy consumption of the customer hosting the PV generator.

Among the above three tariffs, group billing requires a physical connection between the master meter and other distributed meters, which incurs additional installation costs. Meter aggregation and VNM do not have the requirement of physical connection between meters or meters and PV generator. Compared to meter aggregation, VNM breaks the limit of only one qualified customer in a meter aggregation tariff, and it allows multiple participants to share PV generation from a solar installation. Based on relevant studies review, it can be seen that VNM has become the most popular used tariff for community solar program, due to its financial and technical advantages.

VNM is a not new concept, and was initially designed to support Multifamily Affordable Solar Housing (MASH) program launched by the California Public Utilities Commission (CPUC) in early 2009 [53]. It was stated that VNM overcomes one of the biggest barriers of deploying PV retrofit projects in multitenant buildings - the allocation of solar generation credit across multiple separately-metered units. By VNM, a property owner can install an on-site solar system and distribute the credits 'virtually' among tenants. In addition, the problem of split incentives is another challenge for multi-unit buildings to use solar power, which can be resolved by VNM [54]. A split-incentive problem means that tenants desire the utilisation of solar generation, but the building owner is responsible for the costs of solar installation. VNM supports the property owner to recover their capital costs by charging a flat monthly fee for the access to the shared solar energy or incorporating the cost into rental rates.

Currently, U.S. based VNM policies normally require that all on-site solar generation is directly fed back to grid, and a qualified customer can receive a share of on-site PV generation in the form of rolling-over kWh credits under a pre-arrangement between participants. The allocated credits are subtracted from metered utility energy usage at the end of a billing cycle, and charges or credits are applied to the resulting kWh, which are recorded by the bill. The excess credits are carried over to the next billing period until the end of a 12-month billing cycle. Yearly net consumer or net generator would be charged according to the applied utility tariff or compensated at a wholesale rate, which currently is about 0.04$/kWh in the U.S. [55, 56]. It can be seen that the

implementation of VNM tariff is more complex than FiT and NM, because the real-time metered data needs to be treated and then calculate the virtual net, so a VNM agent is required to do the data processing [57]. In terms of the technical issues, a VNM project requires a separate meter solely for PV generation, and all meters for tenant loads and public areas must be behind this separate meter due to the requirement of exporting all on-site solar power to the utility grid. In addition, normally, a VNM generator is sized to load, which is similar to a traditional net metering scheme [58].

From the above reviews, two concerns were raised: too much low repurchase rate for annual remaining credits; and the size of the shared VNM solar system. It can be seen that allocated VNM credits have a value derived from the compensation of utility energy usage and repurchase price for excess credits, but few studies evaluated the value of VNM credits. Therefore, an investigation is required to understand how much the credit is worth and if a potential alternative treatment to the excess credit is applicable to maximize the revenue of implementing VNM tariff. An investigation could also draw lessons from [59] in trading the credits produced by community solar between investors and utilities instead of VNM tariff. In addition, sizing a VNM solar system is typically completed according to participant load demand, whereas the realistic case could face the situation of more available installation area than that required by the energy demand. Therefore, a potential cost-effective size of a VNM solar system may be larger than total power demand in order to fully utilise the solar resource.

In VNM schemes, the argument of charging wheeling costs has been continuing since launching VNM tariff. VNM projects utilise the distribution network to transport locally-produced solar power. In the U.S., it is required that solar generators and participants in non-MASH residential and commercial VNM projects must locate behind a single service delivery point to avoid potentially raised wheeling charges [60, 61]. Some solar parties advocate to extend the VNM boundary beyond a single service delivery point to more widely generalize VNM tariff to a large number of multi-tenant buildings, and consequently, wheeling charges need to be applied. However, previous relevant studies do not develop the evaluation of wheeling costs associated with the VNM tariff in detail, so more research is required to evaluate the wheeling charges raised by implementation of VNM tariff.

On another side, the utility solar tariffs, no matter which of FiT, NM, community solar or VNM, the behaviours of building load demand and the variation of PV generation need to be considered for the potential improvement of solar-based renewable energy utilization, which was presented by [21]-[23] . However, few of the previous relevant studies presented the analyses for utility solar tariffs by linking the performances of building load demand and PV generation to the utility tariffs. This gap remains opportunities to improve the rewards brought by such schemes or tariffs to each of the parties such as utility, generation owner, and energy consumers, .etc.

2.5 Summary

The research on PV system power sharing involves a number of relevant fields, such as PV performance investigation, the evaluation of building load behaviour, network configuration for sharing solar power, and relevant supporting policies, which cover both technical and financial issues. It is known that solar generation and building demand are daily changing, so the variation of generation and consumption would, to some extent, influence the performance of the implementation of power sharing. In addition, a network must be required for sharing solar power, and the type of networks, as stand-alone and grid, determines what strategies are applicable for a potential cost-effective performance of solar power sharing. Furthermore, the policies of utilities and governments are essential to support PV system power sharing via the utility grid, because the fed-in power needs to be valued and the implementation of power sharing programs need to be regulated.

This thesis will focus on using the grid to share solar power and develop re-evaluations for utility solar tariffs due to low-cost financial requirements and simple configuration and control via utility grid for power sharing compared to stand-alone network. The re-evaluations of tariffs will be developed based on the investigations of the profiles of building load demand and PV generation. Proposals will be offered for end users for a cost-effective option of utility solar tariffs and an improved financial performance of the identified cost-effective tariff. In addition, a strategy for solar power sharing will be proposed as a complement for the scenarios without utility scheme support.

Chapter 3 Comparison of Existing and New Tariff Schemes Using Microeconomic Model

3.1 Tariffs for utilising PV power

Existing tariff schemes for utilising PV power, such as Feed-in Tariff (FiT), Net Metering (NM), Net Purchase and Sale, Community Solar Program, and Virtual Net Metering (VNM), have been re-evaluated and improved to assist in the ongoing development of the PV power market and encourage more subscribers. From reviewing related literature, most achievements of previous studies are focused on serving the power market, government and utility [31, 33-36, 62], and the contribution for the end user is much required.

This chapter was developed to compare FiT, NM and VNM tariffs in terms of the end user revenue achieved through implementation. The microeconomic model established by [62] was developed and used for evaluating customer revenue.

3.1.1 Feed-in tariff (FiT)

The U.S. was the first country to implement an early form of feed-in tariff (FiT) in 1978 to encourage energy conservation and development of new energy resources, such as solar, wind and geothermal power [64]. It can be seen that FiT is not only designed for PV power but also available for other types of renewable energy. In addition, FiT allows widespread types of ownership to join in, including homeowners, farmers, business owners and private investors. As a typical scheme for utilizing PV power, FiT has been very applicable and 50 countries have enacted it as of 2010 [65].

Under FiT, the utility or grid company is obliged to purchase overall produced renewable electricity generated by an eligible PV power generator at a set price [66]. In other words, the generator can sell all production to the utility, but they have to pay for all on-site consumed utility electricity at standard retail rates. As a result, two

meters are needed for running FiT, one of which is for metering the consumed utility energy, and another for measuring all on-site renewable generation.

The purchase rates of FiT have been adjusted along with the changing domestic power market of different countries. For example, Canada increased the rate from 42¢/kWh set in 2006 to 80.2¢/kWh in 2010, and cut down to 64.2¢/kWh after July 2010, and then revised the price down to 28-38¢/kWh in 2013. In Japan, the FiT rate was set at 52.5¢/kWh (US$) for 10 years for systems with capacity less than 10 kW, and 50¢/kWh for larger systems, but for 20 years from July 2012. The rates were to be reviewed annually for subsequently connected systems [40]. In Australia, FiT was introduced in 2008 in South Australia and Queensland, and currently rates are around 0.1-0.05$/kWh, cut down dramatically from the original value of around 0.60$/kWh. In addition, NSW and ACT closed FiT to new generators by the middle of 2011, because the installed capacity cap had been reached [41].

From the above introduction, it can be seen that the purchasing rate and the amount of on-site PV generation are two key factors involved in FiT. In latter parts, these two items were used for evaluating the revenue of FiT.

3.1.2 Net metering (NM)

Net metering (NM) is a simplified title of Net Energy Metering (NEM), and was originated in U.S. In 1980, Utilities of Idaho initially used NM, and other states subsequently adopted it, such as Arizona in 1981, Massachusetts in 1982 and Minnesota in 1983. In Europe, it was slowly adopted due to some confusion over addressing economic matters, such as the vague treatment for setting tax over the value in U.K. [43].

As the initiative of encouraging private investments for generating renewable energy, NM gives subscribers with their owned renewable generator more flexibility than FiT, as renewable generation is allowed to offset demand energy of on-site loads, and the owner sells the excess generation to the utility at a set rate for monetary profits. For measuring on-site energy usage and excess generation, a reversible electric meter is required [67].

The set export rate of NM is normally below the import retail rate based on the updated NM schemes of many countries. For example, rates are 8.2-10.0¢/kWh in 2012 in Canada, 2.6¢/kWh in 2016 reduced from last updated 11¢/kWh in Nevada, U.S. In some states of Australia, the rate has been reduced from an early price of 60¢/kWh to currently 6-10¢/kWh, and down to 5¢/kWh in 2016 [12, 13]. The purchase rate has been cut down significantly from the original price as per FiT [68].

Grid-tied PV systems for NM are connected to both the on-site loads and the utility grid enabling the priority of compensating the on-site energy usage. The three key parameters for evaluating the revenue from NM schemes are: the applicable tariff rates; PV generation profiles; and on-site energy.

3.1.3 Virtual net metering (VNM)

Virtual net metering (VNM) originated in the U.S., and initially was implemented in investor-owned utility territories in California in 2009, and then nine other states had enacted relevant VNM schemes by 2012. In addition, solar power is the primary renewable resource for producing electricity in a VNM program [58].

VNM is an allocation of electricity generated from a single PV system at, for example, a multitenant property to multiple utility accounts located at that property. It is required that all the electricity generated by the shared PV system is fed back into the utility grid, and the allocation is applied to customer monthly (or a specified billing cycle) electricity bills in the form of kWh credits based on a pre-arranged agreement. In addition, the title of 'Virtual' means that the shared PV system is not physically tied to the participants' loads, but directly connected to the utility grid through a separate meter for measuring all PV-generated electricity, so VNM is often regarded as a 'billing mechanism' rather than actual NM [69].

Based on the above introduction, the financial profit of VNM subscribers is the cost saving by the subtraction of the utility energy usage by the allocated credits, which is different from the revenue from implementing FiT by selling all generation. In addition, 12-month-cycling net left-over credits would be settled at an applicable rate, which is normally much lower than the retail rates of utility energy, such as 4¢/kWh in California, U.S. [56]. The evaluation of VNM revenue is dependent on the

electricity utility tariff rates, which was used in this thesis to build up the related microeconomic models.

3.1.4 Review of FiT, NM and VNM

From the above introductions, FiT and VNM have a common feature as feeding in all renewable generation. In contrast, NM allows the generation to compensate the loads usage locally, and the excess generation is fed back into the grid. In terms of the reward for the fed-in generation, FiT and VNM, have monetary payments and rolled-over kWh credits respectively, and NM effectively has both.

FiT is an absolute trading agreement based a certain rate set by the utility. NM, as an improved tariff, provides subscribers with more flexibility by allowing the on-site renewable energy to compensate the local load usage and excess generation fed back to the grid for monetary profits. VNM was developed, as a branched and yet closely related net metering protocol to overcome the barriers involved in NM and other later developed solar tariffs [56, 69].

The improvements of VNM includes (i) VNM only requires a shared PV system instead of distributed solar generation plants to provide the renewable energy to the subscribers, which reduces the cost for installing PV systems and makes utilising renewable energy more affordable for low-income household, (ii) VNM overcomes the site limitation not well suited for distributed PV generation, such as roof orientation problems and space limitations. In addition, VNM does not require the physical connection between the customer's site and the solar system. It becomes practical for residents of multi-tenant buildings to utilise solar power by avoiding the hard access from each unit to the roof-mounted solar system. (iii) VNM does not have any property ownership requirement, which encourages businesses and residents who rent property to utilise renewable energy.

It has been claimed that VNM is a more feasible protocol to expand renewable utilisation, because VNM breaks some limitations of NM that constrain many potential users and businesses from utilising PV power, such as ownership of property and geographical location [69].

3.2 Comparison of FiT, NM and VNM by microeconomic model

3.2.1 Microeconomics

The latter comparisons of FiT, NM and VNM were established based on microeconomic models, so it is necessary to understand how microeconomics works. '*Microeconomics is a branch of economics that studies the behaviour of individual units (such as a person, household, firm, or industry) in making decisions regarding the allocation of limited resources. Microeconomics is primarily concerned with the factors that affect individual economic choices, the effects of changes in these factors on the individual decision makers, and advises how their choices are coordinated by markets, and how prices and demand are determined in individual markets, and how individuals make more efficient or more productive decisions*' [70]. From the above description and combining with the purpose of this chapter, the purpose is to demonstrate the best option amongst the three solar tariffs for the subscriber to achieve more revenue. The microeconomic model investigates an individual unit, such as a household or a building, not the aggregate economy issues. Thus, microeconomics is an applicable tool for the financial evaluation of this study.

As an example of the application of microeconomics, [63] established a series of microeconomic models to evaluate the financial performances of FiT, NM and net purchase and sale. The established microeconomic models from [63] were modified and applied here to compare FiT, NM and VNM in this study.

3.2.2 Microeconomic models of FiT, NM and VNM

All the notations involved in the latter microeconomic models are presented in Table 3.1. All notations except B_i, q_l, and p_l, the explanations related to FiT and NM, and equations (3.1)-(3.3), are cited from [63]. Remaining notations, explanations and equations were developed by this research based on the relevant cited items.

TABLE 3.1 Notations

Notation	Description of notation
i	A series of subscribers (household or building) of a solar mechanism, $i = 1, 2, 3, 4 \ldots n$
k_i	A subscriber i's total cost of installing a PV system (FiT & NM) or the share of overall investment for a shared PV system (VNM)
u_i	Benefits by the subscriber 'i' obtained from installing a PV system
r	Retail rates of utility electricity
p	Purchase rate of PV-generated electricity for FiT & NM
B_i	Revenue of a subscriber by selling PV generation (FiT & NM) or saving cost of consumed utility electricity (NM & VNM)
z_i	Subscriber i's PV generation (FiT & NM) or allocated kWh credits (VNM)
z_{gi}	i's PV generation in net generation periods (specifically for NM)
z_{ci}	i's PV generation in net consumption periods (specifically for NM)
q_i	Subscriber i's electricity consumption
q_{gi}	Subscriber i's electricity consumption in net generation periods (specifically for NM)
q_{ci}	Subscriber i's electricity consumption in net consumption periods (specifically for NM)
q_l	Left-over allocated credits of VNM in kWh
p_l	Settlement rate for annual left-over credits
	Remark: $z_i = z_{gi} + z_{ci}$, $q_i = q_{gi} + q_{ci}$

Further explanations for some of the items shown in Table 3.1 are presented as follows. k_i includes the cost of the PV system equipment, metering, and installation, all of which are specific for the customer i, who subscribes to a solar tariff. u_i represents the satisfaction of a subscriber raises from implementing a certain solar tariff, which is evaluated by the cost, k_i, and the revenue by selling solar power (NM & FiT) or sharing rolled-over kWh credits (VNM). For FiT, the expression of u_i is presented by the cost, k_i, minus the income, $p \times z_i$, which represents the net cost or income. It can be understood that the inspiration for a potential customer to subscribe FiT can be presented as (3.1).

$$u_i \geq k_i - p \times z_i \tag{3.1}$$

u_i is absolutely from utilising PV generation, so any issue related to the consumption of the utility electricity is excluded from u_i. Furthermore, the cost k_i is comparatively fixed for installing a PV system with a certain capacity due to the fixed the unit cost as \$/W_p, e.g. 8 \$/W_p cited from [71]. From (3.1), it can be seen that the higher value of $p \times z_i$ causes the lower value of $k_i - p \times z_i$, and consequently, results in a lower value of u_i, which means that it becomes easier to inspire a potential customer to subscribe to FiT. By this, whichever one of FiT, NM and VNM provides the highest revenue, B_i, would be the most attractive option for a potential customer.

The parameters z_{gi}, z_{ci}, q_i, q_{gi}, and q_{ci} from Table 3.1, and two time frames of 'net generation period' and 'net consumption period', which respectively present the time period where PV generation is greater than the on-site load usage, and the time period where PV generation is less than the load usage, were set specifically for NM. The total revenue of NM has two components: the cost saving from compensating the on-site PV generation to the utility energy usage; and the income by selling the excess PV power. By introducing the above time frames, the on-site PV generation and the utility energy usage can be divided into two parts as the generation and consumption during 'net generation period' represented by z_{gi} and q_{gi}, and the generation and consumption during 'net consumption period' represented by z_{ci} and q_{ci}. It can be understood that a NM customer sells a net amount of on-site generation, $z_{gi}-q_{gi}$, at the price of p_{NM} during 'net generation period', and purchases the net consumed utility electricity, $q_{ci}-z_{ci}$, at the retail price of r, during net consumption, and the net revenue is presented as follows:

$$(z_{gi} - q_{gi})\times p_{NM} - (q_{ci} - z_{ci})\times r = (z_{gi} - q_{gi})\times p_{NM} + (z_{ci} + q_{gi})\times r - q_i \times r \quad (3.2)$$

Equation (3.2) can be divided into two components as total revenue by saving utility energy and selling excess PV generation, presented by $(z_{gi}-q_{gi})\times p_{NM}+(z_{ci}+ q_{gi})\times r$, and the cost for consuming utility energy, presented by $q_i \times r$.

In addition, some of the items shown in Table 3.1 have different explanations for VNM, because VNM as a group solar tariff, which means a number of subscribers share a common PV system, has different running principle, and the composition of the subscriber from FiT & NM. In VNM, k_i means the qualified customer i's share of total investment for installing the shared PV systems. In addition, q is equivalent to r, because the value of the rolled-over kWh credits is evaluated by the cost saving from compensating the energy usage of the loads, which has to be calculated based on the retail rates of the utility tariff, r. z_i is the share of the customer i's allocated credits, and q_I is the annual left credits with a repurchase rate as p_I, so the total revenue of VNM from cost saving and selling the remaining credits can be expressed by $(z_i-q_I)\times r+p_I \times q_I$.

Based on the above analyses, the individual expression of the satisfaction of FiT, NM and VNM are presented as the followings,

FiT: $u_{iFiT} \geq k_i - p_{FiT} \times z_i$ (3.1)

NM: $u_{iNM} \geq k_i - [(z_{gi} - q_{gi}) \times p_{NM} + (z_{ci} + q_{gi}) \times r]$ (3.3)

VNM: $u_{iVNM} \geq k_i - [r \times (z_i - q_I) + p_I \times q_I]$ (3.4)

As previously analysed, the first component of (3.1), (3.3) and (3.4), represents the cost for installing an individual (FiT & NM) or shared (VNM) PV system, and the latter presents the revenues from implementing a solar tariff. As previously mentioned, the one with the highest revenue, as B_i, would be the best option for a customer, so the further evaluations were developed for comparing the revenue of FiT, NM & VNM.

FiT: $B_i = p_{FiT} \times z_i$ (3.5)

NM: $B_i = (z_{gi} - q_{gi}) \times p_{NM} + (z_{ci} + q_{gi}) \times r$ (3.6)

VNM: $B_i = r \times (z_i - q_I) + p_I \times q_I$ (3.7)

3.3 Results and analyses in different scenarios

From (3.5) to (3.7), there are three types of items involved: (i) the rate including the retail rate of utility energy, r, the set rate of FiT & NM, $p_{FiT\ \&\ NM}$, and the repurchase rate for the left-over VNM credits, p_I; (ii) PV generation, z_i; and (iii) the demand energy of the loads, q_{gi}. For comprehensive analyses, the research sets three scenarios based on the comparison of PV generation and the demand energy of the loads to evaluate the revenue, B_i, as: (1) no any excess solar power exported and total daily generation less than daily demand energy of the loads; (2) excess solar power occurring but total daily generation less than daily demand energy of the loads; (3) excess solar power occurring and total daily generation more than daily demand energy of the loads. In addition, there are three conditions in terms of the rates as $p_{FiT\ \&\ NM} = r$, $p_{FiT\ \&\ NM} < r$ & $p_{FiT\ \&\ NM} > r$. Furthermore, the repurchase rate for the left-over VNM credits, p_I, was specifically discussed in the analyses related to VNM. The latter evaluations were developed under the above three scenarios, and each scenario has three conditions of the rates.

For a fair comparison, FiT, NM and VNM are with the same capacity as $z_{FiT} = z_{VN} = z_{VNM}$, and all comparisons of the three tariffs are based on a common customer. It is

also noted that the capacity of VNM, z_{VNM}, means a customer' share out of overall rolled-over kWh credits of a VNM group.

3.3.1 Scenario 1 - no excess solar power

Under this scenario, overall the daily PV generation, z_i, is less than the daily demand energy of the loads, q_i, and for NM zero excess solar power is exported, refer to Fig. 3.1.

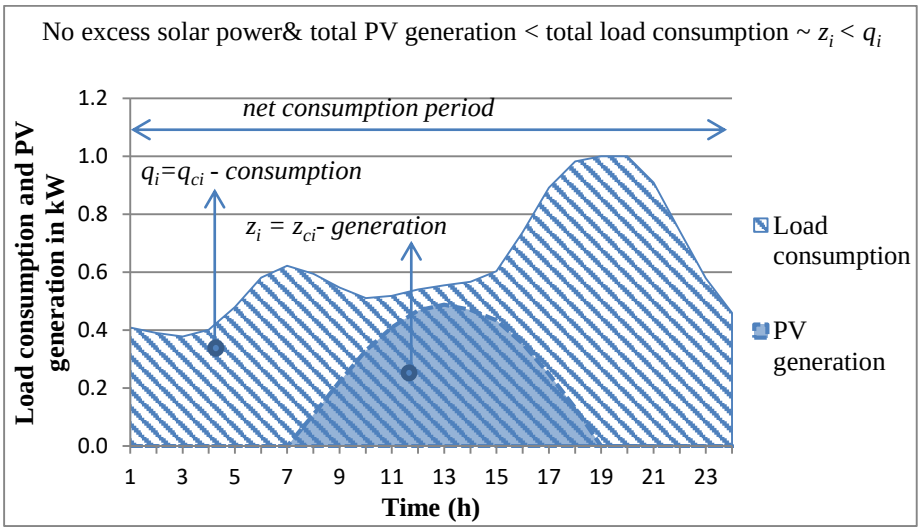

Fig. 3.1 Scenario 1.

Based on (3.6) to (3.8), the revenue - $B_{FiT,\ NM\ \&\ VNM}$ were determined under three conditions of the rates, $p_{FiT,\ NM}$, r.

When $p_{FiT,\ NM} = r$, the revenue of FiT is $B_{FiT} = p \times z_{i,}$. For NM, it has z_{gi} & $q_{gi} = 0$, $z_{ci} = z_i$ due to no excess generation, which means that all daily time is net consumption period, and based on (3.5), $B_{NM} = r \times z_i = p \times z_i$. For VNM, it can be understood that there is not any left-over credit in the end of a billing cycle of VNM under this scenario, so $q_I = 0$, and based on (3.6), $B_{VNM} = r \times z_i$. By comparing the results, it has $B_{FiT} = B_{NM} = B_{VNM}$, and illustrated by the diagram below.

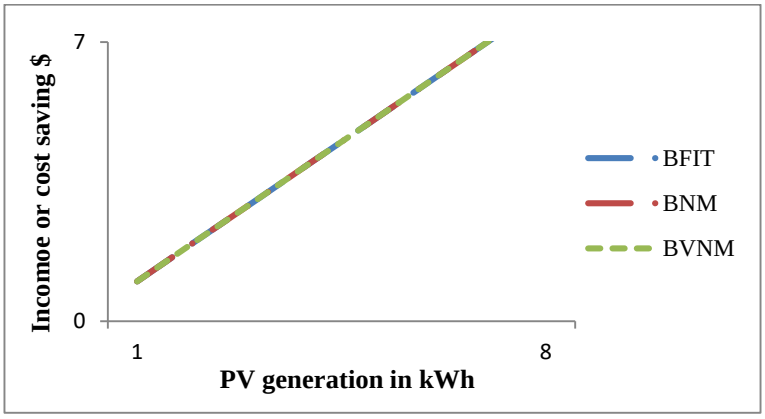

Fig. 3.2 Comparison under condition 1 - $p_{FiT,\ NM} = r$.

When $p_{FiT,\ NM} < r$, it can be assumed $p_{FiT,\ NM} + \wedge p = r$, $\wedge p$ represents the greater value of r minus $p_{FiT,\ NM}$, so it has $\wedge p > 0$, which would be repeatedly used in further related evaluations. For FiT and, it has $B_{FiT} = p \times z_i$. For NM, it still has $q_{gi} = 0$, $z_{ci} = z_i$, so $B_{NM} = p \times z_i + \wedge p \times z_i$. For VNM, it still has $q_I = 0$, so $B_{VNM} = p \times z_i + \wedge p \times z_i$. The result is $B_{FiT} < B_{NM} = B_{VNM}$.

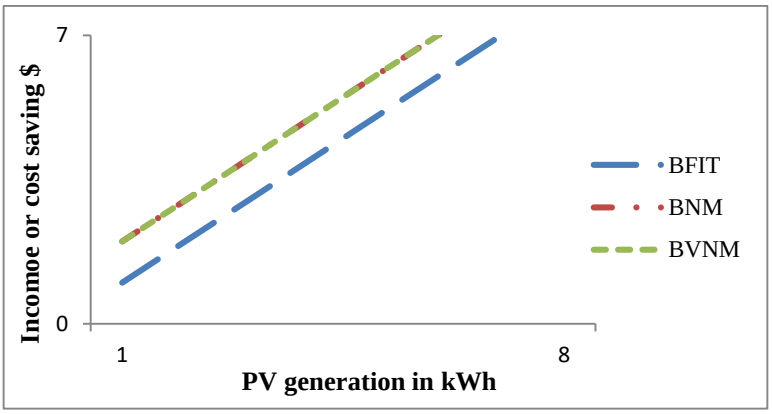

Fig. 3.3 Comparison under condition 2 - $p_{FiT,\ NM} < r$.

When $p_{FiT,\ NM} > r$, by the same means as the second sub-scenario, it can be assumed $p_{FiT,\ NM} = r + \wedge p$, so $r = p - \wedge p$. For three tariffs, It has $B_{FiT} = p \times z_i$, $B_{NM} = p \times z_i - \wedge p \times z_i$, and $B_{VNM} = p \times z_i - \wedge p \times z_i$. The result is $B_{FiT} > B_{NM} = B_{VNM}$.

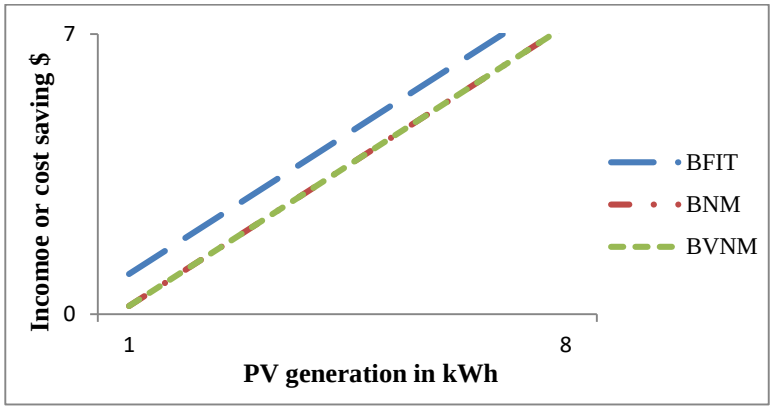

Fig. 3.4 Comparison under condition 3 - $p_{FiT,\ NM} > r$.

From the above evaluations, B_{NM} and B_{VNM} always have same values, because implementing NM has an only function as offsetting the usage of utility electricity without any income by selling on-site generation, which is same as VNM, under the condition of no excess solar power. In addition, the revenue of both of NM and VNM is only the cost saving and has same value due to only the utility rate applied to calculating the cost saving. The revenue of FiT could be greater or lower than NM & VNM depending on the relationship between the purchase price of p_{FiT} and the retail rate of utility energy. In reality, the utility electricity rate is normally much higher than the current purchase price of FiT and NM. For example, the utility electricity rates has different schedules as 0.277$/kWh, 0.396$/kWh, etc. that are much higher than the current rate of FiT of around 0.05$/kWh in Australia, and this situation is globally popular. Therefore, in this context, FiT is the tariff with the lowest revenue, and NM and VNM would bring same revenue to a potential customer, for who it is depending on the related local policy and the realistic situation, such as the architectural structure, the ownership of the property, etc., to choose NM or VNM.

3.3.2 Scenario 2 - excess solar power exported and total generation less than load consumption

Under this scenario, shown by Fig 3.5, the total daily PV generation, z_i, is less than the daily demand energy of the loads, q_i. For NM, the excess generation, z_{gi}, is exported to the grid, and the rest is consumed by the on-site loads. For FiT, overall on-site PV generation, z_i, is fed into the grid, and for VNM, the equivalent rolled-over kWh credits, z_i, are allocated to the customer without any left-over credits as $q_I=0$.

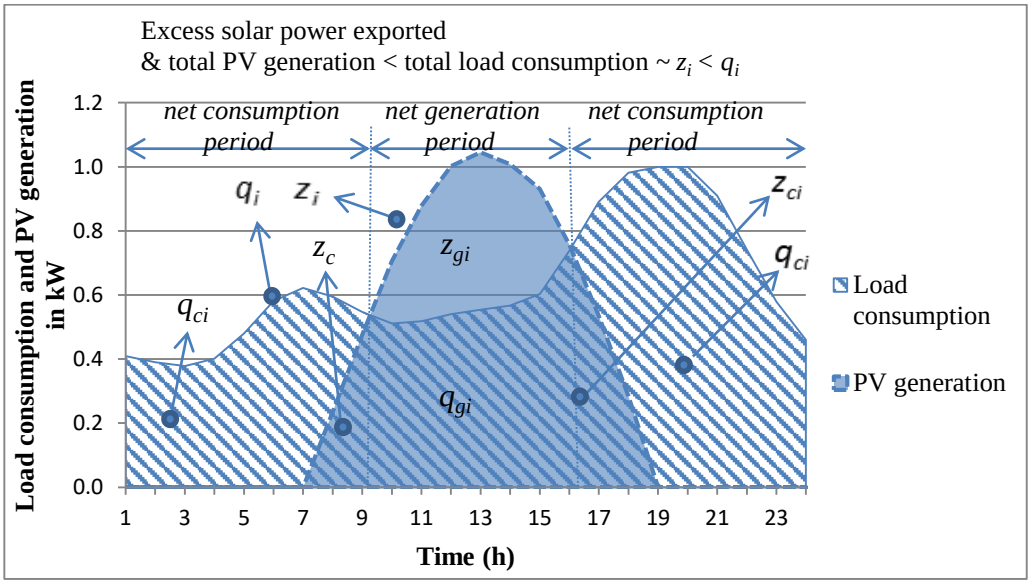

Fig. 3.5 Scenario 2.

When $p_{FiT,\,NM} = r$, the revenue of FiT is $B_{FiT} = p \times z_i$. For NM, the revenue is $B_{NM} = (z_{gi} - q_{gi}) \times p + (z_{ci} + q_{gi}) \times r = p \times z_i$. For VNM, with $q_I = 0$, the revenue is $B_{VNM} = r \times (z_i - q_I) + p_I \times q_I = r \times z_i$. By comparing the result, it has $B_{FiT} = B_{NM} = B_{VNM}$.

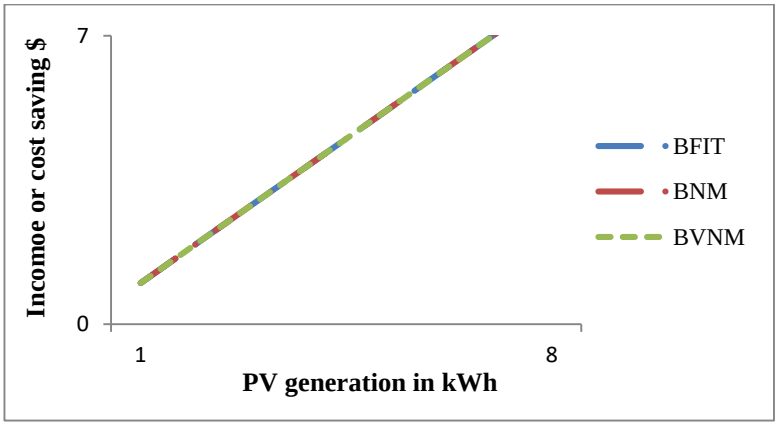

Fig. 3.6 Comparison under condition 1 - $p_{FiT,\,NM} = r$.

When $p_{FiT,\,NM} < r$, it can be assumed $p_{FiT,\,NM\ \&\ VNM} + \wedge p = r$, so it has $B_{FiT} = p \times z_i$, $B_{NM} = p \times z_i + \wedge p \times (z_{ci} + q_{gi})$, and $B_{VNM} = r \times (z_i - q_I) + p_I \times q_I = p \times z_i + \wedge p \times z_i$. In addition, under NM, the consumption must be less than the generation during net generation period as $q_{gi} < z_{gi}$, so $z_{ci} + q_{gi} < z_{ci} + z_{gi} = z_i$. It has $B_{FiT} < B_{NM} < B_{VNM}$.

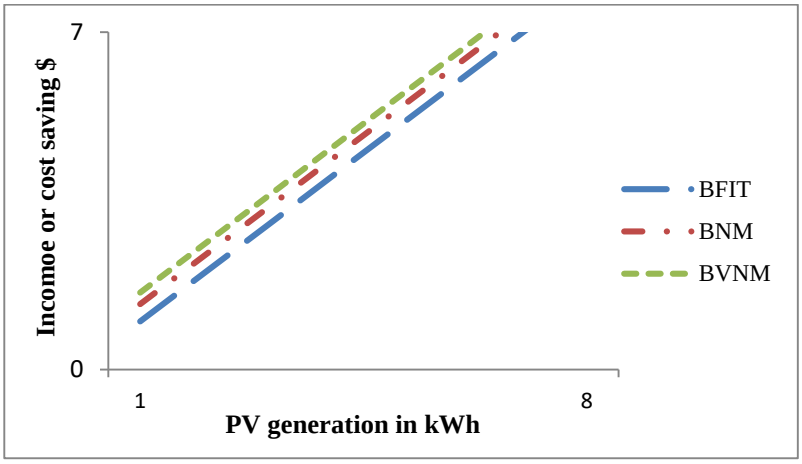

Fig. 3.7 Comparison under condition 2 - $p_{FiT,\ NM} < r$.

When $p_{FiT,\ NM} > r$, it is assumed $p_{FiT,\ NM} = r + \hat{}p$, so $r = p - \hat{}p$. For FiT, NM & VNM, the revenues are，respectively，$B_{FiT} = p \times z_i$, $B_{NM} = p \times z_i - \hat{}p \times (z_{ci}+q_{gi})$, $B_{VNM} = r \times (z_i - q_I) + p_l \times q_{I,} = p \times z_i - \hat{}p \times z_i$. As the above analysis, it has $z_{ci}+q_{gi} < z_i$ under NM, so the comparison result is $B_{FiT} > B_{NM} > B_{VNM}$.

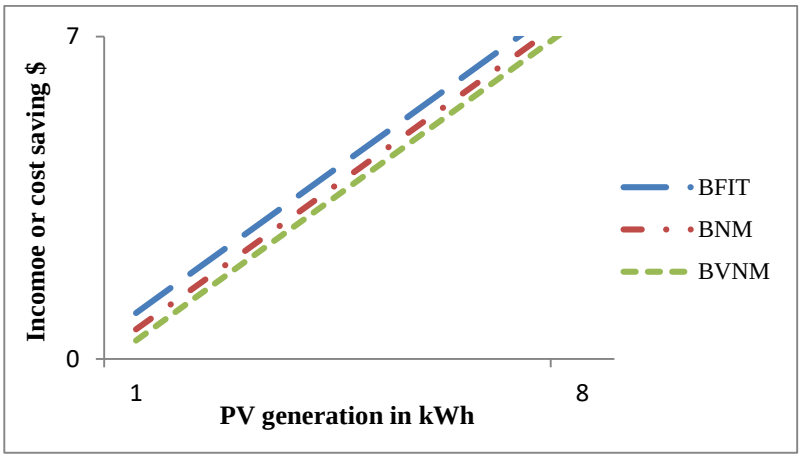

Fig. 3.8 Comparisons under condition 3 - $p_{FiT,\ NM} > r$.

Under this scenario, the three tariffs could have same revenue with $p_{FiT,\ NM} = r$, and are different each other with $p_{FiT,\ NM} <$ or $> r$. The utility electricity rate is much higher than the current purchase price of FiT and NM in the current Australia context. Therefore, based on the results shown in Fig 3.7, VNM is the best option with the highest revenue, and FiT is the worst cost-effective tariff with the lowest revenue due to selling overall on-site generation to the utility at a much lower price. NM stands on the position between VNM and FiT, because portions of the on-site generation bring the cost saving from reducing the utility energy usage same as VNM does, and the excess solar power is sold to the utility, as per FiT.

3.3.3 Scenario 3 - excess solar power exported and total generation more than load consumption

Under this scenario, illustrated by Fig 3.9, the total daily PV generation, z_i, is greater than the daily demand energy of the loads, q_i. The situation for NM and FiT is same as under the second scenario, as the excess generation, z_{gi}, is exported to the grid, and the rest is consumed by the on-site loads under NM, and overall on-site PV generation, z_i, is fed into the grid under FiT. The situation of VNM is, however, different from overall credits consumed under the second scenario, as rolled-over allocated credits would be occurred, i.e., $q_I>0$.

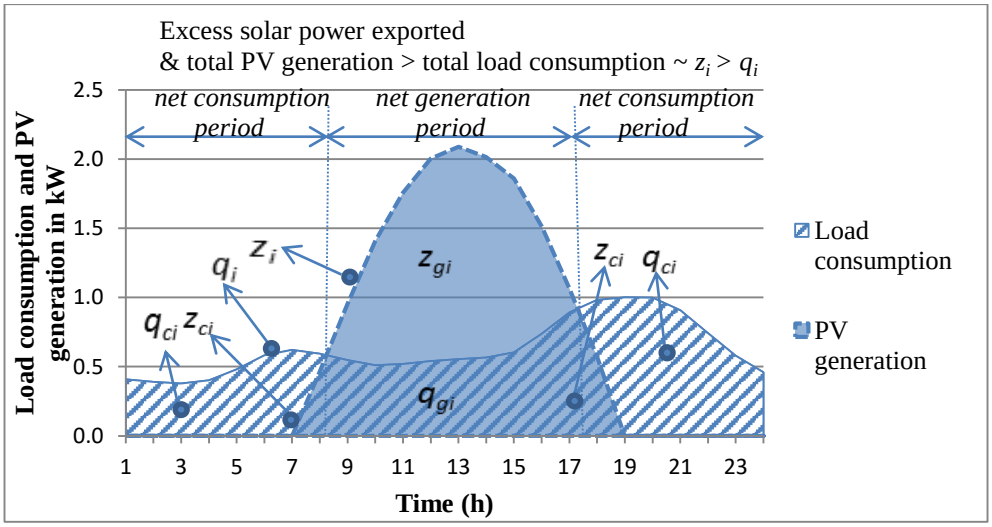

Fig. 3.9 Scenario 3.

When $p_{FiT,\,NM} = r$, the revenue of FiT, NM & VNM is respectively presented as $B_{FiT} = p \times z_i$, $B_{NM} = (z_{gi}-q_{gi}) \times p + (z_{ci}+q_{gi}) \times r = p \times z_i$, and $B_{VNM} = r \times (z_i-q_I) + p_l \times q_I = r \times z_i - q_I \times (r-p_l)$. As shown in Table 3.1, p_l is the repurchase rate for the left-over credits, and it is much lower than the retail rate of r, so $r - p_l > 0$, and with $q_I>0$, it has $B_{FiT} = B_{NM} > B_{VNM}$.

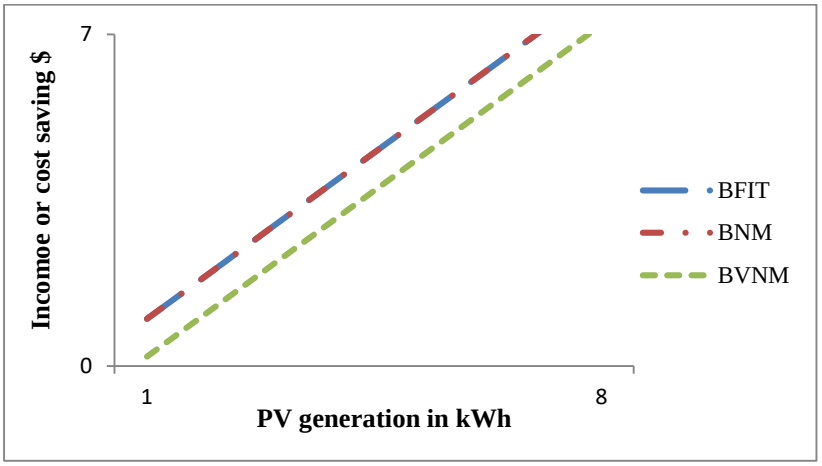

Fig. 3.10 Comparison under condition 1 - $p_{FIT,\,NM} = r$.

When $p_{FiT,\,NM} < r$, by the above means, it is assumed as $\hat{p}>0$, and $p_{FiT,\,NM} + \hat{p} = r$, and consequently, it has $B_{FiT}=p\times z_i$, $B_{NM}=p\times z_i+\hat{p}\times(z_{ci}+q_{gi})$, and $B_{VNM}=r\times(z_i-q_l)+p_l\times q_l=p\times z_i+\hat{p}\times z_i-q_l\times(r-p_l)$. Due to all items involved in the revenue with nonnegative value, it has $B_{FiT} < B_{NM}$. For B_{FiT} & $B_{VNM,}$ when $\hat{p}\times z_i>q_l\times(r-p_l)$, i.e. $z_i/q_l > (r-p_l)/(r-p_{FiT,NM})$, it has $B_{VNM} > B_{FiT}$. Otherwise, $\hat{p}\times z_i < q_l\times(r-p_l)$, i.e.

$$z_i / q_l < (r-p_l)/(r-p_{FiT,NM}) \tag{3.8}$$

and, $B_{VNM} < B_{FiT} < B_{NM}$. Under the scenario of $B_{VNM} > B_{FiT}$, the comparison of B_{VNM} to B_{NM} can be identified by B_{VNM} minus B_{NM}, in addition, it was given as $z_{ci}+z_{gi} = z_i$, so it has $B_{VNM} - B_{NM}=\hat{p}\times(z_{gi}-q_{gi})-q_l\times(r-p_l)$. When $\hat{p}\times(z_{gi}-q_{gi})>q_l\times(r-p_l)$, i.e.

$$(z_{gi}-q_{gi})/q_l > (r-p_l)/(r-p_{FiT,\,NM}) \tag{3.9}$$

and it is $B_{VNM} > B_{NM} > B_{FiT,}$ and otherwise, as

$$(z_{gi}-q_{gi})/q_l < (r-p_l)/(r-p_{FiT,\,NM}) \tag{3.10}$$

it has $B_{NM} > B_{VNM} > B_{FiT}$.

It can be seen that the above three judging conditions as (3.8) to (3.10) were sorted out by the left side presenting the relationship among PV generation, load demand and left-over credits, and the right side showing the relationship among the different rates. In addition, the right side of the three judging conditions is same for a clear evaluation. The comparison of B_{FiT}, B_{VNM} & B_{NM} is illustrated by Fig 3.11, and three conditions of

VNM were numbered as (1), (2) and (3) aligning with the above three judging conditions (3.8), (3.9) and (3.10) respectively.

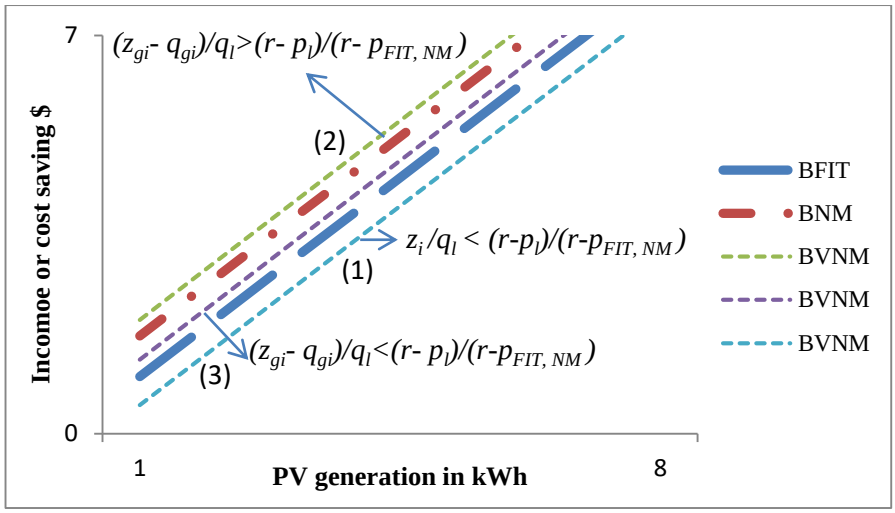

Fig. 3.11 Comparison under condition 2 - $p_{FIT, NM} < r$.

As Fig 3.11 shows, NM is always with more revenue than FiT, because the value of cost saving from a certain amount of PV generation compensating utility energy usage is always greater than the monetary profits by selling the same amount of PV generation to the utility due to $p_{FiT, NM} < r$.

VNM is variable comparing FiT & NM depending on the different situations of the PV generation and load demand, and the values of the utility retail rate, purchase rate of NM & FiT and the repurchase rate for VNM left-over credits. From theoretical view, the above three possibilities as (3.8) to (3.10) are effective, and the realistic situation of these possibilities can be further studied by referring to current market values of r, p & p_l. For example, in Australia context, the purchase rate of FiT, p, is around 0.05-0.1$/kWh depending on different states, and the rate of utility energy is different based on the variant schedules such as 0.277, 0.396, etc. $/kWh, so this chapter took an average value by 0.3 $/kWh for further studies. In addition, it is hard to get the repurchase rate for VNM left-over credits in Australian related policy, and it was introduced from US that is 0.04 $/kWh [56].

The right side of the three judging conditions can be evaluated based on the above values as $(r-p_l)/(r-p_{FiT,NM})$=1.3≈1, based on which, the three possibilities (1)-(3) shown in Fig 3.11 can be studied. There is a trend about the possibility (1) as it becoming more unlikely to occur with the value of $(r-p_l)/(r-p_{FiT,NM})$ getting close to

1, because the total rolled-over VNM credits equivalent to total PV generation, z_i must be much greater than the left-over credits, q_l, which means the value of z_i/q_l must be distinctly greater than 1. For the possibilities (2) & (3), it is hard to identify which one is more likely to occur, because the reliable evaluation for the relationship between the exported generation, the energy usage of the on-site loads during net generation period under NM, and the left-over credits, as $(z_{gi}-q_{gi})/q_l$, must be depending on the specific case.

From the view of the left-over VNM credits, q_l, however, it can be understood that the more left-over VNM credits, the less revenue of VNM, because the repurchase rate for left-over VNM credits is too much low as 0.04$/kWh. This trend is illustrated as the position of B_{VNM} moving from (2) to (3) shown in Fig 3.11 due to the value of $(z_{gi}-q_{gi})/q_l$ getting smaller caused by the bigger value of q_l. The above evaluation demonstrates that VNM can bring more revenue for a customer than NM by cutting down the left-over VNM credits in some ways, which will be further studied in Chapter 5.

When $p_{FiT,\,NM} > r$, based on the above assumption as $r = p-\hat{}p$. It has $B_{FiT} = p \times z_i$, $B_{NM} = p \times z_i - \hat{}p \times (z_{ci}+q_{gi})$, and $B_{VNM} = p \times z_i - \hat{}p \times (z_i-q_I) - q_I \times (p-p_l)$. It is obvious $B_{FiT} > B_{NM}$. In addition, under VNM, it has that total allocated credit minus left-over credits is equal to the total load consumption as $z_i - q_I = q_i = q_{ci} + q_{gi}$, it is obvious that $q_{ci} + q_{gi} > z_{ci}+q_{gi}$, and it has $B_{FiT} > B_{NM} > B_{VNM}$, provided $p > p_l$. Otherwise, as $p < p_l$, it has $B_{VNM} = p \times z_i - \hat{}p \times (z_i - q_I) + q_I \times (p_l - p)$. If q_I is much greater than $z_i - q_I$, B_{VNM} could be greater than both of B_{NM} and B_{FiT}, so the results could be $B_{FiT} > B_{VNM} > B_{NM}$ and $B_{VNM} > B_{FiT} > B_{NM}$. The comparison of B_{FiT}, B_{VNM} & B_{NM} is illustrated by Fig 3.12.

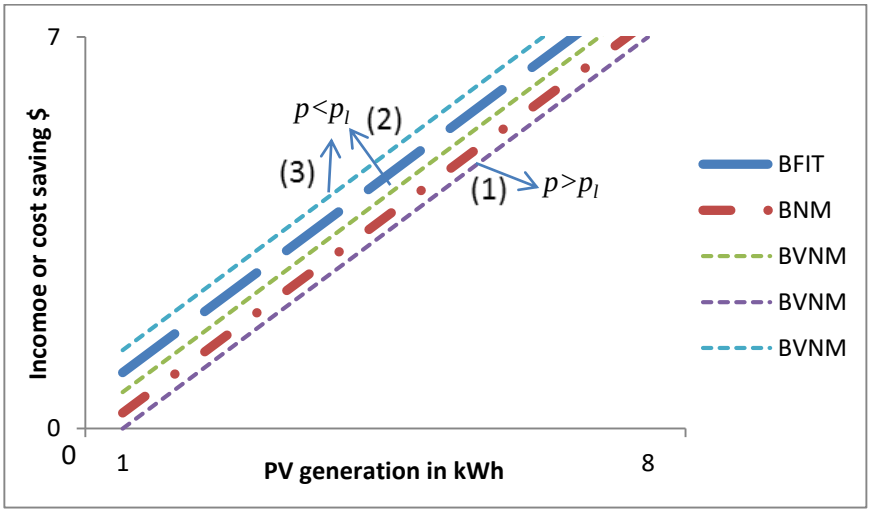

Fig. 3.12 Comparison under condition 3 - $p_{FIT,\ NM} > r$.

Under $p_{FiT,\ NM} > r$, FiT always achieves more revenue than NM due to the higher purchase rate than the utility retail, and the revenue of VNM is floating shown by Fig. 3.12 depending on the relationship of the purchase rate of FiT & NM, $p_{FiT,\ NM}$, and the repurchase rate of VNM, q_l.

Under this scenario, VNM has floating positions with $p_{FiT,\ NM} <$ or $> r$ due to the VNM left-over credits occurring, which causes the revenue of VNM changing with the variation of the amount of the left-over credits. In the realistic context, the utility rate, currently, is quite higher than the purchase rate of FiT & NM, as $p_{FiT,\ NM} < r$, so FiT is the tariff with the lowest revenue, and VNM can be the best option for a customer by using the allocated credits as much as possible.

3.4 Summary

This chapter has evaluated the revenues a potential customer achieving from respectively implementing FiT, NM and VNM by using microeconomic models. The investigations were developed based the three assumed scenarios as shown in Fig. 3.1, 3.5 & 3.9, each of which includes three conditions as $p_{FiT,\ NM} =, < \&\ > r$.

In the current Australia context, the purchase rate of FiT & NM is much lower than the retail rate of utility energy as $p_{FiT,\ NM} < r$. Under this realistic condition, it was demonstrated the FiT is always the worst cost-effective tariff with the lowest revenue, and the better option between NM & VNM is alternating depending on the different study scenarios. NM and VNM are always with same revenue under Scenario 1

(generation less than load), and VNM is the best option under Scenario 2 (net generation less than net load). Under scenario 3 (net generation greater than net load), the revenue VNM brings is floating depending on the amount of rolled-over (surplus) credits. It was demonstrated that VNM can be the tariff with the highest revenue by reducing the surplus credits in some ways, which will be further studied in Chapter 5.

Chapter 4 Daily Profiles of Building Electrical Demand and PV System Generation Based on Australian Fixed and TOU Tariffs

4.1 Daily trends of building demand and PV generation

As discussed in Chapter 1, the evaluation of building consumption and PV system generation is important to the development of this project, because the features of building energy usage and solar system output have significant impact on determining energy costs and subsequent investment recovery of the PV system. In order to comprehensively study on building load behaviour, this study investigated a number of different types of buildings, such as commercial office buildings, retail centres, education buildings and residential apartment-style buildings. Building load includes the various types of electrical appliance and mechanical systems, interior end use equipment, and interior and exterior lightings [71]. Different categories of buildings, such as education buildings, commercial buildings, residential buildings, etc., have different load demand profiles because of the diverse electrical and mechanical system components, the different design requirements of building functions, and activities of their occupants. Even in a certain category of building, the load demand varies along with the changing requirements of the occupants and facilities as well [22, 72]. For the investigation of electric load demand of different types of buildings, this study utilises a public database of building energy consumption, which has been measured from real buildings and sorted for public use [71]. For another, PV system has variable output due to the variation of weather conditions such as temperature, sun insolation, etc. [11]. The work in this chapter uses software simulation to evaluate the variation of PV system output, and yearly data of weather conditions, which is introduced from an Australian database, was utilised for the daily solar generation simulation.

In addition, this study introduced Australian utility tariffs to evaluate the impact on energy costs and the investment recovery of PV system from the behaviour of building load demand and PV system output. The current widely-used 'time-of-use' (TOU) and fixed-rate utility electricity tariffs were applied to the relevant financial evaluation.

4.2 Evaluation of electrical demand and simulation of PV system output

4.2.1 Building daily demand

This study evaluates building load consumption by data analysis based on a US public database [71]. There are fifteen types of buildings involved in this database, i.e. full-service restaurant, quick service restaurant, warehouse, hospital, stand-alone retail, strip mall, supermarket, primary school, secondary school, small office, medium office, large office, small hotel, large hotel and midrise apartment. It is noted that the office buildings and the hotel buildings are classified as small, medium and large scales, which are defined by the amount of load consumption, for instance, the maximum hourly electricity usage of the small hotel and the large hotel, respectively, is 43 kW and 452 kW at 8pm.

By extracting annual 24-hour data points from the database, the daily curve of building electric demand was developed. By the comparison of daily curves all year long, it can be seen that the daily trend of electrical demand of a certain category of building has a similar pattern. Through taking the large hotel, one of fifteen categories of buildings, as an example, the daily curves of electric load demand year-round were illustrated as the table below shown.

TABLE 4.1 Year-round daily trend of electrical load demand of large hotel.

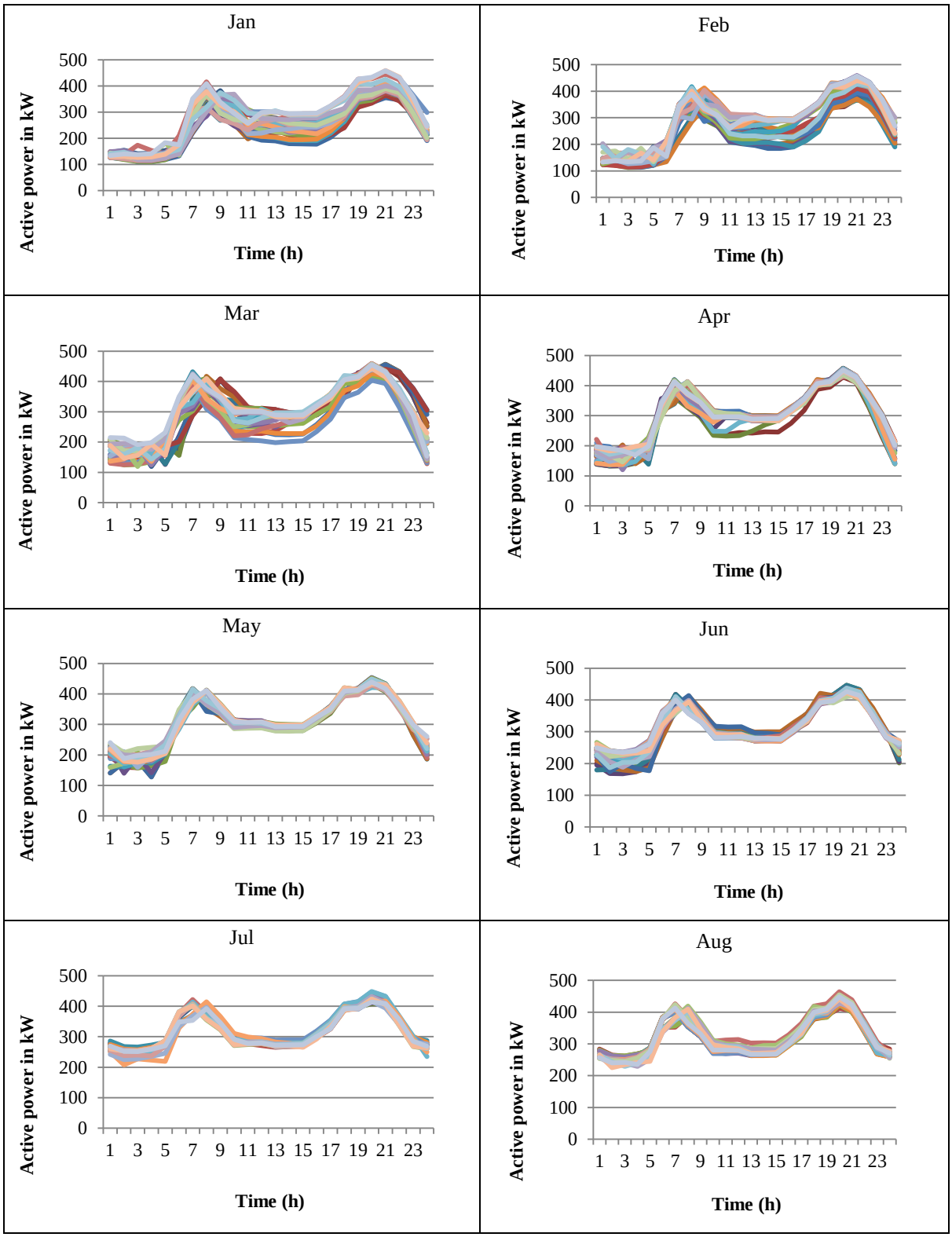

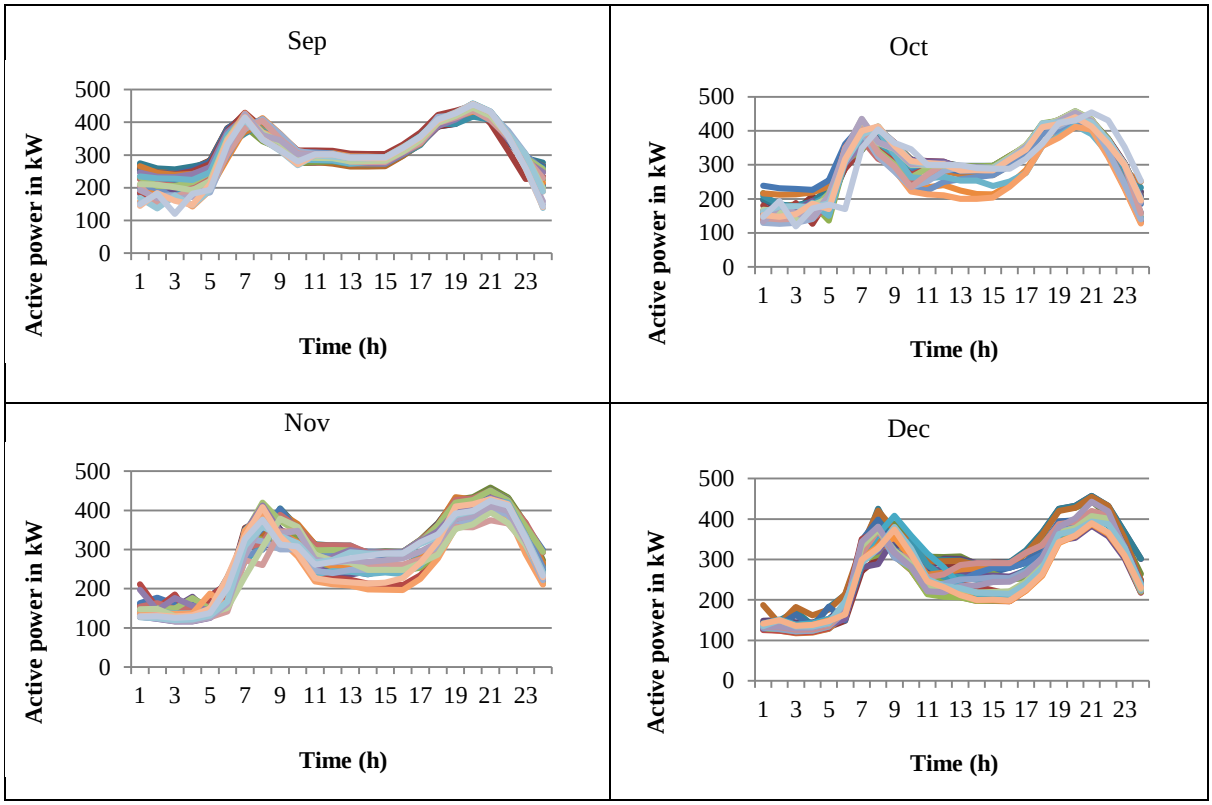

From Table 4.1, the daily trend of load consumption year-round is similar with the demand going up from early morning, and reaching the first peak at around 7am or 8am, and then dropping down until around 10am, and remaining comparatively flat from 10am to 4pm, and then rising to the second peak at around 8pm or 9pm, finally dropping down to the level same as the early morning. This trend can be explained by the general regulation of the occupants' activity and the usage of electric equipment in a hotel, i.e. guests using electric devices (equipment) and the facilities of electrical and mechanical systems operation reaching to the peaks in the morning and at nightfall periods because of living and catering requirements. For other types of buildings, the regulation of the occupants' activities and the facilities of electrical and mechanical systems operation should be in other ways due to the diverse functions of different types of buildings.

The annual maximum, minimum and average data were extracted and calculated for further investigation of the daily trend of large hotel, and the corresponding three curves were illustrated by the diagrams below.

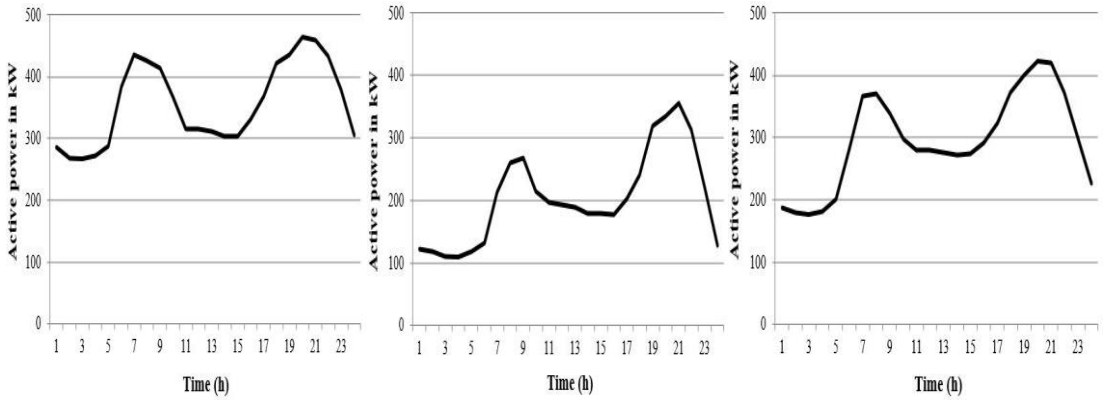

Maximum (a) Minimum (b) Average (c)

Fig. 4.1 Annual maximum, minimum, average daily changing trend.

As Fig. 4.1 shows, the levels of load consumption are slightly different among the three scenarios, but they follow a similar pattern. The annual average data is applied to building up representative profiles of load demand, and further investigation for the applicability of annual average data is provided in Section 4.4.2.1.

It is noted that the load consumption shown in Fig. 4.1 is in kW, but the load profile characteristics is of more concerned rather than the exact value of power usage in this project, and thus the methodology of 'per unit' is applied to demonstrate the daily curve of load demand for unified illustration. In the methodology of 'per unit', the daily peak value of load consumption is set as '1' and consequently the values of other hourly consumptions are less than '1'. The exact value of hourly load consumption in 'per unit' is determined by the kW of hourly consumption being divided by the daily peak value in kW. The hourly load consumption in kW and 'per unit' of large hotel is presented by the following table, and the daily profile of large hotel in per unit is presented by Fig. 4.2.

TABLE 4.2 Daily electrical load consumption in kW and per unit.

Hour	*1*	*2*	*3*	*4*	*5*	*6*	*7*	*8*	*9*	*10*	*11*	*12*
Load demand in kW	188	180	177	182	200	284	367	370	339	297	280	281
Load demand in per unit	0.44	0.42	0.42	0.43	0.47	0.67	0.87	0.87	0.80	0.70	0.66	0.66
Hour	*13*	*14*	*15*	*16*	*17*	*18*	*19*	*20*	*21*	*22*	*23*	*24*
Load demand in kW	275	273	273	293	323	372	401	423	419	372	300	228
Load demand in per unit	0.65	0.64	0.65	0.69	0.76	0.88	0.95	1.00	0.99	0.88	0.71	0.54

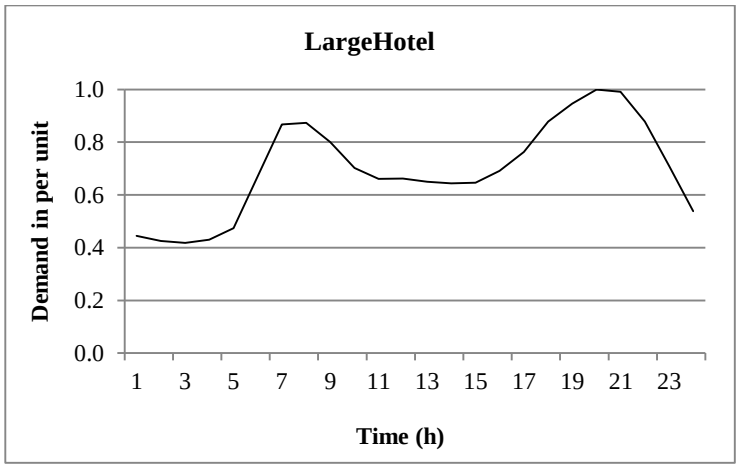

Fig. 4.2 Daily profile of electrical load demand changing of large hotel in per unit.

All daily curves of load consumption of fifteen types of buildings in 'per unit' are presented in Section 4.3.1.

4.2.2 PV system daily output

PV systems utilise solar insolation to generate electricity, and the operation principle can be learned from the two diagrams below.

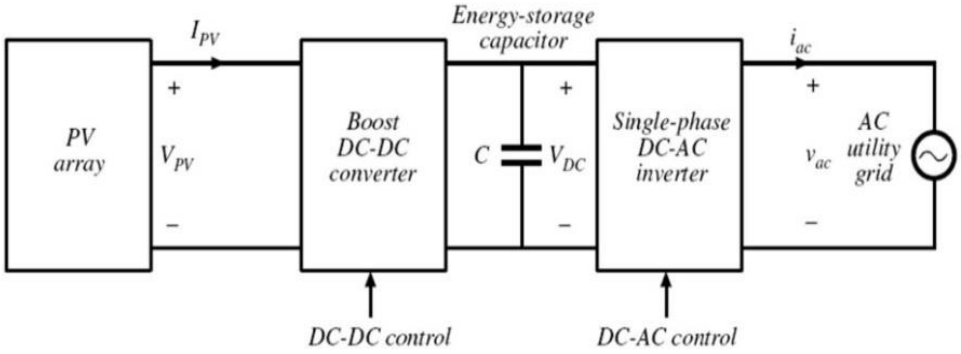

Fig. 4.3 Schematic diagram of grid-connected PV system [71].

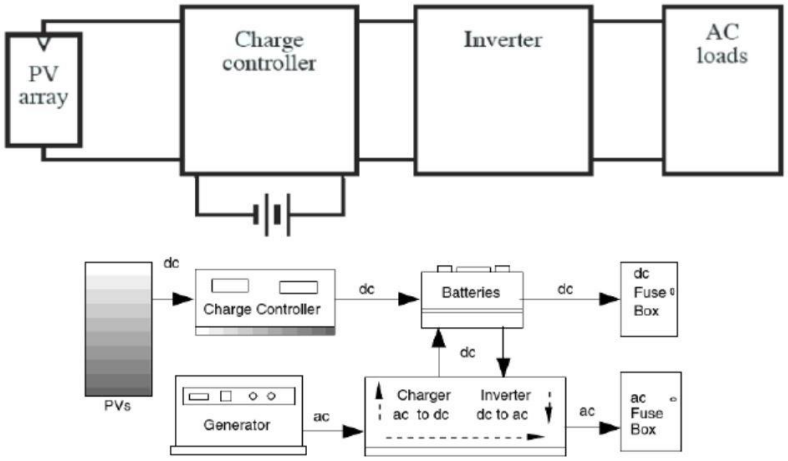

Fig. 4.4 Schematic diagram of stand-alone PV system [71].

It is noted that a grid-connected PV system can be directly connected to either loads or the utility grid. Through the direct connection to loads, the priority of the power supply to building loads can be achieved and the remaining power, if any, is fed into the utility grid. The direct connection to the utility grid is to feed overall PV generation into the grid. The two different connection methods are alternatively applied to different types solar tariffs or schemes, such as direct connection to the grid is for FiT and VNM, and NM requires the direct connection to loads.

By the comparison of grid-connected and stand-alone PV systems, it can be seen that the latter has a battery system to store excess on-site generated energy. Solar sharing tariff (VNM) is the core research interest of this study, which utilise the utility grid to share solar power. Therefore, calculations of the PV generation and ultimately evaluations of the various tariff schemes are limited to grid-connected PV systems.

The generation of grid-connected PV system in Wp can be calculated by (4.1-4.3) [71].

$$T_{cell} = T_{amb} + \left(\frac{NOCT-20}{0.8}\right) S \tag{4.1}$$

$$P_{DC} = P_{NOMINAL} \times (1 - \left(\frac{dp}{100}\right) \times (T_{cell} - 25℃))s \tag{4.2}$$

$$P_{AC} = P_{DC} \times \eta_{mismatchedmodules} \times \eta_{dirtloss} \times \eta_{inverter} \tag{4.3}$$

where T_{amb} in (4.1) is the ambient temperature [°C], T_{cell} [°C] is the PV panel internal cell temperature, which is calculated using PVUSA test condition data [73], in which

the irradiation (S) [W/m^2] is 1 kW/m^2. *NOCT* (module nominal operating temperature) is a constant value that is normally taken as 47 °C [73], which is the cell temperature measured at 20 °C ambient temperature, 800 W/m^2 irradiance, and 1m/s wind speed [11]. In (4.2), $P_{NOMINAL}$ is the rated power of a PV array, dp is the percentage of DC power drops that is normally, in case of mono-crystalline cell, valued at 0.5%/ °C . S is the irradiation on the cell surface, which for this study is a series of variable values introduced from an Australian public database of weather conditions. (4.3) is for the calculation of AC power output of a PV system from the result achieved by (4.2) multiplied by three efficiencies of mismatching modules, dirt covering, and inverter application, which are the main causes for the power loss of grid-connected PV systems [73].

Based on (4.1)-(4.3), a MATLAB simulation model was built up for the evaluation of daily PV system output. An Australian public database of weather conditions was used, from which the data from Wagga Wagga is taken as the input resource of ambient temperature (T_{amb}) and irradiation (S) for the simulation model [74]. Wagga Wagga is located approximately midway between the two largest Australian cities, Sydney and Melbourne, and has a typical temperate climate with a hot dry summer and a cool to cold winter. This temperate climate zone in Australia includes Sydney, Melbourne, Adelaide, ACT (Australian Capital Territory), Newcastle, and Wollongong, etc., which has the greatest population among all Australian climate zones and includes six of the top ten cities and areas of Australia. Therefore, the data of weather conditions of Wagga Wagga has a widespread applicability for the evaluation of PV system generation in the Australian context.

It is noted that the capacity of the simulated PV generator is valuated at 1 kW to match up with the peak load capacity of buildings under the methodology of ‘per unit’. The simulation results are presented in Section 4.3.2.

4.3 Categorising daily profiles of building electrical demand and PV system outputs

4.3.1 The profiles of electrical demand

All 15 types of buildings involved in the U.S. public database applied by this study were investigated and evaluated by the means introduced in Section 4.2.1 and the methodology of 'per unit'. The achieved annual average curves of 15 types of buildings are categorized into seven groups by building function and are presented in Table 4.3 below.

TABLE 4.3 Daily profile of electrical load demand of 15 categories of buildings.

Retail centre building	
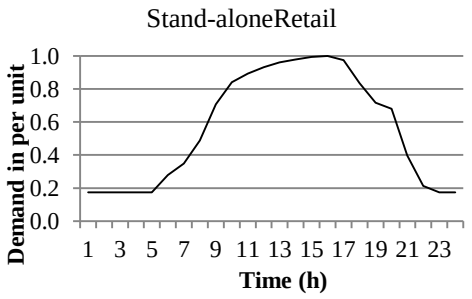	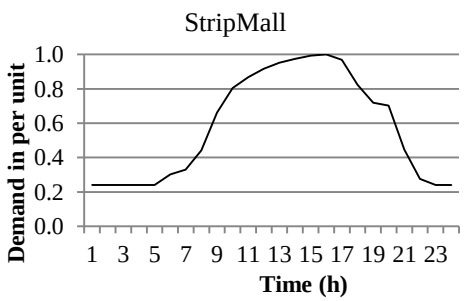
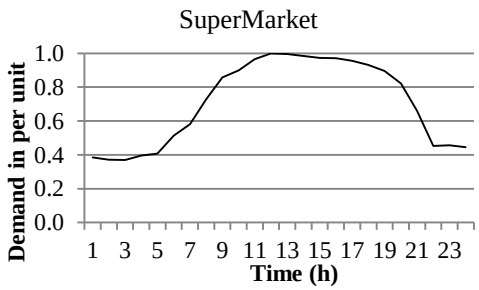	
Catering service building	
	

Education building

PrimarySchool

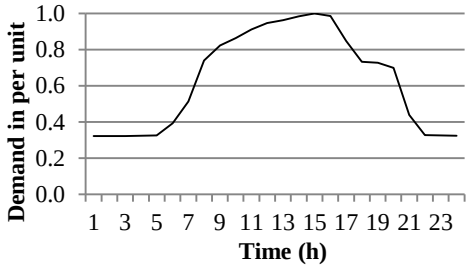

SecondarySchool

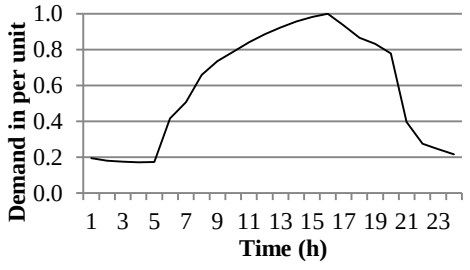

Commercial office building

LargeOffice

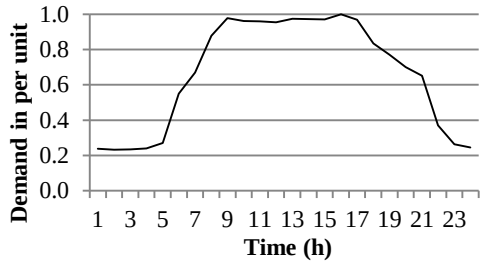

MediumOffice

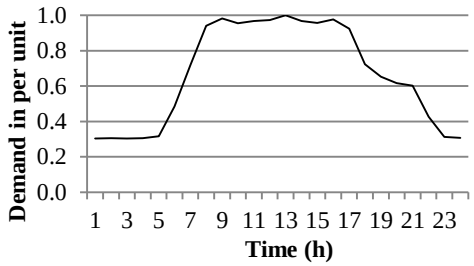

Small Office

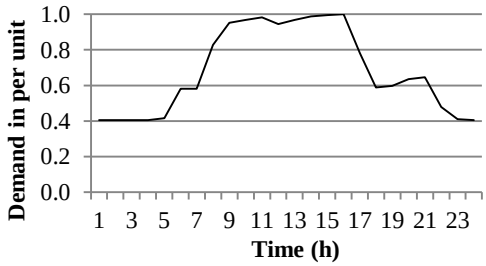

Hotel building

LargeHotel

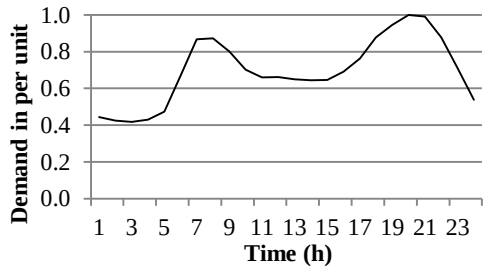

SmallHotel

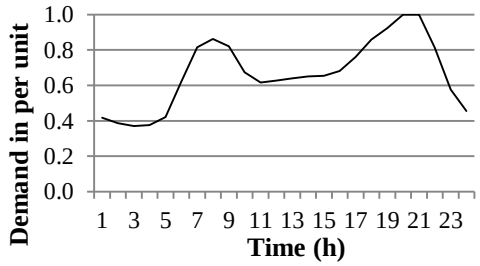

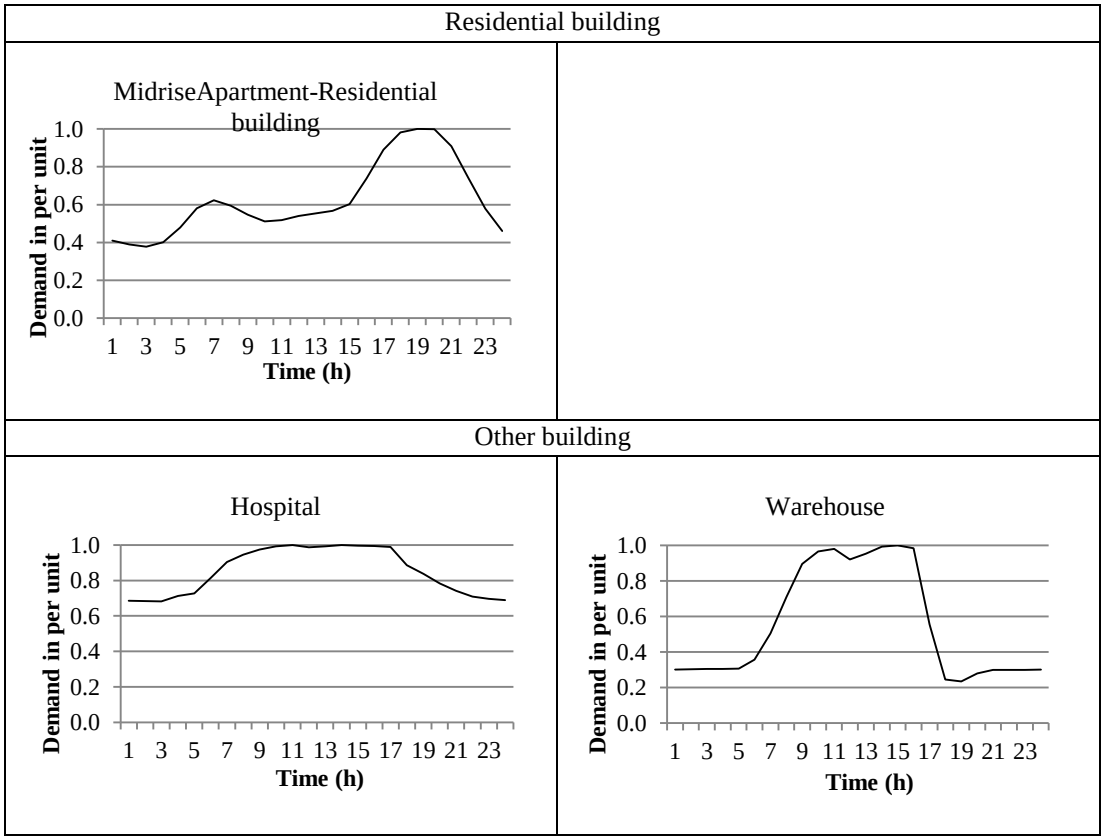

From Table 4.3, it can be seen that the demand curves of the buildings in a certain group have a similar pattern except the group of "other building". The residential building has a load-demand trend similar to the hotel building due to the similar building function of providing accommodation. The demand curves of the hospital and warehouse are with different patterns due to the totally different building functions, but the common feature of the load-demand trend of the two buildings is still shown, i.e. the time period with the peak load consumption covering the daytime from around early morning to late afternoon (7am–6pm), which could be determined by the similar operation hours (outpatient service hours for hospital). In summary, the buildings in a certain group have similar demand trends due to the shared types of occupant activities and the requirements of facility operation.

From Table 4.1, the daily demand trend of a large hotel does not follow a completely common curve. Even though the curves closely overlap together during the time period of from May to September, slight differences of hourly load consumption still can be seen by a more detailed observation. It has to be acknowledged that the annual average profile has less meaning for the calculation or prediction of the exact building load

consumption that [72] was working for. However, the purpose of investigating building demand in this study is to evaluate the impact on the financial performance of solar sharing tariff from the building load behaviour instead of calculating or predicting the exact value of the building consumption. Therefore, the demand curves are applicable to further investigation and evaluation within this study because it can represent the general daily changes of building demand.

4.3.2 The profiles of simulated grid-connected PV system output

By the simulation model introduced in Section 4.2.2, the annual AC outputs of an assumed PV system rated at 1 kW installed in Wagga Wagga are established and presented in Table 4.4 below.

TABLE 4.4 Year-round daily profiles of grid-connected PV system.

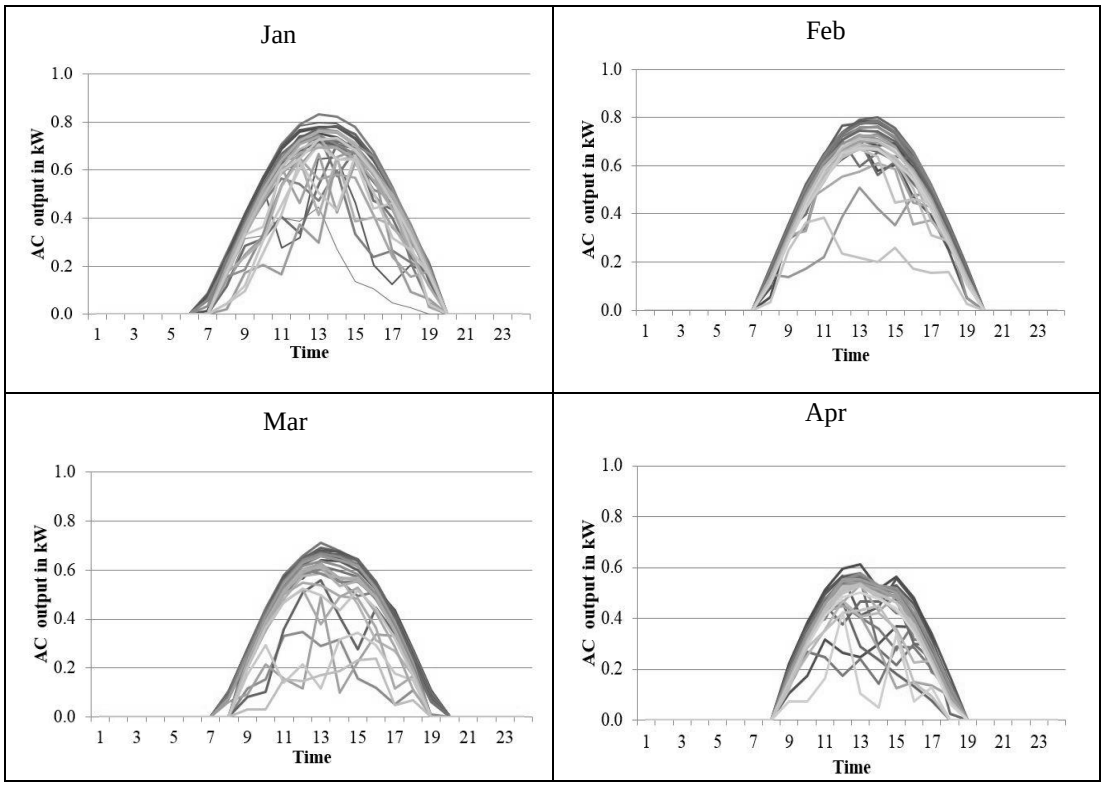

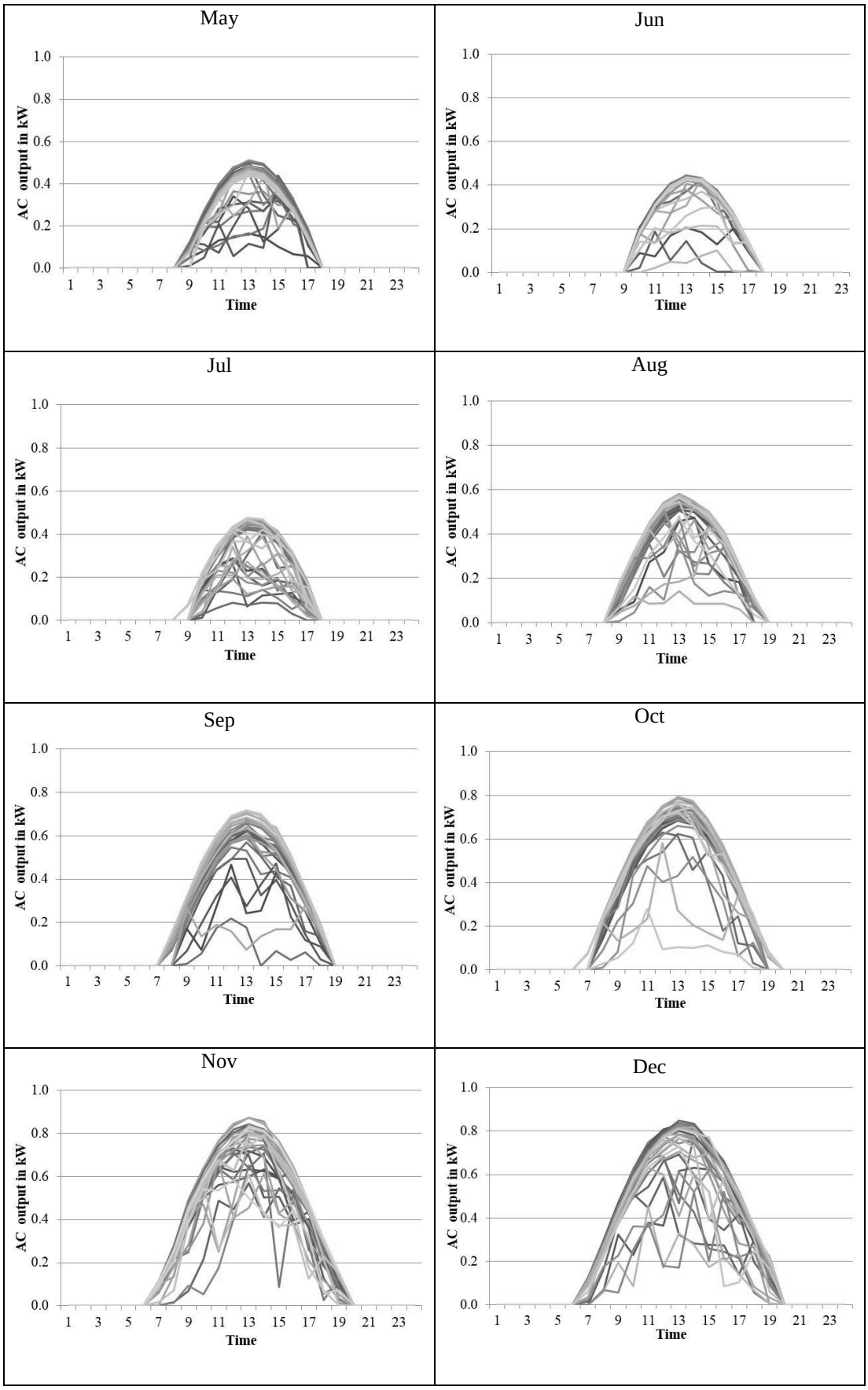
May
Jun
Jul
Aug
Sep
Oct
Nov
Dec
AC output in kW
Time
0.0
0.2
0.4
0.6
0.8
1.0
1 3 5 7 9 11 13 15 17 19 21 23

From Table 4.4, it can be seen that numbers of daily curves follow a common parabola-style shape. The annual average of daily PV output is shown in Fig. 4.5.

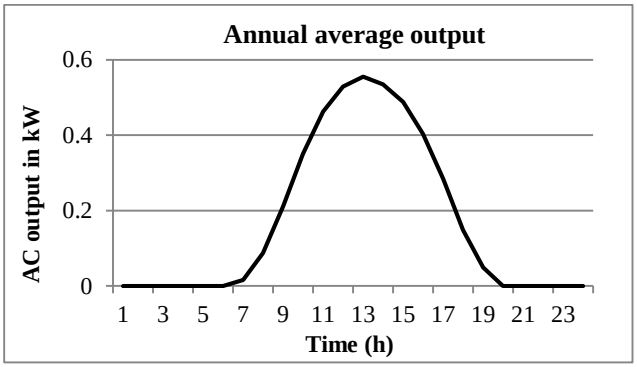

Fig. 4.5 Annual average curve of PV systems generation.

As previously discussed, the purpose of investigating building demand is to evaluate the impact on the financial performance of solar sharing tariff from the building load behaviour. The annual average profile was applied to further relevant evaluation. Similarly, for the development of the solar-generation curve, i.e. evaluating the impact on the financial performance of solar sharing tariff or scheme from the variation of daily PV generation. In addition, the annual average curve of daily solar generation is applied to the evaluation of VNM in Chapter 5. The further explanation for the practicality of the annual average curve is presented in Section 4.4 by introducing Australian utility schemes.

4.4 Profiles of building consumption and PV generation based on utility tariff

In order to study the impact on the financial performance of solar sharing tariff from the behaviour of building demand and PV system output, utility tariff is a key point, because it links the profiles of building demand and PV system output to energy costs and investment recovery of the solar system. Therefore, utility tariff needs to be investigated in detail. This study refers to the schedules of charges of ActewAGL.

4.4.1 Utility tariffs in Australia

ActewAGL comprises a retail joint venture between AGL Energy and ACTEW Corporation and a distribution joint venture between Singapore Power and ACTEW Corporation, and it is one of nation's biggest utilities for generating and selling

electricity and gas. Therefore, the rules involved in the schedules of electricity charges of ActewAGL are representative for further economic evaluation. Some relevant tariff charges, taken from [75], are presented in the diagrams below.

Home

Electricity	Unit	2013-14 GST exclusive	2013-14 GST inclusive
Supply charge	¢ per day	69.8800	76.8680
Supply charge with Controlled load 1	¢ per day	74.6200	82.0820
Supply charge with Controlled load 2	¢ per day	74.6200	82.0820
Consumption for the first 1,750 kWh per quarter	¢/kWh	24.6600	27.1260
Consumption thereafter	¢/kWh	27.4100	30.1510
Controlled load 1 consumption	¢/kWh	8.6000	9.4600
Controlled load 2 consumption	¢/kWh	13.3600	14.6960

Home time-of-use

Electricity	Unit	2013-14 GST exclusive	2013-14 GST inclusive
Supply charge	¢ per day	89.8800	98.8680
Supply charge with Controlled load 1	¢ per day	94.6200	104.0820
Supply charge with Controlled load 2	¢ per day	94.6200	104.0820
Peak consumption	¢/kWh	35.7700	39.3470
Shoulder consumption	¢/kWh	27.5100	30.2610
Off-peak consumption	¢/kWh	13.8800	15.2680
Controlled load 1 consumption	¢/kWh	8.6000	9.4600
Controlled load 2 consumption	¢/kWh	13.3600	14.6960

Fig. 4.6 Electricity charges for residential customer [75].

Business

Electricity	Unit	2013-14 GST exclusive	2013-14 GST inclusive
Access charge	¢ day	87.0700	95.7770
Access charge with Controlled load 1	¢ day	91.8100	100.9910
Access charge with Controlled load 2	¢ day	91.8100	100.9910
Consumption for the first 2,500 kWh per quarter	¢/kWh	23.2700	25.5970
Consumption thereafter	¢/kWh	25.1800	27.6980
Controlled load 1 consumption	¢/kWh	8.6000	9.4600
Controlled load 2 consumption	¢/kWh	13.3600	14.6960

Business time-of-use

Electricity	Unit	2013-14 GST exclusive	2013-14 GST inclusive
Access charge	¢ per day	91.9600	101.1560
Peak energy	¢/kWh	33.9700	37.3670
Shoulder energy	¢/kWh	27.6900	30.4590
Off-peak energy	¢/kWh	13.7700	15.1470

Fig. 4.7 Electricity charges for business customer [75].

From Fig. 4.6 and 4.7, it can be seen that the tariff charges of each of the four schedules can be divided into two components, i.e. service charge (¢/day) and energy charge (¢/kWh). For simplified investigation and evaluation, this study only takes into account energy charge for the financial studies related to utility tariff. In addition, the energy charge can be categorized into two types, i.e. floating price by load type and amount, and time-varying price. For example, in 'Home' and 'Business', the energy charges of *Controlled load 1* and *load 2* are different, and in time-of-use (TOU), the energy charge is classified as peak energy, shoulder energy and off-peak energy, which are, respectively, corresponding to three different daily time periods as 'peak period' - 1pm to 8pm, 'shoulder period' - 7am to 1pm and 8pm to 10pm, and 'off peak period' –

from 8pm to next day 7am [75]. This study applies the time frames of TOU as the time reference to further relevant economic evaluation.

In this study, floating price by load type and amount is defined as fixed-rate due to the single price for a certain amount or type of load and TOU is used to represent time-varying price for brief discrimination of the types of utility tariffs. It is easily understood that fixed-rate utility schedule makes the PV-generated electricity a single rate, and PV-generated electricity can represent different values within TOU if PV generation compensates the customer energy usage in the form of either kWh or kWh credit. Therefore, the application of different types of utility tariffs must result in different financial profits for a solar owner. In addition, it can be understood that the different profile of load demand will cause different energy cost for a customer with the application of TOU, because the proportions of the energy consumed, respectively, in peak, shoulder and off-peak periods with different profile of load demand will also vary.

4.4.2 Proportion of building consumption and PV generation under utility tariffs

4.4.2.1 Proportion of building consumption

As previously analysed, utility tariff is a critical point for the evaluation of energy costs and the investment recovery of the PV systems, and utility schedules of electricity charges can be categorised as fixed-rate and TOU.

Fixed-rate utility scheme charges building energy usage during any time at a single price in terms of a certain type or amount of load, and whereas load consumption is charged at different prices under TOU. For the clear demonstration of the proportions of building load consumption in different daily time period, the above achieved curve of building consumption is transformed into the form of histogram by the reference of fixed-rate and TOU utility tariffs. The example transformed profiles – large hotel are presented by the diagrams below.

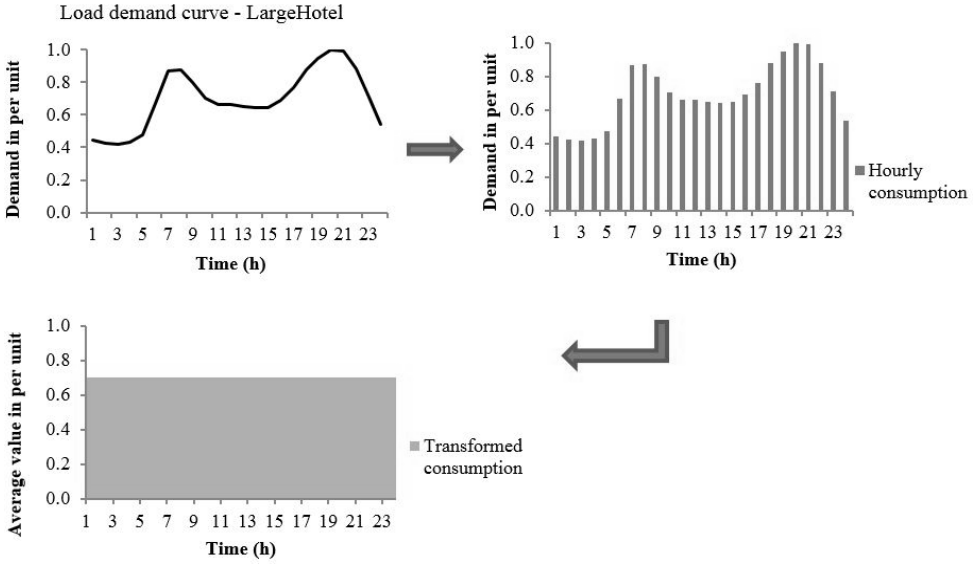

Fig. 4.8 Transformed profile of load demand under fixed-rate tariff.

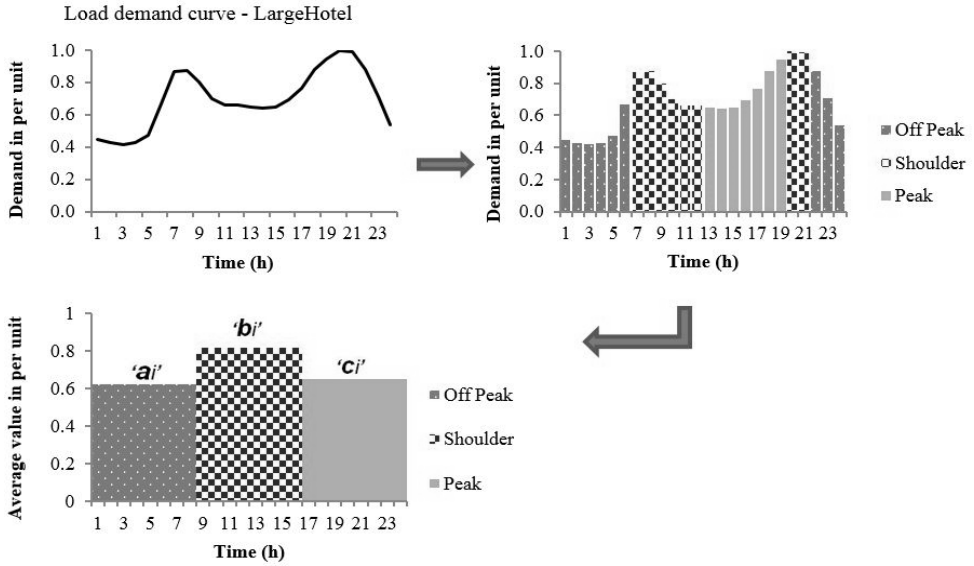

Fig. 4.9 Transformed profile of load demand under TOU.

Fixed-rate schedules do not have any time frame to price the electricity, and consequently daily consumption, i.e. the area under the curve of load demand, is transformed into a single column as shown in Fig. 4.8. By contrast, there are three daily time periods scheduled by TOU - 'peak', 'shoulder', and 'off peak', which are, respectively, labelled by *'ai'*, *'bi'*, and *'ci'*, and consequently, the daily consumption is transformed into three columns as shown in Fig. 4.9.

The applicability of using annual average data to establish the representative profile of load demand is still a concern, as mentioned in Section 4.2.1. On the other hand, from

Fig. 4.8 and Fig. 4.9, it is obvious that the transformed profile can more directly demonstrate the proportion of the energy consumed in the different time periods determined by the utility tariff. Therefore, the transformed profile is applied to further financial evaluation. As shown in Fig. 4.9, daily load consumption is transformed into three columns with the application of TOU, and this study uses the percentage of the energy consumed in peak, shoulder and off-peak periods, respectively, over the total daily consumption to present the three proportions of energy usage. The year-round three percentages of the load consumption of the example building, the large hotel, were investigated to verify the applicability of annual average data, and the results are illustrated by the diagrams below.

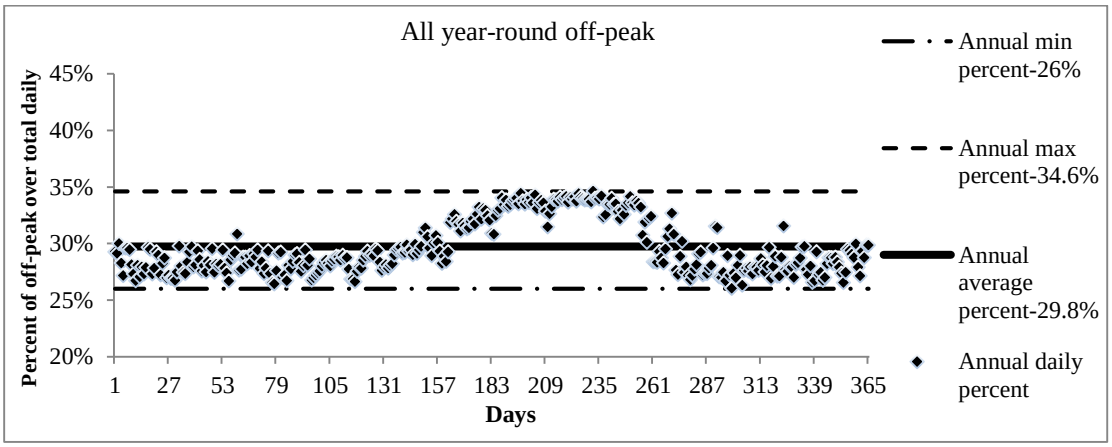

Fig. 4.10 Annual percentage of energy consumed during the shoulder period over total daily energy consumption under TOU.

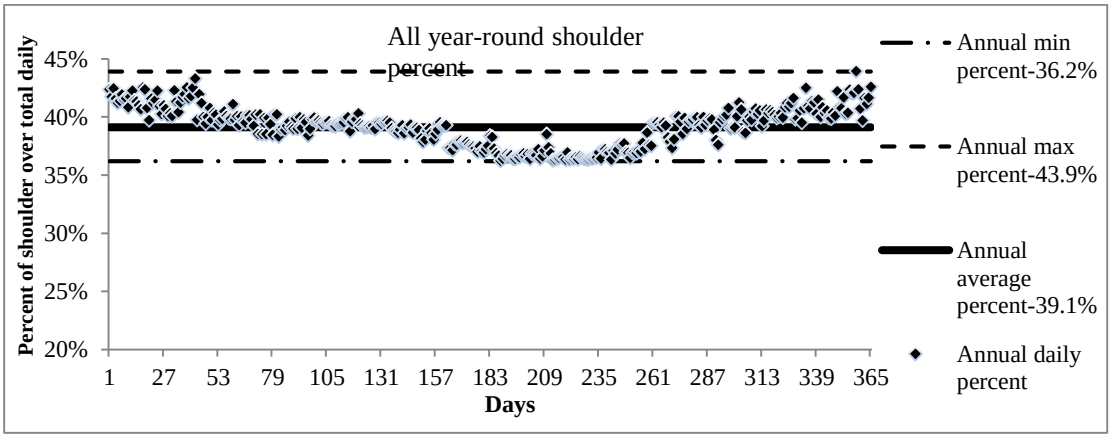

Fig. 4.11 Annual percentage of energy consumed during the off-peak period over total daily energy consumption under TOU.

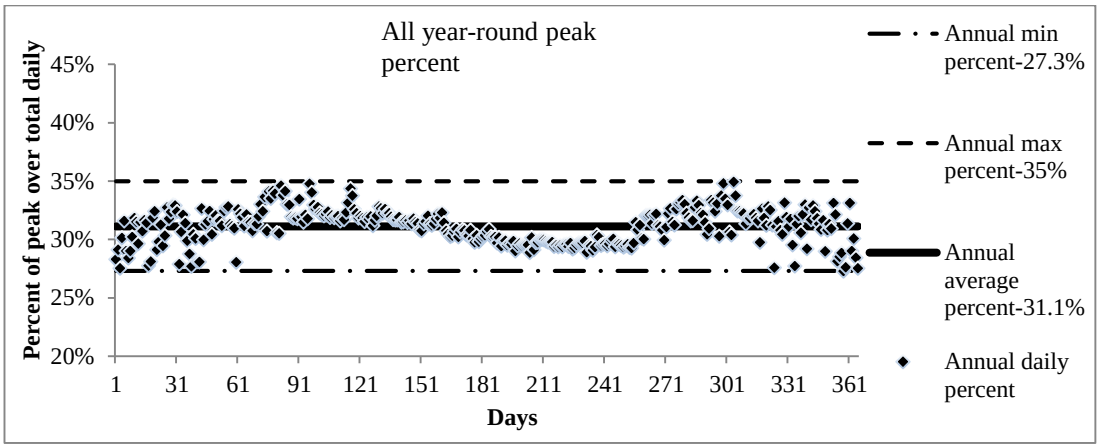

Fig. 4.12 Annual percentage of energy consumed during the peak period over total daily energy consumption under TOU.

From Fig. 4.10 to Fig. 4.12, the off-peak percentage of overall 365 are distributed between 34.6% (annual maximum value) down to 26% (annual minimum value), and the deviation is +4.8% to -3.8% comparing to the annual average percentage of 29.8%. For the shoulder percentage, all data points are distributed between 43.9% - annual maximum value to 36.2% (annual minimum value), and the deviation is +4.8% to -2.9% comparing to the annual average percentage of 39.1%. The annual peak percentage has a deviation between +3.9% (annual maximum value) and -3.8% (annual minimum value) comparing to the annual average percentage of 31.1%. All three deviations of +4.8% to -3.8%, +4.8% to -2.9% and +3.9% to -3.8% demonstrate an obvious central tendency of year-round data to the annual average value. Therefore, this study applies the annual average data to building up the representative profiles of load consumption of 15 categories of buildings for the relevant investigation and evaluation.

As Fig. 4.9 demonstrated, energy costs for consuming utility electricity with the application of fixed-rate utility schedule only depend on the amount of energy consumption, i.e. the area under the load demand curve without any impact from the pattern of building load demand. By contrast, the energy costs by the implementation of TOU can be influenced by both consumption amount and the profile due to the various prices for electricity consumed in the different time periods. The proportions of daily load consumption of 15 categories of buildings are evaluated and presented in the following table.

TABLE 4.5 Proportions of load consumption of the 15 categories of buildings.

	Building Category	The proportion of annual energy consumption during off-peak period- ***'ai'***	The proportion of annual energy consumption during shoulder period- ***'bi'***	The proportion of annual energy consumption during peak period- ***'ci'***	The approximate ratio of three proportions	Daily consumed energy in per unit method (kWh)
1	Full Service Restaurant	25.15%	39.40%	35.45%	1:1.6:1.4	17.68
2	Quick Service Restaurant	26.5%	38.6%	34.9%	1:1.5:1:3	18.15
3	Warehouse	20.9%	41.8%	37.3%	1:2:1.8	13.32
4	Hospital	31.3%	35.9%	32.8%	1:1.2:1.1	20.42
5	Stand-alone Retail	12.7%	39.3%	48.0%	1:3.1:3.8	13.45
6	Strip Mall	16.3%	37.3%	46.4%	1:2.3:2.8	13.86
7	Supermarket	22.3%	38.3%	39.4%	1:1.7:1.8	17.02
8	Primary School	19.7%	39.1%	41.1%	1:2:2.1	15.17
9	Secondary School	14.5%	39.6%	46.0%	1:2.7:3.2	14.12
10	Small Office	23.9%	39.9%	36.1%	1:1.7:1.5	16.37
11	Medium Office	19.1%	42.2%	38.7%	1:2.2:2	16.02
12	Large Office	16.6%	42.5%	40.9%	1:2.6:2.5	15.89
13	Small Hotel	27.7%	40.0%	32.3%	1:1.4:1.2	16.02
14	Large Hotel	29.8%	39.1%	31.1%	1:1.2:1	16.76
15	Midrise apartment	29.5%	35.0%	35.6%	1:1.2:1.2	15.00

Fourteen out of 15 categories of buildings investigated by this study are non-residential buildings (except for the 'midrise apartment'), and consequently, this study takes the values of energy charge of 'Business TOU' shown by Fig. 4.8 as the reference of electricity rates for further financial evaluation. In 'Business TOU', peak and shoulder rates are, respectively, 0.37 and 0.3 $/kWh, which are much higher than the off-peak rate of 0.15 $/kWh. From Table 4.6, the off-peak consumption is always the lowest among the three proportions of energy usage. Therefore, this study takes the shoulder and peak rates as the critical indicators for further financial discussion. By the comparison of the magnitude of the load consumption in shoulder and peak periods, the 15 types of buildings can be categorized into two groups - the buildings with the highest shoulder consumption and the buildings with highest peak consumption.

TABLE 4.6 Transformed profile of load demand of the 15 categories of buildings.

Load consumption profile with highest shoulder	Load consumption profile with highest peak
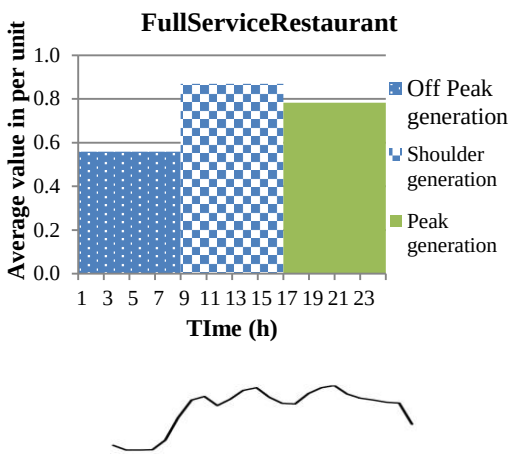	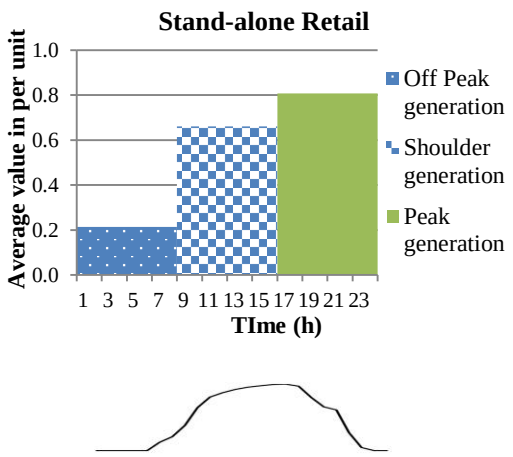
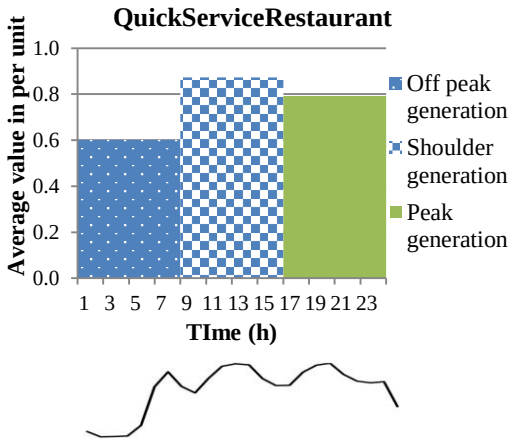	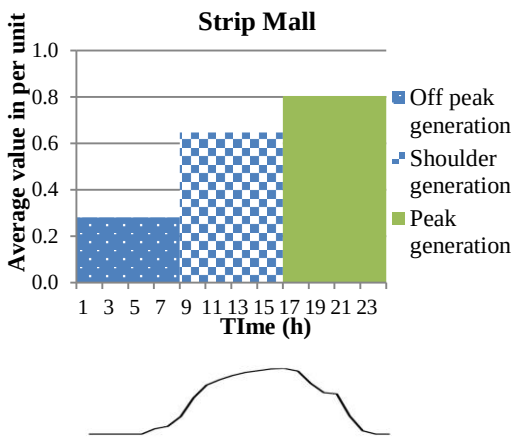
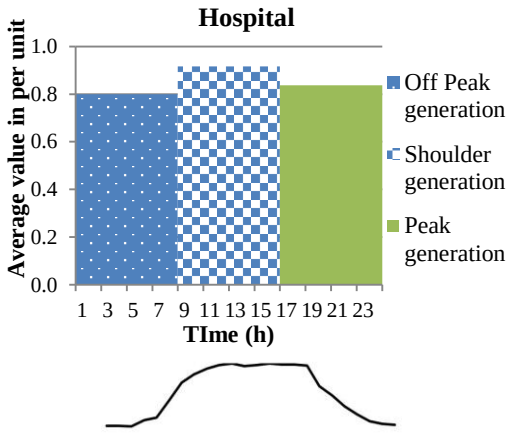	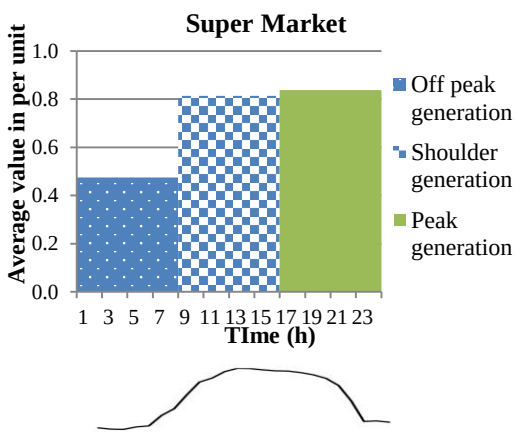

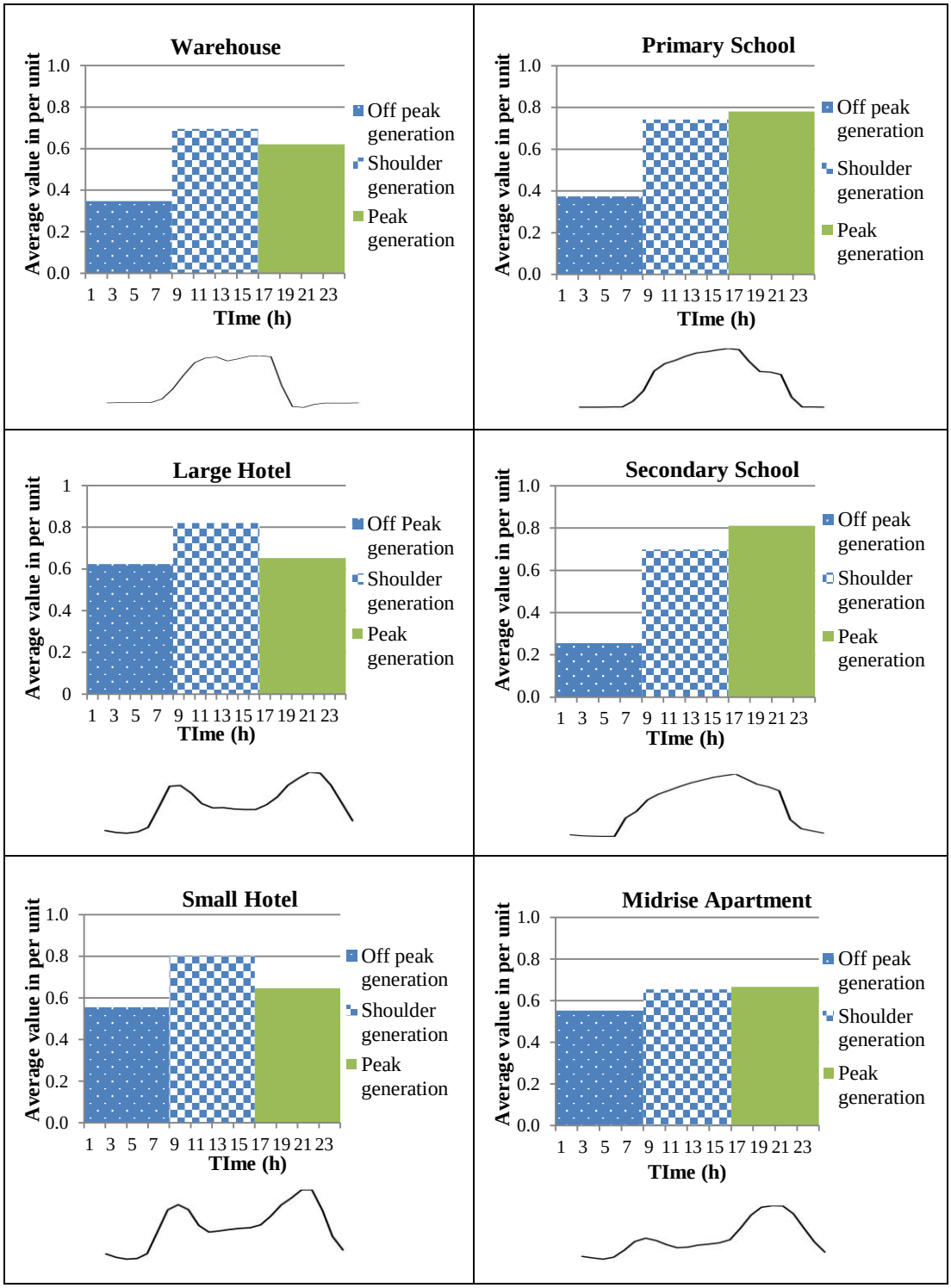
Warehouse
Average value in per unit
1.0
0.8
0.6
0.4
0.2
0.0
1 3 5 7 9 11 13 15 17 19 21 23
TIme (h)
Off peak generation
Shoulder generation
Peak generation
Primary School
Average value in per unit
1.0
0.8
0.6
0.4
0.2
0.0
1 3 5 7 9 11 13 15 17 19 21 23
TIme (h)
Off peak generation
Shoulder generation
Peak generation
Large Hotel
Average value in per unit
1
0.8
0.6
0.4
0.2
0
1 3 5 7 9 11 13 15 17 19 21 23
TIme (h)
Off Peak generation
Shoulder generation
Peak generation
Secondary School
Average value in per unit
1.0
0.8
0.6
0.4
0.2
0.0
1 3 5 7 9 11 13 15 17 19 21 23
TIme (h)
Off peak generation
Shoulder generation
Peak generation
Small Hotel
Average value in per unit
1.0
0.8
0.6
0.4
0.2
0.0
1 3 5 7 9 11 13 15 17 19 21 23
TIme (h)
Off peak generation
Shoulder generation
Peak generation
Midrise Apartment
Average value in per unit
1.0
0.8
0.6
0.4
0.2
0.0
1 3 5 7 9 11 13 15 17 19 21 23
TIme (h)
Off peak generation
Shoulder generation
Peak generation

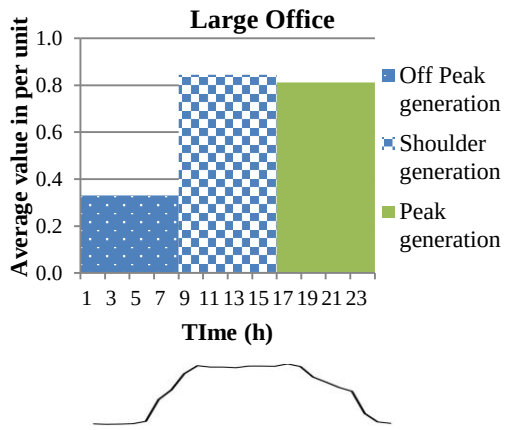

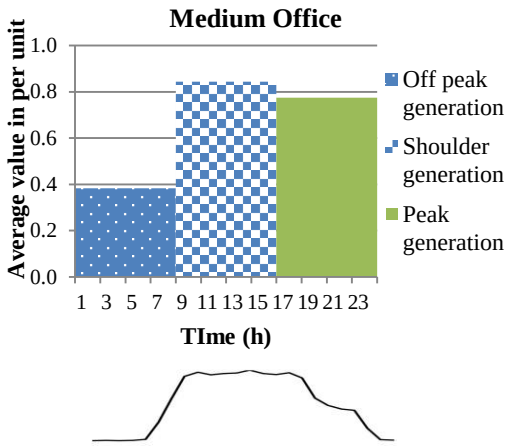

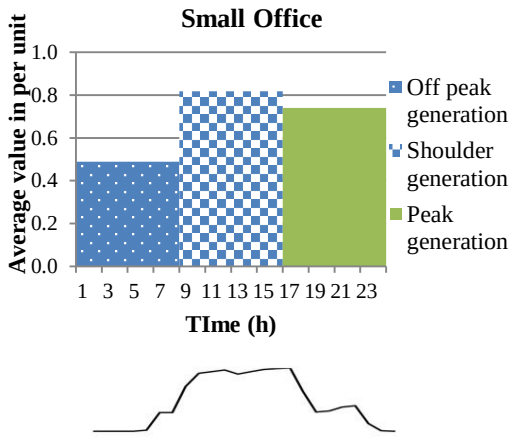

(Note: the histogram-styled profiles and the corresponding curves are both presented for a clear comparison.)

From Tables 4.6 and 4.7, it is clear that the histogram profile is more practical than the curve for financial evaluation, because the energy costs can be easily achieved by the proportions of load consumption (in kWh) multiplied by the rates of utility tariffs. Therefore, the transformed profiles illustrated in Table 4.7 are applied to evaluating

the impact on the financial performance of solar tariff from the profile of building load demand based on utility tariffs. It is very hard, however, to apply overall 15 categories of load profile to relevant evaluation, and consequently, this study takes some types of buildings with typical proportion features, such as small hotel, stand-alone retail and hospital, for later relevant investigation and evaluation.

4.4.2.2 The proportion of PV generation

As the above analysed, the transformed profile of load consumption is more practical than curve for the relevant financial evaluation of this study. Similarly, the transformed profile of PV system generation is required for later relevant studies, and is presented by the diagrams below.

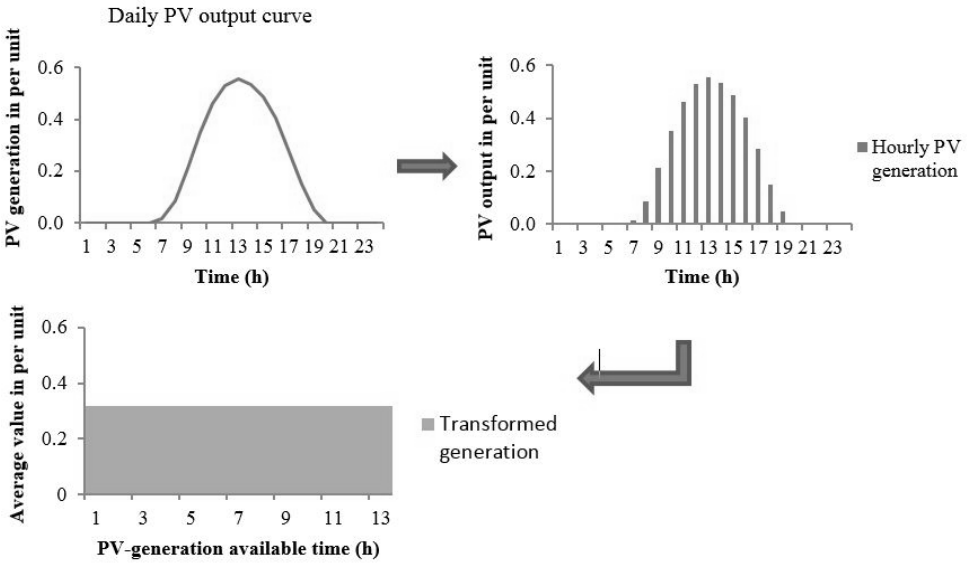

Fig. 4.13 Transformed profile of PV generation under fixed-rate tariff.

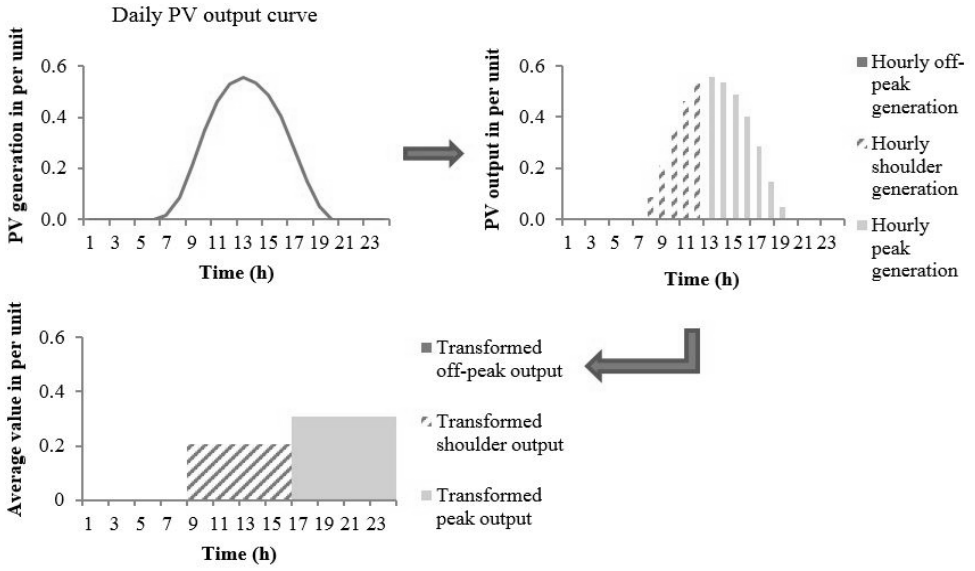

Fig. 4.14 Transformed profile of PV generation under TOU.

As Fig 4.13 shows, daily PV generation is transformed into a single column under the fixed-rate due to the single price for a certain type or amount of load. By contrast, the same PV system generation is illustrated by two columns, as shown in Fig 4.14, by the transformation under TOU due to the various rates for the energy consumed in different time periods. It is noted that the demonstration of only two columns under TOU indicates that solar generation is unavailable during off-peak hours, which has detailed demonstration herein below.

In Section 4.4.2.1, it has been shown that the practicability of annual average data for building up the representative profile of load consumption by Fig. 4.10 to Fig. 4.12. By the same means, the year-round percentages of the PV generation produced in peak, shoulder, and off-peak periods, respectively, over total daily generation are presented by the diagrams below.

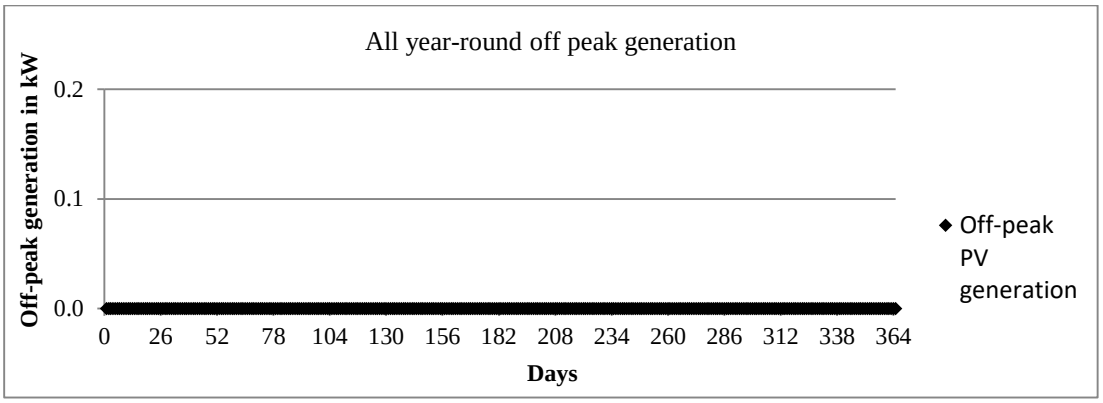

Fig. 4.15 Annual percentage of off-peak PV generation over total daily generation**.**

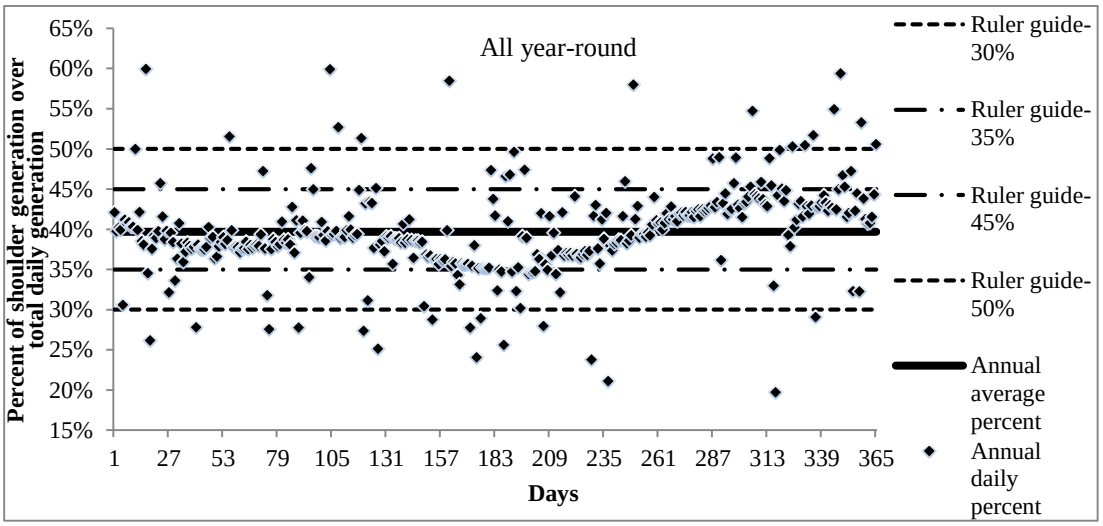

Fig. 4.16 Annual percentage of shoulder PV generation over total daily generation.

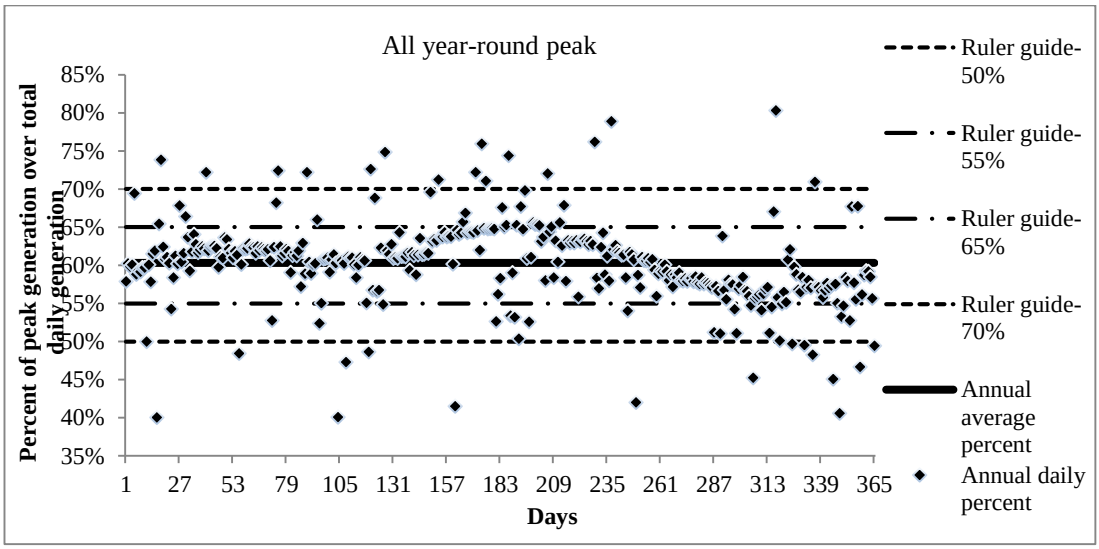

Fig. 4.17 Annual percentage of peak PV generation over total daily generation.

Fig. 4.15 shows there is no PV output in off-peak period every day all year long because sun insolation is very low or zero at night and early morning (from 11pm to next day 6am). As shown in Fig. 4.16, the annual-average shoulder percentage is 39.7%, and there are 334 out of 365 data points distributed between 30% and 50% with the deviation of around ±10% comparing to the annual-average value of 39.7%. 284 out of 365 data points stand between 35% and 45% with the deviation of ±5%. The annual-average peak percentage stands by 60.3% shown by Fig 4.17, and there are 334 out of 365 data points distributing between 50% and 70% with the deviation of ±10% comparing to annual-average value of 60.3%. 284 out of 365 data points stand between 55% and 65% with the deviation of ±5% comparing to the annual-average value of 60.3%.

It is noted that the annual shoulder and peak percentage have same numbers of data points, respectively, by 284 and 334 with the deviations of ±5% and ±10%, because the weather conditions such as sun insolation and temperature have direct impact on PV system output, and consequently, solar generation in shoulder and peak periods each day have similar deviation. The results by 284 and 334 out of 365 year-round data points, respectively, with the deviations of ±5% and ±10% comparing to the annual average percentages of 39.7% and 60.3% shows an obvious central tendency. Therefore, the annual average data is applied to establishing the representative profile of daily PV generation and used for further financial evaluation.

4.5 Summary

This chapter has illustrated the purpose of developing the profiles of load usage and PV system output, i.e. evaluating the impact on the financial performance of solar sharing tariff from the behaviour of building load and solar system output with the reference of utility tariffs. The year-round curves of load demand and PV output achieved by data analysis and software simulation show the daily trend of building consumption and solar generation, respectively, has a representative pattern.

In order to link the profiles of load demand and PV output to the further financial evaluation of this study, two types of utility billing schedules in the Australian context, i.e. fixed-rate and TOU, were introduced. Based on the fixed-rate and TOU, the achieved curves of building consumption and PV generation were transformed into the form of histogram, which is more practical than the curve for the evaluation of the energy cost and the cost saving from the utilisation of solar power. It is demonstrated that the energy cost and the cost saving are only dependant on the amount of load consumption and solar generation under fixed-rate schedule, and the energy cost and the cost saving are determined by both the amount of consumption and generation and the profiles of load demand and PV system output under TOU.

By the application of the fixed-rate and TOU, the applicability of using annual average data to establish the representative profiles of building consumption and PV generation has been verified. The annual maximum deviation of +4.8% ~-3.9% for building consumption and the deviation of ±5% of 284 data and ±10% of 334 data for PV generation compared to annual average value show year-round data points of load consumption and PV generation with obvious central tendency to the annual average data. Therefore, this study applies the annual average profile to evaluating the correlation of the behaviour of load demand and PV output and financial performance of VNM in Chapter 5.

Chapter 5 Economic Performance of VNM Based on Daily Trends of Building Demand and PV Generation

5.1 Financial evaluation of VNM

As introduced in Chapter 3, VNM is a rolling over credit arrangement for allocating credits from a shared PV system [69]. Participants of a VNM program can be either units in a common building or several individual buildings within a local precinct, as shown in Fig. 5.1. This chapter focuses on the situation where the shared solar generation plant(s) serves several individual buildings shown as Fig. 5.1 (b).

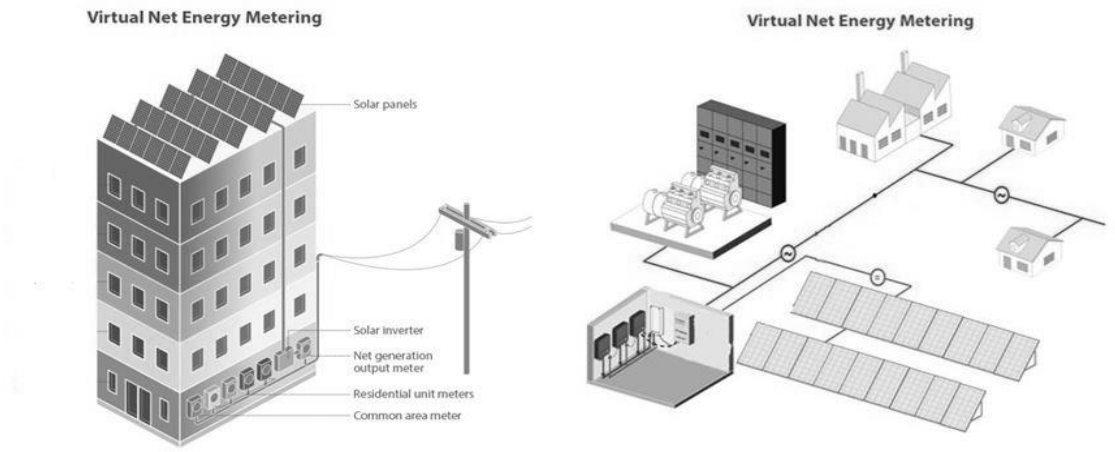

(a) (b)

Fig. 5.1 Schematic of VNM [76].

In this chapter financial evaluations of VNM schemes are undertaken using payback period as the economic indicator. Existing VNM laws for allocating VNM credits to qualified customers are utilised for the evaluations, with the issue of what to do with left over credits addressed. A number of new mathematic models are developed to demonstrate cost of energy consumption and cost saving through the use of VNM. The correlation between payback period and the profile of building energy usage is analysed and shown to be a key factor in impacting the successful VNM implementation for public buildings.

5.2 Establishing mathematic models

Fig. 5.2 introduced from Chapter 4 presents the assumptions used for establishing mathematic models in this chapter.

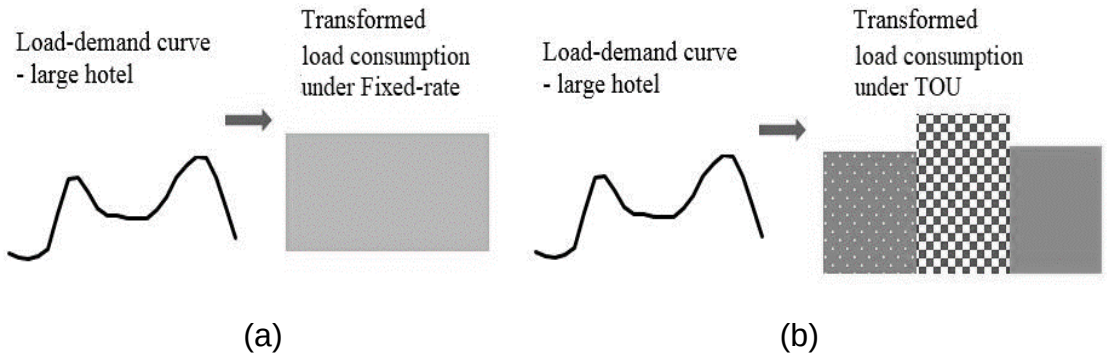

Fig. 5.2 Transformed profile of building demand under (a) fixed-rate and (b) TOU

As Fig. 5.2 (a) shows, fixed-rate tariff charges utility electricity at a time invariable price, so the transformed histogram is presented by a single column. By contrast, as Fig. 5.2 (b) shows, the transformed histogram has three individual parts due to three different rates under TOU, and this research uses *'ai', 'bi'* and *'ci'* to respectively represent the percentages of load usage consumed in different periods (off peak, shoulder and peak) over total daily consumption (represented by *'x'* in kWh). In addition, *'i'* represents individual participant involved in a VNM group, so *i = 1, 2, 3… n*. 'r_1', 'r_2' and 'r_3' respectively represent the different rates set for off peak, shoulder and peak periods. Under the fixed-rate, it can be understood that 'r_1', 'r_2' & 'r_3' have the same value, and a single column represents daily consumption instead of individual *'ai', 'bi'* & *'ci'* parts.

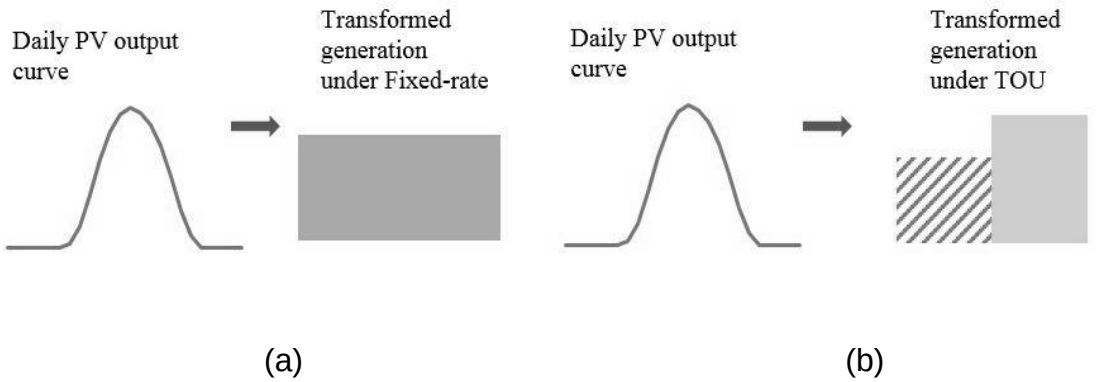

Fig. 5.3 Transformed profile of PV generation under (a) fixed-rate and (b) TOU.

Under the fixed-rate, daily PV generation was presented by a single column due to the fixed price for any time shown by Fig 5.3 (a). As Chapter 4 presented, PV system generation occurs only in the TOU periods of shoulder and peak, and the output during off-peak is zero. 'd_i' and 'e_i' are used to respectively represent the percentages of solar power generated in shoulder and peak periods over total daily generation, as Fig. 5.3 (b) shows. This chapter uses *'y'* to represent total daily generation (in kWh). As Chapter 3 outlined, PV generation kWh credits are rolled over to customer bills to offset load usage in a VNM program, so the allocated credits can be valued by the cost saving of customers. This study uses the shoulder and peak rates of TOU, as 'r_2' & 'r_3', to evaluate the reflected value of PV generation when TOU is applied. Overall variables related to building consumption and PV generation are summarized in Table 5.1 below.

TABLE 5.1 Variables.

x_i	Building consumption during a certain period (such as daily, monthly, or annual) in kWh
y_i	Generation or allocated credits from PV generation under VNM during a certain period (such as daily, monthly, or annual) in kWh
a_i	Percentage of load consumption in off-peak period, %
b_i	Percentage of load consumption in shoulder period,%
c_i	Percentage of load consumption in peak period,%
d_i	Percentage of PV generation in shoulder period,%
e_i	Percentage of PV generation in peak period,%
r_1	Price for off-peak period, $/kWh
r_2	Price for shoulder period, $/kWh
r_3	Price for peak period, $/kWh
	$a_i + b_i + c_i = 1$; $d_i + e_i = 1$
	('i' is participant set of a VNM program, $=1, 2, 3, \ldots\ldots n$)

5.2.1 Cost of building consumption

Based on the established variables shown in Table 5.1, the cost for consuming utility electricity can be presented as below,

Cost of building consumption

$$= r_1 \times (a_i \times x_i) + r_2 \times (b_i \times x_i) + r_3 \times (c_i \times x_i) = x_i \times (r_1 \times a_i + r_2 \times b_i + r_3 \times c_i) \quad (5.1)$$

As the above analyses, it is given $r_1 = r_2 = r_3$ under fixed-rate utility tariff and $a_i + b_i + c_i = 1$, so the specific form of (5.1) under the fixed-rate can be expressed as,

$$\textit{Cost of building consumption}_{\textit{ under fixed-rate}} = x_i \times r \quad (5.2)$$

(5.1) and (5.2) are used for further economic analyses. In addition, based on the above two formulas, 'x_i' is the metered building load consumption, the last part of '$r_1 \times a_i + r_2 \times b_i + r_3 \times c_i$' is variable depending on the profiles of building load consumption and the rates of utility tariffs. A study was developed to evaluate the correlation between building demand profiles and the costs of load usages. A function was built up as per the below to develop the relevant further evaluations for the last part of (5.1),

$$f(a,b,c) = r1 * a + r2 * b + r3 * c \tag{5.3}$$

From mathematic knowledge, (5.3) can be geometrically demonstrated by a plane, and all possible points of a, b, c, the sum of which is '1' as the defined in Table 5.1, are within the plane. The linear function of (5.3) attains its critical points at the boundaries, the values of which are r_1, r_2 and r_3. By introducing the values of TOU rates, which are 0.15 \$/kWh for off-peak period, 0.3 \$/kWh for shoulder period, and 0.37 \$/kWh for peak period, a 3D figure was established and presented by Fig 5.4.

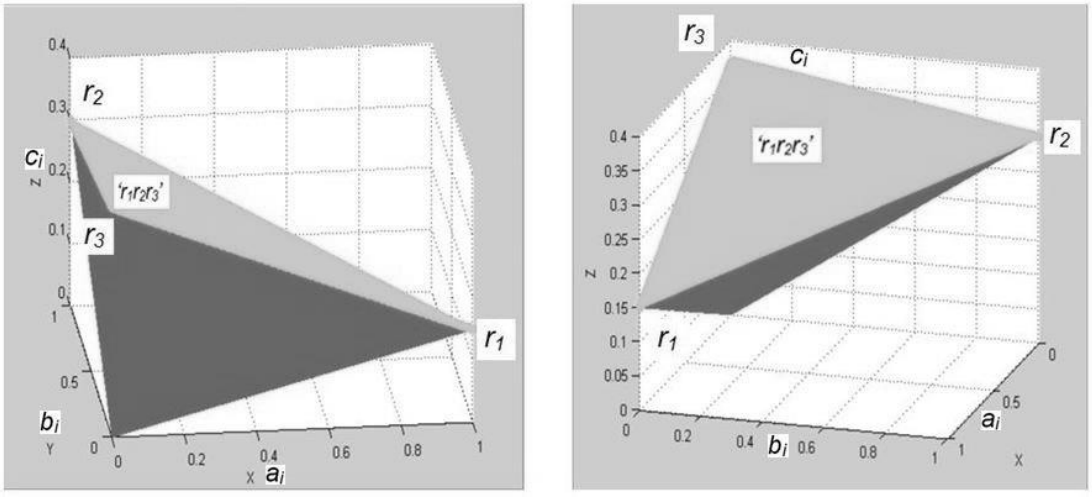

Fig. 5.4 Financial presentation of load profile under TOU.
(Note: the left and right graphs illustrate a same 3D figure from two views.)

As the above mentioned, put TOU rates of 0.15, 0.3 & 0.37 respectively on r_1, r_2 & r_3, so $r_1 = 0.15$ with a_i=1, b_i & c_i = 0, $r_2 = 0.3$ with b_i=1, a_i & c_i = 0, and $r_3 = 0.37$ with c_i =1, a_i & b_i = 0 are the three extreme points, and the flat surface of '$r_1\, r_2\, r_3$' presents overall values of $f(a,b,c)$ as Fig. 5.4 shows. The correlation between the profile of building demand and the cost for consuming energy can be seen as higher percentage of a_i tends to have a lower cost of building consumption, and higher shoulder or peak

percentage of b_i or c_i would cause higher costs. The above demonstration visually links the profile of building consumption to the costs for consuming energy, which presents an easy-understood method to analyse financial issues.

5.2.2 Cost saving from VNM

Based on (5.1) and the above analyses on PV generation, the cost saving from VNM can be expressed as below,

$$Cost\ saving_{\ max} = y_i \times (r_2 \times d_i + r_3 \times e_i) \tag{5.10}$$

(5.10) was used in later financial evaluations for payback period and overall value. It needs to be noted that the above formula is marked as 'max cost saving', because it is available when overall credits are used up by the buildings/customers, but if any credit is left in the end of a VNM billing cycle, the cost saving would reduce because a baseline repurchasing price of the utility would be applied [56]. In Chapter 4, It was demonstrated that a PV system has comparatively fixed annual generation during shoulder and peak periods under TOU, and the corresponding percentages as '*d*' & '*e*' is 39.7% and 60.3%, therefore, cost saving is depending on the utility rates of r_2 & r_3 and the generation of y_i.

5.3 VNM credits allocated to customer's bill

The method for allocating VNM credits can be demonstrated as the allocated credits are subtracted from the metered consumer's usage, and the bill could consequently reflect either a credit or a charge according to the resulting kWh. The qualified customer with net consumed kWh is billed in accordance to the customer's utility tariff, such as the fixed-rate and TOU, and the net kWh generated would settle accounts using an applicable baseline rate [56, 69]. The above description is cited from the previous researches, based on which this study detailed the method of allocating VNM credits to develop further financial evaluations. The detailed method can be presented by three points: (1) VNM allocated credits are directly subtracted from metered consumption under fixed-rate utility tariff; (2) The allocated VNM credits should correspondingly offset shoulder and peak building usage, because the PV generation of a VNM program can be valued at shoulder and peak rates under TOU as previously analysed, and the corresponding allocation can guarantee the value of the VNM

credits; and (3) The surplus allocated credits after offsetting shoulder and peak usage offset the off-peak usage.

According to point (3), there are two further scenarios for addressing the surplus allocated credits. (a) The left credits of *'d'* and *'e'* offset the off-peak usage of *'a'*, or (b) The left credits of *'e'* offset the shoulder and peak usage of *'b'* and *'a'*. It can be seen that the usages of *a & b* share the left credits of *e* in Scenario 2, and there is a priority of offsetting usage *b* due to the higher rate in shoulder period than in off-peak period. The percentages of the left credits of *e* respectively offsetting *a & b* can be identified based on the above priority. The left credits of *'d'* can't be allowed to offset the peak usage of '*c*', because this would impair utility interests. This assumed method for allocating VNM credits can be illustrated by the diagrams below.

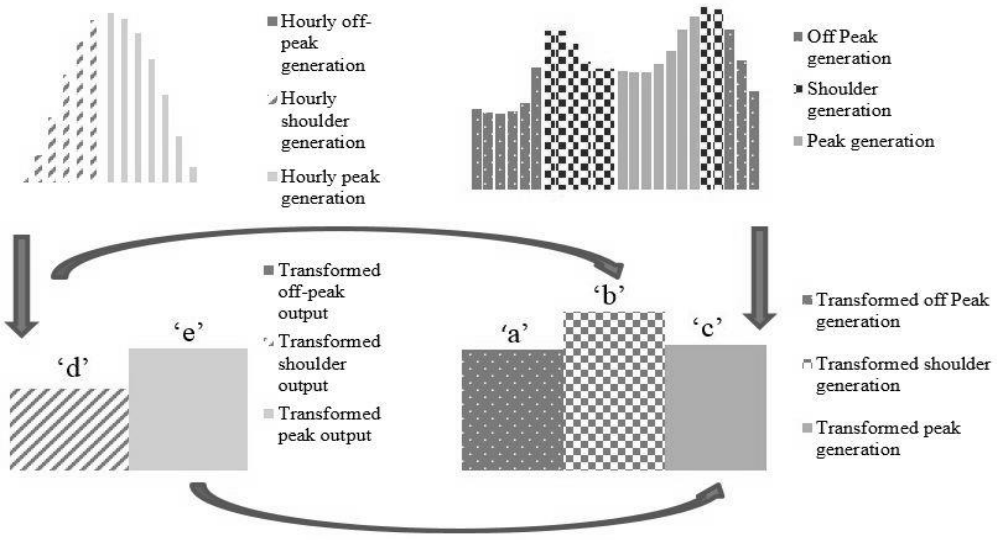

Fig. 5.5 Assumed allocation of VNM credits.

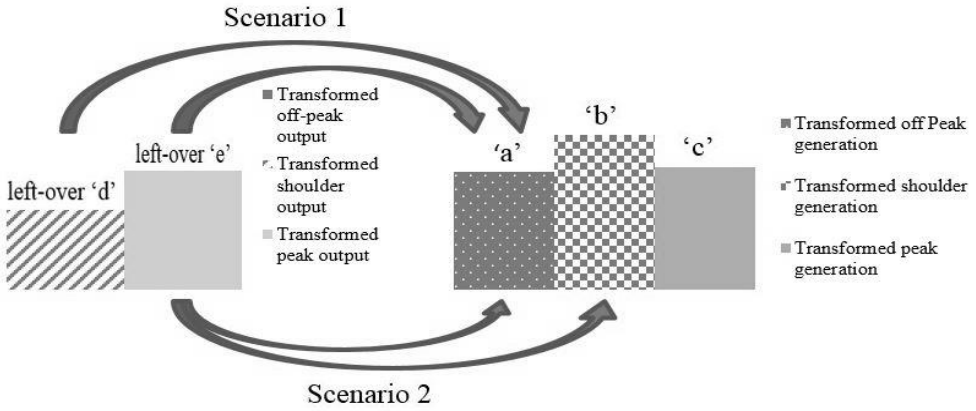

Fig. 5.6 Assumed allocation of VNM 'left-over' credits.

The above assumptions can be summarized as the credits (allocated or left) with a certain equivalent rate of TOU are allowed to offset customers' usage with the rates of TOU that is equal or less than the credits'. All further financial evaluations are developed based on the above assumption.

5.4 Financial evaluation

5.4.1 Payback period

Payback period is used for evaluating the performances of an investment, and some previous researchers use it for analysing financial issues of investing in a PV system [19]. This project used payback period as the economic indicator in order to evaluate the correlation of the financial profits from implementing a VNM program and the daily profiles of building demand. The general expression for payback period is presented as the followings.

$$\text{Payback Period} = \frac{Investment}{Cash\ inflow} \tag{5.11}$$

The investment shown in above formula only considers the cost for installing a shared PV system, because the main cost for launching a VNM program is installing the PV system for participants. In addition, cash inflow presents the financial profits for the generator or customer involved in a VNM program, and this project investigated

current types of VNM in Australian in order to understand more about cash inflow in the local context, and the details are presented by the below table.

TABLE 5.2 Types of VNM in Australia.

Type of VNM	**Description**	**Generator**	**Consumer**	**Electricity sale or transfer**	***Cost saving of customers***
Single entity VNM	An entity transfers exported generation from one site to offset electricity demand at its other site(s)	Entity A *Meter A*	Entity A *Meter B, C .etc.*	Transfer *(No trading involved in)*	*1. The investor or generator is the consumer.* *2. Cost saving is valued at utility rates based subtracted usage from customers' bill.*
Third Party VNM	An entity sells exported generation to separate entity(s)	Entity A *Meter A*	Entity B, C, D etc. *Meter B, C, etc.*	Sale *(There is a form of trading)*	*1. The investor or generator is not the consumer.* *2. There are two prices involved in, as the selling price (from Seller) and cost saving (Buyer).*
Community Group VNM	A collectively owned generator transfers exported generation to shareholders	Entity A *Meter A* (i.e. generator owned by core group of investors)	Entity B, C ,D .etc. *Meter B, C, ..etc.* (shareholders in core group)	Transfer *(No trading involved in)*	*Same as 'type 1'*
Retail Aggregation VNM	Multiple entities sell exported generation to retailer for resale to multiple consumers.	Entity A,B,C .etc. *Meter A,B,C .etc.*	Entity X,Y,Z via Retailer *Meter X, Y, Z .etc.*	Sale *(There is a form of trading)*	*1. The retailer is not investor or generator or consumer. The retailer is a middleman.* *2. There are three prices involved in, as 'selling price' from generator to retailer, 'the selling price' from retailer to final consumer, and consumer's cost saving.*

The first five columns of Table 5.2 are cited from a UTS report [60], and the last column about cost saving is added by this research based on the principle of running VNM [56]. It can be seen that no matter which type of VNM, the cost saving is parts or the whole of cash inflow achieved by implementing VNM. In Type 1 & 3, the generator is the customer, so there is no trading activity involved, and the cost saving is equivalent to cash inflow. In Type 2 & 4, the generator directly or via a third party sells PV generation to the customers, so there must be a difference between the generator's profits from the trading and the customers' cost saving. For the simplified evaluations, the cost saving is regarded as cash inflow to study payback period in this research.

For installing a PV system, the initial investment can be evaluated by (5.12).

$$Investment_{\ Installing\ a\ PV\ system} = G \times 1000 \times \$8/Wp \tag{5.12}$$

G is the rated DC capacity of a PV system in kW, and $\$8/Wp$ is the estimated unit cost for installing a PV system [71].

As the introduction in Section 5.1.1.2, the cost saving from implementing VNM under TOU or the fixed-rate can be calculated by (5.10).

$$Cost\ saving_{\ max} = y_i \times (r_2 \times d_i + r_3 \times e_i) = y_i \times d_i \times r_2 + y_i \times e_i \times r_3 \tag{5.10}$$

$y_i \times d_i$ *and* $y_i \times e_i$*'* represents the allocated credits rolled over from shared PV power generated respectively in shoulder and peak periods, and this research takes the annual PV generation for calculating the exact cost saving for matching the relevant period, which consists of any 12 monthly billing cycles introduced in [56]. The annual PV generation are evaluated based on the simulated data in Chapter 4.

In addition, (5.10) presents the maximum cost saving based on the analysis in Section 5.1.1.2. Depending on the two scenarios of the assumed method for addressing left-over allocated credits shown in Fig. 5.8, the cost saving with left credits can be presented by (5.13) & (5.14).

For Scenario 1:

Cost saving $_{with\ left\ credits}$ *= [(shoulder credits – shoulder consumption) + (peak credits –peak consumption)] × r_1 + shoulder consumption × r_2 + peak consumption × r_3*

$$= [(y_i \times d_i - x_i \times bi) + (y_i \times e_i - xi \times ci)] \times r_1 + (b_i \times x_i) \times r_2 + (c_i \times x_i) \times r_3 \quad (5.13)$$

For Scenario 2:

Cost saving $_{with\ left\ credits}$ *= [(peak credit – peak consumption)] × p_a× r_1 + [(peak credit – peak consumption)] × p_b× r_2 + shoulder consumption × r_2 + peak consumption × r_3*

$$= [(y_i \times e_i - xi \times ci)] \times p_a \times r_1 + (y_i \times e_i - xi \times ci)] \times p_b \times r_2 + (b_i \times x_i) \times r_2 + (c_i \times x_i) \times r_3 \quad (5.14)$$

where, p_a & p_b respectively represent the percentages of left peak credits allocated to off-peak and shoulder load usage, which are identified based on the analyses of Scenario 2. Based on (5.10) to (5.14), the maximum cost saving has a shortest payback period, presented as below equations,

$$Payback\ Period_{\ shortest} = \frac{G * 1000 * 8}{G * 8760 * (r2 * di + r3 * ei)} \quad (5.15)$$

And the payback period under the condition with left allocated credits is expressed as two equations below,

For Scenario 1:

Payback Period $_{with\ left\ credits}$

$$= \frac{G * 1000 * 8}{[(yi * di - xi * bi) + (yi * ei - xi * ci)] * r1 + (bi * xi) * r2 + (ci * xi) * r3} \quad (5.16)$$

For Scenario 2:

Payback Period $_{with\ left\ credits}$

$$= \frac{G * 1000 * 8}{[(yi * ei - xi * ci)] * pa * r1 + (yi * ei - xi * ci)] * pb * r2 + (bi * xi) * r2 + (ci * xi) * r3} \quad (5.17)$$

The latter case studies were established based on (5.15) to (5.17).

5.4.2 Assumptions for case study

A series of case studies were established based on (5.15) to (5.17) for evaluating payback period. From these three equations, the building consumption and the PV generation as *'x_i'* & 'y_i' in kWh and the capacity of a shared PV system as *'G'* in kW are needed to be identified. As analysed above, this study took annual PV generation as 'y_i', so for a match, annual building consumption was taken as 'x_i', which can be evaluated based on the database of load consumption introduced in Chapter 4. *'G'* was assumed and presented by latter sections. The percentages of building consumption and PV generation as *'a_i'*, *'b_i' & 'c_i'*, and *'d_i' & 'e_i'* have been investigated in Chapter 4, which are presented by Table 4.7, Fig. 4.16 and Fig. 4.17.

For simplified calculations, assuming the load capacity of each building involved in the case studies is 20 kW. To investigate on the correlation of payback period and the profiles of building consumption, 3 out of 15 categories of buildings introduced in Chapter 4 as quick service restaurant, stand-alone retail and hospital are used for the case studies of an individual building. Another three buildings plus above three are taken and categorized by three groups for the case studies of group buildings as Group 1 - small hotel & quick service restaurant, Group 2 - supermarket & apartment, Group 3 - stand-alone retail & secondary school, and three groups are respectively with highest shoulder consumption, even shoulder and peak consumption and highest peak consumption as Fig 5.7 shown.

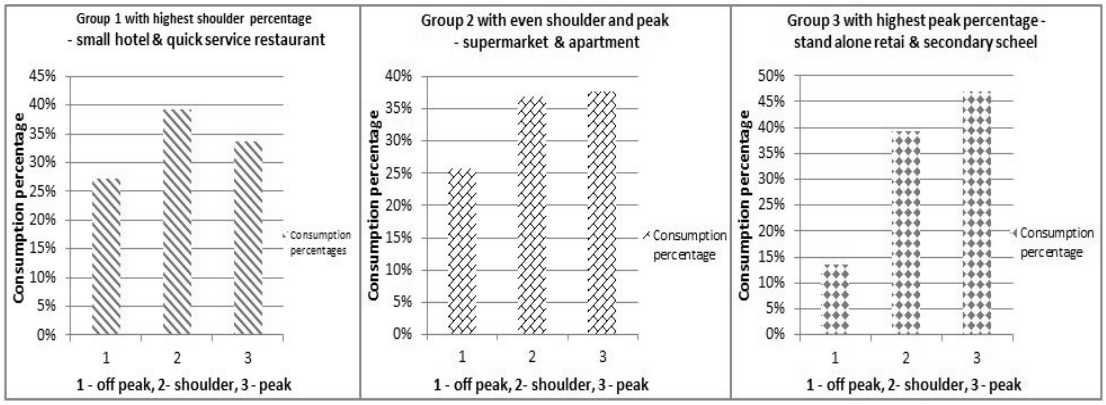

Fig. 5.7 Three groups of buildings with different profiles of demand.

Each group with two buildings has an assumed load demand of 40 kW based on the above assumption of 20 kW for each studied building. As introduced in [58], the

capacity of a VNM PV system is same as the load capacity of all participants, so this research set 40 kW as the origin capacity of a shared PV system, as *'G_{origin}'* = 40 kW. A comparison was made to demonstrate the difference between the annual consumption of a group of buildings with a load demand of 40 kW and the annual generation of a shared PV system with the same capacity as 40 kW, which aims to further study the match of the size of a shared-VNM PV system and the load capacity of the qualified customers in a VNM program. The third group as stand-alone retail & secondary school with the lowest annual consumption is used for the above comparison. The comparison shows that the annual PV generation is much less than the annual load consumption and the details were illustrated as the below diagram.

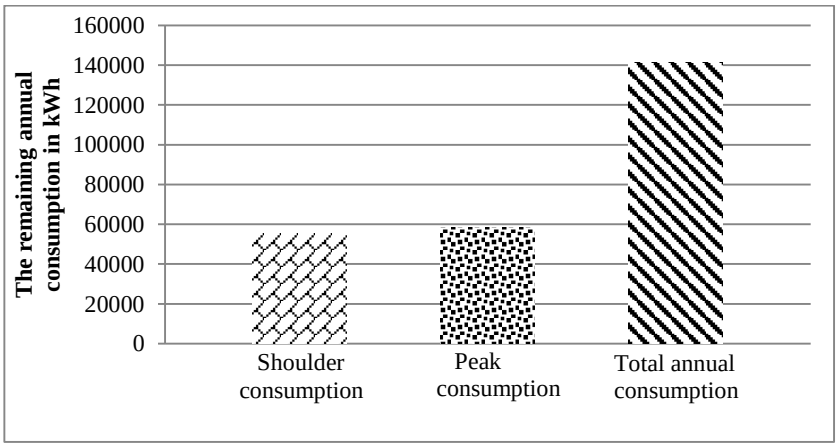

Fig. 5.8 Comparison of annual building demand and PV generation.

As Fig. 5.8 shows, the shoulder & peak-period & the total annual usage of Group 3 are respectively much more than the shoulder & peak-period & total annual generation of a shared PV system with the capacity of 40kW same as the load capacity of group 3. If the site is enough to install a shared PV system, what potential sizes of a VNM PV system can cover or better match the consumption of the served buildings is one of the interests this chapter studies for.

To identify the potential sizes of a shared PV system, this project uses shoulder and peak load consumption as the indicators for exploring the bigger sizes, which respectively assumes that the shoulder (peak) generation of a VNM PV system covers the shoulder (peak) building consumption. The sizes of covering shoulder and peak consumption can be calculated by the following expressions.

Annual shoulder PV generation = annual shoulder building consumption,

d_i × *annual PV generation* = b_i × *annual consumption,* d_i *(*e_i*)* is achieved as 60.3% (39.7%) in Chapter 4,

60.3% × annual average daily generation in per unit × 40 kW × 365 = b_i *× annual average daily consumption in per unit × 40 kW × 365,*

0.603 × 4.12 kWh × capacity of the shared PV system × 365 = b_i *× annual average daily consumption in per unit × 40 kW × 365,*

So,

Capacity of the shared PV system *by shoulder consumption*

$$= \frac{bi * annual\ average\ daily\ consumption\ in\ per\ unit * 40\ kW}{0.603 * 4.12\ kWh} \quad (5.18)$$

In the similar way,

Capacity of the shared PV system *by peak consumption*

$$= \frac{ci * annual\ average\ daily\ consumption\ in\ per\ unit * 40\ kW}{0.397 * 4.12\ kWh} \quad (5.19)$$

The results calculated by (5.18) & (5.19) for the three groups are presented as the tables bellow.

TABLE 5.3 Potential sizes of the shared PV system.

group 1 *with daily consumption 34.17 kWh*		
PV size (DC rated or Peak) by annual peak consumption	(kW)	93.10
PV size (DC rated or Peak) by annual shoulder consumption	(kW)	162.77
group2 *with daily consumption 32.02 kWh*		
PV size (DC rated or Peak) by annual peak consumption	(kW)	97.45
PV size (DC rated or Peak) by annual shoulder consumption	(kW)	142.80
group 3 *with daily consumption 27.57 kWh*		
PV size (DC rated or Peak) by annual peak consumption	(kW)	105.0
PV size (DC rated or Peak) by annual shoulder consumption	(kW)	132.0

It is noticed that the daily consumption of three groups are different, and the exact values are presented as the table below.

TABLE 5.4 Daily consumption of individual and group of building(s).

Group 1			
Feature of buildings	Highest shoulder		
Building categories	Quick service	Small hotel	Total-group1
Daily building load consumption in per unit (kWh)	18.15	16.02	34.17
Group 2			
Feature of buildings	Even shoulder and peak		
Building categories	Supermarket	Residential	Total-group2
Daily building load consumption in per unit (kWh)	17.02	15	32.02
Group 3			
Feature of buildings	Highest peak		
Building categories	Stand-alone retail	(Secondary) School	Total-group3
Daily building load consumption in per unit (kWh)	13.45	14.12	27.57

Each group daily consumption shown in the last column of Table 5.4 is different, and for a comprehensive evaluation, this research makes another assumption as valuing the daily group consumption of Group 2 & 3 at 34.17 kWh same as Group 1, and the new potential sizes of covering shoulder and peak consumption were calculated and presented as the table below,

TABLE 5.5 Potential sizes of the shared PV system with normalized daily consumption by 34.17 kWh.

group 1 *with daily consumption 34.17 kWh*	
PV size (DC rated or Peak) by annual peak consumption (kW)	93.10
PV size (DC rated or Peak) by annual shoulder consumption (kW)	162.77
group2 *with daily consumption 34.17 kWh*	
PV size (DC rated or Peak) by annual peak consumption (kW)	103.99
PV size (DC rated or Peak) by annual shoulder consumption (kW)	152.39
group 3 *with daily consumption 34.17 kWh*	
PV size (DC rated or Peak) by annual peak consumption (kW)	129.85
PV size (DC rated or Peak) by annual shoulder consumption (kW)	165.59

The six extension sizes of the shared PV system are shown in Table 5.3 and the original capacity is 40 kW. For comprehensive evaluations, this research put another five assumed random sizes to assist in the development of the related case studies as 65 kW, 85 kW, 110 kW, 185 kW and 200 kW, and to distinguish the extension sizes and

randomly assumed sizes, the former were annotation as ‘critical’, the critical sizes in round-off number plus randomly assumed sizes were presented by the table below.

TABLE 5.6 Summary of shared PV system sizes with different daily demand.

Each group with different daily consumption								
Serial	1	2	3	4	5	6	7	8
Annotation	origin			critical		critical		
Group 1 in kW	40	65	85	93	110	163	185	200
Group 2 in kW				97		143		
Group 3 in kW				105		132		

The extension sizes of three groups with the normalized daily consumption shown in Table 5.5 in round-off number plus randomly assumed sizes were presented by Table 5.7, and were used for further related case studies.

TABLE 5.7 Summary of shared PV system sizes with normalized daily demand.

Three groups with normalized daily consumption												
Serial	1	2	3	4	5	6	7	8	9	10	11	12
Annotation	origin			critical	critical		critical	critical	critical	critical		
Size of PV system in kW	40	65	85	93	104	110	130	152	163	166	185	200

The latter case studies evaluated payback period that were calculated by (5.16) to (5.18) based on different sizes of an assumed shared PV system as shown in Tables 5.6 & 5.7.

5.4.3 Evaluation under assumed ‘pure’ TOU schedule

As previously introduced, the two types of schedules considered are TOU and fixed-rate. This research focuses on TOU to develop the latter case studies, because the profile of building consumption has impacts on customer cost saving from implementing VNM under TOU, but the cost saving is independent of the profile under the fixed rate, which is pointed out by Chapter 4. For clear and comprehensive evaluations, this research studies the payback period under two conditions as assuming all VNM customers implementing TOU notated as ‘pure’ TOU schedule and both TOU and the fixed-rate are, respectively, applied by VNM customers notated as ‘hybrid’ schedule.

In addition, as the beginning of this chapter introduced, this work focuses on the situation where a VNM group consists of several individual buildings shown in Fig. 5.1 (b). For a comprehensive evaluation, this research studies individual buildings and the whole group.

5.4.3.1 Investigation for individual building

The case studies evaluated three points: (1) evaluating payback period by taking two different assumed methods for addressing left credits as Fig. 5.6 shown; (2) investigating payback period changing along with the different amount of allocated credits; and (3) evaluating the correlation of payback period and the profiles of building demand. In order to investigate point (2), it is assumed that the amount of credits is directly proportional to the cost of a customer investing in a VNM program. For example, a customer pays 50% cost of installing the shared PV system, and 50% out of overall allocated credits would be allocated to this customer in return.

Three categories of buildings are used as quick service restaurant with highest shoulder consumption, stand-alone retail with highest peak consumption and hospital with even shoulder and peak consumption, which were illustrated in Table 4.5, were used for developing the case studies of individual customer (building). It is assumed all individual buildings have a normalized power demand of 20 kW. In addition, 93 kW, which is the smallest critical size and closest to power demand of the building of 20 kW shown in Tables 5.6 & 5.7 is used as the capacity of a shared-VNM PV system. The results of payback period, building consumption, allocated credits and surplus allocated credits are illustrated in Fig. 5.9 to Fig. 5.11.

The indication of each line labelled with a number is listed by the legend of Fig. 5.9. It is needed to explain that two symbols as rhombus and square were used for marking the lines of payback period. The points with rhombus represents the payback period evaluated by compensating left shoulder and peak credits to off-peak consumption as the Scenario 1 shown in Fig. 5.6, and the points with square represents the payback period evaluated by allocating left peak credits to shoulder and off-peak consumption as the Scenario 2 shown in Fig. 5.6.

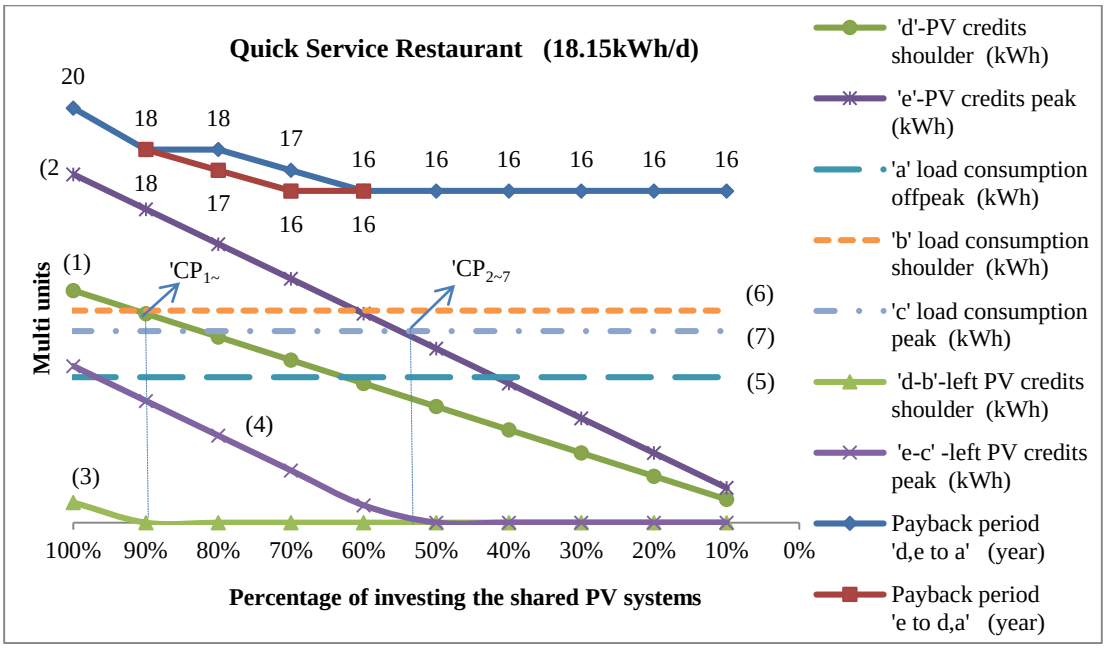

Fig. 5.9 Results of quick service restaurant.

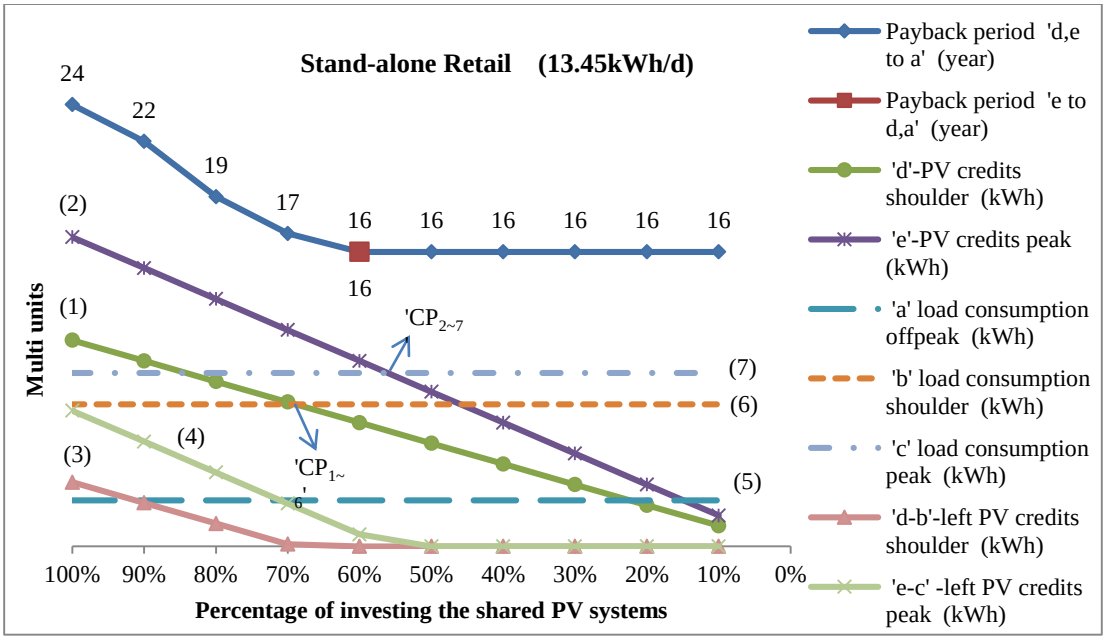

Fig. 5.10 Results of stand-alone retail.

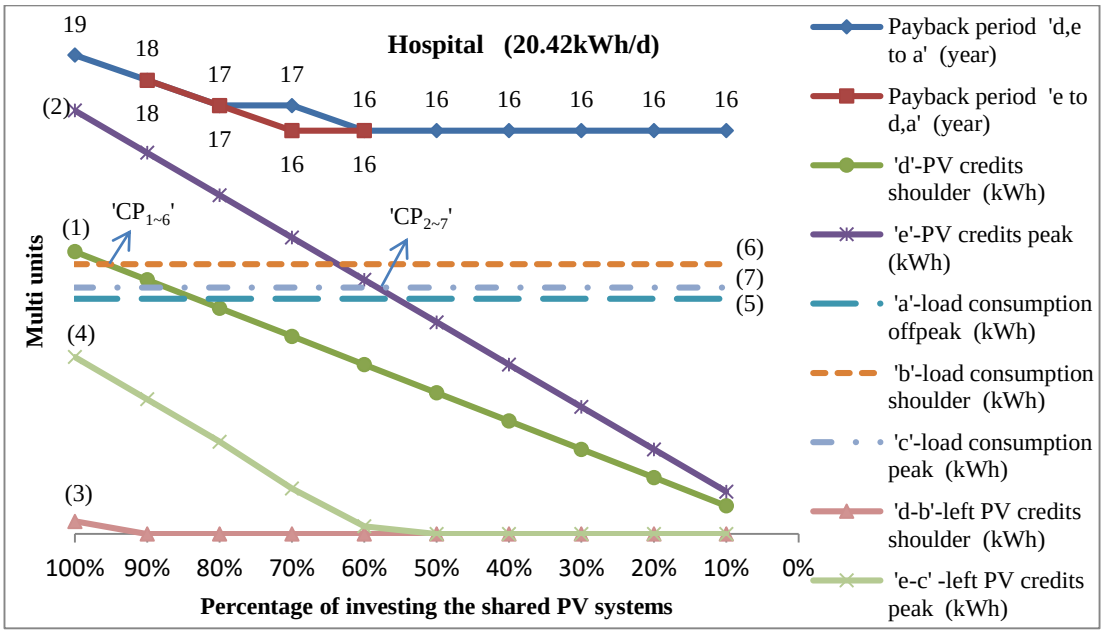

Fig. 5.11 Results of hospital.

It can be seen by oblique lines (1) & (2) that the amount of allocated shoulder (d) and peak (e) credits are reducing along with the investment shrinking. In addition, oblique lines (3) & (4) representing the left shoulder and peak credits were obtained by shoulder and peak credits labelled as line (1) & (2) respectively minus shoulder and peak usage labelled as line (6) & (7). The crossover points as ‘CP1-6’, ‘CP2-7’, demonstrate the shoulder and peak credits would be completely used out respectively corresponding to the proportion of customer participating ratio of 0.9 and 0.56. These two ratios can be directly read from the crossover points of oblique lines (3) & (4) with x-axis as well.

From Figs. 5.9 to Fig. 5.11, the line marked by square is always under or overlap the line marked by rhombus, which indicates the Scenario 2 shown in Fig 5.6 as compensating peak left allocated credits to off-peak and shoulder usage is a better option than the Scenario 1 as compensating shoulder and peak credits to off-peak consumption. This result indicates the better option for a customer to addressing the surplus credits is to maximize the value of the surplus credit by allocating them to the usage with higher utility rate. While, the Scenario 2 is not always applicable when the shoulder usage on a customer’s bill is zero after subtracting allocated shoulder credits from shoulder usage. Under this condition, only Scenario 1 can be applied to addressing the left shoulder and peak credits.

From above three graphs, it can be seen that the payback period always remains fixed after a certain ratio, which is annotated as the critical ratio in this research, and the critical ratio is around 0.6 for stand-alone retail and 0.6-0.7 for quick service restaurant and hospital. The critical ratio can be identified by line (4) of each graph as well, i.e. the first ratio resulting in a zero-left peak credit. The critical ratio is a useful indicator for potential customers of a VNM program to have cost-effective investment. It needs to be noticed that an over-reduction of the investment should be avoided for a maximal utilization of PV generation due to the payback period remaining fixed after the critical ratio.

From Fig. 5.9 to Fig. 5.11, the relative positions of the flat lines (5), (6) & (7) indicate the different profiles of building consumption of three categories of buildings, such as line (6) being on the top of line (7) in Fig. 5.9, which illustrates quick service restaurant has highest shoulder consumption. By this means, the profiles of consumption of stand-alone retail and hospital can be read from Fig. 5.10 & Fig. 5.11. As the above graphs show, the hospital has a shorter payback period, 19 years corresponding to the ratios of 1, than the quick service restaurant with payback periods of 20 years corresponding to the ratios of 1. The hospital and quick service restaurant have same payback periods as 18, 17, and 16 years corresponding to ratios of 0.9, 0.8, and 0.7. Stand-alone retail has the longest payback periods of 24, 22, 19, 17 years corresponding to the ratios of 1, 0.9, 0.8, and 0.7, in terms of payback period (marked by squares). This result can be explained by the daily consumption of each building. The hospital has the highest daily consumption of 20.42 kWh/d, then quick service restaurant with 18.15 kWh/d, and stand-alone retail with 13.45 kWh/d. This makes the hospital consume more allocated credits than the two other buildings. As previously analysed, both the daily consumption and the profile of load usage have impacts on cost saving of a VNM customer under TOU. In order to evaluate the correlation of the profile and payback period without any impact from the daily usage, it was assumed that the daily consumption of 18.15 kWh/d (i.e. the same as quick service restaurant) was assigned to above stand-alone retail originally with 13.45 kWh/d, and repeated the same evaluations, as shown by Fig. 5.12.

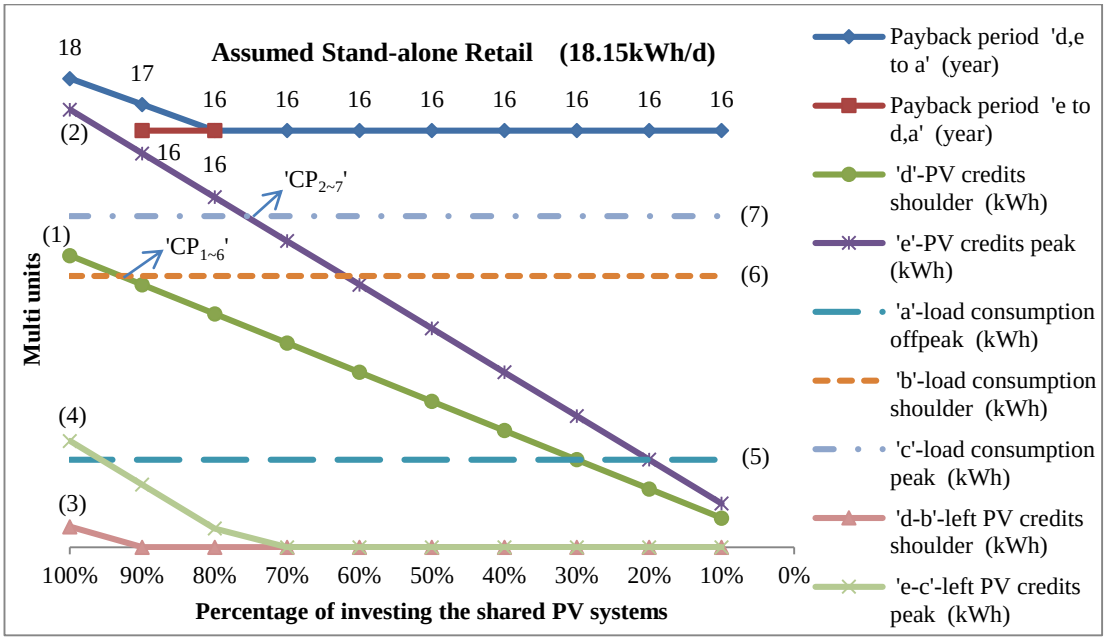

Fig. 5.12 Results of assumed stand-alone retail.

From Fig. 5.12, the assumed stand-alone retail with highest peak consumption same as original stand-alone retail shown in Fig 5.10 has the best performance of payback period among three buildings with nine ratios having the shortest payback period as 16 years, and the payback period of 18 years corresponding to the ratio 1 is the shortest amongst the corresponding values of the buildings. This result can also be indicated by a comparison of the line (4) shown in Fig. 5.9, Fig. 5.11 & Fig. 5.12, which demonstrates that the lowest surplus peak credits due to the profile with highest peak usage results in the shortest payback period. It can be concluded that the profile with highest peak usage has the shortest payback period when the daily consumption is similar or even smaller as 18.15 kWh/d of the assumed stand-alone retail being lower than 20.42 kWh/d of the hospital.

5.4.3.2 Investigation for a group of buildings

This section evaluated the same three points listed in the beginning of Section 5.4.3.1 but with a different objective to the above investigations. Three groups of buildings with three different types of profiles as highest shoulder usage, even shoulder and peak usage, and highest peak usage as shown in Fig. 5.8 were used. A number of capacities of a shared PV system shown in Tables 5.6 and 5.7 instead of the ratio of the investment an individual customer (building) affords are used for evaluating more

optional sizes of a VNM PV system. The load demand of each group is normalized to 40 kW, but the daily consumption of three groups are different as 34.17, 32.02, and 27.57 kWh/d, which were selected from the outcomes of Chapter 4. The results are illustrated by Fig. 5.13 to Fig. 5.15.

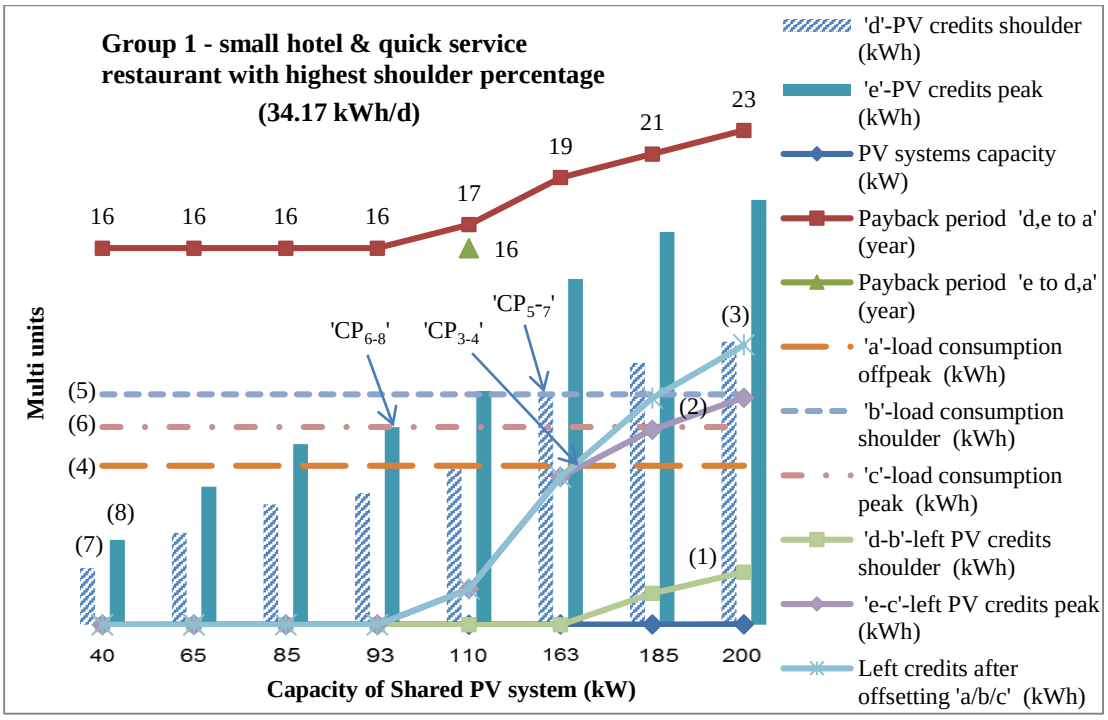

Fig. 5.13 Results of Group 1.

The indication of each line labelled with a number is listed by the legend of Fig. 5.13. It is needed to explain that only one point marked by the triangle sign indicates it is applicable only for the capacity of 110 kW to compensate the surplus peak credits to shoulder and off-peak usage comparing to other points only with the applicability of allocating peak and shoulder left credits to off-peak usage. As Fig. 5.13 shows, the curve (3) is always under flat (4) before the crossing point of '$CP_{3\text{-}4}$' (around 166 kW corresponding to the capacity of the shared PV system), which means that the allocated credits can be used out by compensating off-peak usage corresponding to all capacities less than around 166 kW. The crossover points at '$CP_{6\text{-}8}$' & '$CP_{5\text{-}7}$' respectively demonstrate that the peak and shoulder credits being equal to building peak consumption and shoulder consumption, which are corresponding to two critical capacities as 97 kW and 143 kW. The results of Group 2 & 3 are shown by Fig. 5.14 and Fig. 5.15.

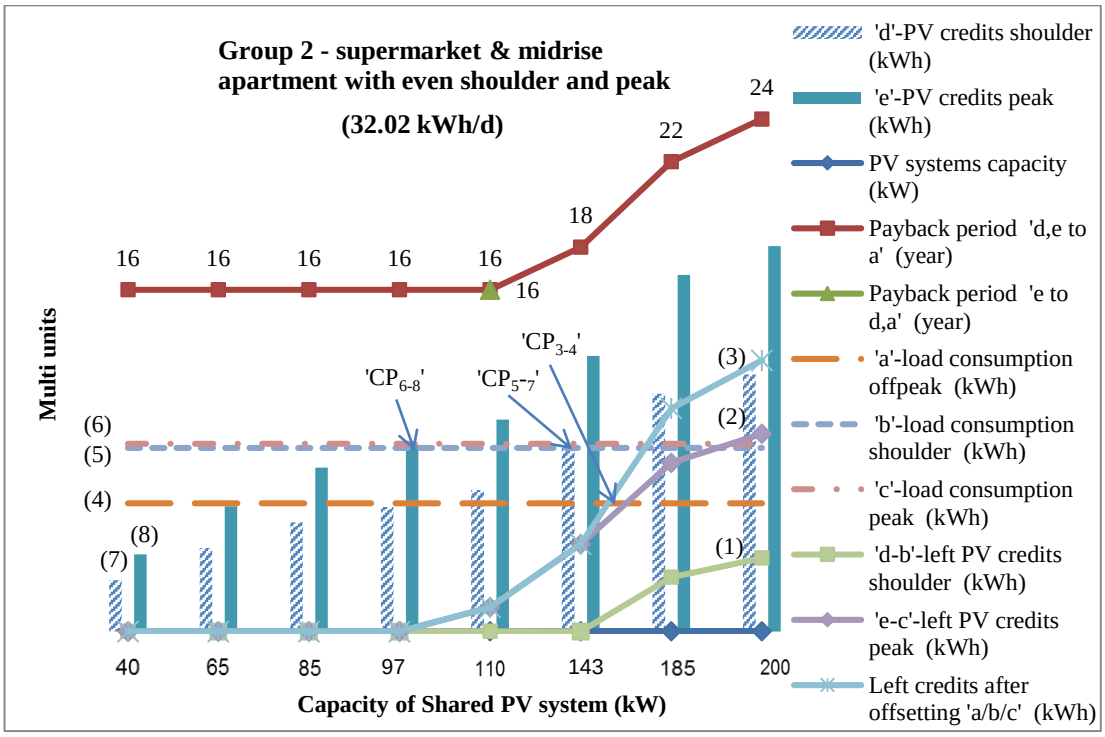

Fig. 5.14 Results of Group 2.

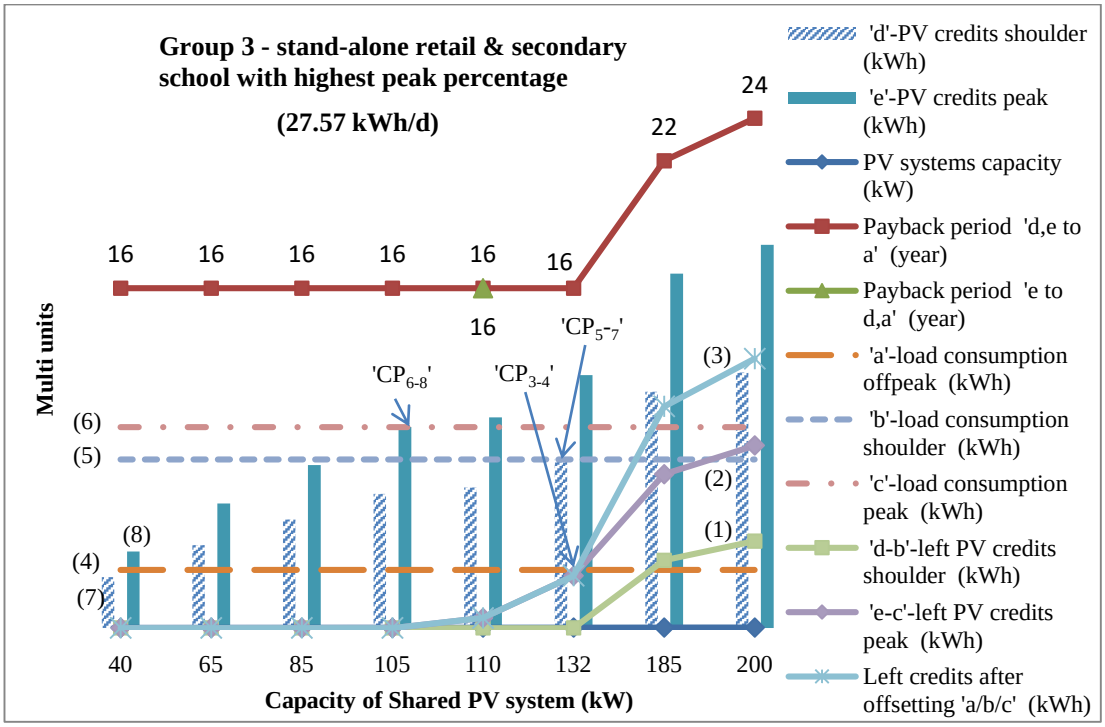

Fig. 5.15 Results of Group 3.

From the comparison of Fig. 5.13 to Fig. 5.15, only one point signed by triangle for each group and the triangle points of Group 2 & 3 overlap the corresponding square points. This result indicates that the two assumed methods for addressing the left

credits are almost the same for a VNM group. The reason is that the difference between the values of the left credits achieved respectively by the two assumed methods is not obvious and is very small compared to the overall cost saving of the whole VNM group, so the resulting payback period is almost same. While, it has to be noticed that the Method 2 of allocating peak left credits to shoulder and off-peak usage, is effective for shortening the payback period under a certain condition as the original was 17 years but was cut down to 16 years at the capacity of 110 kW for Group 1, so the evaluation for the two assumed methods for addressing the surplus credits is necessary for a realistic case.

It can be seen that the payback period of the three groups starts to go up from the smallest value by 16 years after a certain size of the shared PV system. The start point of Group 1 is the first critical size covering the peak usage as 93 kW, the point of Group 2 is 110 kW between two critical sizes respectively covering peak and shoulder usage, and the Group 3' is the second critical size covering the shoulder usage as 132 kW. This result indicates that payback period must remain fixed without any the left credits, and the first critical capacity covering peak usage is an applicable option for identifying the size of a VNM PV system, which provides more PV power than the original size as 40 kW same as the load capacity introduced by [58] and guarantees a shortest payback period. For Group 2 & 3, the capacities having the shortest payback period are larger than the first critical size, because discounted value of the left peak credits caused by compensating shoulder or off-peak usage is not too much comparing to the overall cost saving. Therefore, the applicable capacity, which provides as much as possible PV power and guarantees the shortest payback period, must be located in the range between the first and the second critical sizes, and the exact value of the applicable capacity should be individually evaluated.

As to the correlation of payback period and the profile of building consumption, the Group 1 has shortest payback periods as 20 & 21 years corresponding to 185 & 200 kW, and both Group 2 & 3 have 22 & 24 years respectively corresponding to the same capacities. However, the Group 3 has the most points of 6 with the shortest payback period as 16 years among three groups. It is not convincing which type of profile results in the best performance of payback period. By referring to the case study for individual buildings, the different daily consumption as three groups

respectively with 34.17, 32.02 and 27.57 in kWh/d would impact the evaluation for the correlation of payback period and the profile of load usage. For a clear and comprehensive comparison, another two groups respectively with same profiles of Group 2 & 3 and with daily consumption as 34.17 kWh/d same as Group 1 are assumed. The results are presented by Fig. 5.16 to Fig. 5.18.

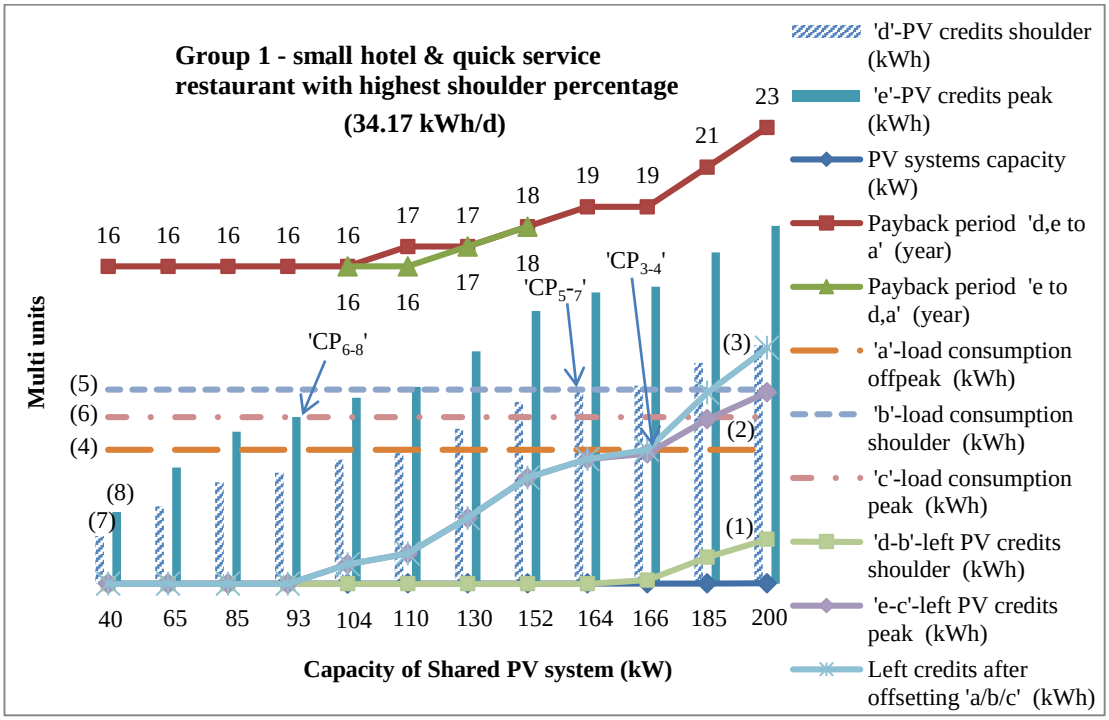

Fig. 5.16 Results of Group 1 under full sizes of PV system.

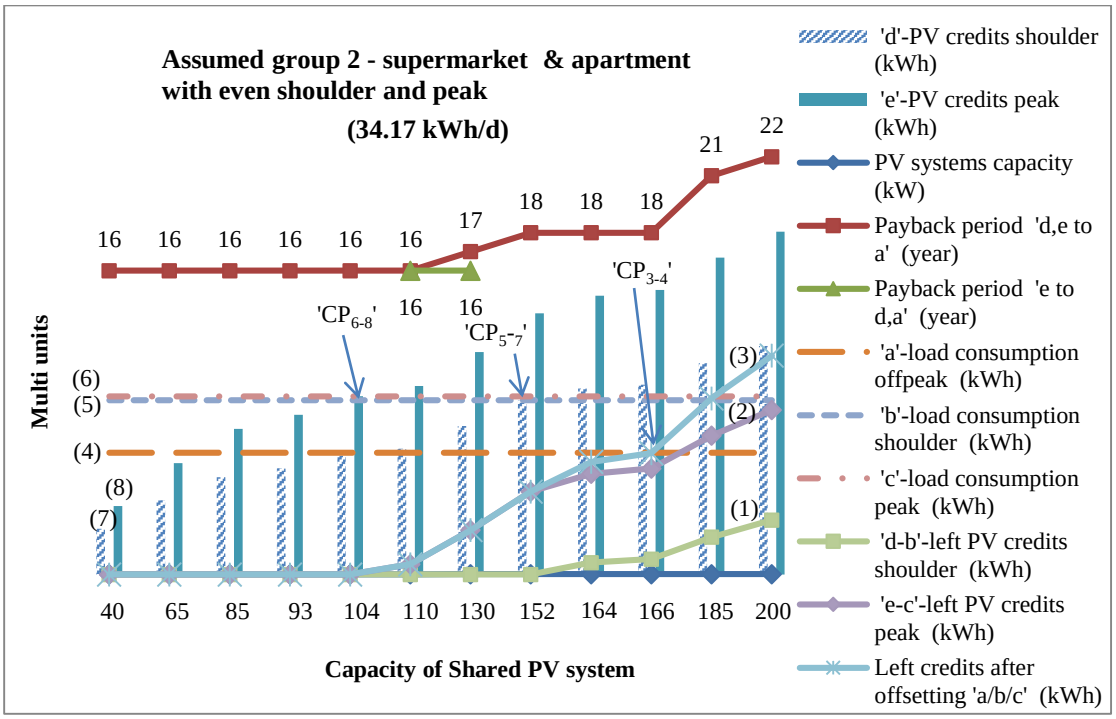

Fig. 5.17 Results of assumed Group 2 under full sizes of PV system.

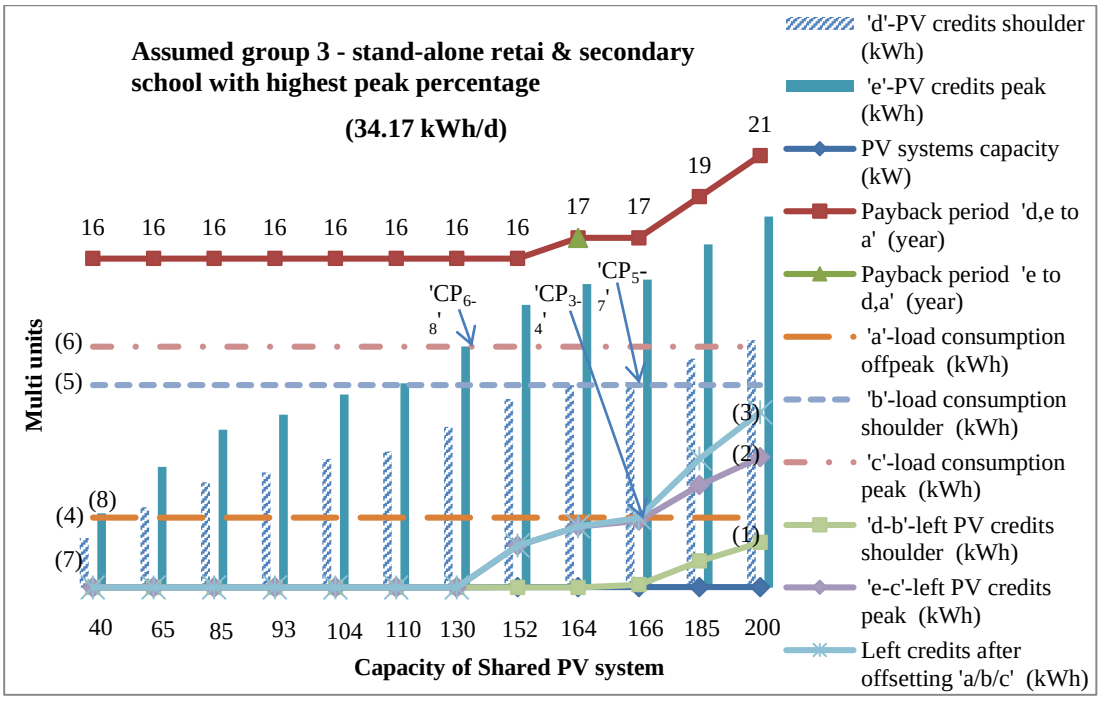

Fig. 5.18 Results of assumed group 3 under full sizes of PV system.

From the above three figures, there are 12 tested capacities of the shared PV system from Table 5.7, are used for a normalized comparison. The payback period illustrated by Fig. 5.16 are same as Fig. 5.13 except five more added capacities as 104, 130, 152,

and 166 in kW. Fig. 5.17 & Fig. 5.18 have different scenarios as Fig. 5.14 & Fig. 5.15 due to the normalized daily consumption as 34.17 kWh/d. By a comparison of Fig. 5.16 to Fig. 5.18, the assumed Group 3 has the best performance among three groups as all capacities less than 130 kW with 16 years of payback period, which are same as Group 1 and assumed Group 2, and each capacity larger than and equal to '130 kW' always has shortest payback period than another two groups. It can be concluded that the profile with highest peak consumption has the shortest payback period than another two types of profiles when the daily consumption of the different building groups are close, because of the more peak usage, the more allocated credits consumed, which maximizes the value of PV-generated credits.

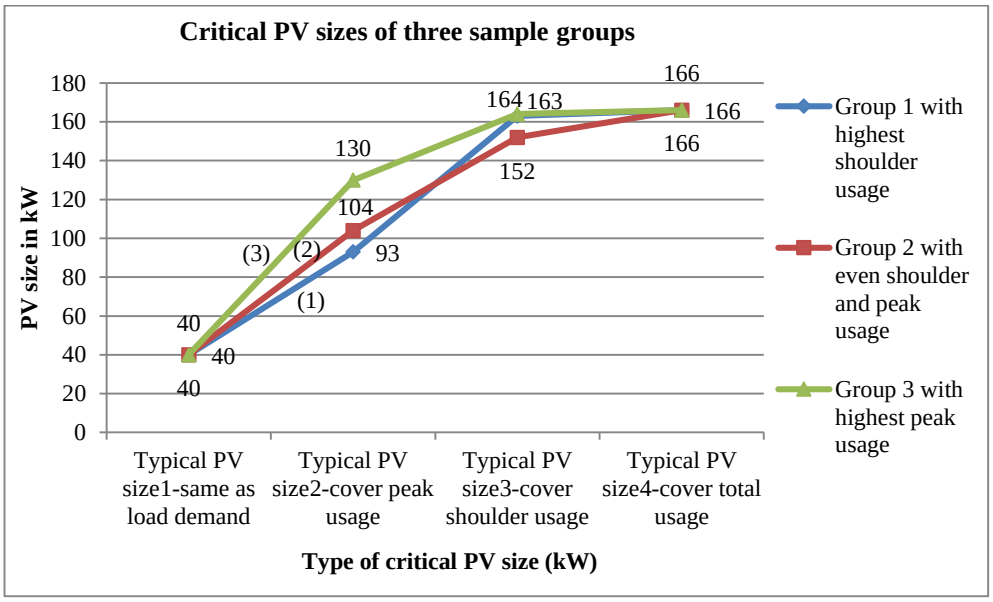

Fig. 5.19 Comparison of critical PV sizes.

Fig. 5.19 shows all critical capacities of three groups respectively shown by curves (1), (2) & (3). The illustration starts from the common point as the original size of 40 kW, and ends up at another common point as 166 kW. The Group 1 with the highest-shoulder profile has smallest peak critical capacity as 93 kW, the Group 2 with the even-shoulder & peak profile has smallest shoulder critical capacity as 152 kW, and the Group 3 with highest-peak profile has both largest shoulder and peak critical capacities as 130 and 164 kW. From Fig. 5.19, the highest-shoulder and the even-shoulder & peak profiles are better than the highest-peak profile for the lower critical sizes, which would lead to a lower cost for installing the shared PV system. Based on

above analyses, if re-shaping the profile of load usage of a VNM group is practical, a certain type of the profile can be applied to achieve a shorter payback period of investing a VNM program or a lower cost based on a certain critical size of the shared PV system. In addition, re-shaping the profile of load usage of a VNM group could be achieved by adjusting the composition of the potential participants (buildings) with different types of the profiles, which needs to be further studied.

5.4.4 Evaluation under assumed 'hybrid' schedule

As introduced in Section 5.4.2, the 'hybrid' schedule assumed a composition of the participants respectively implementing TOU and the fixed-rate. By comparing to the above evaluations under 'pure' TOU, this section focuses on evaluating the correlation of the ratio of the building loads with TOU over the loads with the fixed-rate and the payback period of a VNM group. A further explanation for this ratio is that, for example, 20% building usage in kW of a VNM group is charged by TOU, and the left 80% is charged by the fixed-rate, and correspondingly 20% of overall VNM credits are allocated to the loads with TOU, and 80% of credits put to the loads with the fixed-rate. This assumption is set up by considering only two buildings involved in each sample group shown in last section, which causes that it is hard to set the ratio by the number of the customers (buildings). It needs to be noticed that the assumption proportionating the allocation of the VNM credits to the above ratio is one of methods for the same evaluations, such as based on the ratios of the investment the 'TOU customers' and 'the fixed-rate customers' respectively afford, which would have different scenarios.

The profile of load usage and the critical extension capacities of a VNM PV system are not the research interest of this section, because the profile impacts payback period only under TOU as previously analysed, and the related evaluations under 'hybrid' schedule are similar with the corresponding studies of the last section.

Based on the above assumptions, the assumed power demand of a group as 40 kW and two capacities of PV system as 40 kW and 200 kW are used for a distinct comparison of the related tested results. Two existing fixed prices introduced from utility price schedules [75] as 0.277 & 0.396 in $/kWh and the rates of TOU are used for the evaluation of payback period. In addition, the building information of the Group 1, as

daily consumption, annual total consumption and the profile of building usage, was used for calculating payback period, and the results were presented as the follows.

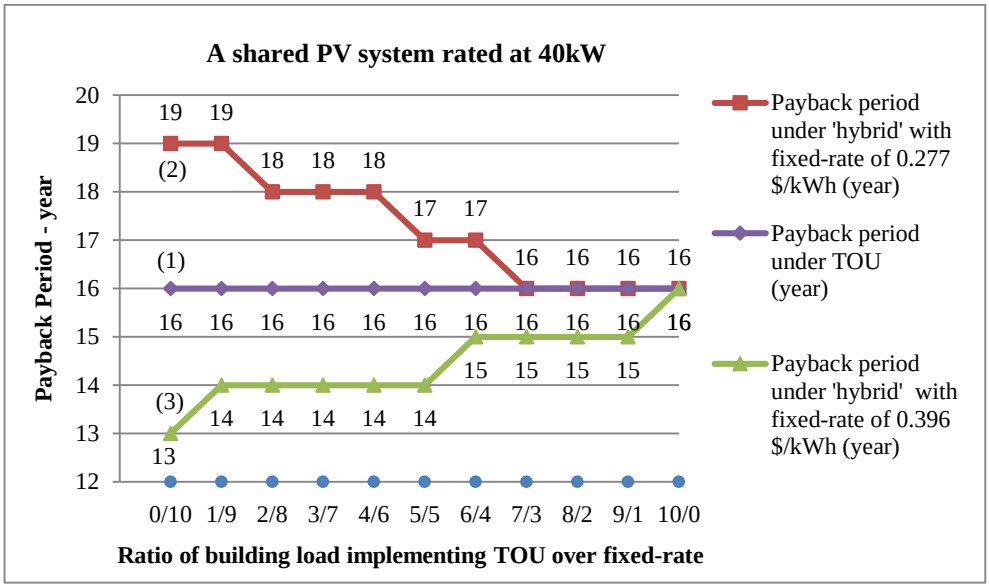

Fig. 5.20 Comparison of payback periods – 40 kW PV system.

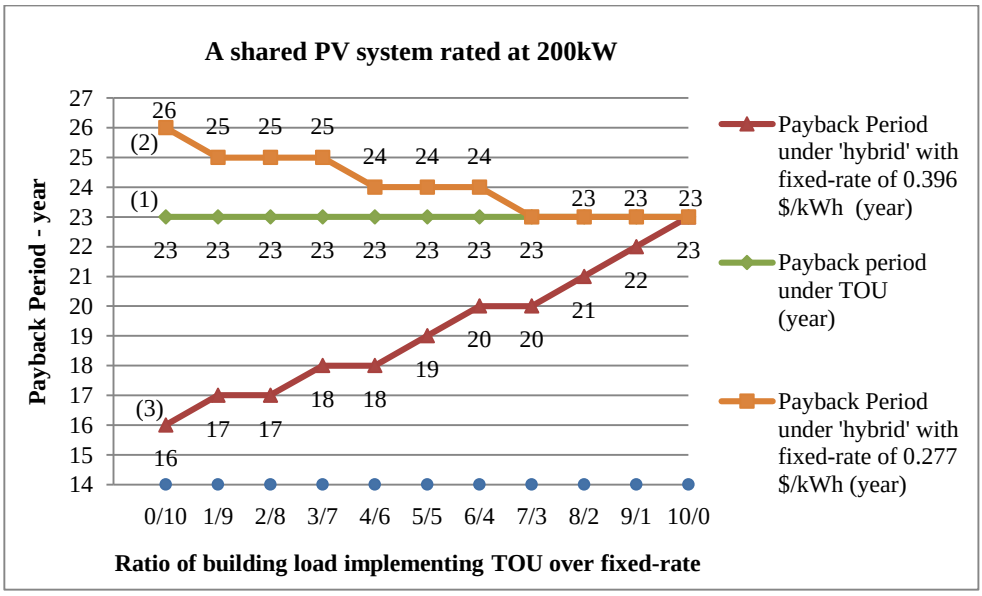

Fig. 5.21 Comparison of payback periods – 200 kW PV system.

From Figs 5.20 & 5.21, line (1) represents the payback period under 'pure' TOU as 16 and 23 years respectively corresponding to the capacity of the shared PV system as 40 kW and 200 kW. Lines (2) & (3) respectively illustrates that the payback period changes along with the different ratios of the building loads with TOU over the loads

with the fixed-rate under two utility fixed rate as 0.277 & 0.396 $/kWh. It can be seen that the higher percentage of the fixed-rate loads, the shorter payback period, which is always shorter than under 'pure' TOU as 16 & 23 years, when the fixed utility rate is higher than the peak and shoulder rates of TOU, such as 0.396 $/kWh for the fixed-rate, and the situation of payback period is opposite with a lower fixed rate than the shoulder and peak rates of TOU, such as 0.277 $/kWh.

The results demonstrate that the ratio of the loads respectively charged by TOU and the fixed-rate and the value of the utility's fixed rate have impacts on the payback period. Under the study conditions assumed by this section, the more users of a VNM group implementing the fixed-rate tariff tends to have a shorter payback period, when the utility's fixed rate is higher than shoulder and peak rates of TOU. On the contrary, the more VNM customers applying TOU would have a shorter payback period, when the fixed rate is cheaper than shoulder and peak rates of TOU. The above results can be explained by that allocating more VNM credits to the customers with a higher utility's fixed rate than shoulder and peak rates of TOU can maximize the reflected value of the VNM credits, which results in more cost saving, and otherwise allocating more credits to TOU customers is a better option for more cost saving.

This section demonstrates that the evaluation for the ratio of the potential VNM customers implementing different types of utility tariffs is necessary to seek a shorter payback period for launching a VNM program. Further studies to test the same issue under other study scenarios as mentioned in the begging of this section is needed to a more comprehensive evaluation.

5.4.5 Reflective value

From the references, it is easy to find the rate schedules of FiT and NM, such as 0.05~0.072 $/kWh in Australia for FiT [41], and the paid price for NM being same as the utility retail in U.S. [77]. As to the price of VNM, no exact value was assessed based on the collected references by this research, but a previous study has clearly stated that the value of the shared VNM power can be determined from the subtraction of the usage by the allocated VNM credits [56], based on which, the equation (5.20) was developed to evaluate the reflected values of VNM, and all arguments involved in, such as cost saving, left credits and PV generation, are counted by year-round

values aligning with the regulated 12-month relevant period for settling accounts for a VNM customer [56]. In addition, the baseline rate for the utility to re-purchase the net left allocated credits as 0.04 $/kWh cited from [56] was applied.

Reflective value $_{VNM}$ =

$$\frac{Annual\ cost\ saving\ from\ allocated\ credits + (annual\ net\ left\ credits * 0.04\ \$/kWh)\ \ (in\ \$)}{Annual\ total\ generation\ of\ the\ shared\ PV\ system\ (in\ kWh)}$$

(5.20)

By applying the above equation and related assumptions used for the previous case studies, the reflective value of VNM of three groups with the normalized daily usage as 37.14 in kWh/d is evaluated and presented by the follows.

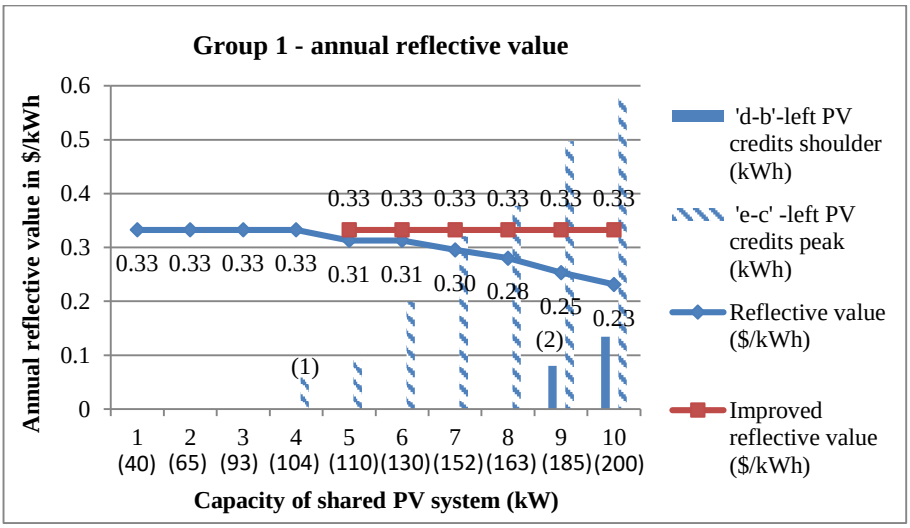

Fig. 5.22 Annual reflective value of VNM credits of Group 1.

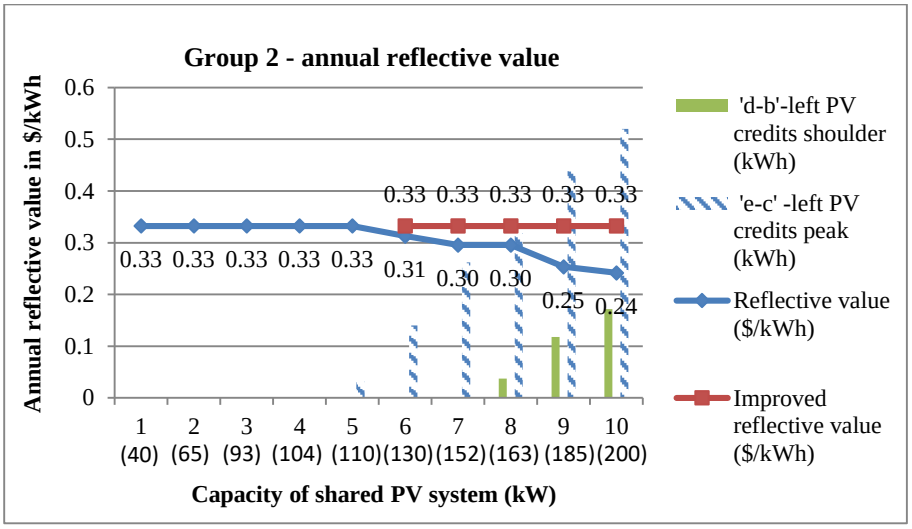

Fig. 5.23 Annual reflective value of VNM credits of Group 2.

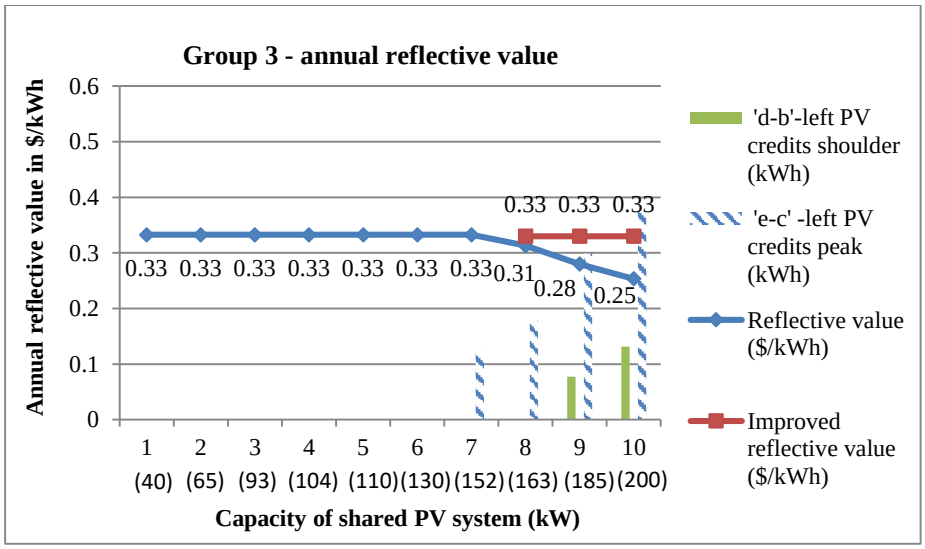

Fig. 5.24 Annual reflective value of VNM credits of Group 3.

As Fig. 5.22 to Fig. 5.24 show, ten developed capacities of PV system shown in Table 5.7 were used for evaluating the reflective value. The columns labelled as (1) & (2), respectively, present the left peak and shoulder credits. It can be seen that the reflected value is not always fixed as feed-in tariff and Net Metering, which are set by the government or the utility, and starts to be lower from the maximum number as 0.33 along with left peak and shoulder credit increasing.

It can be seen that the point where the reflected value starts to reduce is different among the three groups due to the different profiles of building consumption, which shows that the reflected value is an indicator to identify the best extension capacity of the

shared PV system for each group in term of the maximum reflected value. In addition, the Group 3 has the best performance of the reflected value as seven points with the maximum value as 0.33, and with the highest values as 0.28 & 0.25 corresponding to 185 & 200 kW among the three groups, which demonstrates that the highest-peak-usage profile is the best pattern, under the condition of a close daily consumption for each studied VNM group, among three types of profiles as highest-peak, highest-shoulder and even-shoulder & peak the of are close in term of reflected value of VNM.

In addition, based on the result as the three groups with the same maximum reflected value as 0.33, it can be deduced that the maximum reflected value is only decided by the utility rates without any impact from other factors, such as the profile of building usage, the capacity of the shared PV system, etc. Furthermore, the line marked by square sign means the reduced reflected value can be somehow improved to the maximum. According to the analyses in Section 5.4.1, in order to achieve the shortest payback period, the shoulder and peak allocated credits should be maximally consumed respectively by shoulder and peak building usages and the left credits could cause the loss of the reflected value of VNM credits. Two methods for increasing reflected value can be identified as reducing the size of the shared PV system down to a right critical capacity. For instance, an original over-large capacity can be cut down to 153 kW or smaller to achieve the maximum reflected value for Group 3 as Fig 5.18 shows. Another is adding more building loads (customers) into the VNM program for consuming the original left shoulder and peak credits.

5.5 Summary

This chapter has presented the financial evaluation of VNM tariff including payback period and reflective value of VNM credit considering the daily profiles of building consumption and PV generation. The evaluation of payback period indicates that the profile with the highest-peak usage always has the shortest payback period when the daily consumption of the compared buildings or building groups are similar. It is also demonstrated that the shortest payback period of investing a VNM program can be achieved by reducing the capacity of the shared PV system or adding more customers (buildings) to maximally consume allocated VNM credits. An over reduction of the

capacity, however, should be avoided, because the payback period remains fixed beyond a threshold value of the capacity.

In order to provide more options to size a VNM PV system besides the existing method – based on the load capacity, this chapter has developed and evaluated three extension sizes. The evaluation under the 'hybrid' condition indicates that the ratio of the numbers of participants, respectively, implementing TOU and the fixed-rate should be evaluated based on the retail rates of utility electricity tariff, because the ratio of participants composition is one of critical factors to shorten the payback period.

This chapter studied the equivalent value of VNM credit reflected by the subtraction of metered usage, and this value in $/kWh is unfixed, which is different from the purchasing rates of NM and FiT set by the utility. The case studies show that the reflective value getting reduced along with the left-over allocated credits increasing. It is also indicated that VNM is much more worth implementing than NM and FiT by comparing the reflective value to the rates of NM & FiT. For example, the results show that lowest value of 0.23 $/kWh is much higher than the rate of NM & FiT by around 0.05 $/kWh in current Australia context [41, 42]. It should be noted that the reflective value is evaluated only from the side of the end user without considering other fees involved in implement a VNM program, such as wheeling cost associated with using the utility grid to distribute the shared PV power. The reflective value, however, could be a price reference for selling the left-over VNM credits in some way, which needs further studies, instead of repurchasing them at a too low price by utilities.

Chapter 6 Wheeling Cost Associated with Using Utility Grid to Share PV Power

6.1 Wheeling cost associated with sharing PV power

PV systems as one type of distributed generator (DG) has been popularly applied to residential and commercial power supply systems for compensating grid electricity consumption. The schemes of sharing PV power have been developed to more widely spread the benefits of utilising renewable-generated electricity as well. The wheeling cost should be counted in the full selling rate of grid power in the deregulated electricity market [78]. A wheeling cost is defined as a currency fee charged by a transmission owner for providing energy transportation services to other parties. By this sense, a wheeling charge would be raised by using grid networks to share PV power for customers (generator and consumer) involved in a solar power sharing scheme, such as Virtual Net Metering (VNM) [60]. The argument whether customers should be charged for using grid networks to wheel shared PV power has been continuing [56, 60]. In U.S., for a balance between network service providers and customers of VNM, one of the rules for implementing VNM is that the generator and all of beneficiary accounts must be connected behind a single distribution service point (DSP) of a utility [56]. The limit for a single DSP, however, would be broken sooner or later with the extent of using grid to share PV power increasing, so the study for wheeling cost, which is involved in implementing a solar power sharing scheme with crossing multi-DSPs, is required.

This chapter was developed to present and analyse potential wheeling cost associated with using grid networks to share PV power by crossing multi-DSPs. Note that this research specifically focuses on LV distribution system because precinct-level DG is normally connected to local LV distributed feeders. In terms of wheeling cost evaluation, ‘MW-Mile’ is one of the methodologies to assess the services of Transmission Use of System (TUoS) and Distributed Use of System (DUoS), and tracing power flow is critical for applying ‘MW-Mile’ to calculate wheeling cost [79-

81]. 'Generation matrix' is one of tools for tracing grid power flow especially with the advantage of addressing multi-generators [82]. This research combines these two methodologies as 'generation matrix' and 'MW-Mile' to evaluate the potential wheeling costs associated with using LV distribution systems to share local-generated PV power.

In addition, this study developed a series of case studies to present and evaluate wheeling cost and related issues. In embedded cost-based methods, the range transmitted power passing and the amount of wheeled power, which normally are described by the extent of utilising the grid, are the key factors to assess wheeling cost [83, 84]. Based on the achievements of this chapter, it is demonstrated that 'sharing percentage' is a more sensitive indicator to reflect wheeling cost than the extent of utilising the grid, and more factors, such as the install location of a shared PV power, the profile of load demand, need to be considered for comprehensive evaluation of wheeling cost associated with precinct-level solar power sharing.

6.2 The methodology for evaluating wheeling cost

6.2.1 MW-Mile for wheeling cost evaluation

There are several methodologies for the calculation of wheeling charges raised by transmitting and distributing grid electricity, such as post-stage stamp, path contract, MW (MVA)-Mile, and marginal cost [85, 86]. The various methods value wheeling cost from different views of technical and economic issues. Among them, 'MW (MVA)-Mile' is the method focusing on both the amount of wheeled power and the distance wheeled power passes. Based on the statements as the range transmitted power passing and the amount of wheeled power are key factor to assess wheeling cost [83, 84], this study sets wheeling distance and the amount of wheeled power as the research objects, so 'MW (MVA)-Mile' was used to evaluate wheeling charges involved in utilising LV distribution system to share PV power. Note that only active power is considered by this study for simplified evaluation.

In terms of 'MW-Mile', there are various expressions shown in previous studies [79, 80, 81, 87], but wheeled-power amount and wheeling distance are two common factors involved in each expression. Equations for determining 'MW-Mile' are presented as the followings.

Example 1 [79]

$$TC_t = TC \times \frac{\sum_{k\in K} C_k \times L_k \times P_{tk}}{\sum_{t\in T}\sum_{k\in K} C_k \times L_k \times P_{tk}} \tag{6.1}$$

where *t* is network user set and *k* is transmission line set. TC_t is wheeling cost allocation of user *t* in \$/MW, *TC* stands for the total transmission cost in \$/MW, C_k is the cost per mw per unit length of line *k* in \$/MW (MVA)-Km, L_k is the length of transmission line *k*, P_{tk} stands for the power flow contributed by user *t* in line *k*.

Example 2 [80]

$$C_{CT} = C \times \frac{\sum_f (MW_f)_T \times L_f}{\sum_T \sum_f (MW_f)_T \times L_f} \tag{6.2}$$

where *T* is user set and *f* is line branch of a network set. C_{ct} stands for the network charge for user *T* in \$/h, *C* is total annual revenue requirement per hour in \$/h, MW_f stands for power flow in line branch *f* due to the user *T*, L_f is length of the network branch *f*.

Example 3 [81]

$$TC_n = \sum_{i=1}^{l} \frac{C_i \times L_i \times P_{in}}{p_i^c} \tag{6.3}$$

where *n* is user set and i is transmission line set, l represents the lth line. TC_n stands for the transmission cost to network user *n* in \$/MW (MVA). C_i is the cost per mw per unit length of line *i* in \$/MW (MVA)-Km. L_i stands for the length of transmission line *i*. P_{in} is power flow contributed by user *n* in line *i*, p_i^c is the power capacity of line *i* in MW.

Example 4 [87]

$$R_{kl} = \sum_{l=1}^{n} C_f \times \frac{P_{kl}}{\sum_k P_{kl}} \tag{6.4}$$

where l is component line set, *n* represents the nth line and *k* is network user set. R_{kl} stands for wheeling charge allocation to use *k* in \$/h, P_{kl} is power flow contributed by

user *k* in line l, C_f stands for the total annual revenue requirement per hour for line l in $/h based on an expected payback period.

It can be seen that the above each expression can be divided into two components as the economic factor, such as *TC, C, C_i, C_f* representing total transmission cost or expected annual revenue, and the ratio related to power and distance. In addition, it is easy to see two groups of (6.1) & (6.2) and (6.3) & (6.4), respectively, have similar forms. The critical difference between these two groups is the economic indicator as *TC & C* is for the total network, and *C_i & C_f* represent the economic issues of each line, so the summation calculation of all lines is required to evaluate full wheeling cost as (6.3) & (6.4) show. Furthermore, for (6.3) and (6.4), *C_i* is an economic indicator for per unit length of a line *i*, so *C_i* needs to be multiplied by the length *L_i* for evaluating the whole line, and *C_f* has already considered the length of a line branch.

In terms of this research, the shared PV power would pass through related feeders one after another based on the radial nature of LV distribution network, so the accumulation of wheeling cost in each related feeder is reasonable for the evaluation of full wheeling cost under the scenario of this study. In addition, for simplified evaluation of financial issues, this study calculated the cost of each feeder by considering the length of a whole line branch, which is same as *C_f*. Therefore, (6.4) is the best option for the calculations in the latter case studies. Note that wheeling cost evaluated by this study only considers the fixed investment of a network without counting the power loss, the administrative fees, etc.

6.2.2 Generation matrix for tracing power flow

From (6.4), $\sum_i P_{kl}$ is the power flow contributed by user *k* in line l, and $\sum_k \sum_i P_{kl}$ is the total power flow in line l, so how to identify the power injected by a certain generator out of overall transmitted power in a distribution feeder is a key point for the calculation of wheeling cost [88-91]. From the review of related previous studies, there have been some methodologies developed to trace power flow within grid networks [82, 92 and 93], and no matter which method, it was established based on a common assumption as proportional principle [94]. As a general knowledge, electrons can't be coloured to identify their source. The proportional principle is a fair treatment for

addressing this unproven issue [95, 96], and it can be demonstrated by the following diagram.

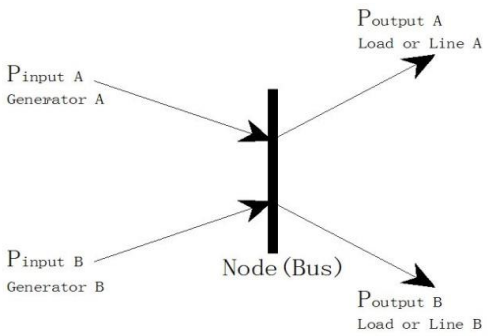

Fig. 6.1 Proportional sharing principle [19].

$$P_{outputA} = P_{outputA} * (\frac{P_{input\ A}}{P_{input\ A}+P_{input\ B}} + \frac{P_{input\ B}}{P_{input\ A}+P_{input\ B}}) \quad (6.5)$$

$$P_{outputB} = P_{outputB} * (\frac{P_{input\ A}}{P_{input\ A}+P_{input\ B}} + \frac{P_{input\ B}}{P_{input\ A}+P_{input\ B}}) \quad (6.6)$$

In this study, $\frac{P_{input\ A}}{P_{input\ A}+P_{input\ B}}$ and $\frac{P_{input\ B}}{P_{input\ A}+P_{input\ B}}$ are called 'tracing factor' notated as T_f.

In terms of the above mentioned three applications of proportional principle, the method without matrix [92] and generation matrix [82] were developed especially for calculating the contribution of a generator to a common as a node or a bus, and 'incidence matrix multiplication' [93] is for tracing the path of a power flow contributed by a certain generator. The application of matrix for power flow tracing has the advantages of explicit expression and addressing multi-generators by the comparison of 'generation matrix' & 'incidence matrix multiplication' to the method without matrix. For clear and concise evaluation of power flow tracing, this study applies 'generation matrix' to investigate the contributions from distributed PV systems and grid and the path wheeled solar power passing.

$$M_g = \begin{bmatrix} a_1 \\ \cdots \\ a_i \end{bmatrix} \quad (6.7)$$

(6.7) is called generator matrix, and

$$M_b = \begin{bmatrix} b_1 \\ ... \\ b_i \end{bmatrix} \tag{6.8}$$

(6.8) is called node (or bus) matrix. Where *i* is generator set including grid and DG. Assuming the Generator 1 is grid, and the generator *i* is a shared PV system, the individual generator matrixes can be expressed as the followings.

$$M_{g1\text{-}grid} = \begin{bmatrix} 1 \\ 0 \\ ... \\ 0 \end{bmatrix}, M_{gi\text{-}pv} = \begin{bmatrix} 0 \\ 0 \\ ... \\ 1 \end{bmatrix} \tag{6.9}$$

In addition, for clear evaluation, this study categorizes nodes (buses) into 'source node' notated as M_{bs} with load & generator and 'load node' notated as M_{bb} with only load besides upstream and downstream power flow. Node matrix can be presented by the followings.

$$M_{bsk} = T_{f1} \times M_{g1\text{-}grid} + T_{f2} \times M_{g2} + \dots T_{fi} \times M_{gi\text{-}pv} = \begin{bmatrix} b_1 = T_{f1} \times 1 \\ b_2 = T_{f2} \times 0 \\ ... \\ b_i = T_{fi} \times 1 \end{bmatrix} \tag{6.10}$$

$$M_{bb(k1)-(kn)} = M_{bsk} \tag{6.11}$$

where *k* is source node (bus) set, and T_f is tracing factor shown by (6.5) and (6.6). The node '*bsk*' is the upstream source node closest to the load node '*bb(k1)'*. 'Upstream' indicates the direction towards power resource, which includes pole transformer and distributed PV systems in this study. Based on (6.11), it can be known that the contributions at a source node M_{bsk} would be carried by all the downstream load nodes, as $M_{bb(k1)} \sim M_{bb(kn)} = M_{bsk}$, until the next source bus $M_{bs(k+1)}$. In addition, b_i is the contribution of individual generator at a certain source node. By (6.10) and (6.11), the contributions of all generators at overall nodes of a studied network can be solved.

So far, two methodologies were investigated and explained in detail, which is, respectively, for calculating wheeling cost and tracing power flow. In addition, based on (6.5) and (6.6), it can be understood that b_i shown in (6.10) is actually the ratio of

$\frac{P_{kl}}{\sum_k P_{kl}}$ shown in (6.4), provided the fixed cost of each feeder of a studied LV distribution network C_f is assumed, the wheeling cost can be presented by (6.4).

6.3 Demonstration on model LV network and evaluation

6.3.1 Model LV network and scenarios

This section established related assumptions and equations (6.4), (6.10) and (6.11) to calculate wheeling cost associated with using LV distribution systems to share PV power. Therefore, a distribution network needs to be built up for further calculations. This study established a network by referring to a segment of LV distribution system in Wollongong City, which is presented by the diagram below.

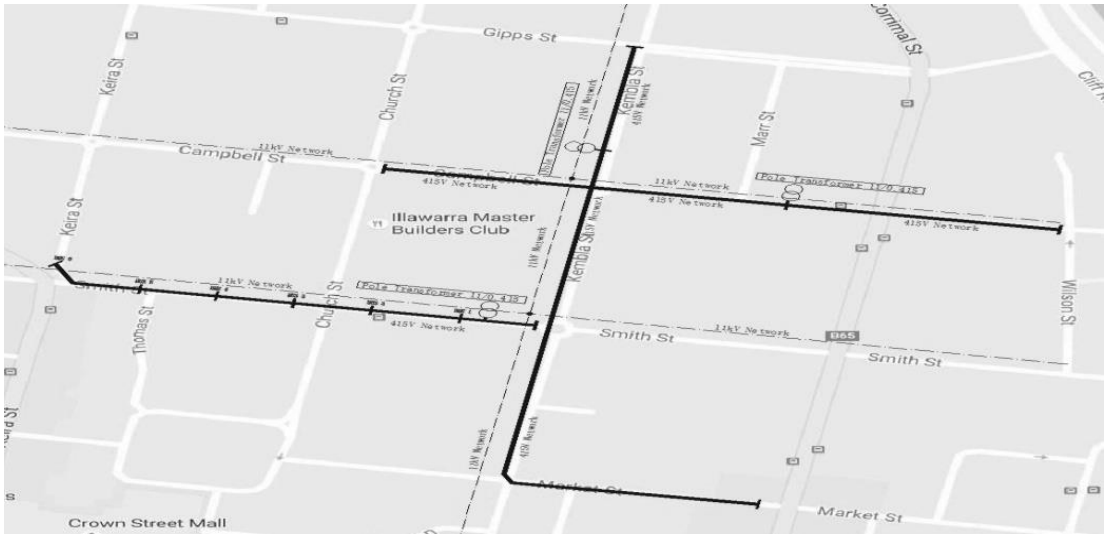

Fig. 6.2 Segments of MV and LV residential distribution networks in Wollongong City.

The dash lines represent segments of local 11kV networks, and the solid lines illustrate LV distribution feeders. Three pole transformers were marked to show the power supply boundary of the illustrated segments. The distribution feeder with the length of around 0.5 km serving western Smith St was used by this study. For simplified calculation and analysis, it was assumed that six buses (nodes) and every two neighbour buses has equal spacing distance. The assumptions for further calculations are presented by the following tables.

TABLE 6.1 Assumptions related to power flow.

Item	Values							
Capacity of Pole transformer (kVA)	160 (11kV/0.415kV)							
Rated capacity of PV systems (AC) (kW)	100							
Consumer's peak load demand (kW)	Load1	Load2	Load3	Load4	Load5	Load6	Load7	Load8
	5	25	5	5	10	25	20	5
Location of buses (the distance from each bus to pole transformer (km)	Bus1	Bus2	Bus3	Bus4	Bus5	Bus6		
	0	0.1	0.2	0.3	0.4	0.5		
Distribution line length (km)	Line1	Line2	Line3	Line4	Line5			
	0.1	0.1	0.1	0.1	0.1			

Eight loads were assumed, and the individual load demand and the total load demand capacity were assigned by integral value for simplified calculation. In addition, the total load demand capacity as 100 kW is satisfied to the acceptable voltage drop 6% of the rated voltage of LV distribution system in Australia context by referring to national code [AS 60038, AS 61000.3.100].

This study considers the daily profiles of PV generation and building load demand to evaluate the related impacts on wheeling cost. The profiles were introduced from Chapter 4. Note that the assumed shared solar system rated at 100 kW, and the changing hourly PV generation is presented by Table 6.2.

TABLE 6.2 Daily change of PV generation.

Time (h)	7	8	9	10	11	12	13	14	15	16	17	18	19
PV generation (kW)	0	22	46	68	84	96	100	97	89	72	51	30	0

Two categories of building profiles were applied, and each assumed load capacity shown in Table 6.1 needs to be multiplied by the ratios shown in Tables 6.3, 6.4 in order to calculate the exact hourly load demands. Note that the time period was taken from 7 o'clock to 19 o'clock to align with the available time of daily PV generation.

TABLE 6.3 Daily change of residential-building load demand.

Time (h)	7	8	9	10	11	12	13	14	15	16	17	18	19
Building demand (per unit)	0.62	0.59	0.55	0.51	0.52	0.54	0.55	0.57	0.60	0.74	0.89	0.98	1

TABLE 6.4 Daily change of office-building load demand.

Time (h)	7	8	9	10	11	12	13	14	15	16	17	18	19
Building demand (per unit)	0.67	0.88	0.98	0.96	0.96	0.95	0.97	0.97	0.97	1	0.97	0.83	0.77

Based on Fig 6.2 and related assumptions, the study LV distribution network can be presented by the diagram below.

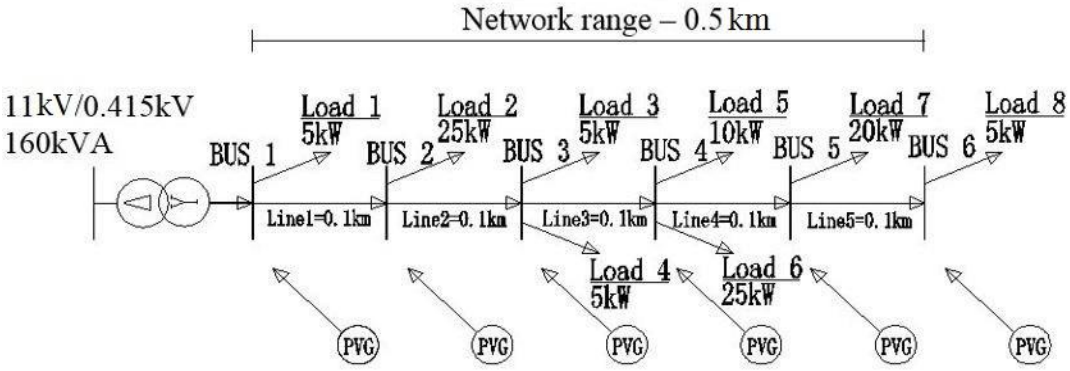

Fig. 6.3 LV distribution network model.

Note that this study assumes only a PV system, labelled by *PVG*, connected to this network for sharing solar power, and marked six *PVG* stand for that the shared PV system is assumed to be, respectively, connected to Bus 1 to 6 in order to evaluate the potential impacts on wheeling cost from the install location of PV systems.

It also needs to be clarified that the simulation of the power network were undertaken in MATLAB, which was for simulating the assumed PV system, and MSExcel, which was applied to all the calculations related to building loads.

For presenting the value of wheeling cost, the fixed investment of distribution feeder C_f needs to be assumed. The related financial formulas are shown as the followings.

Net Present Value (NPV):

$$PV = \frac{C\ (1+i/100)^{(n-1)}}{(1+d/100)^{n}} \tag{6.12}$$

where,

C = any cost element at n^{th} year

i = inflation rate

d = discount rate/ interest rate

n = expected payback years

By the results calculated by (6.12), annual revenue requirement of a certain feeder per hour in \$/h based on an expected payback period can be evaluated by (6.13).

$$C_f = \frac{C}{n \times 8760 \times 5} \tag{6.13}$$

where,

C and n are same as in (6.12),

'5' means the whole network have five segments (lines), and each line is 100m long.

The related economic assumptions and the calculated result of fixed investment of each feeder are presented by the table below.

TABLE 6.5 Financial assumptions and calculated results.

Items	Assumed values	Calculated results	Remarks
Total cost of 0.5 km LV distribution lines - *PV*		\$143,935	Including cable 500m (95m^2), 20 wooden poles , and insulator string (5% cable cost)
C		\$217,794	
i	3%		1.3%~4.5% in recent 15 years in Australia context
d	5%		1.5%~7.25% in recent 15 years in Australia context
n	20 years		
C_f		\$0.2486/h	Each feeder

Based on the above assumptions and calculated results, the wheeling cost can be evaluated by (6.4), (6.10) and (6.11). In addition, two study scenarios were set as static condition and dynamic condition. In Scenario 1-static condition, overall eight loads take peak values shown in Table 6.1, and six PV outputs as 22kW, 30kW, 52kW,

72kW, 89kW, 100kW are selected from Table 6.2. Each output was studied by respectively connected to six buses, so six groups of tested results about the buses were achieved in Scenario 1. In Scenario 2-dynamic condition, PV outputs and all load demands are changing with time by applying the daily profiles of PV generation and residential building load demand shown in Tables 6.2 and 6.3. The shared PV system was studied by respectively connected to 6 buses, and achieved each group of results is about time due to the time-varying PV generation and load demand.

Note that Bus 4 has two different loads as load 5 - 10kW and load 6 - 25kW shown in Fig. 6.3, so the net PV power injected to the network must be different when the shared PV system is respectively connected to Load 5 and 6. Therefore, for the shared PV system there are two different install locations at Bus 4 notated as B4(a) and B4, so the whole network has total 7 locations for installing the shared PV system.

6.3.2 Modelling result and discussion

The case studies has evaluated four points including: (1) the potential wheeling cost associated with using utility LV distribution system to sharing PV power; (2) the relationships between wheeling cost and the extent of utilising grid including the distance shared PV power passing and the amount of wheeled PV power; (3) the potential install location of the shared PV system with lowest wheeling cost; and (4) the potential impacts on wheeling cost from the daily change of PV output and building load demand. The related test items illustrated in latter graphs were presented by the table below.

TABLE 6.6 Notation of testing parameters.

Items		Notation
D from PT (km)		Distance from each bus to the pole transformer listed on table1
D down passing (km)		Distance from the shared power passing towards the loads direction
D up passing (km)		Distance from the shared power passing towards the pole transformer direction
Assessment approach	WC ($/kWh)	Wheeling cost caused by distributing solar power in $ per kilowatt hour
MW-Mile	WC ($/h)	Wheeling cost caused by distributing solar power in $ per one hour
Sharing percentage %		The ratio of net PV power exported from a node over total power supply (the sum of PV power and grid power)
Wheeled power (kW)		The amount of wheeled net PV power (hourly PV output minus all loads connecting to the common bus)

Note that there are two types of wheeling cost with different units as $/kWh and $/h. Based on (6.4), the calculated result should be in $/h, and in order to evaluate wheeling cost from a different view, this result is assigned to per kilowatt of wheeled solar power in $/kWh. In addition, sharing percentage is actually the tracing factor T_f at a source bus shown by (6.5) and (6.6), and this study demonstrated that sharing percentage is a critical indicator for evaluating wheeling cost associated with sharing PV power.

6.3.2.1 Evaluation under Scenario 1

Under this scenario, there are six tests based on six selected daily PV outputs. In each test, PV output is fixed, and all loads always remain the peak values of daily demand capacity. Six groups of results are presented by Fig. 6.4 to Fig. 6.9.

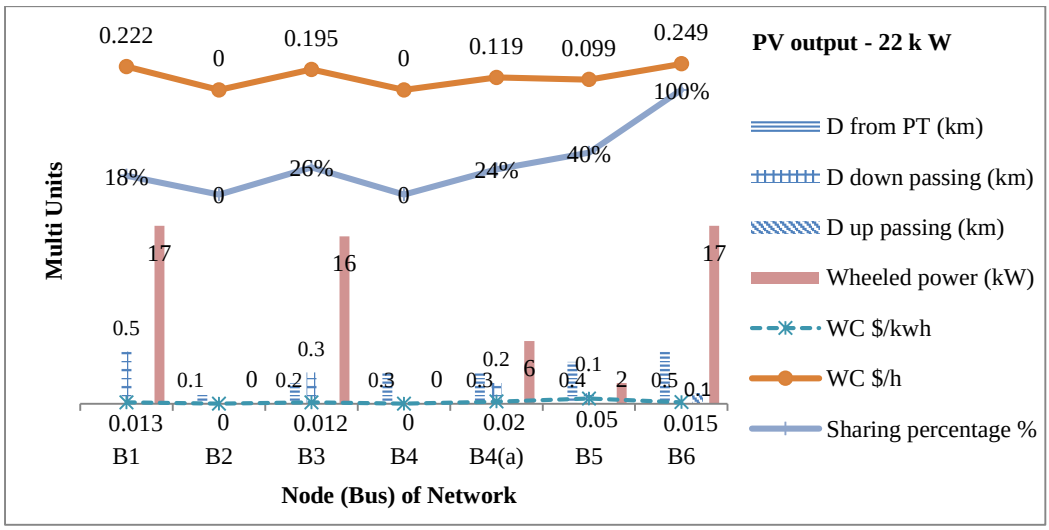

Fig. 6.4 results with 22kW PV output.

As previously mentioned, there are two different install locations for the shared PV system at Bus 4, which are illustrated by B4 and B4(a) shown in Fig. 6.4. It can be read by 'D from PT' as well, as 0.3 labelled at two locations. In order to study the second point mentioned in the beginning of this section, as the relationships between wheeling cost and the extent of utilising grid, the shared PV system was, respectively, connected to 7 locations as B1 ~ B6 shown in the above diagram. In addition, from Fig. 6.4, four locations B1, B3, B4(a), B5 have 'D down passing' as 0.5, 0.3, 0.2, 0.1, which means that PV power is distributed to the downstream direction (towards load 8 shown in Fig. 6.3), when the solar system is respectively connected to these four locations, and otherwise no PV power shared at B2 and B4 due to PV generation completely consumed by the on-site loads. Only at B6 is the shared solar power distributed upstream (towards pole transformer), as 0.1 km. The exact distance shared solar power passing and the amount of wheeled solar power can be read from the labelled numbers shown by Fig. 6.4. Note that the total wheeling distance shared PV power passing should be the summation of 'D down passing' and 'D up passing'. The test results based on other PV outputs were illustrated by Fig. 6.5 to Fig. 6.9.

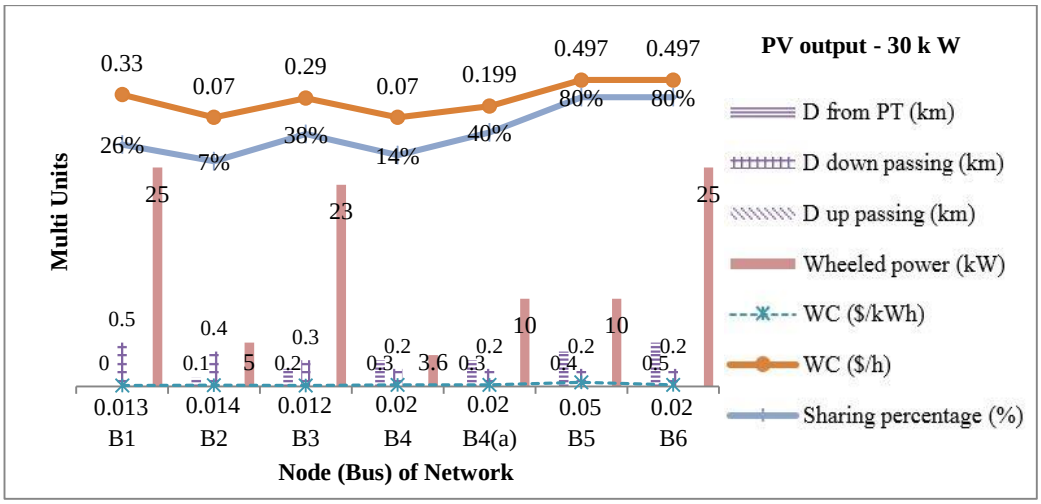

Fig. 6.5 Results with 30kW PV output.

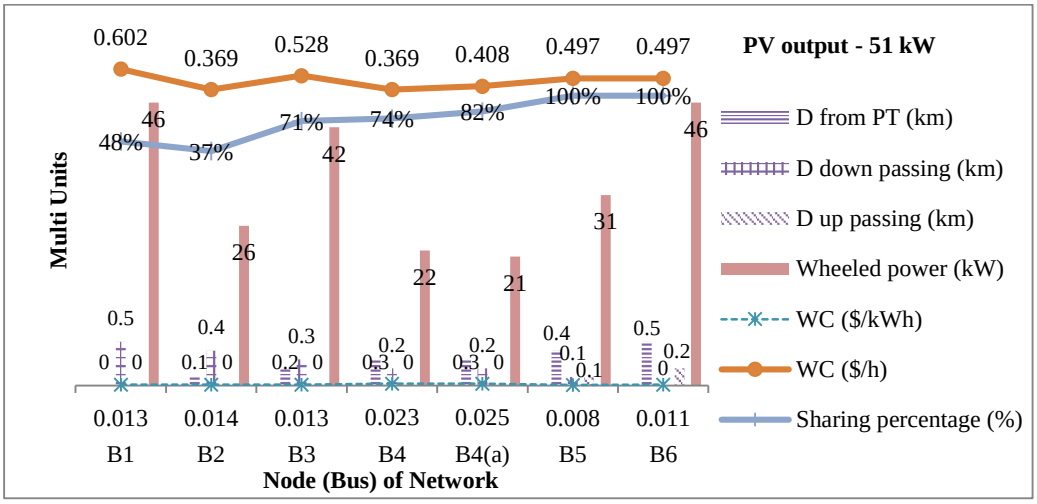

Fig. 6.6 Results with 51kW PV output.

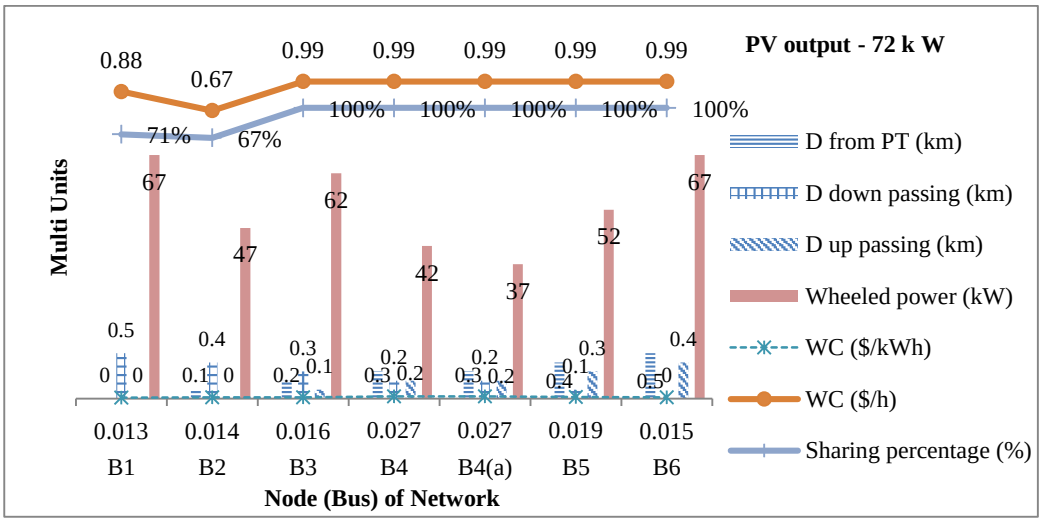

Fig. 6.7 Results with 72kW PV output.

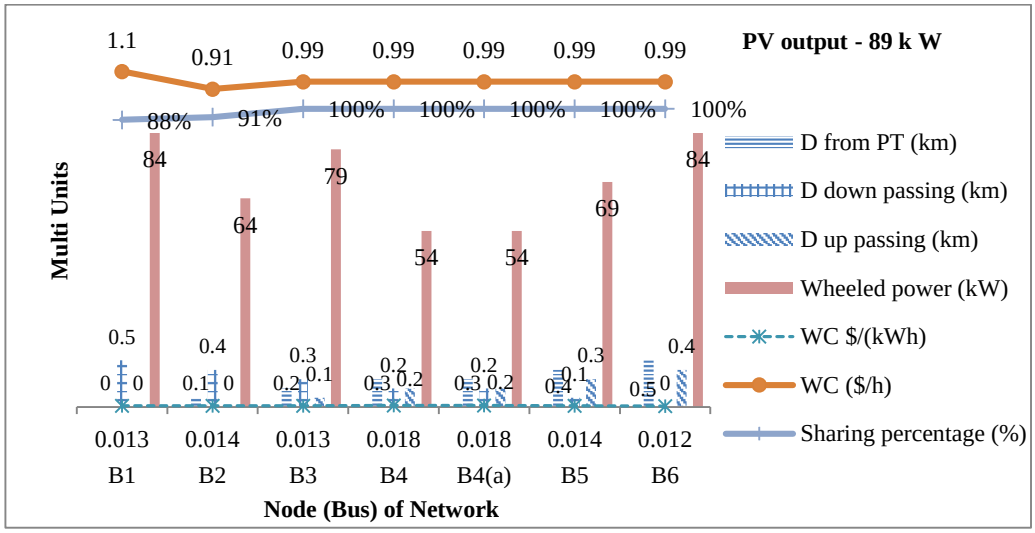

Fig. 6.8 Results with 89kW PV output.

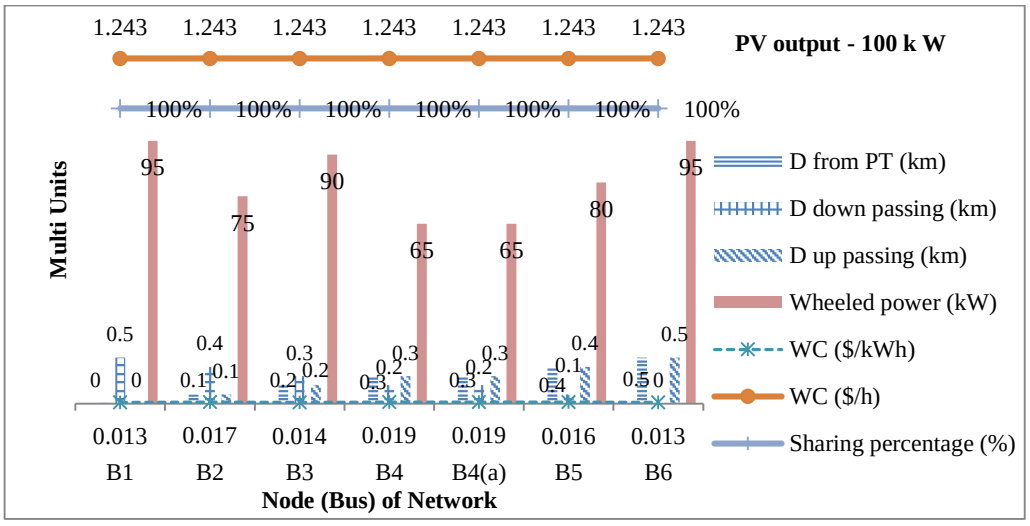

Fig. 6.9 Results with 100kW PV output.

By comparing Fig. 6.5 to Fig. 6.9, it is demonstrated that the wheeling cost for sharing PV power is not in direct proportion to the extent of utilising grid (the distance distributed solar power passing and the amount of wheeled power). For example, in Fig 6.4, wheeling cost is 0.222$/h with downstream distance 0.5km at B1, but a higher cost is 0.248$/h with upstream distance 0.1km at B6. In Fig. 6.5, 0.07$/h with downstream distance 0.4km at B2, and the costs at B3, B4(a), B5, B6 are always higher than at B2 but with shorter distance as 0.3km for B3 and 0.2km for B4(a), B5, B6. The same situation as longer distance shared solar power passing with lower wheeling cost is presented by Fig. 6.6 to Fig. 6.8 as well. The opposite situation as longer distance with higher wheeling cost only occurs at B1 and B2 in Fig. 6.4 to Fig. 6.8. For example,

wheeling cost 0.33$/h with 0.5km at B1, and lower value as 0.07 with 0.4km at B2 in Fig. 6.5. Wheeling cost is 0.602 with 0.5km at B1, and 0.369 with 0.4km at B2 in Fig. 6.6. In Fig. 6.9, wheeling cost remains fixed as 1.243 with any distance, and the same situation as wheeling cost regardless of the distance is presented by B3 ~ B7 in Fig. 6.7 and Fig. 6.8. From the above comparisons, firstly, there is no proportion relationship between the wheeling distance and wheeling cost. Secondly, there is no a constant rule between the distance and wheeling cost.

In terms of the relationship between the amount of distributed solar power and wheeling cost, the situation is same as the above. For example, wheeling cost is 0.479$/h with 10kW transmitted solar power at B5, and a lower value 0.29$/h but with greater amount of solar power as 23kW at B3 in Fig. 6.5. The same situation is presented by Fig. 6.6 as 0.602$/h with 6kW transmitted power at B1, and lower cost 0.369$/h with a greater amount 26 kW. In addition, the same amount of transmitted PV power can cause different wheeling costs as 10kW respectively with 0.109$/h and 0.497$/h at B4(a) and B5. Furthermore, from B3 – B6 in Fig. 6.7 to Fig. 6.9, it is shown wheeling cost is independent of the amount of transmitted PV power.

In summary, ‘MW-Mile’ mainly considers the amount of transmitted power and wheeling distance, but the above analyses demonstrate that the amount of shared solar power and wheeling distance can’t be literally used to assess potential wheeling cost for using utility LV distribution system to share PV power.

As previously introduced, this study tested two types of wheeling cost respectively shown by ‘WC $/h’ and ‘WC $/kWh’ in Fig. 6.4 to Fig. 6.9. From the above illustrations, it is demonstrated that two types of wheeling cost at a same install location of the shared PV system have different situations in terms of values. For example, Fig. 6.4 shows B1 with higher ‘WC $/h’ 0.222 but with much lower ‘WC $/kWh’ 0.013 than B5 with ‘WC $/h’ 0.099 and ‘WC $/kWh’ 0.05. This is caused by the much different kW at B1 with 17kW and B5 with 2kW. Another example by B2 with 26kW and B6 with 46kW in Fig. 6.6, it has B2 with lower ‘WC $/h’ 0.369 but higher ‘WC $/kWh’ 0.014 than B6 with ‘WC $/h’ 0.497 and ‘WC $/kWh’ 0.011. It is easily to understand that ‘WC $/kWh’ is a value allocated to per kW based on ‘WC $/h’, so the quantity of kW of transmitted PV power is the critical factor to cause the different situations of two types of wheeling cost.

The more important point involved in the difference of two types of wheeling cost is what they respectively imply to identify install location of shared PV system with lower allocated wheeling cost. In deregulated electric market, wheeling cost must be considered for calculating the total charge for consuming utility energy, so lower wheeling cost could result in cheaper price of grid electricity for both utility and consumers [78]. For this study, in terms of 'WC $/h', B2 is the best location for installing the shared solar system, because B2 always has the lowest wheeling cost shown in Fig. 6.4 to Fig. 6.8. For 'WC $/kWh'. B1 is the best location in Fig. 6.7 and Fig. 6.9 due to the lowest wheeling cost 0.013 $/kWh. B3 is the best location in Fig. 6.4 and Fig. 6.5 with the lowest (nonzero) wheeling cost 0.012 $/kWh, and B6, respectively, with the lowest value 0.011, 0.012, and 0.013 in Fig. 6.6, Fig. 6.8, and Fig. 6.9. Note that the best install location judged by 'WC $/kWh' is at different buses in the above 6 diagrams instead of at a same bus B2 identified by 'WC $/h'. A common feature is, however, that the different buses with lowest 'WC $/kWh' always have the greatest value (or close) of wheeled PV power in individual test, such as B3, respectively, with the second highest value 16kW and 23kW in Fig. 6.4, and Fig. 6.5, B6, respectively, with greatest values 46 kW, 84 kW, 95kW in Fig. 6.6, Fig. 6.8, and Fig. 6.9, and B1 with greatest value 67 kW, 95 kW in Figs 6.7, 6.9. Based on the above different situations of two types of wheeling cost, this study proposes that 'WC $/h' can be an indicator specifically for credit-based solar power sharing scheme, such as VNM, to identify a PV-system install location with lower wheeling cost. 'WC $/kWh' can be an indicator for a group-solar scheme, which supplies substantial kW of PV power instead of the rolled-over credits, to identify PV-system install location with lower wheeling cost. Based on (4), 'WC $/h' states for a whole wheeling service, on another hand, credit-based group solar scheme normally measures total generation. When 'WC $/h' is allocated to each customer based on the quantity of roll-over credits, which is only depending on the measured total PV generation, for a same PV output, the lowest 'WC $/h' would have the lowest allocated value for customers. Therefore, for credit-based sharing solar scheme, the 'WC $/h' directly indicates the install location with the lowest wheeling cost. In contrast, 'WC $/kWh' varies depending on the substantial shared power, so in a common sense, it is expected that more solar power sharing with lower wheeling cost. Therefore, for power-based sharing solar scheme, both exported kilowatts power and wheeling cost need to be considered, and 'WC $/kWh' is an appropriate indicator.

In conclusion, the above evaluation implied the method of allocating wheeling cost to each customer depending on different types of sharing solar scheme is another critical factor for the site-specific identification of wheeling cost associated with using LV distribution system to share PV systems.

As the above evaluated, wheeling distance and kilowatts of wheeled power are not the reliable indicators for assessing the potential wheeling cost for using utility LV distribution system to share PV power. Based on Figs 6.4 ~ 6.9, it is demonstrated that 'sharing percentage' can be a more convincing factor than kilowatts of wheeled solar power and wheeling distance to reflect wheeling cost. As shown in these Figs, the curves of sharing percentage and wheeling costs ('WC $/h') have almost same profiles. Note that several data points in the above diagrams have, however, different scenarios by detailed comparison. For example, B4(a) has a higher 'WC $/h' 0.119 but with lower sharing percentage 24% than B5 with 'WC $/h' 0.099 and sharing percentage 40% in Fig 6.4. In Fig 6.5, B1 has higher 'WC $/h' 0.33 but with lower sharing percentage 26% than B3 with 0.29 & 38%, and B4(a) with 0.199 & 40%. By further study, wheeling distance is the factor causing the above mismatch between 'WC $/h' and sharing percentage. For example, In Fig 6.8, B1 has lower sharing percentage 88% than B2 91%, but the wheeling distance at B1 is 0.5km longer than B2 0.4km, so B1 has higher wheeling cost 1.1$/h than B2 0.91$/h. The same situation is also demonstrated by the above two examples as B4(a), B5 in Fig 6-4, and B1, B3, B4(a) in Fig 6.5. Note that sharing percentage has more significant impact on wheeling cost than wheeling distance based on a comprehensive comparison.

Based on the above analyses, this study proposes the combination of sharing percentage and wheeling distance can be a reliable indicator to evaluate wheeling cost for utilising LV distribution system to sharing PV power.

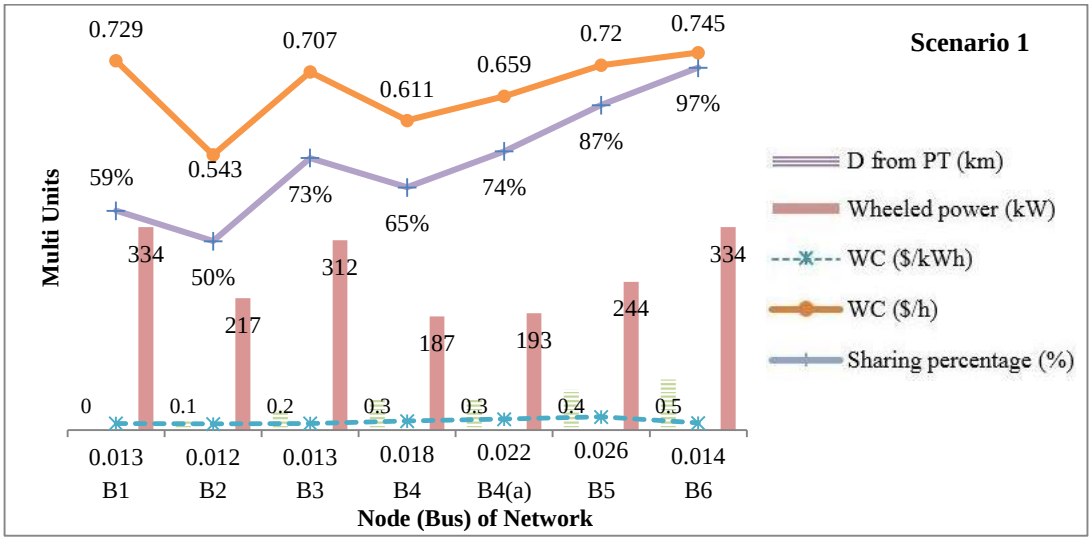

Fig. 6.10 Integrated illustration of the above 6 groups.

In Fig. 6.10, wheeling cost ('WC $/h' & 'WC $/kWh'), sharing percentage are average value, and wheeled power is the sum corresponding value based on the above 6 groups. This diagram shows comprehensive trends of these three main items. It is demonstrated as well that the curves of sharing percentage and 'WC $/h' have almost same profile, so sharing percentage is regarded as a reliable indicator to reflect wheeling cost by this study. The curve of 'WC $/h' & 'WC $/kWh' have different profile due to the different quantity of kilowatts of wheeled power. By B2 with the lowest 'WC $/h', it is indicated that B2 is the best install location of a shared PV system for credit-based sharing solar power scheme. B1, B3, B6 and B2 have very low values of 'WC $/kWh', but the former three buses with much higher exported power by 334kW, 312 kW, 334 kW than 217kW at B2. From the expectation of more solar power sharing, B1, B3, B6 are, respectively, the best PV-system install location for power-based solar scheme depending on different PV outputs.

6.3.2.2 Evaluation under Scenario 2

Under scenario 2, load demand and PV output are time-varying, so each test is based on a certain bus and time shown in Fig. 6.11 ~ 6.17, which is different from each test about a certain PV output and different buses under Scenario 1. For matching up total 8 loads demand, this study only takes 100kW as the capacity of the shared PV system under this scenario.

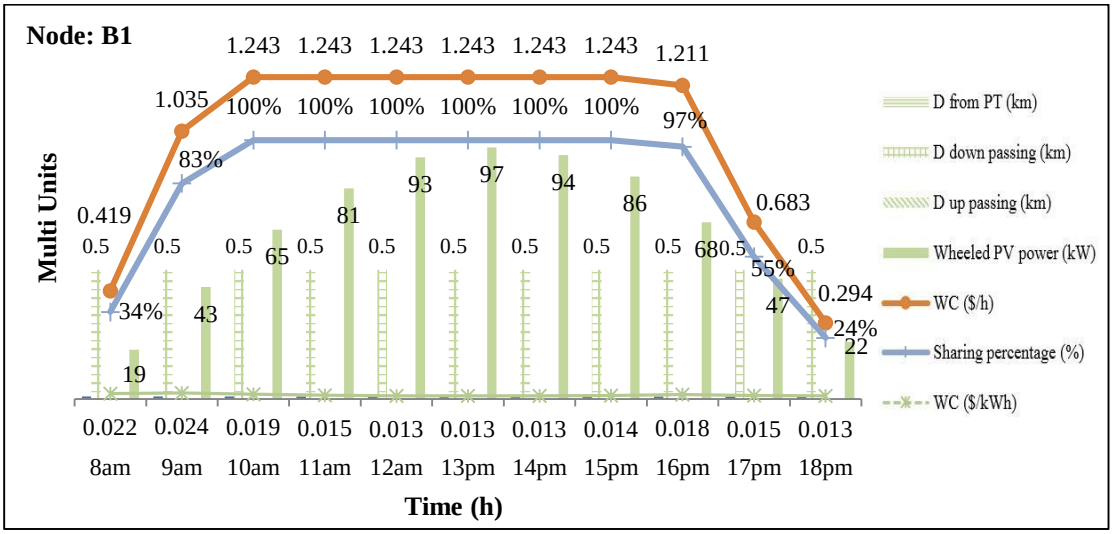

Fig. 6.11 Results at B1.

Fig. 6.11 shows the calculated results of wheeling cost ('WC $/h' & 'WC $/kWh'), sharing percentage and kilowatts of wheeled solar power when the shared PV system connected to the bus B1. It can be seen that the kilowatts of wheeled solar power is changing along with time. Note that this chapter used the annual average profiles of daily PV generation and building load demand, which were achieved in Chapter 4, to evaluate wheeled power changing, so the profile of wheeled PV power shown in Fig. 6.11 is not available to demonstrate the exact situation of wheeled PV power changing in a certain day, but for presenting annually classic trend. As Fig 6.11 shows, wheeling cost and sharing percentage are changing along with time as well due to the time-varying wheeled solar power. Note that the flat segment of the curves of 'WC $/h' and sharing percentage shows the daily peak values of these two items and indicates that the PV generation is the only power supply resource for all 8 loads from 10am to 15pm. In addition, as evaluated under scenario 1, sharing percentage is a sensitive factor to wheeling cost (WC $/h), which is also demonstrated by Fig. 6.11 as the two curves of sharing percentage and wheeling cost (WC $/h) have a very similar profile. The assigned wheeling cost 'WC $/kWh' has a generally opposite trend to WC $/h as higher values occurring at early and late time and the middle of the day with the lowers due to the profile of wheeled PV power. Furthermore, the downstream wheeling distance is 0.5km for any time, because the shared PV system is only connected to B1 in this test. The test results at B2 to B6 are illustrated by Fig. 6.12 to Fig. 6.17.

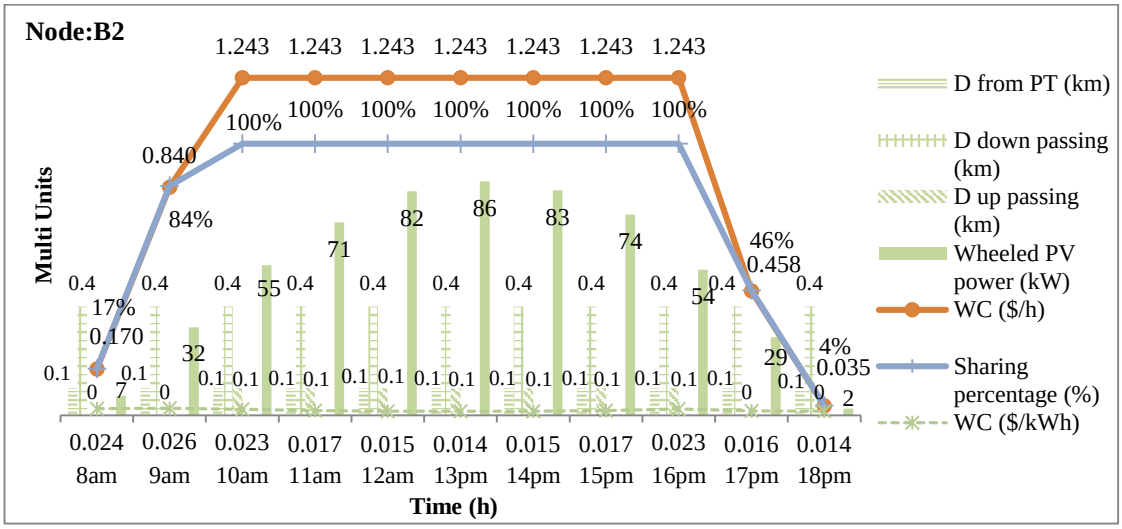

Fig. 6.12 Results at B2.

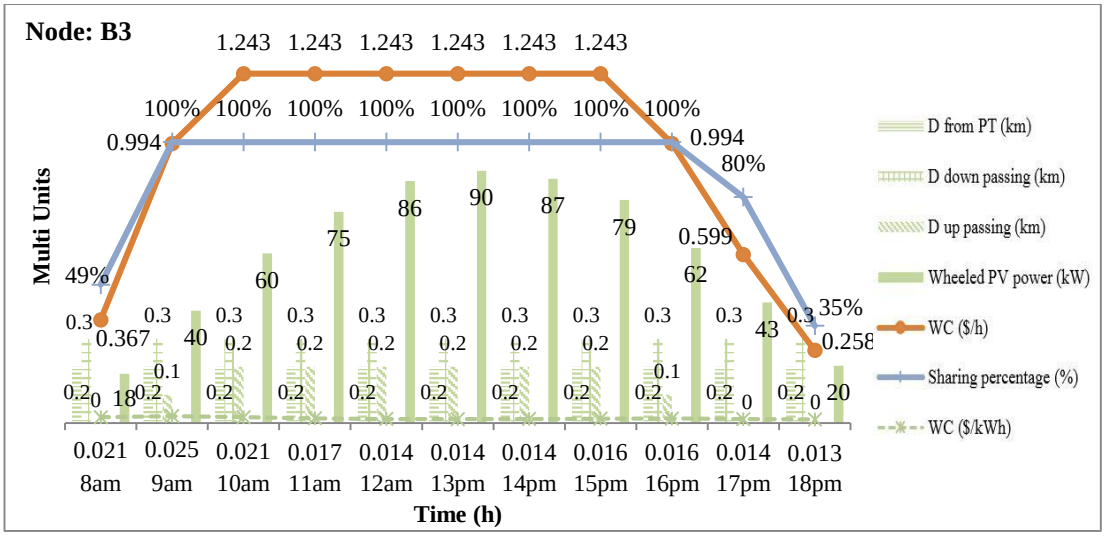

Fig. 6.13 Results at B3.

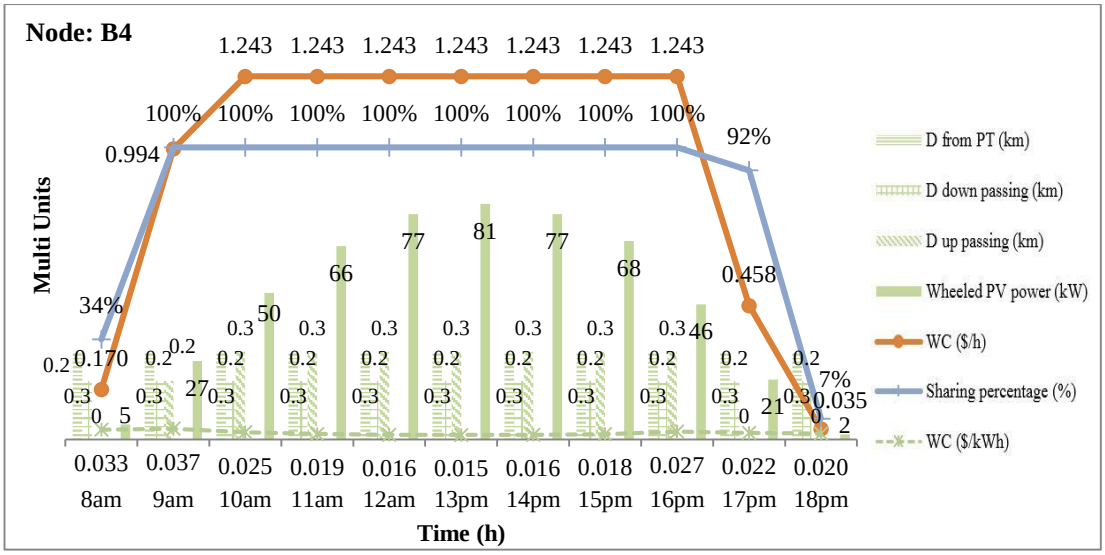

Fig. 6.14 Results at B4.

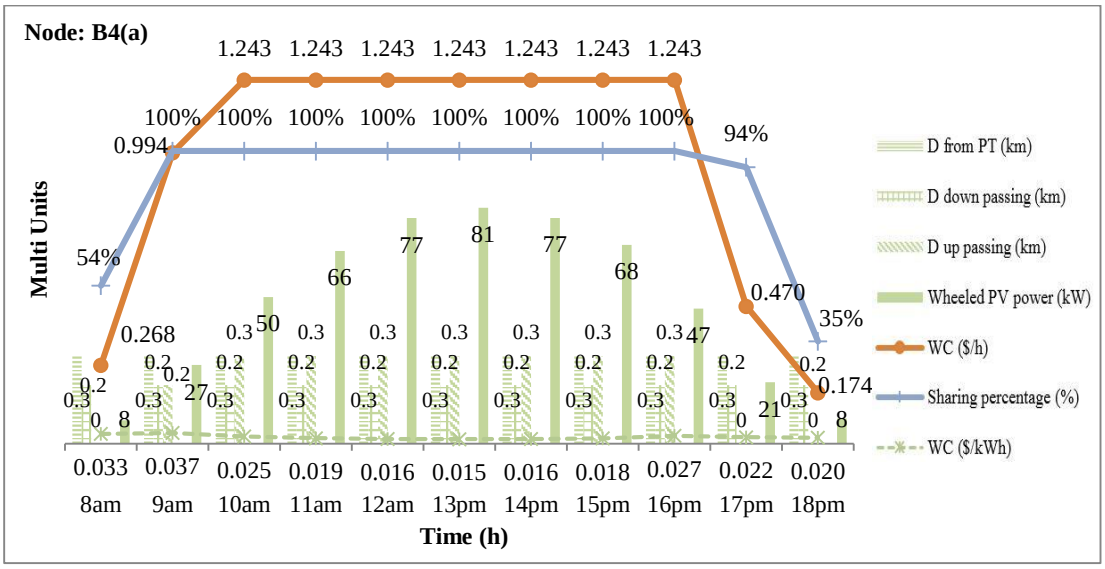

Fig. 6.15 Results at B4(a).

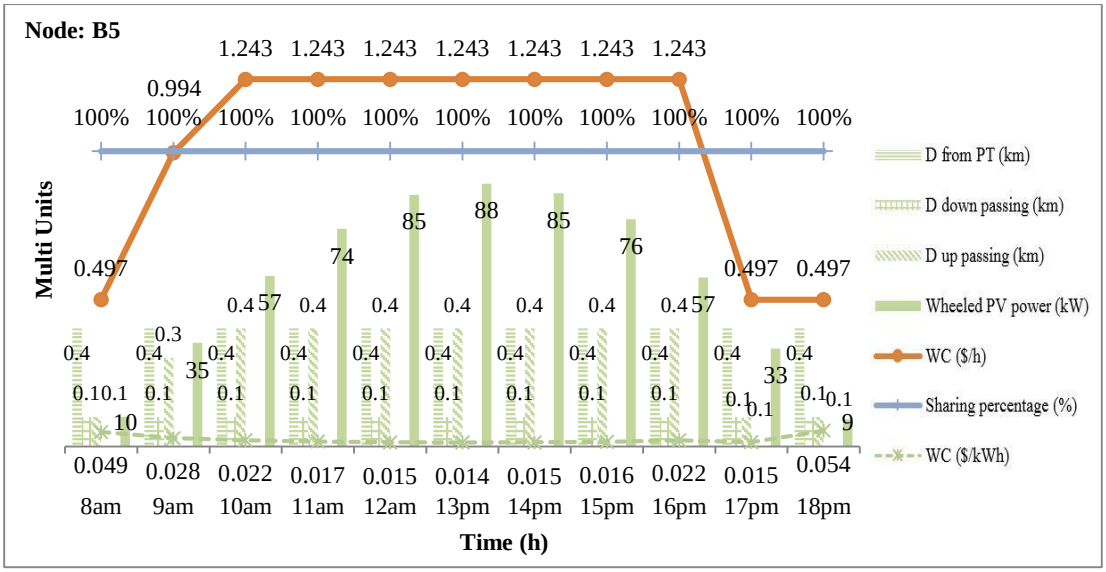

Fig. 6.16 Results at B5.

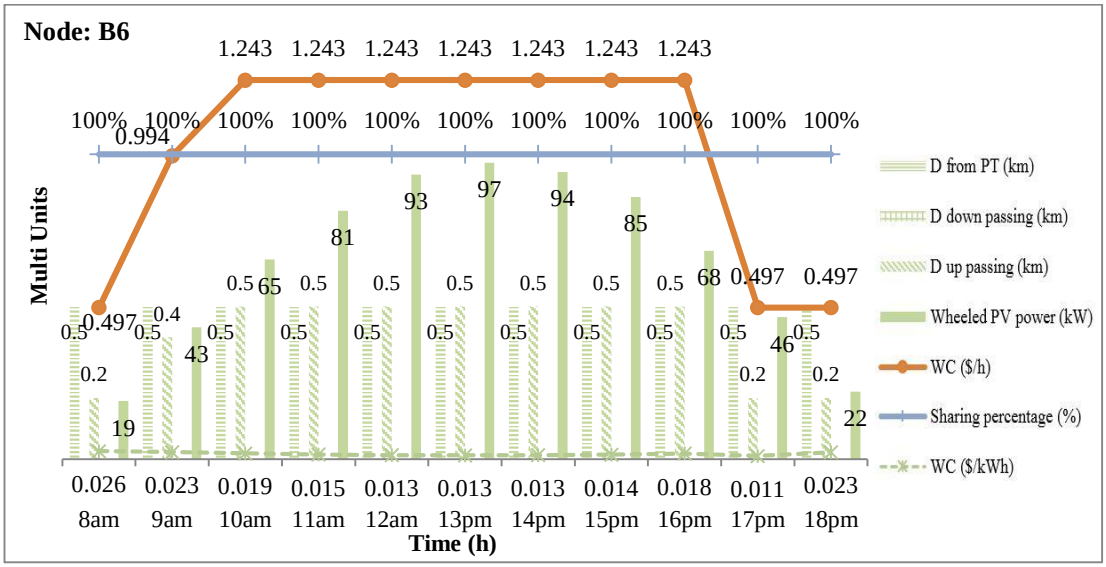

Fig. 6.17 Results at B6.

From the comparison of Fig. 6.11 to 6.17, it can be seen that wheeling cost remains the peak value of 1.243$/h from 10am to 15am (B1&B3) or 16am (B2, B4~B6), and it matches high kilowatts of wheeling solar power. During out of the above time period as 8am – 10am and 16pm – 18pm, the greater (less) wheeled power causes the higher (lower) wheeling cost. In terms of wheeling distance, the peak value 1.243$/h always corresponds to the longest distance 0.5km. Note that the total wheeling distance is the sum of downstream and upstream distance shown in Fig. 6.12 to Fig. 6.16. However, other values of wheeling cost and the corresponding wheeling distance have no a clear rule. For example, at B1, wheeling distance is fixed as 0.5km for each hour, but all hourly wheeling cost is not always same. At B2, wheeling distance 0.4km corresponds to different wheeling cost as 0.17, 0.84, 0.458 and 0.035. The same situation is shown by B3 0.3km, B4 0.2km and 0.3km, B4(a) 0.2km illustrated, respectively, in Fig. 6.13 to Fig. 6.15 as well. The above comparisons demonstrate that there is no a distinct rule between wheeling cost and the extent of utilising grid as wheeling distance and the kilowatts of wheeled power.

On another side, it can be seen that the curve of sharing percentage has a very similar profile as wheeling cost (WC $/h) shown in Fig. 6.11 to Fig. 6.15, so as evaluated under scenario 1, sharing percentage is a more sensitive factor to reflect wheeling cost varying than wheeling distance and the amount of wheeled power. There is, however, a different scenario for the curves of wheeling cost and sharing percentage shown by Fig. 6.16, Fig. 6.17, as the sharing percentage of 100% does not always cause peak

wheeling cost of 1.243$/h. It can be understood that wheeling distance results in this different scenario by comparing the difference value between two neighbours 'wheeling distance' and 'wheeling cost' in Fig. 6.16 and Fig. 6.17. For example, at B5 shown by Fig. 6.16, when wheeling distance increases from 0.2km at 8am up to 0.4km at 9am by a double increment, wheeling cost rises up from 0.497$/h to 0.994$/h by a double increment as well. At B6 shown by Fig. 6.17, the distance decreases from 0.5km at 16pm to 0.2km at 17pm by a 2.5 times reduction, wheeling cost drops from 1.243$/h down to 0.497$/h by 2.5 times reduction as well. It can be seen that wheeling cost varies along with wheeling distance in proportion. Based on the above evaluation, one of conclusions under scenario 1, as the combination of sharing percentage and wheeling distance can be a reliable indicator to reflect the value of wheeling cost for using utility LV system to share solar system, is demonstrated as well by scenario 2.

As analysed under Scenario 1, two types of wheeling cost as 'WC $/h' and 'WC $/kWh', respectively, can be indicators for evaluating the install location for a shared PV system with lower allocated wheeling charges for customers depending on different types of sharing solar tariff. Under this scenario, Fig. 6.11 to Fig. 6.17 is unable to illustrate the clear comparisons of wheeling cost and sharing percentage between different buses due to the time-varying test method. Fig. 6.18 was made for comprehensively comparing the related situations of all 7 nodes.

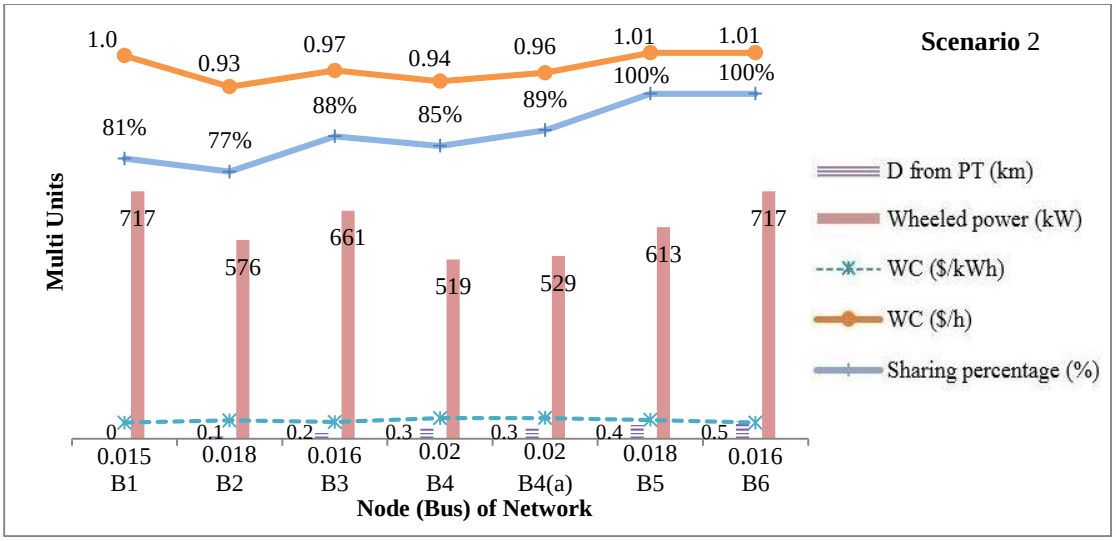

Fig. 6.18 Daily illustration under scenario 2.

In Fig 6.18, the kilowatts of wheeled power are presented by daily accumulated hourly values at a certain node shown by Fig. 6.11 to Fig. 6.17, wheeling cost of 'WC $/h'

and sharing percentage are shown by daily average value, and wheeling cost of 'WC $/kWh' is calculated by the division of daily accumulated 'WC $/h' by daily total kilowatts of wheeled power. It can be seen that the curves of 'WC $/h' and sharing percentage have almost completely same profiles, which demonstrates once again sharing percentage is a very sensitive factor to wheeling cost of 'WC $/h'.

In terms of the difference between two types of wheeling cost 'WC $/h' and 'WC $/kWh', from Fig. 6.18, B2 has the lowest value of 'WC $/h', and B1, B3 and B6 have obviously lower 'WC $/kWh' than other buses, which is completely same with the corresponding evaluation under Scenario 1. Therefore, as one of conclusions under Scenario 1 demonstrated, 'WC $/h' and 'WC $/kWh' can be applicable, respectively, for credit-based and power-based sharing solar schemes to identify the install location of a shared PV system with lower allocated wheeling cost and more revenue from utilising renewable energy to customers.

6.3.2.3 Evaluation related to the profile of load demand

As one of the research interests of this chapter, the impact on wheeling cost from the different profile of building load demand was evaluated, and the related results are presented by Fig. 6.19. Note that all study items under the above two scenarios were tested based on the load-demand profile of residential building. Under this test, for concise and explicit comparison, this study assumes an office building is connected to Bus 4 instead of previous residential building, and the office building has same peak load demand of 25kW shown in Fig. 6.3. In addition, this test was done under Scenario 2.

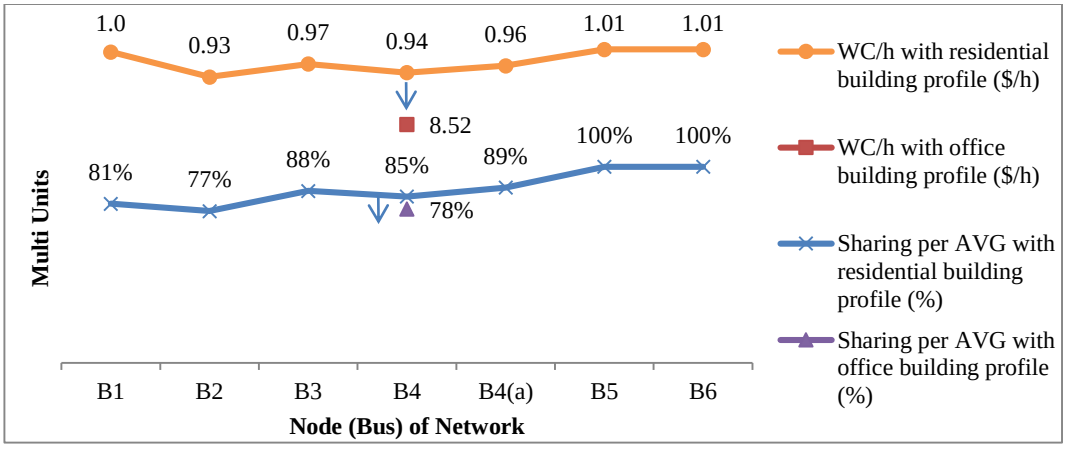

Fig. 6.19 Impact on typical arguments from load-demand profile.

From Fig. 6.19, both wheeling cost and sharing percentage with office-building profile are lower than the originals with residential-building profile at B4, and the reduction of wheeling cost is significant by B4 substituting B2 as the location with the lowest wheeling cost. This result can be explained by the proportion of load consumption. As Table 6.7 shows, office building has, respectively, higher shoulder and peak consumption than residential building, and office building hence locally consumes more PV generation than residential building. It causes less kilowatts solar power wheeled, so sharing percentage drops and consequently wheeling cost is reduced. Note that the above evaluation was made based on the assumption of close or same peak load demand, because load demand capacity is one of factors impacting wheeling cost and sharing percentage as well illustrated by Fig. 6.10, 6.19.

TABLE 6.7 Proportion of load consumption.

Building Category	The proportion of ***annual energy*** consumption during off-peak period	The proportion of ***annual energy*** consumption during shoulder period	The proportion of ***annual energy*** consumption during peak period	The approximately ratio of three proportions	Daily consumed energy in per unit method (kWh)
Large Office	16.6%	42.5%	40.9%	1:2.6:2.5	15.89
Midrise apartment	29.5%	35.0%	35.6%	1:1.2:1.2	15.00

In conclusion, it is obviously demonstrated that different building-consumption profiles could vary the situations of wheeling cost and related issues. When the load demand capacity of neighbouring buildings is close or same, a node of LV distribution system, which is connected to a building with higher shoulder and peak consumption, can be a good install location for the shared PV system to reduce wheeling cost (WC $/h). Further study by testing more categories of building is needed to comprehensively evaluate the impact on wheeling cost from the load-demand profile.

6.4 Summary

This chapter has presented a methodology by combining ‘generation matrix’ and ‘MW-Mile’, which are used for evaluating wheeling charges of grid power transmitting, to evaluate potential wheeling costs associated with using LV distribution system to share PV power. Note that although this study focuses on LV distribution system, the proposed methodology can be applicable to evaluate wheeling cost

utilising MV network to share solar power as well due to the similar structure nature of LV and MV networks. In addition, 'generation matrix' and 'MW-Mile' are two general applications suitable for tracing power flow and assessing wheeling cost, so there is no a constrain for the type or voltage class of grid network.

This study was developed with considering the daily change of PV output and load demand, so two scenarios were set for related studies as Scenario 1 with fixed solar power output and load demand, and Scenario 2 with varying hourly solar generation and load consumption. In addition, it is shown that all corresponding evaluations studied, respectively, in two scenarios have similar results.

This chapter shows that the kW of wheeled power and wheeling distance are not reliably to reflect the value of wheeling cost associated with using LV distribution system to sharing solar power, and sharing percentage is more sensitive factor to assess wheeling cost than wheeled kW and wheeling distance. This study hence proposes sharing percentage associating with wheeling distance can be a reasonable application for reliable assessment of wheeling cost for precinct-level solar power sharing. In addition, the illustration of two types of wheeling cost ('WC $/h' and 'WC $/kWh') demonstrates wheeling cost varying as the install location of the shared PV system changing, and these two items can be, respectively, used to identify a PV-system install location with lower wheeling cost for different types of group solar schemes. Furthermore, it was shown that the profile of load demand has impacts on wheeling cost and related issues, but load demand capacity needs to be considered when evaluating this issue.

For practical schedule of wheeling cost associated with using grid to sharing solar power, further study is still needed, such as the allocation of wheeling cost to customers, the evaluation for the power loss, power wheeling safety by considering current-carrying capacity of lines, and the cooperation with existing wheeling cost involved in customers' bill, etc.

Chapter 7 Improvements Arising from the Application of Sharing PV Power

7.1 Solar tariff limitations

The solar tariffs including Feed-in tariff (FiT), net metering (NM) and virtual net metering (VNM) have been re-evaluated utilising profiles of building demand and PV system output throughout Chapters 3 to 6. However, some limitations of the three solar tariffs have been demonstrated by the investigations. This Chapter provides a summary on the financial and policy-issued limitations of FiT, NM and VNM for sharing PV power, and provides an alternative that is completely disconnected from solar tariff schemes for the utilisation of PV power and precinct solar sharing.

7.1.1 Pricing of FiT and NM for distributed generation projects

In Chapter 3, it is mentioned that the purchase rate of FiT and NM for the fed-in solar power is, currently, lower than utility retail price in the Australian context, as the purchase rate is 5-10 ¢/kWh compared to the average retail of 25 ¢/kWh. In other countries, the purchase rate of FiT and NM has been significantly cut down, such as the FiT rate from 80.2¢/kWh in 2010 reduced to 28-38¢/kWh in 2013 in Canada, and the NM purchase rate from 11 ¢/kWh cut down to 2.6 ¢/kWh in 2016 in Nevada, U.S.

It is demonstrated that the fed-in solar power of a subscriber of FiT or NM is, in fact, locally used by the neighbours behind a common utility service delivery point (SDP) of the subscriber by the analysis of tracing power flow in Chapter 6. However, the fed-in solar power consumed by neighbouring consumers is priced for the customers at the retail price by the utility, which is nearly three times the purchase price for solar households. This issue is criticized as “daylight robbery” by the advocators of the campaign for a fair price for solar in Australia [97].

Research involved in the campaign for a fair price for solar points out that solar power is undervalued in Australia and suggests exported PV power is worth 10-18 ¢/kWh by considering all the benefits including the network, environment and health [98]. The

suggested price of 10-18 ¢/kWh is nearly two times the current purchase rate of 5-10 ¢/kWh in Australia. In this situation, another study claims that the best way for solar owners to achieve maximal value of their solar investment is to consume as much of the on-site PV generation as they can at the time they generate it [99]. It can be understood that the above method is, actually, to enlarge self-consumption, so a methodology or strategy to realize self-consumption enlargement is required for solar owners to reduce the economic loss caused by undervalued price for solar power.

7.1.2 Addressing PV generation by VNM

As an upgraded solar tariff, VNM overcomes some barriers related to the issues of the ownership of property and the space of solar PV installation, which is introduced in Chapters 2 & 3. However, VNM requires that all locally-generated PV power must be fed back into grid, and the total fed-in PV generation is shared to all participants in accordance with a pre-arrangement. Therefore, it is clear that the rules and policies of VNM do not include the means to address the excess locally-generated solar power. In addition, it is also introduced in Chapter 2 that the on-site PV generation is allowable to be sold to a third party or retailer by some types of VNM in Australia context. However, the undervalued pricing for solar power presented in section 7.1.1 could be involved in the trading of VNM, which would cause financial loss for the solar owners of VNM.

In conclusion, the existing solar tariffs either have undervalued price for PV generation or have deficiencies for addressing locally-generated solar power. By contrast, self-consumption of on-site PV generation is easier and more financially beneficial than participating in utility solar tariffs.

7.2 A conceptual network for limitation breaking

7.2.1 Application range

A conceptual network is proposed to proffer solutions for maximizing financial profits of excess solar generation and sharing solar with the unavailability of solar tariff. From the analyses in section 7.1, the undervalued pricing of solar tariffs must result in the economic loss of solar owners, and the deficiencies of the rules and polices involved in existing solar tariffs would hinder the flexibility of utilising solar power. In addition,

the solar tariff such FiT, NM and VNM, etc., has not been globally enacted or applied, and hence many areas and countries do not have policy support for the utilisation of solar power and solar sharing. As the aforementioned, self-consumption is a more cost-effective for the investment recovery of solar owners than solar tariff in current relevant context. The proposed strategy is, in fact, of enlarging the self-consumption of on-site generated PV power to nearby loads.

7.2.2 Network structure and operation principle

7.2.2.1 Network structure

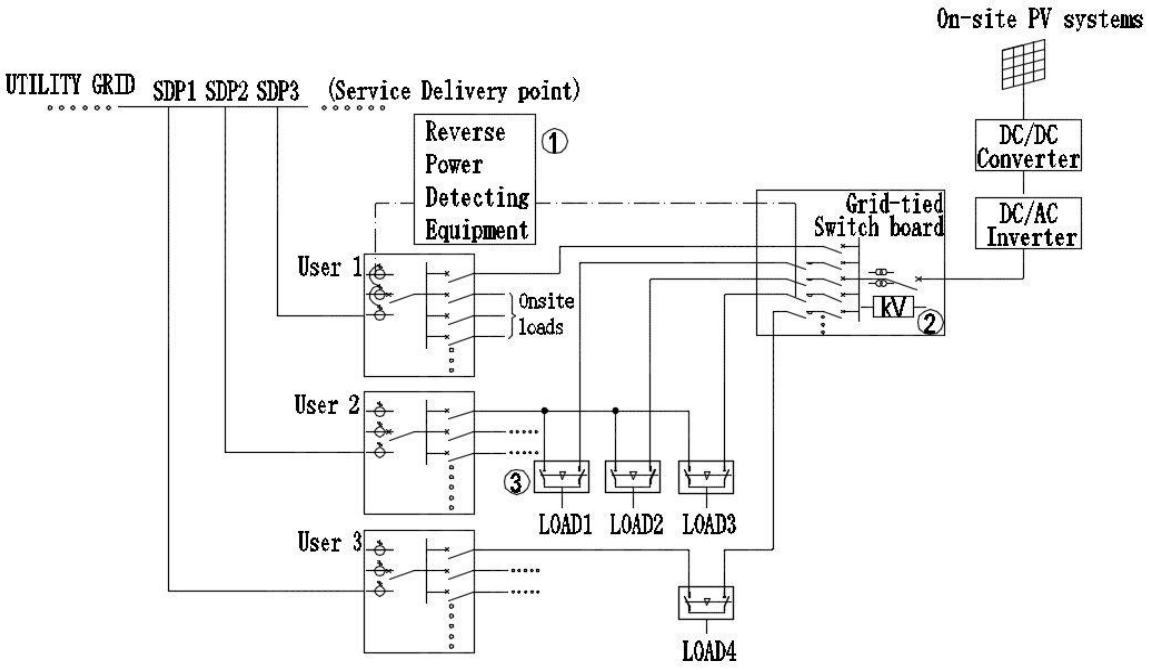

Fig. 7.1 Structure of proposed network.

From Fig 7.1, it can be seen that the proposed network is, in fact, an extensive grid-connected PV system, which is normally connected only to on-site loads. In order to share the potential excess solar power, the distribution lines of the PV system installed on the site of user1 is extended to user2 and user3. Note that the exact supply range of the proposed network must be identified by detailed evaluation of the amount of potential excess PV generation and the load capacity of neighbouring consumers' the loads. In addition, three critical devices are applied to operate the network: ①reverse power detection equipment (RPDE), ②voltage relay, ③automatic transfer switch equipment (ATSE). RPDE and voltage relay are, respectively, monitor the reverse power and voltage drop at the point of common coupling (PCC), the changes of which

control AC contactors to switch in and disengage the neighbouring loads. ATSE addresses the transition of the distribution feeders between two power sources to prevent loop circuit from forming. The transient power supply interrupt must be acceptable for selected neighbouring loads, and hereunder 'switchable load' is used to represent the neighbouring loads that can be operated to consume the potential excess solar power.

From the above introduction, the core operation of the proposed network is monitoring the changes of PCC reverse power and voltage drop by RPED and voltage relay, and the detailed evaluation of PCC reverse power and voltage drop has been presented by next section.

7.2.2.2 Utilisation of PCC voltage and reverse power for switchable loads control

This study proposes using the voltage and reverse power at the point of common coupling (PCC) as the control indicators to operate the network. The analysis of load flow, which is a tool to analyse the distributed active and reactive power and the voltage at each node through electric distribution networks, is applied to evaluating PCC voltage and reverse power. For the proposed network, this study assumes the reverse power only comprises active power for simplified analyses and calculations. In addition, PV systems mainly output active power due to the inverter set to a high power factor, which is usually unified to the grid', so this assumption should not influence the relevant results too much. Furthermore, in the analysis of load flow, the line-to-earth capacitance of distribution networks can be ignored when the distribution distance is less than 100km [100], so the proposed network has a zero line-to-earth capacitance due to its application range of on-site or small-scale precinct. Based on the above analyses, the network as Fig 7.1 shown can be equivalent to a simplified circuit presented as the following diagram.

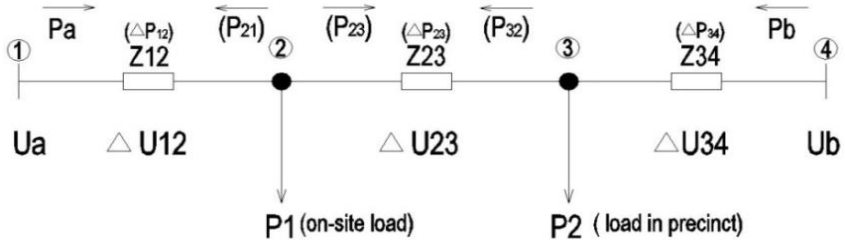

Fig. 7.2 Simplified equivalent circuit of sharing PV power.

As Fig 7.2 shows, U_a represents the voltage of the grid, and U_b is the output voltage of a grid-tied PV system. U_2 & U_3 are the voltage at node 2 & 3. Δp_{12}, Δp_{23}, Δp_{34}, and ΔU_{12}, ΔU_{23} & ΔU_{34} are, respectively, the power loss and the voltage drop of the feeders caused by the resistance of the distribution feeders, R_{12}, R_{23} & R_{34}. By the analysis of load flow, when the on-site loads, p_1, is supplied only by PV system without switchable loads, p_2, it has,

$$p_1 = p_b - \Delta p_{34} - \Delta p_{23} \tag{7.1}$$

$$U_3 = U_b - \Delta U_{34} \tag{7.2}$$

$$U_2 = U_a - \Delta U_{12} \tag{7.3}$$

$$U_3 = U_2 + \frac{(p_b - \Delta p_{23} - \Delta p_{34}) * (R_{34} + R_{23})}{U_3} \tag{7.4}$$

For a simplified expression of the relationship between the electric arguments of the grid and the on-site PV system, R_{12}, R_{34} and the power loss of the feeders are ignored, it has $U_2 = U_a$, and $U_3 = U_b$. U_3 is the PCC voltage. So (7.26) can be rewritten as the following.

$$U_3 = U_a + \frac{P_b * R_{23}}{U_3} \tag{7.5}$$

Based on (7.5), PCC voltage, $U3$, is varying completely along with the changes of PV output, p_b, when the grid is regarded as a constant voltage source and the feeder is certainly given. As Chapter 4 shows, daily PV output changes and has a representative profile. When PV output exceeds p_1, as $p_b - p_1 > 0$, reverse power would occur and feed back into the grid. It is noted that this study regards on-site loads, p_1, being constant

by ignoring the variation of load demand for simplified evaluation. The reverse power can be expressed by the following formula.

$$p_{reverse}=p_b-p_1 \tag{7.6}$$

It can be seen that reverse power, in fact, is the excess solar power, so the study on excess solar power is needed to identify the operation principle of the proposed network, which is devised to share excess power to switchable on-site or nearby loads, p_2, for the restriction of reverse power. From Chapter 4, it is known that daily PV output is constantly varying within generation available hours (same situation for excess PV power), so it is required that the switchable loads can be adjustable to match up with the changing excess solar power as approximate as possible. This study uses several switchable loads to realize the desired matching, and it can be explained by the diagram below.

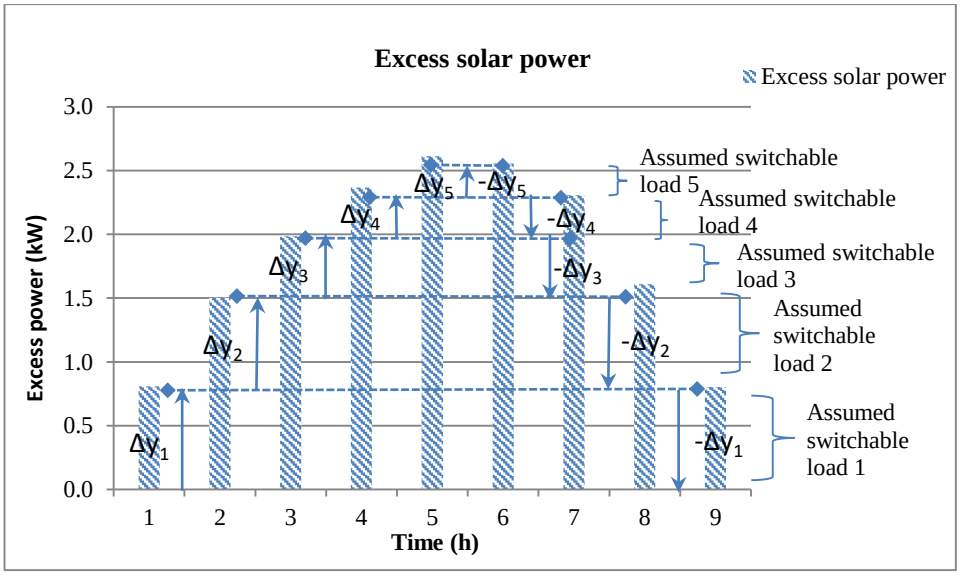

Fig. 7.3 Daily change of excess solar power.

As Fig 7.3 shows, the excess power lasts nine hours, and the power reaches to the peak value by five step-ups during five hours, and then it drop down to zero by four step-downs during four hours. Five switchable loads are used to match up with the changes of excess solar power, and the identification of the capacity of each load is according to the increment value between two adjacent hourly generations as Δy_1~Δy_5. The five loads should be switched into the network step by step along with the five times step-up of the excess power, and then the five loads would be disengaged in four times

corresponding to the four step-downs. It is noted that the third and fourth loads should be disengaged together that decided by the difference value between the 7th and 8th hourly generation. In addition, it can be seen that the five loads stay in the network for different hours. As Fig 7.3 shows, load 1 has the longest connection for 9 hours, and load 2 has a 7-hours connection, five hours for load 3, four hours for load 2 and two hours for load 1. However, it should be noted that the increment value of excess power is not always equal to the corresponding reduction value, for example, Δy_2 being less than $-\Delta y_2$, and Δy_4 & Δy_5, respectively, being slightly greater than $-\Delta y_4$ & $-\Delta y_5$. This phenomenon indicates a remaining reverse power still exists after the excess power shared, but it could be tolerant by controlling the value of remaining reverse power below to the upper limit required by relevant codes or standards.

As the above analysed, extra loads need to be switched into the network for the consumption of excess solar power, so a control device must be required for the connection of extra loads. Reverse-power detect equipment (RDPE) is widely applied to detecting the reverse power, and it can pre-set the control and operation threshold values to control other equipment such as AC conductor [101]. Therefore, this study uses RDPE to detect the changes of reverse solar power, and control switchable loads to connect to the network by pre-setting several operation values based on the increment values of excess power, $\Delta y_1 \sim \Delta y_5$. The excess power is declining from 6th hour as Fig 7.3 shows, and reverse power would be disappeared because all switchable loads still connect to the network, and the sum capacity of on-site and switchable loads must be greater than the declining PV output, which means part of power supply to loads would depend on the grid. Consequently, another device is required to address the power flow from grid to loads due to the function limit of RDPE. On the other hand, (7.5) shows the relationship between PCC voltage and power flow, and a general expression of PCC voltage can be achieved based on (7.5) and the analysis of power flow, and it is presented as (7.7) by a formula-transform.

$$U_3 = \frac{U_a + \sqrt{{U_a}^2 + 4 * R * (P_1 \pm \Delta P_{excess})}}{2} \tag{7.7}$$

In (7.7), ΔP_{excess} is the changing value of excess power presented by $\pm\Delta y_1 \sim \pm\Delta y_5$ shown in Fig 7.3. The part of '$P_1 \pm \Delta P_{excess}$' shows the change of power flow between node

2 and node 3. From this part, it can be seen that the power flow is increasing by ΔP_{excess}, as $P_1+\Delta P_{excess}$, from the 1st hour to the 5th hour shown by Fig 7.3, if without switchable loads added into the network. The power flow would be remaining p_1 from the 1st hour to the 5th hour if switchable loads joined in step by step with the gradual increment of excess solar power, as $P_1+\Delta P_{excess}-\Delta P_2$, $\Delta P_{excess}=\Delta P_2$. The power flow would drop down to $P_1-\Delta P_{excess}$ from the 6th hour to the 9th hour shown by Fig 7.3 if the switchable loads still staying in the network with the excess power declining. This study proposes utilising voltage relay to disengage switchable loads based on the voltage drop of U_3. So far, the control principle has been presented, and (7.6) & (7.7) have been derived for the calculation of the operation values of RPDE and voltage relay.

7.3 Case study implementation

This section uses a case study to show the correlation between the parameters involved including P_1, P_2, ΔP_{excess}, P_{excess}, U_a, & U_3, and demonstrate the practicability of the proposed network. Some relevant assumptions are developed and presented by the table below.

TABLE 7.1 Assumptions of case study.

Electrical arguments	Symbol	Value	Remark
Resistance of distribution line	R	0.05 Ω	In LV distribution system, the reactance of lines is very small, so only considering resistance. The value is calculated by an assumption of the utilisation of 70m electrical cable with the resistance of 0.725 Ω / kM.
The rated voltage of grid	U_a	400 V	
On-site load	P_1	50 kW	Assuming a constant load
Capacity of a grid-tied PV system	P_{pv}	500kW	Citing the achieved annual average profile of daily PV generation in Chapter 4. The hourly excess power can be got by minus the above P_1, and the exact values are presented in Fig 7-4.

It is noted that this case study chooses the demand capacity of on-site loads and the capacity of the grid-tied PV system with a significant difference value for a distinct demonstration of parameters involved and clear relevant analyses. Based on the (7.6) & (7.7) and the above assumptions, P_1, P_2, ΔP_{excess}, P_{excess}, and U_3 were calculated and illustrated by Fig 7.4.

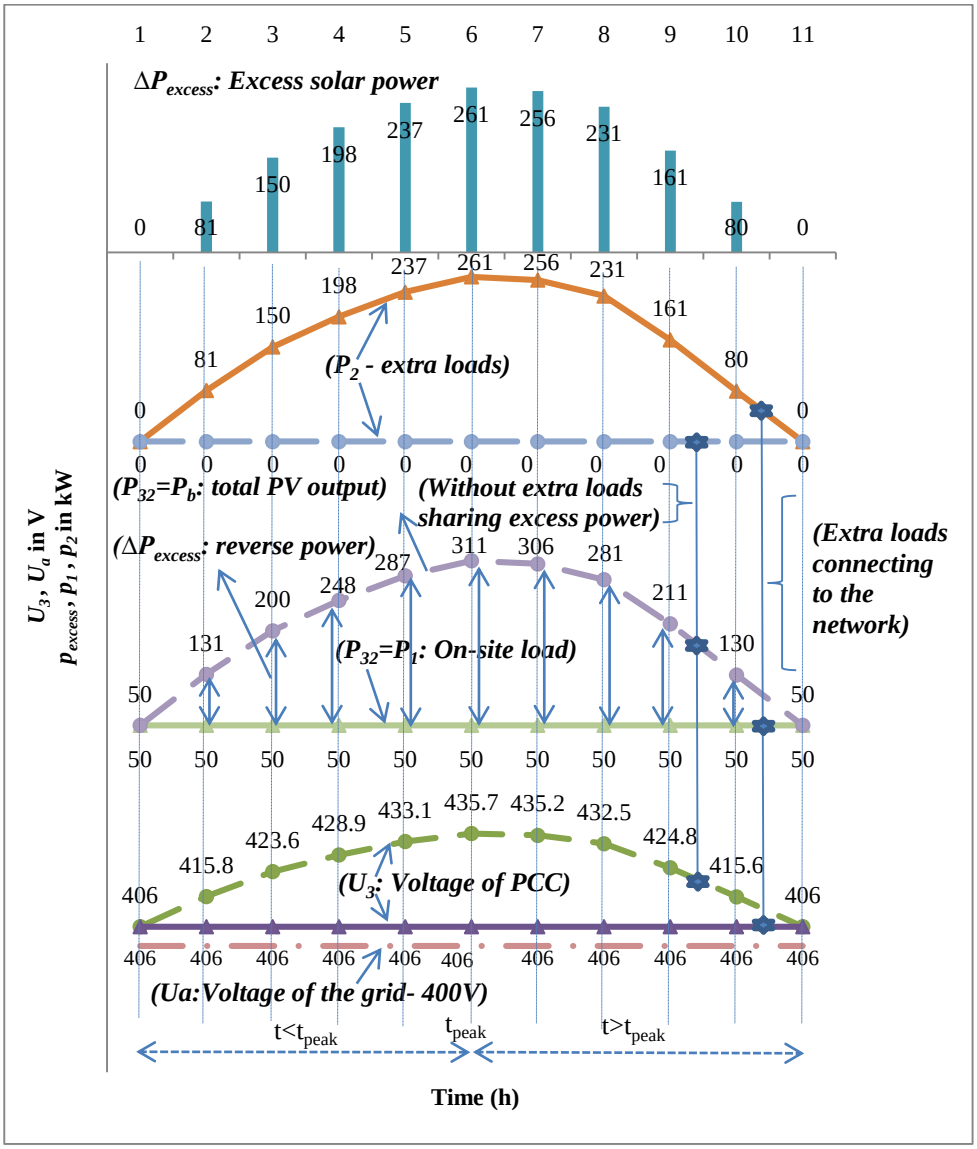

Fig. 7.4 Simulation of PCC reverse power and voltage.

It needs to be noted that the changing trend of excess PV power, ΔP_{excess}, in Fig 7.4 was achieved by introducing the annual average profile of PV generation achieved in Chapter 4. This pattern cannot present the exact change of excess solar generation on a certain day, but it is a representative annual average profile, so it is applicable for a general evaluation of the parameters involved.

As aforementioned, extra loads are controlled to switch into the network by using RDPE to detect the change of reverse power, ΔP_{excess}, and extra loads are disengaged from the network by applying voltage relay to monitor the PCC voltage drop, U_3. Fig 7.4 clearly illustrates the changing trend of ΔP_{excess} and U_3 to demonstrate the effect of the application of switchable loads, P_2. From Fig 7.4, when no extra loads switch into

to the network, as $P_2=0$, reverse power is actually the excess solar power, ΔP_{excess}, which is increasing from zero up to the peak value of 261 kW and then declining, finally to zero. The power flow from node 3 to node 2, P_{32}, goes up from 50 kW to the peak value of 311 kW and then reduces, finally down to 50 kW. PCC voltage, U_3, is changing along with the variation of ΔP_{excess} as rising up from 406 V at the 1st hour to the peak value of 435.7 V at the 6th hour, and then dropping down from 435.7 V to 406 V at 11th hour. When extra loads are used to switch into and disengage from the network step by step in response to the changes of reverse power, as $P_2=0\sim261\sim0$ kW, P_{32} and U_3, respectively, remains 50 kW and 406 V. It is noted that the network must guarantee the priority of the power supply to on-site loads, which can be seen by that the minimum P_{32} remains 50 kW and the corresponding U_3 is 406 V.

From the above comparison, it is shown that the application of switchable loads, P_2, can result in PCC voltage, U_3, and power flow P_{32} staying at a constant level, which both guarantees the power supply to on-site loads, P_1 and utilise the excess solar power, ΔP_{excess}, to supply other loads without reverse power fed into the grid. In addition, the operation value of RDPE can be set based on ΔP_{excess}, because the value of ΔP_{excess} directly reflects the changes of power flow from node 3 to node 2. However, the values of U_3 from the 7th hour to the 11th hour can't be used to set voltage relay because they reflect the situation of PCC voltage without the application of switchable loads. Therefore, an evaluation of U_3 with the application of switchable loads is required to show the reference value for setting the voltage relay. It can be understood that U_3 would be below to 406 V if switchable loads still connect to the network after the 6th hour, and if switchable loads are disengaged from the network step by step along with the gradual decline of excess solar power, U_3 would drop down before each switch-off, and rise up to 406 V after that. The potential value of U_3 can be calculated by (7.6) & (7.7), and the results are presented by the following diagram.

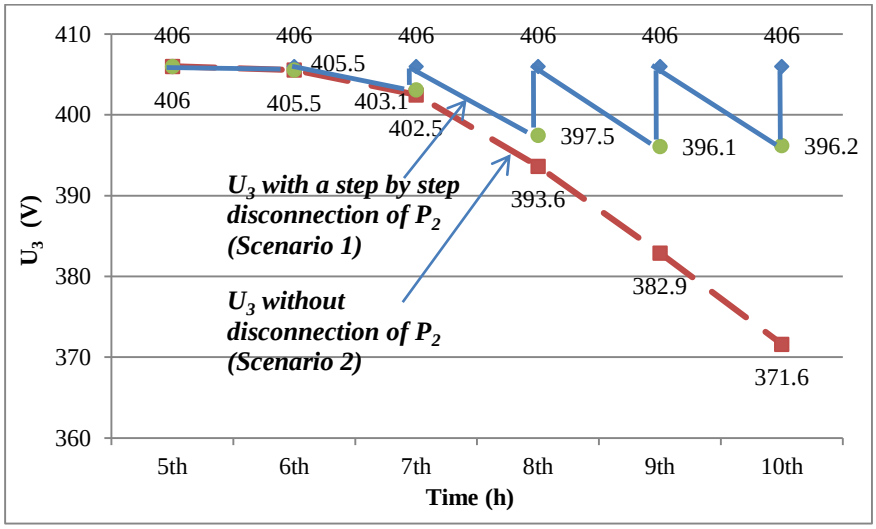

Fig. 7.5 PCC voltage drop.

From Fig-7.5, it can be seen that U_3 is constantly declining under scenario 2. By contrast, U_3 follows a cycle as drops to a certain level and then rising up to 406 V under scenario 1. It is clear that scenario 1 is the expected operation for the switchable loads, and the values of U_3 achieved under scenario 1 lower than 406 V are the references for setting the operation value of voltage relay.

So far, the running principle of the proposed network has been presented, and it can be concluded as the extra loads are switched into the network by RPDE detecting the change of reverse power, ΔP_{excess}, and disengaged from the network by voltage relay measuring PCC voltage drop, U_3. In addition, it is clear that a step by step operation of the switchable loads is required to match up with the changes of excess solar power. From Figs 7.3 and 7.4, there are ten step changes of excess solar power, $\pm\Delta y_1 \sim \pm\Delta y_5$, within the generation available hours. Therefore, ten corresponding step operations of switchable loads are needed in response to the ten step changes of excess solar power. It can be known that Fig 7.4 demonstrates an ideal operation of switchable loads as the load capacity of each switchable load is completely equal to the corresponding step change of excess solar power, as $P_2=\Delta P_{excess}$. However, this situation is impossible for a realistic case. It can be understood that each extra load must have a pair of connect-disconnect operation, which means ten step changes of excess solar power correspondingly are corresponding to five switchable loads. In addition, the first five changes of excess power must be not always equal to corresponding last five changes as $+\Delta y_{1\text{-}5} \neq -\Delta y_{1\text{-}5}$. Furthermore, the load capacity of switchable loads must be identified based on the realistic electrical facilities and equipment, and cannot be

discretionarily assigned. All the above analysed matters cause that the load capacity of switchable loads cannot completely match up with the changes of excess solar power. Fig 7.6 was developed to demonstrate the realistic situation of switchable loads operation.

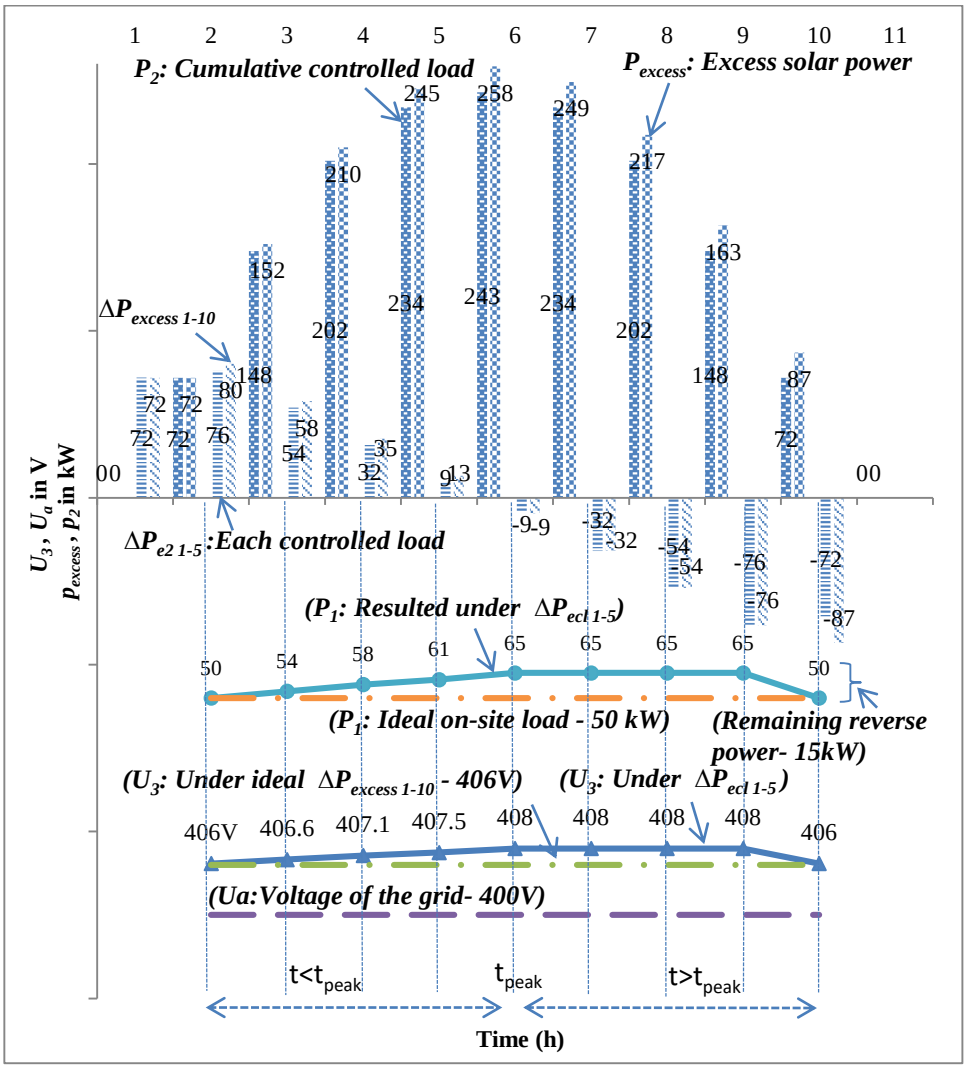

Fig. 7.6 Simulation of switchable-loads operation.

From Fig 7.6, $\Delta P_{excess\ 1\text{-}10}$ show the 10 different step changes of excess PV power, and $\Delta P_{e2\ 1\text{-}5}$ represent the load capacity of 5 extra loads. $\Delta P_{excess\ 1\text{-}10}$ is determined based on the difference value of two neighbouring hourly excess solar power, and $\Delta P_{e2\ 1\text{-}5}$ is always less than or equal to the corresponding $\Delta P_{excess\ 1\text{-}10}$, such as ΔP_{e2} equal to ΔP_{excess} on the 1st & the 7th ~ 10th hours, and ΔP_{e2} less than ΔP_{excess} on other 5 hours. This consideration, as $\Delta P_{e2} \leq \Delta P_{excess}$, prevents from a potential over consumption of excess PV power, which would cause a lower PCC voltage, U_3, than the desired value of 406 V, and an insufficient power supply to an on-site load. However, this method

of assigning load capacity of extra loads results in another problem of higher U_3 and over power supply of P_1 because excess PV power cannot be completely consumed by the extra loads, and a remaining reverse power is fed back into the grid. From Fig 7.6, it can be seen that the cumulative controlled loads are always not more than excess PV power on 10 hours. Consequently, the power flow, P_1, is greater than or equal to the load capacity of the on-site load as P_1 is above 50 kW for eight hours and remains the peak value of 65 kW for four hours. Correspondingly, U_3 is over 406 V and lasts 4 hours at the peak value of 408 V. As a result, the remaining reverse power occurs from the 2nd hour and goes up to 15 kW, and maintains the peak value of 15 kW for 4 hours since the 5th hour.

By this means, the peak reverse-current fed back the grid is about 24 A based on the peak reverse power of 15 kW. On the other hand, the assumed grid-tied PV system is 500 kW, so the rated output of a matching invert is around 800A. It can be seen that the peak reverse current of 24 A is below to the upper limit of 5% of rated output of the inverter as 40 A by Chinese code - JGJ16-2008 [102]. Therefore, the switchable loads operation under the scenario shown by Fig 7.6 is available for both the mitigation of revere power and the utilisation of excess solar power.

7.4 Challenges of the network operation and solutions

7.4.1 Challenges

From the relevant analyses in last section, the proposed network is incapable to completely prevent from reverse power fed into the grid, because it is impractical that the load capacity of each switchable load completely matches up each step change of excess solar power. However, the irregularity of daily PV generation changing is a bigger challenge than the mismatch between the load capacity and step change for practising this network. The irregularity means daily PV generation does not always follow a parabola curve as presented in Figs 7.3, 7.4 and 7.6. In Chapter 4， it was presented that the profile of daily PV output is a smooth parabola curve on the days with good weather (sunny or slightly cloudy), and the profile is irregular variation on other days. The irregularity of PV generation would result in irregular variation (non-parabola) of excess solar power, ΔP_{excess}, and PCC voltage, U_3, and the load capacity

of switchable loads devised based on the parabola profile of excess solar power must be unavailable to match up with the irregular step change. In another word, the load capacity of switchable loads devised based on a certain-day profile of excess solar power is not of universal availability. The irregularity of PV generation and the caused problem can be demonstrated by the diagrams below.

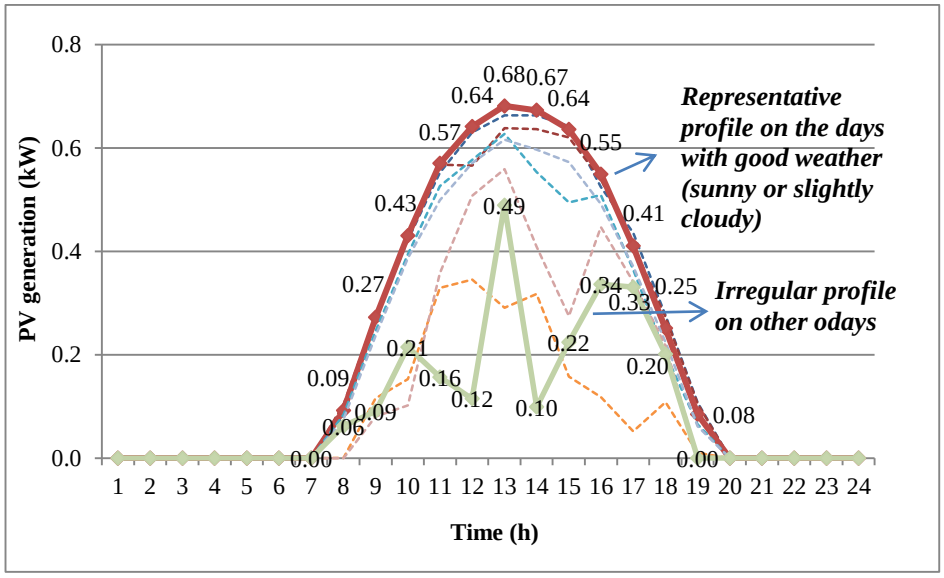

Fig. 7.7 Irregularity of PV generation.

Fig 7-7 shows the daily profile of PV output on some days in per-unit methodology developed in chapter 4. It is illustrated that there are some days with the pattern similar as the representative profile, and there are various irregular patterns for other days. In addition, the difference between the representative and the irregular profiles is significant. The example difference values of PV generation and PCC voltage were calculated by applying the representative and irregular profiles to the assumed 500 kW PV system in the case study, and are presented by the diagram below.

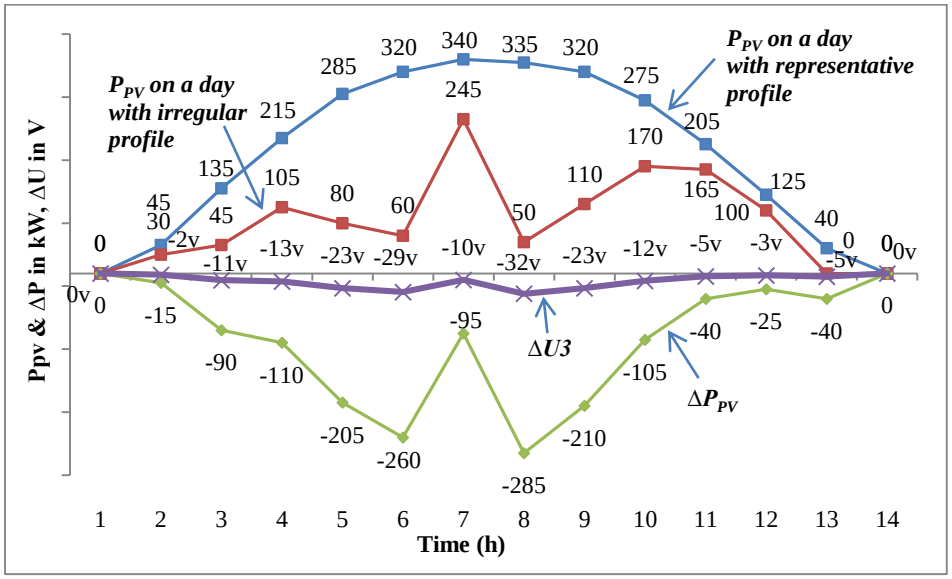

Fig. 7.8 Comparison of *P & V* under different PV-generation profiles.

From Fig 7.8, ΔP_{PV} shows the difference value of hourly PV generation with a range of 15 kW to 285 kW on day1 and day2, respectively, with representative and irregular profiles. ΔU_3 shows the difference value of PCC voltage with a range of 2 V to 32 V on the same two days. Note that the negative value of ΔP_{PV} and ΔU means the decrement of PV generation and PCC voltage between day1 and day2. The significant difference values of PV generation indicate the load capacities of switchable loads devised based on day1 profile must be unavailable to match up with the step changes of excess solar power on day2. In addition, the set operation values of RPDE and voltage relay based on day1 profile must be ineffective to control the switchable loads on day2, which causes the switch-transfer operation of the switchable loads failed.

Another challenge for the proposed network is the operation order of the switchable loads. As the aforementioned, RPDE and voltage relay control AC contactors to switch in and disengage the extra loads based on the respective set operation values, but AC contactor is incapable to intelligently choose a certain load to be operated for a desired match to the unpredictable step changes of excess solar power. Therefore, the switchable load operation must be failed due to non-intelligence of AC contactor, even though some of the load capacities devised based day1 profile are similar with the certain step changes of excess solar power on day2.

From the above analyses, it can be seen that the irregularity of daily PV generation, the mismatch between the load capacity of switchable loads and step change of excess

solar power and the non-intelligence of the operation system are three main challenges for the availability of the proposed network, and comparatively, the irregularity of daily PV generation more critically influences the network operation. On the other hand, the identification of the load capacity of switchable loads is a critical factor for the proposed network operation because it is related to the above both challenges.

7.4.2 Solutions

Based on the above relevant analyses, this study proposes two solutions to address the two challenges as 1) setting equal load capacity to each switchable load, 2) using probability-based methodology to devise the load capacity. Equal load capacity assigned for all switchable loads can cover the third challenge analysed in last section as the shortage of the non-intelligence of AC contactor. The extra loads are switched into the network one by one until reverse power reduced to a set value of RPDE that being greater than 0, which is for preventing from over consumption of excess solar power, and are disengaged one by one until PCC voltage, U_3, dropped down to a set value of voltage relay. For example, in Fig 7.6, the first two loads of 72 & 76 kW, correspondingly, matching up with the first two hourly excess PV power of 72 & 80 kW, $\Delta P_{excess\text{-}1\&2}$, would be, respectively, substituted by 7 and 8 groups of loads each of that with equal load capacity of 10 kW. The last disengaged load of 72 kW would be displaced by 8 groups of 10 kW loads to guarantee the priority of power supply for the on-site loads. The number of the switchable loads can be evaluated by the equation below,

$$N = \frac{\Delta P_{excess-max}}{\Delta P_{2-n}} \tag{7.8}$$

where, $\Delta P_{excess\text{-}max}$ is the greatest hourly excess solar power, and $\Delta P_{2\text{-}n}$ is the equal load capacity. It is obvious that $\Delta P_{excess\text{-}max}$ can't always have exact division by $\Delta P_{2\text{-}n}$, which indicates a reverse power is still remaining. However, it can be understood that the greater is N, the more reduced would be the remaining reverse power, i.e., the smaller load capacity of, $\Delta P_{2\text{-}n}$ for each switchable load. From (7.8), it can be seen that the identification of the load capacity of switchable loads, $\Delta P_{2\text{-}n}$, must be depending on the step changes of excess solar power, ΔP_{excess}. In addition, as the aforementioned, the load capacity of switchable loads devised based on a certain-day profile of excess solar power is not of universal availability for all PV generation available days. The

second solution - probability-based methodology to determine the value of $\Delta P_{2\text{-}n}$ considers the annual step changes of hourly excess solar power and finds out a value of ΔP_{excess} that repeatedly occurs at the same time period of as many as possible days within a year. It can be explained by the following diagram.

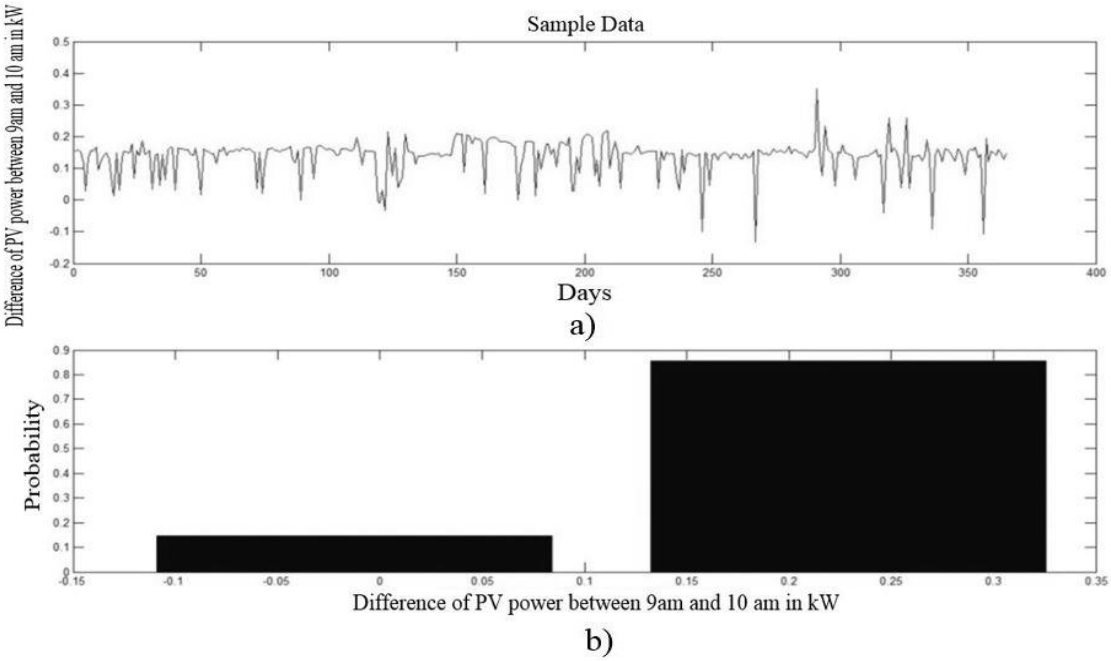

Fig. 7.9 Annual probability distribution of hourly step changes of PV generation.

Fig 7.9 (a) shows a sample step change between 9am and 10am for a year. It can be seen that the step change with several extreme values, such as -0.1 or 0.3, etc., mostly locates between 0 and 0.2. Fig 7.9 (b) shows the probability distribution of the sample step change, which is stratified to Bernoulli distribution, so it can be presented as the followings,

$$P(X = k_1) = 0.82 \text{ , } 0.13<k_1<0.32 \tag{7.9}$$

$$P(X = k_2) = 0.18, \text{ } -0.07<k_1<0.07 \tag{7.10}$$

(Note: All numbers are approximate values by reading the above diagram.)

$P(X = k)$ is the probability of the step change, ΔP_{excess}, happening at the same time period within a year, and k is the value of the hourly step change, ΔP_{excess}. $P(X = k)=0.82$ means there are 299 days (365×0.82) between 9am and 10am with ΔP_{excess}, the value of which ranges from 0.13 to 0.32 kW. By this means, it can be understood that a 0.13 kW load can be guaranteed to be switched into the network at the time

interval of 9am to 10 am for 299 days, and the probability of the switch-in operation would be greater along with the value of $\Delta P_{2\text{-}n}$ decreasing below to 0.13. In addition, there are at most two 0.13 kW extra loads can be switched into the network between 9am and 10 am in this example year, because the annual maximum $\Delta P_{excess\ 9\text{-}10}$ is 0.32, and the total capacity of the switchable loads between 9am and 10 am should be less than or equal to 0.32 kW, as $0.13\times2=0.26<0.32$. However, it should be noted that the exact value of P and k involved in (7.9) and (7.10) can't be identified by the probability distribution, which can only demonstrate the general situation of the distribution of ΔP_{excess} but showing the exact value of probability and ΔP_{excess}. In order to cover the shortage of probability distribution methodology, this study proposes using probability density curve for the identification of the exact value of the hourly step change, ΔP_{excess}, under a certain probability. In addition, the probability of the switch-in operation of the extra loads can be regarded as an expectation for an utiliser of the proposed network, which should be considered in advance. Based on the expectation, the corresponding annual minimum value of ΔP_{excess} is actually the load capacity of each switchable load, $\Delta P_{2\text{-}n}$.

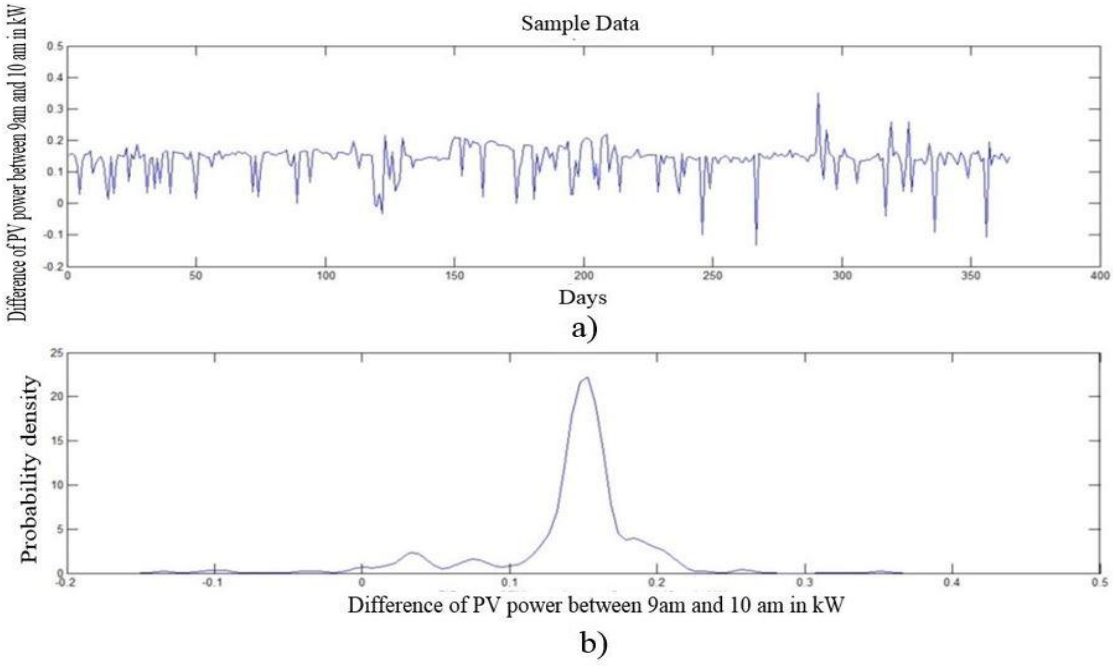

Fig. 7.10 Annual probability density curve of hourly step changes of PV generation.

Fig 7.10 (a) shows the annual step change of excess solar power from 9am to 10am same as Fig 7.9 (a), and Fig 7.10 (b) demonstrates the probability density of the year-

round step change. The relation of probability and probability density is presented as the following equation.

$$P(X = k) = \int_{P_1}^{P_2} f(p)\, dp \tag{7.11}$$

$f(p)$ is the function of probability density in terms of the hourly step change of excess PV power, and the definite integration of $f(p)$ presents the corresponding probability in the range of the upper limit, P_2, to lower limit, P_1. The annual maximum value of ΔP_{excess} is the upper limit, and the lower limit, P_1, is the target value of the load capacity of each switchable load under an expected probability. (7.11) can be manipulated by the followings for a simplified evaluation of P_1.

$$\int_{P_1}^{P_2} f(p)\, dp = \frac{P_2 - P_1}{n}(y_1 + y_2 + \cdots y_n) \tag{7.12}$$

$$P(X = k) = \frac{P_2 - P_1}{n}\sum_{i=1} y_n \tag{7.13}$$

where, $y_{1\sim n}$ is the exact value of the probability density, n is the corresponding number of $y_{1\sim n}$. (7.12) is the approximate treatment for integration, and otherwise, the curve fitting needs to be applied to determine the function of probability density. It can be understood that the greater is n, which means the more are y taken, the more accurate is the value of $P(X = k)$. As the aforementioned, the probability, $P(X = k)$, represents the expectation of the successful switchable-load operation for an utiliser of this proposed network, so it is a target value. On the other hand, the values of P_1, P_2, n and $\sum_{i=1} y_n$ can be achieved by using software such as MATLAB or EXCEL. The calculated result of $P(X = k)$ can be obtained by (7.13) and the tentative value of P_1, which can be identified from probability distribution diagram by referring to a rough probability close to the target value of $P(X = k)$. The desired result of P_1 is corresponding to the calculated value of $P(X = k)$ that is closest to target value. It is noted that the identification of P_1 based on an expected probability can be achieved completely by data analysis via MATLAB or EXCEL as well.

It can be known that a complete probability-based evaluation for the daily step changes of excess PV power would cover several hours, and the load capacity of switchable loads is the minimum value of the several achieved P_1. As previously analysed, a reverse solar power would still remain in a realistic case because a complete match of

switchable loads and excess solar power is impossible. However, the probability-based methodology can maximally reduce the reverse power and consequently sharing as much as possible excess solar power to other nearby loads. In addition, the negative impact on the network operation from the irregularity of daily PV generation can be mitigated by the probability-based methodology, because it considers year-round situation of hourly change of excess solar power, and the methodology of taking annual minimum value can make the switchable-load operation maximally fit to the irregular change of excess solar power.

In conclusion, the barriers to the proposed network operation caused by the mismatch of load capacity and step change of excess power and irregularity of PV generation can be mitigated by the probability-based methodology, and the challenge from the non-intelligence of AC contactor can be resolved by the implementation of equal load capacity for each switchable load. In addition, the operation value of RPDE and voltage relay is easy to be identified by the proposed two solutions because the exact values of step increment of excess PV power, $\Delta \boldsymbol{P}_{excess}$, and the PCC voltage drop, U_3, do not need to be measured. The operation value can be set by only referring to the annual minimum $\Delta \boldsymbol{P}_{excess}$, and the upper limits for reverse power and voltage rise of relevant codes or standards. However, it is noted that the practicability of application of annual minimum value of $\Delta \boldsymbol{P}_{excess}$ to the identification of the load capacity of switchable loads is a concern for a realistic case because the load capacity cannot be assigned by optional value, and it must be determined by the load capacity of actual electrical facilities and equipment. In addition, the fluctuation of PV generation due to the transient changes of weather conditions could influence the stability of the network operation. Furthermore, the variation of load demand of the switchable loads must result in undesirably poor consumption of excess solar power, which would cause the disturbance to the network operation. This study suggests that the switchable loads should be selected from the loads with slight fluctuation of load demand and the tolerance of transient power supply interruption, such as the lightings on hallway and other not important areas, ventilators, etc. It can be seen that further study must be required to more comprehensively evaluate the practicability of the proposed network.

7.5 Financial analysis

As Fig 7.1 shows, the proposed network needs to build up extra precinct LV distribution lines, which cause additional investment mainly including the costs for cable materials and control equipment, installation costs for cable laying. As analysed in Chapter 2, one of the shortages of the utilisation of separate networks for solar sharing is the additional cost comparing to using utility grid. This section uses a case study to financially evaluate the feasibility of the proposed network, and the relevant assumptions were presented as the followings.

It is assumed that a building with the load capacity of 100 kW and the on-site PV system is rated at 100 kW to cover the overall on-site load demand. A RPDE is installed in the main switch panel of the user to monitor the potential reverse solar power fed into the utility LV distribution systems based on the network structure shown by Fig 7.1. The load capacity of the on-site electrical loads has a seasonal reduction ranging from 0-50% of peak value of 100 kW in the year-round time except the summer, i.e. 0-50 kW. That means that the on-site PV system has 0-50 kW potential excess power during the corresponding time period. Based on the operation principle of the proposed network, twenty loads each of that with equal load demand of 3 kW installed on neighbouring consumers' sites are selected as the switchable loads to consume the potential excess solar power. Depending on the above assumptions, the relevant economic issues are presented by Table 7-2.

TABLE 7.2 Assumed economic issues.

Item of materials and equipment	Unit costs ($/per unit)	Numbers of the applied items	Total costs for the extra network ($)
ATSE (<125A)	40	20	22880
RPDE	80	1	
Switch box including breaker, the housing, and the accessories	100	20	
On-site separate network including cable materials and cable laying	100	200 (m)	
Payback period (y) = Total cost / (shared solar power (0~50 kW) × daily peak Sun hours (3 h) × average utility electricity retail price ($ 0.28/kWh) × assumed days with excess PV power (120 d/y))			

(Note: the unit prices involved in the above table are referred to the online resources in the U.S. context [103, 104])

The calculated payback period based on the above economic assumptions is illustrated by the following diagram.

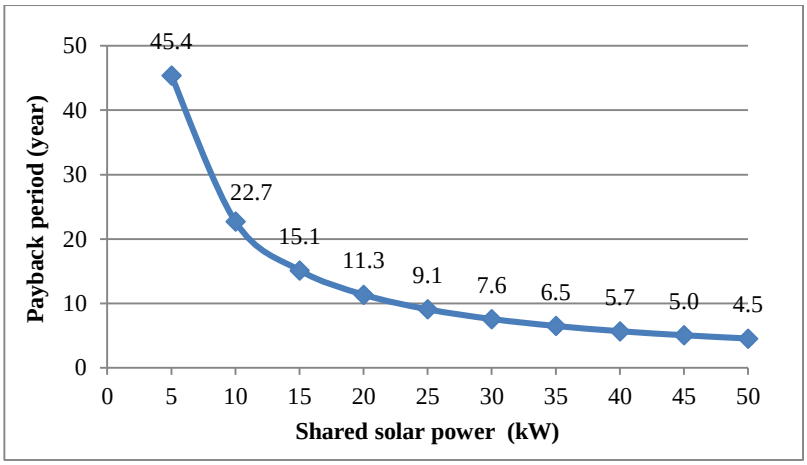

Fig. 7.11 Payback period under different kW of excess solar power.

From the formula of payback period in Table 7.1, it can be seen that the amount of shared solar power, the potential days with excess power and the utility electricity retail are the main factors to influence the financial performance of the proposed network. In addition, the first two factors are varying along with the combination of the behaviours of PV generation and load consumption. Therefore, an accurate evaluation for the financial performance of the proposed network is very hard. However, Fig 7.11 still can present a possible situation of financial issues of the conceptual network. It can be seen that the longest payback period of 45.4 years is too long, but other payback years are acceptable comparing to the normal lifespan of solar PV of 25 years. In addition, from the correlation of payback period and the kW of excess solar power, this proposed network has a decent financial performance, such as 11.3 years corresponding to 20 kW, 25 kW with 9.1 years, etc. The potential excess solar power of 20 kW or 25 kW makes up a comparative small percentage of the capacity of 100 kW of the assumed PV system, which means the probability of the occurrence of 20 kW or 25 kW excess power is realistically not small. This study believes that the economic efficiency of the proposed network would be acceptable for the potential uses, provided this network is devised in a small scale such as installed inside a building or in a precinct ranging from tens of to one or two meters. In addition, the costs are varying too much with the different national context, and consequently,

the detailed financial pre-investigation is required for the application of the proposed network.

7.6 Summary

In the beginning of this chapter, it was pointed out that the undervalued price for solar by some existing solar tariffs, such as FiT and NM, and the limitation of service target of some group solar schemes like VNM have constrained the utilisation of solar power based on relevant investigation and evaluation in previous Chapters. In response to addressing the limitations involved in the current widely-applied solar tariffs, this Chapter has proposed a stand-alone network without energy storage for solar sharing disconnected from utility solar tariffs and schemes.

This network applies the variation of PCC reverse power and voltage to operating switchable loads for the excess locally-produced solar power sharing. Two widely-used electric equipment RDPE and voltage relay are applied to monitoring the changes of PCC reverse power and voltage to triggering the switchable loads operation. The simulations demonstrate the switch-in and disengagement of the switchable loads realize the excess solar power sharing and guarantee the priority of power supply to on-site loads with the function of restricting the reverse power and voltage rise caused by grid-tied PV systems. However, as shown in Fig 7.6, a reverse power up to 15 kW still remains for 7 hours with excess solar generation due to the difference value between step changes of excess solar power and the load capacity of switchable loads. In order to reduce the remaining reverse power as much as possible and other operation challenges of the proposed network including the irregularity of daily PV generation and non-intelligence of AC contactor, this Chapter proposed two solutions as the probability-based methodology and the equal allocation of the load capacity to each switchable load. The relevant evaluation demonstrates the theoretical effect of the two solutions to overcome the aforementioned challenges. In addition, the proposed probability-based methodology by using probability contribution and probability density curve could be applicable for the relevant studies on the behaviour of PV generation and building load demand due to its comprehensive evaluation of the long-term data. The financial analysis suggests that the proposed network is economically acceptable, provided the application range is controlled in a small-scale, such as the on-site 200 meters long used in the financial case study.

The proposed network has simple control configuration and structure, but the network operation is related to some complex and uncertain issues such as the behaviour of PV generation and load demand, the power supply continuity to the building load, which are the critical issues involved in the utilisation of solar power in buildings. Therefore, much further study, such as software simulation, the improved approaches for the evaluation of the profiles of PV output and load demand, etc., is required for the practicability of the proposed network.

Chapter 8 Conclusions and Future Work

8.1 Conclusions

The literature review shows that numbers of studies have been done on popularly implemented utility solar tariffs such FiT and NM. However, little work provided a detailed evaluation of VNM, which is one of most promoted solar sharing tariffs, from either financial or technical perspective. In addition, the impact of the behaviour of PV system output and building load demand on the performance of solar sharing program were barely considered. FiT, NM and VNM are three of the most widely applied solar tariffs in numbers of countries, however, few studies were found for a comprehensive investigation of the three representative tariffs.

In order to fill the above-mentioned research gaps, this study has developed a financial comparison of FiT, NM and VNM. A detailed evaluation of financial performance of VNM has been presented considering the profiles of PV generation and building consumption. The wheeling costs associated with solar sharing has been evaluated as well. Furthermore, this study proposed a strategy for precinct small-scale solar sharing as an alternative to solar tariffs.

The major findings and contributions of this thesis are:

- A review that specifically analyses the technical issues related to the performance of PV systems and the models and strategies of the utilisation of solar power. A detailed review on utility solar tariffs including FiT, NM, community solar and VNM. Using utility grid to share solar power has advantages of low investment and simple requirements of control and configuration compared to building up a separate network. The variation of PV output and load demand is barely considered in the relevant studies of solar sharing. VNM as one of the important solar sharing tariffs lacks the detailed financial and related technical evaluations.

- A financial comparison of FiT, NM and VNM by using micro-economic models was completed. Through the comparison, it is presented that FiT is the tariff with the lowest revenue, and the best cost-effective option is alternating between NM and VNM in current Australian context as purchase rate of FiT and NM is much lower than utility retail rate. VNM can be the best option, provided the annual surplus VNM credits are few. The above findings proffer advice for customers to choose a cost-effective solar tariff, whilst it is demonstrated that the left VNM credit is an important factor that critically impacts the financial performance of VNM tariff as well.

- The daily profiles of 15 categories of buildings electric consumption and PV generation were analysed. Histogram patterns of building consumption and PV generation were developed to evaluate time of use (TOU) tariff. The methodology of linking the profiles to economic issues by using utility retail tariffs proffers a new perspective to study the financial performance of solar tariffs and schemes.

- A detailed financial evaluation of VNM that focuses on payback period and reflective value of allocated credits. It was found that the profile of building consumption with the highest-peak usage always has the shortest payback period when the daily consumption of the investigated building or building groups is similar. The evaluation shows that the factors such as that profile of load demand, participant composition, surplus credits and the size of VNM PV system, are critical to achieve a successful implementation of VNM tariff.

- The investigation and evaluation of wheeling costs associated with solar sharing developed by using MW-mile and an approach of tracing power flow, which are applied to the evaluation of transmission and distribution service of utility power. It is demonstrated that ‘sharing percentage’ is a more reliable index than the extent of utilising utility grid to reflect the value of the potential wheeling charges raised by using utility grid to share solar power.

- A conceptual small-scale network proposed as an alternative of utility solar tariff for PV power sharing. It is presented that sharing excess local-generated solar power to the precinct loads is positive for the mitigation of voltage rise and reverse power caused by the penetration of PV systems. In addition, it is demonstrated that the fluctuation of the voltage and reverse power at the point of common coupling (PCC) can be used as the indicators to control the precinct loads connected and disengaged.

8.2 Constraints and recommendations

This study has presented financial evaluation of VNM from a new perspective of the profiles of building consumption and PV generation. The related results achieved by using historical data need to be validated by future work due to the potential constraints of the application of the historical data. It is recommended that the further studies can use data mining technologies such as neural network method, decision-making tree, etc., to achieve improved profiles or a type of more general expression of load demand and PV output.

The micro-economic model of VNM in Chapter 3 only focuses on the monetary profits brought to customers. For a more comprehensive evaluation of VNM, the social welfare related to environmental contributions and the relevant issues of utility, such as resulting electricity rates, need to be modelled by future work.

The investigation of wheeling costs applies MW-mile due to the lack of the studies on wheeling costs associated with solar sharing. A specific approach for the assessment of wheeling costs associated with solar sharing could be proposed by the further studies.

The study on the conceptual network is at the initial stage. The operation stability, the impacts on power supply continuity of extra loads, etc., need further work to be evaluated. In addition, the financial issue of the small-scale network is another concern due to the additional investment for cable materials and cable laying. Therefore, a more comprehensive financial evaluation of this network is required.

REFERENCES

[1] Advantages of Solar Power Over Alternate Energy Sources, *Soluxe Energy Solutions*, viewed 23 July 2017, <http://www.soluxesavings.com/advantages-solar-power-over-alternate-energy-sources-a-122.html>.

[2] Fares, R 2016, The Price of Solar Is Declining to Unprecedented Lows, *Science American*, weblog post, 27 August, viewed 7 July 2016, <https://blogs.scientificamerican.com/plugged-in/the-price-of-solar-is-declining-to-unprecedented-lows/>.

[3] Sharing the Sun: Solar Power for Tenants and Solar Disadvantaged Homeowners, *Catalyst*, weblog post, June, viewed 7 July 2016, <http://catalyst.energy.gov/a/idea-v2/56853>.

[4] Community solar energy projects give renters access to cheap solar power, Energy Matters, viewed 7 July 2016, <https://www.energymatters.com.au/renewable-news/community-solar-energy-projects-renters-access/>.

[5] Community Solar Project Map, *Community Solar Hub*, viewed 8 July 2016, <https://www.communitysolarhub.com/>.

[6] Community Solar, *Farmingthesun*, <http://farmingthesun.net/about/community-solar/>.

[7] C. P. Cameron, W. E. Boyson and D. M. Riley, "Comparison of PV system performance-model predictions with measured PV system performance," *2008 33rd IEEE Photovoltaic Specialists Conference*, San Diego, CA, USA, 2008, pp. 1-6.

[8] H. G. Beyer, G. H. Yordanov, O. M. Midtgård, T. O. Saetre and A. G. Imenes, "Contributions to the knowledge base on PV performance: Evaluation of the operation of PV systems using different technologies installed in southern Norway," *2011 37th IEEE Photovoltaic Specialists Conference*, Seattle, WA, 2011, pp. 003103-003108.

[9] H.G. Beyer et al., “Identification of a general model for the MPP performance of PV-modules for the application in a procedure for the performance check of grid connected systems”, *Nineteenth EUPVSEC*, 2004, Paris, France, pp.3073-3078.

[10] A. Drews, H.G Beyer, and U. Rindelhardt, “Quality of performance assessment of PV plants based on irradiance maps”, *Solar Energy* 82, 2008, pp. 1067-1075

[11] Ádám, G & Baksai-Szabó, K & Kiss, P. (2012). Energy production estimating of photovoltaic systems. Renewable Energy and Power Quality Journal. 1347-1352. 10.24084/repqj10.701.

[12] J. Guerrero, Y. Munoz, F. Ibanez, A. Ospino. Analysis of mismatch and shading effects in photovoltaic array using different technologies. In: Proceedings of the the international congress of mechanical engineering and agricultural sciences, Valencia, Spain; 2014, pp. 1–9.

[13] Maghami, MR, Hizam, H, Gomes, C, Radzi, MA, Rezadad, MI, & Hajighorbani, S 2016, 'Power loss due to soiling on solar panel: A review', *Renewable and Sustainable Energy Reviews*, vol. 59, pp. 1307-1316. Available from: 10.1016/j.rser.2016.01.044. [1 August 2017].

[14] Ponoum, R, Rutberg, M, & Bouza, A 2013, 'Energy storage for PV power', *ASHRAE, Emerging Technologies*, pp. 82. Oct.

[15] M. Arif, A. Oo, A. Ali and G. Shafiullah, "Significance of Storage on Solar Photovoltaic System—A Residential Load Case Study in Australia," *Smart Grid and Renewable Energy*, Vol. 4 No. 2, 2013, pp. 167-180.

[16] G. T. Samson, T. M. Undeland, O. Ulleberg and P. J. S. Vie, "Optimal load sharing strategy in a hybrid power system based on PV/Fuel Cell/ Battery/Supercapacitor," *2009 International Conference on Clean Electrical Power*, Capri, 2009, pp. 141-146.

[17] Chimtavee, A, Ketjoy, N, Sriprapha, K, & Vaivudh, S 2011, 'Evaluation of PV Generator Performance and Energy Supplied Fraction of the 120 kWp PV Microgrid System in Thailand', *Energy Procedia*, vol. 9, no. 9th Eco-Energy and Materials Science and Engineering Symposium, pp. 117-127. Available from: 10.1016/j.egypro.2011.09.013. [1 August 2017].

[18] S. Sharma and D. W. Galipeau, "Optimization of residential grid-tied PV systems without net-metering using load management," *2012 IEEE Third International Conference on Sustainable Energy Technologies (ICSET)*, Kathmandu, 2012, pp. 6-11.

[19] N. A. M. Amir, N. Y. Dahlan, W. N. A. W. Abdullah, Z. M. D. Zain and H. Mohamad, "Energy saving analysis of a 16kWp grid connected photovoltaic (PV) system at Green Energy Research Centre (GERC), UiTM Shah Alam," *2014 IEEE 8th International Power Engineering and Optimization Conference (PEOCO2014)*, Langkawi, 2014, pp. 390-395.

[20] Eltawil, MA, & Zhao, Z 2010, 'Grid-connected photovoltaic power systems: Technical and potential problems—A review', *Renewable and Sustainable Energy Reviews*, vol. 14, pp. 112-129. Available from: 10.1016/j.rser.2009.07.015. [1 August 2017].

[21] Y. K. Penya, C. E. Borges and I. Fernández, "Short-term load forecasting in non-residential Buildings," *AFRICON, 2011*, Livingstone, 2011, pp. 1-6.

[22] Abdelsalam, AA, Gabbar, HA, Musharavati, F, & Pokharel, S 2014, 'Dynamic aggregated building electricity load modeling and simulation', *Simulation Modelling Practice and Theory*, vol. 42, pp. 19-31. Available from: 10.1016/j.simpat.2013.12.005. [1 August 2017].

[23] National Renewable Energy Laboratory Report, Balcomb, JD, Hayter, SJ, Weaver, NL: Hourly simulation of grid connected PV systems using realistic building loads. NREL/CP, 550–29638 (2001).

[24] Dakkak, M, Hatori, K, & Ise, T 2006, 'The concept of distribution flexible network PV system', *Renewable Energy*, vol. 31, no. 12, pp. 1916-1933. Available from: 10.1016/j.renene.2005.09.022. [1 August 2017].

[25] M. Zeyringer *et al*., "Solar buildings in Austria: Methodology to assess the potential for optimal PV deployment," *2013 10th International Conference on the European Energy Market (EEM)*, Stockholm, 2013, pp. 1-5.

[26] E. Yao, P. Samadi, V. W. S. Wong and R. Schober, "Residential Demand Side Management Under High Penetration of Rooftop Photovoltaic Units," in *IEEE Transactions on Smart Grid*, vol. 7, no. 3, pp. 1597-1608, May 2016.

[27] S. J. Steffel, P. R. Caroselli, A. M. Dinkel, J. Q. Liu, R. N. Sackey and N. R. Vadhar, "Integrating Solar Generation on the Electric Distribution Grid," in *IEEE Transactions on Smart Grid*, vol. 3, no. 2, pp. 878-886, June 2012.

[28] H. Hatta, M. Asari and H. Kobayashi, "Study of energy management for decreasing reverse power flow from photovoltaic power systems," *2009 IEEE PES/IAS Conference on Sustainable Alternative Energy (SAE)*, Valencia, 2009, pp. 1-5.

[29] H. Sugihara and T. Funaki, "An analysis on photovoltaic output restrictions and load management under voltage constraints in a residential low-voltage distribution network," *2016 IEEE Innovative Smart Grid Technologies - Asia (ISGT-Asia)*, Melbourne, VIC, 2016, pp. 771-775.

[30] Perera, BK, & Ciufo, P 2013, *Power sharing among multiple solar photovoltaic (PV) systems in a radial distribution feeder*, Research Online.

[31] Devine, MT, Farrell, N, & Lee, WT 2017, 'Optimising feed-in tariff design through efficient risk allocation', *Sustainable Energy, Grids and Networks*, vol. 9, pp. 59-74. Available from: 10.1016/j.segan.2016.12.003. [1 August 2017].

[32] Dong, Y, & Shimada, K 2017, 'Evolution from the renewable portfolio standards to feed-in tariff for the deployment of renewable energy in Japan', *Renewable Energy*, vol. 107, pp. 590-596. Available from: 10.1016/j.renene.2017.02.016. [1 August 2017].

[33] Grau, T 2014, 'Responsive feed-in tariff adjustment to dynamic technology development', *Energy Economics*, vol. 44, pp. 36-46. Available from: 10.1016/j.eneco.2014.03.015. [1 August 2017].

[34] Couture, T, & Gagnon, Y 2010, 'An analysis of feed-in tariff remuneration models: Implications for renewable energy investment', *Energy Policy*, vol. 38, no. 2, pp. 955-965. Available from: 10.1016/j.enpol.2009.10.047. [1 August 2017].

[35] Campoccia, A, Dusonchet, L, Telaretti, E, & Zizzo, G 2014, 'An analysis of feed'in tariffs for solar PV in six representative countries of the European Union', *Solar Energy*, vol. 107, pp. 530-542. Available from: 10.1016/j.solener.2014.05.047. [1 August 2017].

[36] G. C. Christoforidis, A. Chrysochos, G. Papagiannis, M. Hatzipanayi and G. E. Georghiou, "Promoting PV energy through net metering optimization: The PV-NET project," *2013 International Conference on Renewable Energy Research and Applications (ICRERA)*, Madrid, 2013, pp. 1117-1122.

[37] Vermont Public Service Department 15 January 2013, Evaluation of Net Metering in Vermont Conducted Pursuant to Act 125 of 2012, viewed 20 June 2015, <https://appsrv.pace.edu/VOSCOE/?do=viewFullResource&resID=J69GMS03116012024>.

[38] U.S. Department of Energy SunShot Rooftop Solar Challenge I, City University of New York On behalf of New York City June 2013, *Net Metering and Interconnection Working Group Final Report*, viewed 20 June 2015, <http://fliphtml5.com/ytip/fsel>.

[39] Koumparou, I, Christoforidis, GC, Efthymiou, V, Papagiannis, GK, & Georghiou, GE 2017, 'Configuring residential PV net-metering policies – A focus on the Mediterranean region', *Renewable Energy*, vol. 113, pp. 795-812. Available from: 10.1016/j.renene.2017.06.051. [1 August 2017].

[40] *Canada, Japan, by country, Feed-in tariff from Wikipedia*, viewed 1 May 2017, <https://en.wikipedia.org/wiki/Feed-in_tariff>.

[41] *Information On Australian Solar Feed-In Tariffs*, viewed 1 May 2017, <https://www.engergymatters.com.au/rebates-incentives/feedintariff/>.

[42] *Utilities Clean (FiT) Program - City of Palo Alto*, viewed 10 June 2017, <http://www.cityofpaloalto.org/gov/depts/utl/business/sustainability/clean.asp>.

[43] *Net metering from Wikipedia*, viewed 1 May 2017, <https://en.wikipedia.org/wiki/Net_metering>.

[44] Parkinson, G 2015, Shared Solar could be the future of distributed PV installations, *RENEWECONOMY*, weblog post, 29 April, viewed 11 May 2016, <http://reneweconomy.com.au/shared-solar-could-be-the-future-of-distributed-pv-installations-92117/>.

[45] Barth, B., Enbar, N. "Assessing utility community solar programs" (*2012) World Renewable Energy Forum, WREF 2012, Including World Renewable Energy Congress XII and Colorado Renewable Energy Society (CRES) Annual conference*, 2, pp. 1544-1551.

[46] Farrell, J 2010, *Community Solar Power - Obstacles and Opportunities*, New Rules Project, viewed 11 May 2016, <https://ilsr.org/wp-content/uploads/files/communitysolarpower2.pdf>.

[47] Monica Oliphant Research 2012, *Community Owned Solar*, Monica Oliphant Research, viewed 11 May 2016, <https://www.campbelltown.sa.gov.au/contentFile.aspx?filename=COS%20Exec%20Summary%20Stage%201.pdf>

[48] Chavez, J, & Coughlin, J, 2013, *Community Solar Programs in Iowa: Issues and Options*, NREL, viewed 11 May 2016, <http://c.ymcdn.com/sites/members.iamu.org/resource/resmgr/Services/Energy_Services/Iowa_Community_Solar.pdf>.

[49] The Massachusetts Department of Energy Resources (DOER) 2013, *Community Shared Solar Review and Recommendations for Massachusetts Models*, The Massachusetts Department of Energy Resources (DOER), viewed 16 September 2016, <http://www.mass.gov/eea/docs/doer/renewables/solar/community-shared-solar-model-frameworks-032813.pdf>.

[50] Bulman, E 2012, *Community Solar Models Nationwide and Possibilities for New York City*, Urban Studies Department, Eugene Lang College, The New School University, viewed 16 September 2016, <http://solargardens.org/CommunitySolarModels.pdf>.

[51] Coughlin, J, Crove, J, Irvine, L, Jacobs, JF, Phillips, SJ, Sawyer, A, & Wiedman, J 2012 *'A Guide to Community Shared Solar: Utility, Private, and Non-profit Project'*, Development, U.S. Department of Energy, viewed 10 September 2015, <http://www.nrel.gov/docs/fy12osti/54570.pdf>.

[52] Centre for Energy and Environmental Policy 2012, *'Policies To Support Community Solar Initiatives: Best Practices To Enhance Net Metering Final Report'*, Centre for Energy and Environmental Policy University of Delaware, viewed 10 September 2015, <http://sites.udel.edu/ceep/files/2013/08/2012_es_READY_CommunitySolar_2.pdf>.

[53] McCutchan, M, Treadwell, T, Fortune, JV, Real, JD 2011, *'Solar PV Retrofits in Multifamily Affordable Housing - Impacts of Virtual Net Metering and MASH Incentives on Project Economics'*, Centre for Sustainable Energy California, U.S. Department Of Energy, Solar America Cities, The City Of San Diego, viewed 10 September 2015, <https://energycenter.org/sites/default/files/docs/nav/policy/research-and-reports/CCSE_VNM_MASH_Report_July_28_2011.pdf>.

[54] Inskeep, B, Daniel, K, & Proudlove, A 2015, *'Solar on Multi-Unit Buildings Policy and Financing Options to Address Split Incentives'*, NC Clean Energy Technology Center, U.S. Department Of Energy, Solar Outreach Partnership, viewed 15 July 2016, <http://solaroutreach.org/wp-content/uploads/2015/02/Multi-unitFactsheet_FINAL.pdf>.

[55] San Diego Gas & Electric Company 2013, *'About your SDG&E® Virtual Net Metering billing'*, San Diego Gas & Electric Company, viewed 20 July 2016, <https://www.sdge.com/sites/default/files/documents/713942219/VNM%20FACT%20SHEET%20FINAL%2011-24-15.pdf?nid=5131>.

[56] Centre for Sustainable Energy, California Solar Energy Industries Association, Interstate Renewable Energy Council (2015), *'Virtual Net Metering Policy Background and Tariff Summary Report'*, Centre for Sustainable Energy, viewed 20 May 2016, <https://energycenter.org/sites/default/files/docs/nav/programs/solar-pathways/(6902)_Virtual_Net_Metering_Policy_Background_and_Tariff_Summary_Report.pdf>.

[57] Cockburn, P 2015 'Response to AER Request for Submissions - Regulating Innovative Energy Selling business models under the National Energy Retail Law' Virtual Energy, viewed 14 May 2015, <https://www.aer.gov.au/system/files/Submission%20-%20Virtual%20Energy_0.pdf>.

[58] San Francisco's Department of the Environment 2013, *'Virtual Net Energy Metering at Multitenant Buildings'*, San Francisco's Department of the Environment, viewed 14 September 2015, <https://sfenvironment.org/sites/default/files/fliers/files/virtual_net_energy_metering_at_multitenant_buildings_0.pdf>.

[59] Gottlieb, J 2014, Virtual Net Metering and the Future of Community Solar Energy, *the energy collective*, weblog post, 10 January, viewed 11 July 2015, <http://www.theenergycollective.com/jeremy-gottlieb/325231/virtual-net-metering-and-future-community-solar>.

[60] Langham, E, Cooper, C, & Ison, N 2013, *'Virtual Net Metering In Australia: Opportunities & Barriers'*, Institute for Sustainable Futures (ISF), University of Technology Sydney, viewed 11 July 2015, <https://opus.lib.uts.edu.au/bitstream/10453/31943/1/2012004596OK.pdf>.

[61] Anich, A 2011, *'Virtual Net Metering Programs in the U.S.'*, Karbone Renewables Research, viewed 11 July 2015, <http://www.karbone.com/wp-content/uploads/2012/02/Karbone-VNM-Research.pdf>.

[62] Rami´rez, F, Honrubia-Escribano, A, Go´mez-La´zaro, E, & Pham, D 2017, 'Combining feed-in tariffs and net-metering schemes to balance development in adoption of photovoltaic energy: comparative economic assessment and policy implications for European countries', *Energy Policy*, vol. 102, pp. 440-452. Available from: 10.1016/j.enpol.2016.12.040. [2 August 2017].

[63] Yamamoto, Y 2012, 'Pricing electricity from residential photovoltaic systems: a comparison of feed-in tariffs, net metering, and net purchase and sale', *Solar Energy*, vol. 86, no. 9, pp. 2678-2685. Available from: 10.1016/j.solener.2012.06.001. [2 August 2017].

[64] *Feed-in tariff from Wikipedia*, viewed 20 May 2017, <https://en.wikipedia.org/wiki/Feed-in_tariff>.

[65] REN21. 2010, '*Renewables 2010 Global Stuatus Report'*, Renewable Energy Policy Network for the 21st Century, viewed 15 July 2017, <http://www.ren21.net/Portals/0/documents/activities/gsr/REN21_GSR_2010_full_revised%20Sept2010.pdf>.

[66] Hirsh, R. F. (1999). "PURPA: The Spur to Competition and Utility Restructuring," The Electricity Journal, Vol. 12, Issue 7, pp. 60–72.

[67] Maehlum, MA 2014, What`s the Difference Between Net Metering and Feed-In Tariffs?, *energy informative*, weblog post, 15 March, viewed 11 May 2016, <http://energyinformative.org/net-metering-feed-in-tariffs-difference>.

[68] J. Heeter, R. Gelman, and L. Bird 2014, Status of Net Metering: '*Assessing the Potential to Reach Program Caps'*, National Renewable Energy Laboratory, viewed 18 May 2015, <http://www.nrel.gov/docs/fy14osti/61858.pdf>.

[69] Shannon, H. 2013, *'Community and Virtual Net Metering: Overcoming Barriers to Distributed Generation'*, The George Washington Journal of Energy and Environmental Law, viewed 19 June 2016, <https://gwujeel.files.wordpress.com/2013/11/shannon-huecker.pdf>.

[70] Microeconomics, Investopedia, viewed 22 September 2016, <http://www.investopedia.com/terms/m/microeconomics.asp>.

[71] *Commercial load data USA*, OpenEI, <http://en.openei.org/datasets/files/961/pub/COMMERCIAL_LOAD_DATA_E_PLUS_OUTPUT/USA_CA_Twentynine.Palms.690150_TMY3/>.

[72] Grandjean, A, Adnot, J, & Binet, G 2012, 'A review and an analysis of the residential electric load curve models', *Renewable and Sustainable Energy Reviews*, vol. 16, no. 9, pp. 6539-6565. Available from: 10.1016/j.rser.2012.08.013. [2 August 2017].

[73] Masters, GM 2013, 'Photovoltaic Materials And Electrical Characteristics', *Renewable and efficient electric power systems / Gilbert M. Masters*, Hoboken, New Jersey: John Wiley & Sons Inc., [2013], pp. 445-504.

[74] *Wagga Wagga Amo* 2006, viewed 3 March 2017, <http://www.bom.gov.au/climate/data/>.

[75] ActewAGL 2013, Our NSW electricity prices, ActewAGL, viewed 14 March 2017, <https://www.actewagl.com.au/.../ActewAGL/ActewAGL.../Retail.../Electricity-retail.../...>.

[76] CSE, *About Virtual Net Metering*, online picture, Centre for Sustainable Energy, Solar Market Pathways California And Beyond, viewed 11 May 2017,

<https://energycenter.org/solar-market-pathways/research-and-analysis/about-virtual-net-metering>.

[77] Solar feed-in tariff meets with mixed reviews, *Metering & Smart Energy International*, weblog post, 13 MAY 2008, viewed 23 May 2017, <https://www.metering.com/solar-feed-in-tariff-meets-with-mixed-reviews/>.

[78] Wei-Jen Lee, C. H. Lin and K. D. Swift, "Wheeling charge under a deregulated environment," in *IEEE Transactions on Industry Applications*, vol. 37, no. 1, pp. 178-183, Jan/Feb 2001.

[79] A. Saxena, S. N. Pandey and L. Srivastava, "Genetic algorithm based wheeling prices allocation for Indian power utility by using MVA-mile and MW-mile approaches," *2016 International Conference on Emerging Trends in Electrical Electronics & Sustainable Energy Systems (ICETEESES)*, Sultanpur, 2016, pp. 60-63.

[80] F. Li, N. P. Padhy, J. Wang and B. Kuri, "MW+MVAr-miles based distribution charging methodology," *2006 IEEE Power Engineering Society General Meeting*, Montreal, Que., 2006, pp. 5 pp.-.

[81] Avinash D. and B. Chalapathi, "MW-Mile method considering the cost of loss allocation for transmission pricing," *2015 Conference on Power, Control, Communication and Computational* Technologies *for Sustainable Growth (PCCCTSG)*, Kurnool, 2015, pp. 128-131.

[82] D. Das and D. Divan, "Individual generator contributions towards loads and line flows in networks with loop flows," *41st North American Power Symposium*, Starkville, MS, USA, 2009, pp. 1-6.

[83] J. W. Marangon Lima, "Allocation of transmission fixed charges: an overview," in *IEEE Transactions on Power Systems*, vol. 11, no. 3, pp. 1409-1418, Aug 1996.

[84] D. Shirmohammadi, X. V. Filho, B. Gorenstin and M. V. P. Pereira, "Some fundamental, technical concepts about cost based transmission pricing," in *IEEE Transactions on Power Systems*, vol. 11, no. 2, pp. 1002-1008, May 1996.

[85] H. H. Happ, "Cost of wheeling methodologies," in *IEEE Transactions on Power Systems*, vol. 9, no. 1, pp. 147-156, Feb 1994.

[86] Jiuping Pan, Y. Teklu, S. Rahman and K. Jun, "Review of usage-based transmission cost allocation methods under open access," in *IEEE Transactions on Power Systems*, vol. 15, no. 4, pp. 1218-1224, Nov 2000.

[87] Gu. N, Ling. X, & Hou. Z, “A new approach for pricing of fixed costs in wheeling rates by modified mile-power method”, *Power System Technology*, vol. 23 no. 2 pp. 66-68, 71 Feb. 1999

[88] J. Bialek, "Tracing the flow of electricity," in *IEE Proceedings - Generation, Transmission and Distribution*, vol. 143, no. 4, pp. 313-320, Jul 1996.

[89] Ching-Tzong Su and Ji-Horng Liaw, "Power wheeling pricing using power tracing and MVA-KM method," *2001 IEEE Porto Power Tech Proceedings (Cat. No.01EX502)*, Porto, 2001, pp. 6 pp. vol.1-.

[90] Zhou Ming, Sun Liying, Li Gengyin and Yixin Ni, "A novel power flow tracing approach considering power losses," *2004 IEEE International Conference on Electric Utility Deregulation, Restructuring and Power Technologies. Proceedings*, 2004, pp. 355-359 Vol.1.

[91] A. Tiwari and V. Ajjarapu, "Modified Methodology for Tracing Power Flow," *2006 38th North American Power Symposium*, Carbondale, IL, 2006, pp. 317-322.

[92] D. Kirschen, R. Allan and G. Strbac, "Contributions of individual generators to loads and flows," in *IEEE Transactions on Power Systems*, vol. 12, no. 1, pp. 52-60, Feb 1997.

[93] K. Xie, C. Li and Y. Liu, "Tracing power flow from generators to loads and branches using incidence matrix multiplication," *2009 IEEE Power & Energy Society General Meeting*, Calgary, AB, 2009, pp. 1-7.

[94] Hongbo Sun, D. C. Yu and Qionglin Zheng, "AC power flow tracing in transmission networks," *2000 IEEE Power Engineering Society Winter Meeting. Conference Proceedings (Cat. No.00CH37077)*, 2000, pp. 1715-1720 vol.3.

[95] J. Bialek, "Topological generation and load distribution factors for supplement charge allocation in transmission open access," in *IEEE Transactions on Power Systems*, vol. 12, no. 3, pp. 1185-1193, Aug 1997.

[96] Zhaoxia Jing and Fushuan Wen, "Discussion on the Proving of Proportional Sharing Principle in Electricity Tracing Method," *2005 IEEE/PES Transmission & Distribution Conference & Exposition: Asia and Pacific*, Dalian, 2005, pp. 1-5.

[97] Sign the petition for a fair price for solar, *SolarCitizens*, viewed 2 July 2017, <http://www.solarcitizens.org.au/fairprice?gclid=Cj0KEQjwnazLBRDxrdGMxKm4oQBEiQAQJ1q635vMUow2yHDUWwmvOgVRR6POy6HP3qW8y448BLdyMEaAlJg8P8HAQ>.

[98] National fact sheet, *Why Is Solar Power Undervalued In Australia?*, viewed 12 July 2017, <http://www.backroad.com.au/wp-content/uploads/2016/12/Fair-price-factsheet-SC-2016-12-06.pdf>.

[99] RenewEconomy 2017, *Fair Value of Distributed Generation project*, RenewEconomy articles, viewed 25 July 2017, <http://www.backroad.com.au/wp-content/uploads/2017/07/2017-03-20-RenewEconomy-fair-value-articles.pdf>.

[100] Yang, Y, & Yang, Q 2007, 'Electrical system component parameters and equivalent circuit', *Power system analysis / Yongyuan, Yang, Qiwen, Yang*, China Electric Power Press, [2007], pp. 18.

[101] Hai, H 2010, “Reverse Power Protection Function of PV Power Station”, Machine Building & Automation, vol. 39, no. 5, pp. 159-161, Oct 2010, viewed 23 October 2016, <https://wenku.baidu.com/view/630f1aabd1f34693daef3ee7.html>.

[102] Code for electrical design of civil buildings, JGJ_16-2008, Industrial Code of the People's Republic of China, viewed 23 July 2017, <https://wenku.baidu.com/view/e1c0e21ba8114431b90dd8cb.html?from=search>.

[103] Reverse power protection relay price Trends, Aliexpress, viewed 05 August 2017, <https://www.aliexpress.com/price/reverse-power-protection-relay_price.html>.

[104] Automatic transfer switch Trends, Aliexpress, viewed 05 August 2017, <https://www.aliexpress.com/price/automatic-transfer-switch_price.html >.

APPENDIX A Simulation Models of Grid-Connected PV System

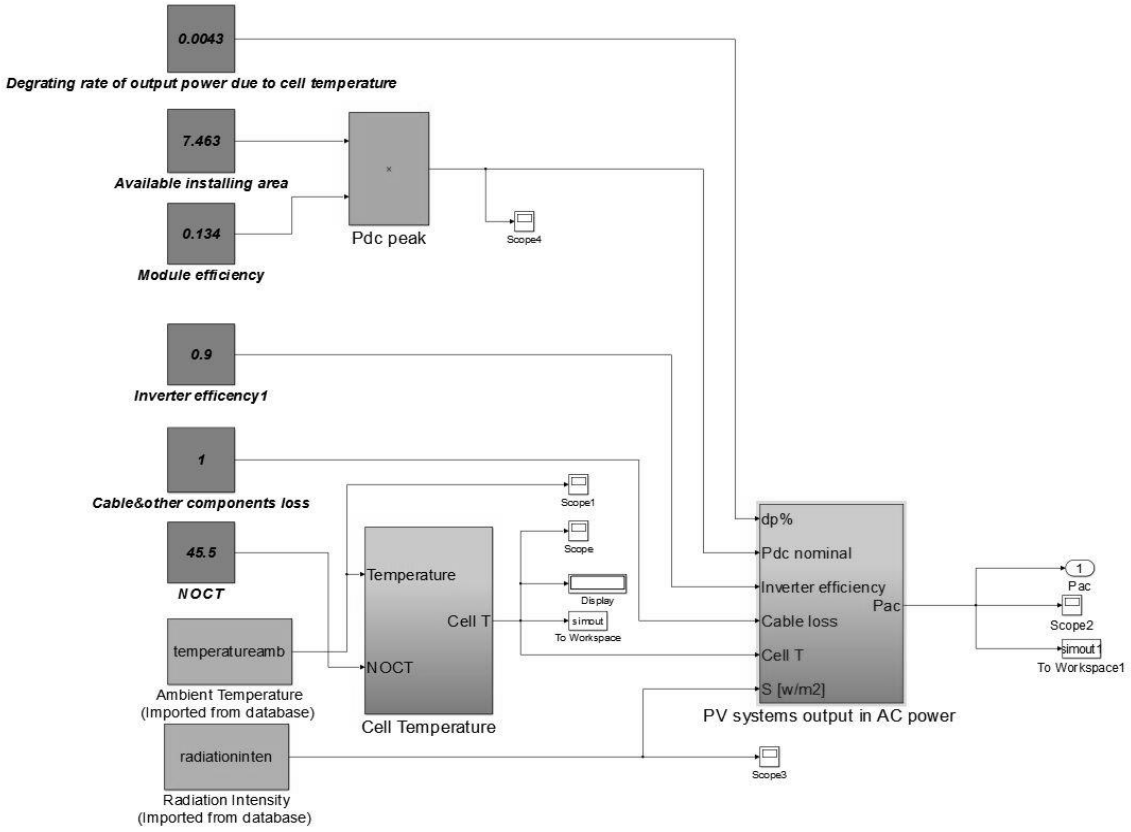

Fig. A.1 Integrated model of PV systems output

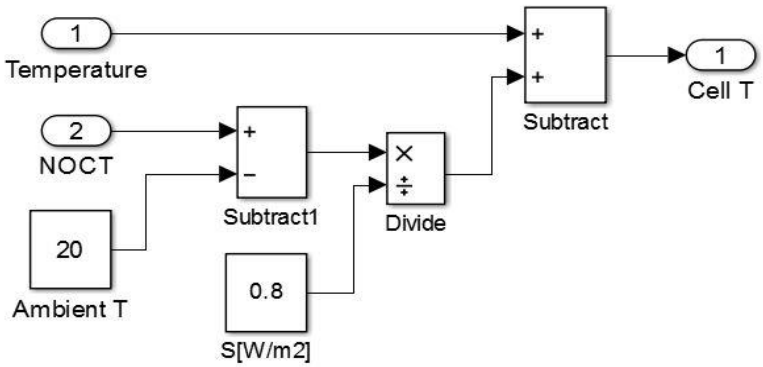

Fig. A.2 Model of cell temperature

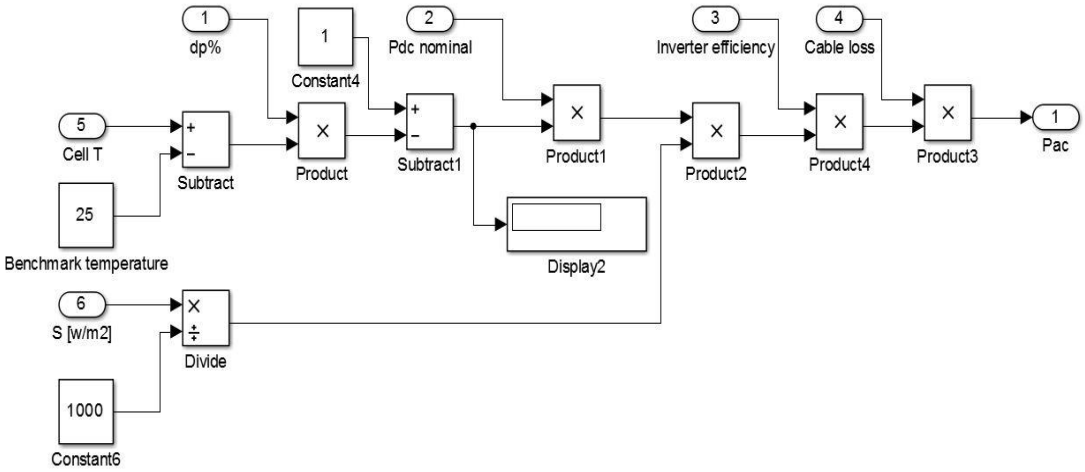

Fig. A.3 Model of PV systems AC output